Investigation into the Effects of High Shear Blending and Storage on Powders for Inhalation

John Willetts

A Thesis Submitted to the School of Chemical Engineering,
University of Birmingham for the Degree of Doctor of Philosophy

November 2011

The School of Chemical Engineering, University of Birmingham

Investigation into the Effects of High Shear Blending and Storage on Powders for Inhalation

by

John Willetts

January 2012

Summary

Dry powder inhaler (DPI) formulations are usually comprised of a mixture of micronised active pharmaceutical ingredient (API) with aerodynamic diameter 1-5 μm to allow deposition in the lower airways, and a coarse (~70 micron) excipient, typically α-lactose monohydrate, used to aid the handling, metering and dosing of the formulation. These components are usually combined in a secondary manufacturing process such as high shear blending (HSB), which is used primarily to distribute the cohesive drug particles throughout the bulk excipient to create a chemically homogeneous formulation.

This thesis explores the use of HSB to produce mimic DPI formulations and assesses the effect of different blending and storage regimes on various physicochemical properties of such powders. A novel fluidised bed elutriation (FBE) technique was developed to test the ability of fine mimic drug particles to separate from coarse particles in such formulations, along with conventional air jet sieve (AJS) and Next Generation Impactor (NGI) studies.

Results showed that, generally, blending regimes were seen to have little effect on the *in vitro* performance of these mimic formulations, with extended storage at high humidity having a more profound effect on the separation of fine particles. Tests on the performance of formulations using the FBE technique showed that fluidisation performance alone is insufficient to identify blending-induced changes; however, analysis of the fine elutriated fraction has shown subtle changes in the populations of particles due to HSB. Notable differences were observed between the mimic cohesive and adhesive drugs, indicating the ability of these tests to identify formulations with different adhesive properties. In addition, a study to determine the specific energy input (SEI) required to achieve chemical homogeneity suggested that extended high shear blending beyond a given energy input may only alter the size distribution of the formulation, and not improve homogeneity, thus having implications for the manufacture of such products.

Acknowledgements

This thesis owes its existence to the help, support and inspiration of many people. Firstly, I wish to acknowledge the EPSRC, GlaxoSmithKline and the University of Birmingham for financial support during the three years of study and the use of laboratory facilities which enabled this work to be carried out.

I would especially like to thank my supervisors Dr Rachel Bridson and Dr Phil Robbins for their continued support, guidance and invaluable input. Thanks also go to industrial supervisors at GSK, Mike Bowley, Trevor Roche and Ian Bridle for valuable advice and ideas throughout the project, and hospitality whilst at their manufacturing and research and development sites. In addition, I would like to thank Kenny Smith and Andrew Savage from GSK for their time and help in the time spent at the Harlow research facility, and Drs Andy Ingram (UoB) and Marcel de Matas for a stimulating and interesting viva.

I would like to thank friends and colleagues within the School of Chemical Engineering at The University of Birmingham. Bob Sharpe, Bill Harris, and Dave Boylin for their help and advice in technical matters, lending of tools, making various pieces of equipment, and fixing apparatus; Tom Eddleston for his support and advice on technical matters and instruments; Steve Williams in the School of Chemistry Glassblowing Workshop for initially making, and numerous repairs to the fluidised bed; Matt Barea, Ben Millington, Drs Catherine Kelly, Aman Dhir and Yan Sim Lee for their support and encouragement throughout the project and finally, Dr James Bowen for his assistance on technical matters and use of Science City laboratory equipment.

In addition, thanks are extended to Mark Ware (Sympatec) for training and support on their laser diffraction equipment, Paul Van Den Branden and John Booth (Scientific and Medical Products Limited) for their support with both DVS instruments used in the department.

Finally, and most importantly, I would like to thank my Mom and Dad for their constant support and encouragement throughout my education.

The DVS Advantage II and Sympatec HELOS laser diffraction system and RODOS dispersion unit used in this research was obtained through Birmingham Science City: Innovative Uses for Advanced Materials in the Modern World (Advanced Materials 2), with support from Advantage West Midlands (AWM) and part funded by the European Regional Development Fund (ERDF)

Contents

List of Figures

List of Tables

Abbreviations

AFM	Atomic Force Microscopy
AJS	Air Jet Sieve
API	Active Pharmaceutical ingredient
ARG	Analytical Reagent Grade
BET	Brunauer Emmet Teller
CFC	Chlorofluorocarbon
CI	Cascade Impactor
cGMP	current Good Medical Practice
cLogP	Octanol/water Partition Coefficient
cLogD	Octanol/water Distribution Coefficient
COPD	Chronic Obstructive Pulmonary Disorder/Disease
CV	Coefficient of variation (%)
DC	Direct Current
DPI	Dry Powder Inhaler
DSC	Differential Scanning Calorimetry
DVS	Dynamic Vapour Sorption
FB(E)	Fluidised bed (elutriation)
FCA	Force Control Agent
FF	Flow Function
FPF	Fine Particle Fraction
FPF	Fine Particle Dose
FTIR	Fourier Transform Infrared Spectroscopy
GI	Gastrointestinal
HFC	Hydrofluorocarbon
HSB	High Shear Blending
ICS	Inhaled Corticosteroid
IGC	Inverse Gas Chromatography
LABA	Long-acting β_2 adrenergic agonists
NGI	Next Generation Impactor
PAT	Process Analytical Technology
MDI	Metered Dose Inhaler
PSD	Particle Size Distribution
QbD	Quality by Design
R&D	Research and Development
RFT	Right First Time
RH	Relative Humidity
SABA	Short-acting β_2 adrenergic agonists
SEI	Specific Energy Input
SEM	Scanning Electron Microscopy
SFC	Supercritical Fluid Crystallisation
SGV	Superficial Gas Velocity
SOP	Standard Operating Procedure
SSA	Specific Surface Area
TDH	Transport Disengagement Height
UV	Ultraviolet

Symbols

Ar	Archimedes Number
c	Constant
C_d	Drag Coefficient
d_{p}	Average Particle Diameter
d_{x}	The particle size at which x% of particles are found in a particle size distribution
d_t	Column Diameter
ΔP	Pressure Drop
D_{sed}	Sedimentation Distance in the Lungs
E_1	Heat of Adsorption (first layer)
E_L	Heat of Adsorption (subsequent layers)
ε	Voidage
$\varepsilon_{\mathrm{mf}}$	Voidage at Minimum Fluidisation
F	Force
Fr	Froude Number
g	Acceleration due to Gravity
μ	Gas Viscosity
N	Rotational Speed (revolutions per minute)
ω	Angular Velocity
P	Pressure, Power
ϕ_{agg}	Effective Diameter of Agglomerate
R	Impeller/Bowl Radius
R_T	Radial distance from centre of bowl to force transducer
Re	Reynolds' Number
ρ_p	Average Particle Density
Stk	Stokes' Number
t	Time
τ	Consolidation Stress
U	Gas Velocity
U_{mf}	Minimum Fluidisation Velocity
U_{sgv}	Superficial Gas Velocity
v	Adsorbed Gas Quantity
v_{tip}	Impeller Tip Velocity

1.0. Introduction

ABSTRACT

Dry powder inhalers (DPIs) are commonly used devices employed to facilitate the delivery of drug formulations designed to treat a range of lung disorders including asthma and chronic obstructive pulmonary disease (COPD). The powders used in such treatments often consist of a near-homogeneous, interactive mixture of micronised (1-5 μm) active pharmaceutical ingredient (API) and coarse (~70 μm), inert excipients (usually α-lactose monohydrate) added to aid the dispensing, filling and metering of the formulation. These formulation components are usually combined in a secondary manufacturing process; with high shear blending (HSB) being the focus of this thesis. During an inhalation event, drug particles separate from excipient and deposit in the lower airways – the site of action. This chapter reviews the many factors influencing the efficiency of drug-carrier detachment, along with methods to test the adhesive strength between drug and excipient.

A key area of focus for DPI formulation production is the establishment of techniques to monitor the properties of the formulation throughout the manufacturing process, in an attempt to identify and correct problems as soon as possible in order to reduce batch wastage.

This chapter introduces the possibility of employing a novel fluidised bed elutriation (FBE) method to assess the bulk-scale properties and characteristics of DPI formulations – work which forms the basis of chapters 5 and 7 of this thesis.

1.1. History of Inhalation Therapy and Devices

The use of dry powder inhalers (DPIs) in the medical treatment of a range of lung-related and systemic conditions requires the careful design and manufacture of an array of products and formulations in order to deliver the desired therapeutic effect. Considerations need to be made regarding the patient's lung physiology, and design of both the inhaler and the formulations containing the active pharmaceutical ingredient (API). Key factors involved in the delivery of powders include the physiology and deposition mechanisms associated with the various regions within the lungs and the physicochemical properties of the formulations, including particle size, shape, morphology, and chemistry (Hickey *et al*., 1994). In addition, the processing stages involved in formulation manufacture play a vital role in the product's efficacy, along with the mechanisms responsible for transferring powder from a static bed within the device to an aerosol for delivery to the lungs. Each of these factors is described in this chapter; however, the key focus of this thesis involves the effect of high shear blending (HSB) – a secondary manufacturing process for combining drug and excipient - on the *in vitro* performance of DPI formulations.

Delivery via the respiratory tract is one the oldest and most common methods for administering drugs into the human body. Aerosols, smoke, vapour, and gases have been inhaled for many centuries in an attempt to cure or treat a wide range of ailments. Pulmonary administration is desirable for several reasons, not only for local therapy in the lungs but also for systemic treatments throughout the body (Grossman, 1954; Gonda, 1990, 2006; Siekmeier and Scheuch, 2008; Allen, 2008).

Inhalation therapy has a long history, with leaves of the Atropa Belladonna plant and the leaves and flowers of the Datura Stramonium smoked as cough suppressants, up until the 1950s (Grossman, 1954). Modern inhalation therapy began in the nineteenth century when nebulisers were introduced, although more compact treatments began with the first pressurised metered dose inhaler (MDI) developed in the 1950s (Medihaler®, Riker). However, MDIs were reliant on ozone-depleting chlorofluorocarbons (CFCs) as propellants, consequently, the Montreal Protocol (1987) required the substitution of CFCs with hydrofluoralkanes (HFAs) and subsequent reformulation of MDI formulations (Ashurst *et al.,* 2000).

In 1970, the first breath-actuated DPI was introduced onto the market (Fisons Spinhaler®). Since then, many different varieties of DPIs have been developed, both multi- and single-dose devices, using technologies drawn from a range of disciplines. These developments were stimulated by the dramatic increase in patients suffering from asthma and chronic obstructive pulmonary diseases (COPDs) in the twentieth century, along with the desire to develop a non-invasive method of drug delivery for formulations that cannot be delivered orally to the gastrointestinal (GI) tract, or have a low bioavailability via the oral route, such as therapeutic peptides and proteins for systemic action (Zijlstra *et al.,* 2004; van Drooge *et al.,* 2005).

The differences between MDIs, DPIs, and nebulisers are based on the physical states of the dispersed phase and continuous medium; within each category, there are different types of system based on the method of metering and dispersion.

The clinical performance of the various types of inhalation devices has been extensively reviewed (Barry and O'Callaghan, 2003; Dolovich *et al.,* 2005), with conclusions made that no class of device is superior, and that choice should be based on convenience, cost, patient preference, and treatment required. With a global market share of about 80%, the MDI remains the most widely used device (O'Connor, 2004). Since a MDI is pressurised, the dose is emitted at high velocity, hence premature deposition in the oropharynx is likely (Newman and Clarke, 1993; Ganderton, 1997). It has also been found that due to incorrect use of MDIs - in particular, the poor coordination of actuation and inhalation - decreased asthma control has been found in a substantial proportion of patients treated with corticosteroid MDIs (Giraud and Roche, 2002).

1.2. Dry Powder Inhalers

Since the introduction of the first DPI in 1970 (Ashurst *et al.,* 2000), many variations of the DPI have been developed, although they are generally classified as being either unit-dose or multi-dose inhalers. The sharp rise in the number of cases of lung-related illnesses in the 20th century stimulated the development of DPIs, although possibly the most crucial event leading to the advance in technology was the prohibition of chlorofluorocarbons (CFCs) as propellants in MDIs. Since CFCs are known ozone depleters, the introduction of hydrofluorocarbons (HFCs) as a replacement propellant required the formulations used in MDIs to be redesigned.

One of the advantages of DPIs over MDIs is removal of the need for patient coordination in administration of the drug. DPIs in common use today are often breath-actuated and the energy for powder dispersion and generation of the aerosol is derived from the patient's inhalation. This method alleviates the problem of coordination of actuation and inhalation that many patients (particularly children and the elderly) have with MDIs. DPIs are thus far easier to use, and offer more stable and efficient systems.

DPIs comprise various types (multi-unit dose, multi-dose reservoir, single-unit dose, single-use disposable – shown in Fig. 1.1). A more detailed description of each type of DPI is given by Daniher and Zhu, (2008).

Reservoir systems that have simple designs where the formulation is stored in a bulk chamber within the device are far cheaper to produce than the factory metered designs; however, they have the disadvantages of having lower dose reproducibility due to inconsistent powder dispensing and having less moisture protection. Factory-metered blister strips allow greater reproducibility of dose due to the consistency in controls for metering, however due to the large number of components required, the costs of pre-metered DPIs is a drawback.

The active ingredients within these systems typically comprise particles with aerodynamic particle size that allows deposition in the tracheobronchial regions of the lungs (1-5 μm – Newman and Clarke, 1983). However, powders of this size are notoriously cohesive and in order to improve handling, dispersion and metering, the active ingredient is often mixed with an excipient carrier of larger (~70 μm) mean geometric particle size (Bridson *et al*., 2007).

The major factor in the design of DPIs is the need to overcome the strong interparticle forces between API and excipient to produce an aerosol consisting primarily of de-agglomerated particles with an aerodynamic diameter suitable for lung deposition at the target area (Hickey *et al*., 1994; Timsina *et al*., 1994). Often, forces generated in passive DPIs are insufficient to overcome these interparticle forces, thus only a small fraction of dose is available for efficient inhalation. Engineers specialising in fluidised bed technology have suggested numerous mechanisms to reduce interparticle forces in DPI formulations, in order to improve aerosolisation. Such methods include: passing aerosol through Venturi tubes to increase velocity; impaction against baffles, plates, or

other surfaces; circulation and cyclone chambers, or by using pressurised air and vacuum chambers (Finlay, 2001). In addition, external energy may be applied to enhance deagglomeration within the device – these are known as active DPIs. Active DPIs have integrated energy and dispersion sources (compressed air, battery, or spring mechanisms to store energy – Crowder and Hickey, 2006) and enhance the dose reproducibility and reduce dependence of the patient's inspiratory flow rate, coordination and ability to generate sufficient pressure (Tobyn, *et al*., 2004). In addition, several power-assisted devices have been developed that utilise vibration (Crowder, 2004); pneumatics, or impaction forces (Crowder *et al.,* 2001). Naturally, these are preferred for children and patients who cannot generate sufficient pressure or flow rate on their own.

Despite these advantages, active DPIs are complex and expensive to both develop and manufacture and their intricate nature leads to regulatory approval issues; however since they require little or no coordination, active DPIs frequently achieve better lung delivery than analogous MDIs (Dunbar *et al*., 1998; Labiris and Dolovich, 2003).

Different available DPI designs result in varying resistances to airflow during inhalation; the fine particle output of the device depends on the generated inspiratory flow profile, the inhaler design, and the powder formulation. Therefore, for a particular device-formulation combination, there exists an optimal flow profile at which maximum fine particle generation occurs (de Koning *et al*., 2002).

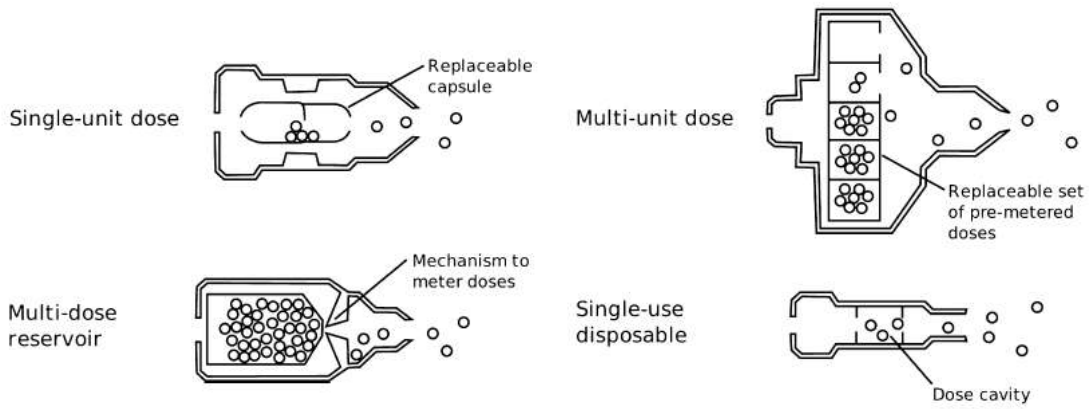

Fig. 1.1. Illustration of four dose design options available for DPIs (adapted from Daniher and Zhu, 2008).

Since DPI formulations are typically one-phase, solid particle blends, they are preferential to MDIs from a stability and processing standpoint (Borgstrom *et al.,* 1996; Ashurst *et al.,* 2000). Dry powders are at a lower energy state, which reduces the rate of chemical degradation and the likelihood of reaction with contact surfaces. In addition, MDI formulations, which include propellant and cosolvents, may extract organic compounds from the device components, thus subjecting the patient to unnecessary chemical exposure (Norwood *et al.,* 1995). However, since administration is controlled by inspiration alone, patients with COPDs and subsequently low inhalation flow rates, certain DPIs may be unsuitable (deBoer *et al.,* 1997).

Generation of a DPI aerosol begins when movement initiated by a patient's inspiratory airflow disperses a static bed. When the patient inhales, airflow through the device creates shear and turbulence; air is introduced into the powder bed, the static bed becomes *aerosolised* and enters the patient's airways (Fig. 1.2). The drug particles then separate from the carrier particles and are carried deep into the lungs, while the carrier particles impact into the oropharynx and are removed into the GI tract (Cegla, 2004). Therefore, the degree of deposition into the lungs is determined by the patient's variable inspiratory airflow (Newman *et al.,* 1994; Dunbar *et al.,* 2000). Ineffective separation between drug and carrier is one of the main reasons (along with dose uniformity) behind low deposition efficiency associated with DPIs (Zeng *et al.,* 2000a).

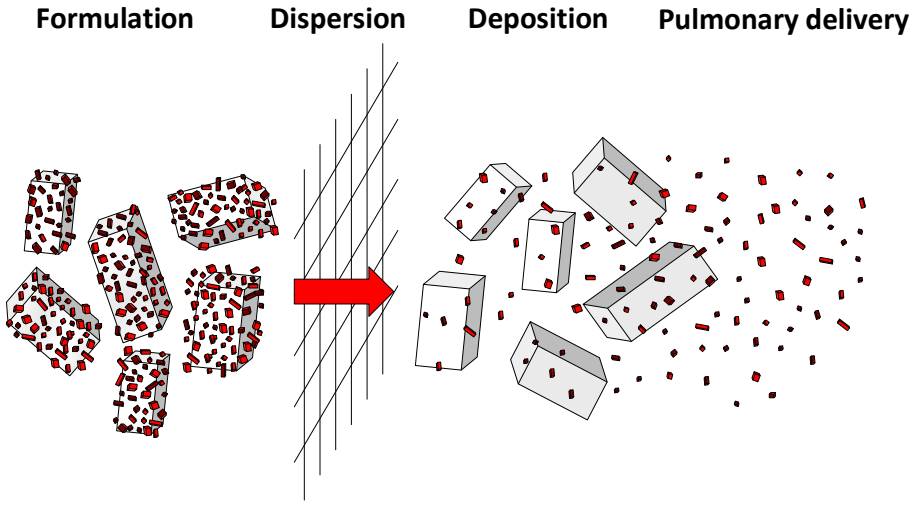

Fig. 1.2. Principle of DPI design. The formulation comprises micronized drug (red particles) blended with larger carrier particles (white blocks). The formulation is dispensed by a metering system, before being dispersed by an active or passive system that entrains the particles into the patient's airways, where drug particles separated from the carrier particle and are carried into the lung (adapted from Telko and Hickey, 2005).

The degree to which drug detachment from carrier particles occurs during inhalation is related to the strength and efficiency of de-agglomeration forces generated within the inhaler, relative to the adhesive forces in the mixture (Clarke *et al.*, 2002). The detachment force and adhesive force need to balance in order to achieve the required powder homogeneity and stability, and sufficient detachment of drug particles to deliver the required dose (Brown *et al.*, 2003).

Obtaining this balance requires the ability to control the parameters that affect the drug-carrier interaction in adhesive mixtures, an effective inhaler device, and an understanding of the detachment forces generated within the inhaler. Unfortunately, not all aspects of the drug, carrier, or inhaler can be controlled; both the drug and carrier will have natural variations in their size and shape, and their level, and nature of surface impurities. Variations in the manufacturing and storage conditions and in patient physiology make optimising performance difficult. Fig. 1.3 summarises the factors that affect the adhesive and de-agglomeration forces in a DPI formulation and their impact on the fine particle fraction (FPF) generated by the inhaler device. The FPF is a commonly used measure of the amount of fine drug particles in a formulation that can be deposited in the lower airways at the site of action; this is usually defined as the fraction of particles with aerodynamic diameter between 1-5 μm (Newman and Clarke, 1983; Zanen *et al.,* 1994).

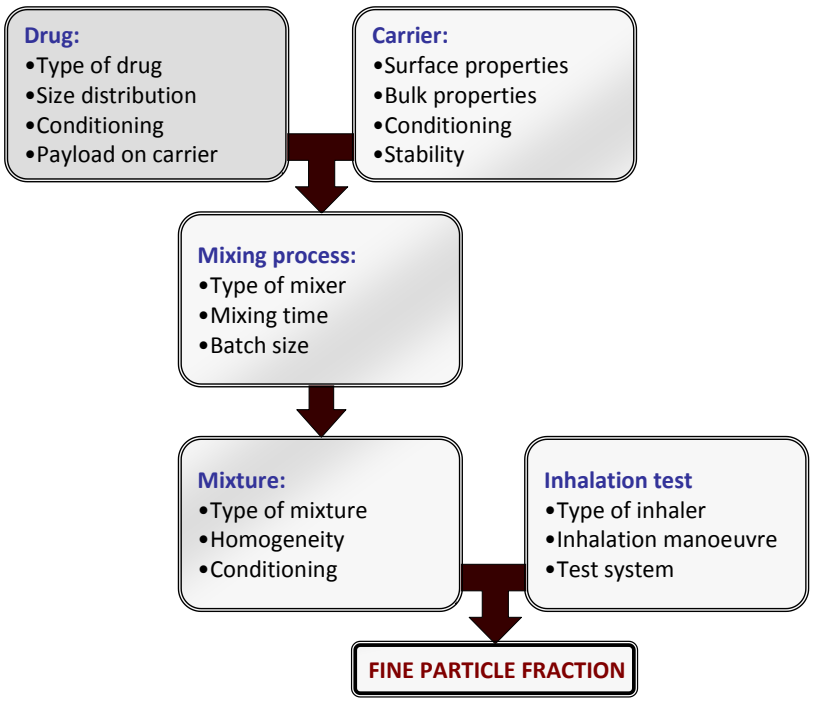

Fig. 1.3. Summary of factors that affect aerosol generation in a DPI (adapted from de Boer *et al.*, 2003b).

1.3. Respiratory Tract Physiology and Deposition

The human respiratory system is divided into three main sections, the upper respiratory tract consisting of the nasal passages, sinuses and throat (pharynx); the respiratory airways consisting of the larynx (voice box), trachea, bronchi, and bronchioles; and finally the lungs consisting of the alveolar ducts, sacs, and alveoli. Moving down the system, the airways decrease in size (Table 1.1) and numerous bifurcations occur, with between 20 and 23 divisions common from trachea to alveoli (Weibel, 1963).

There are major advantages in administering drugs for local therapy by inhalation; firstly, the drug is delivered direct to the target area, hence a rapid and controllable effect is achieved (Niven *et al*., 1994). Secondly, its dose can be dramatically reduced in relation to oral or parenteral administration, hence systemic side effects can be reduced (Patton, 2000). Advantages of the systemic action of inhalation therapy include the non-invasive nature of the treatment, removal of first-pass metabolism of drug by the liver and degradation by high pH and enzyme levels (Crooks and Damani, 1990) in the GI system (Byron and Patton, 1994; Patton, 2000; Zijlstra *et al.,* 2004; van Drooge *et al.,* 2005). In addition, the large surface area of the alveoli (80-100 m^2), and the thin absorption barrier allow for swift uptake into the blood stream (Frijlink and de Boer, 2004).

Target areas in the lungs vary with the type of disease to be treated, and subsequently, the type of drug to be administered. For example, asthma is usually associated with the lymphocytes and eosinophil cells (Krishna *et al.,* 1997; Carroll *et al.,* 1997). As there have been discrepancies about whether central or peripheral inflammation of the airways is more important in asthma treatment, it is recommended that inhaled steroids are deposited throughout the airways (Leach, 1998), and can therefore reach the optimal site of the small airways (Jackson and Lipworth, 1995).

Pulmonary drug delivery is also the most efficient method to treat obstructive airway diseases such as asthma and COPDs. These drugs are typically β_2 adrenergic agonists such as salbutamol and formoterol, corticosteroids or anticholinergics. Such locally acting drugs do not need to be absorbed into the bloodstream to exert their pharmacologic effect, instead, they target specific regions of the respiratory tract for which their effect is desired (de Jongh, 1995). For example, both corticosteroids, which

target inflammatory cells, and anticholinergics, which target muscarinic receptors, are both deposited throughout the lower airways and alveoli (Labiris and Dolovich, 2003).

1.3.1. Deposition In The Respiratory Tract

The deposition of particles in the lungs is reliant upon the same mechanisms that control collection of particles in filters. However, filtration normally occurs within a system at a fixed (constant) flow rate; whereas deposition in the respiratory tract occurs at varying flow rates due to the various geometries experienced (Table 1.1).

Table 1.1. Characteristics of the respiratory tract with respect to drug deposition in different pulmonary regions, assuming a steady inspiratory flow rate of 60 l min^{-1}. D_{sed} is the distance that a 1 μm particle will sediment during transport to the region, *Stk* is the Stokes' number for a 1 μm particle in that region, whilst *Re* is the Reynolds' number for that region (adapted from Davies, 1961).

Region	Number	Diameter *(cm)*	Length *(cm)*	Residence time *(s)*	D_{sed} *($\times 10^{-4}$ cm)*	*Stk* *($\times 10^{-3}$)*	*Re*
Mouth	1	2	7	0.022	0.7	0.48	
Pharynx	1	3	3	0.021	0.7	0.14	
Trachea	1	1.7	12	0.027	0.9	0.78	5010
Main bronchi	2	1.3	3.7	0.010	0.3	0.88	3300
Lobar bronchi	5	0.8	2.8	0.007	0.2	1.5	2220
Segmental bronchi	18	0.5	6	0.021	0.7	1.71	942
Intrasegmental bronchi	252	0.3	2.5	0.045	1.5	0.57	225
Bronchioles	504	0.2	2.0	0.032	1.1	0.95	84
Secondary bronchioles	3024	0.1	1.5	0.036	1.2	1.27	28
Terminal bronchioles	12,100	0.07	0.5	0.023	0.7	0.93	10
Respiratory bronchioles	1.7×10^5	0.05	0.2	0.067	2.2	0.18	1
Alveolar ducts	8.5×10^5	0.08	0.1	0.44	14.5	0.01	0
Atria	4.2×10^6	0.06	0.06	0.71	23.4	0.01	0
Alveolar sacs	2.1×10^7	0.03	0.05	0.75	24.8	0.01	0
Alveoli	5.3×10^8	0.015	0.015	4	132		

The amount and site of particle deposition depends on several factors relating to the physical properties of the particles (size, shape, and density) and lung physiology (geometry, respiratory flow rate, tidal volume). The three major deposition mechanisms in the lung (Fig. 1.4) are impaction due to the inertia of particles, sedimentation due to gravitational forces, and diffusion, which is linked to the Brownian motion of surrounding gas molecules (Agnew, 1984; Schulz, 1998).

Impaction

The probability of particle deposition by impaction is governed by the momentum (mass and velocity) of the particle; it becomes significant during shallow breathing for particles >2 μm and is most likely to occur in the extra-thoracic and large conducting

airways where flow velocities are high, and rapid directional changes in airflow occur (Hahn *et al*., 1993; Swift *et al*., 1988).

Sedimentation

The probability of sedimentation is proportional to the settling distance of a particle within the airways, which in turn, is dependent on the residence time and settling velocity (Schulz *et al*., 1998). As with impaction, the particle mass influences the settling velocity such that sedimentation becomes negligible for particles <0.5 μm. Therefore, deposition by sedimentation occurs most frequently in larger particles with relatively long residence times, this primarily occurs in the small conducting airways and alveolar regions of the lung (Schulz *et al*., 1998).

Diffusion

The random displacement of a particle due to diffusion increases with time and decreasing particle diameter. The highest probability of particle deposition due to diffusion occurs for very small particles (<0.5 μm) inhaled into the peripheral regions of the lung with their small airway dimensions.

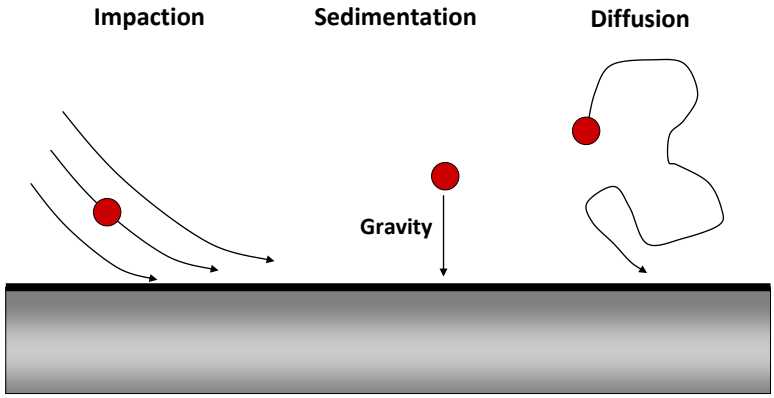

Fig. 1.4. Deposition mechanisms in the lung.

A crucial parameter in inhalation therapy is the mass of active ingredient delivered by the deposited particles to the oro-laryngeal, tracheobronchial or alveolar regions. Hence, the particle mass deposited is crucial to the dose delivered; for example, a 2 μm particle delivers approximately the same dose as 60 × 0.5 μm particles. The mass deposited in the oro-larynegeal regions is highest for forced breathing, with particles larger than 4-6 μm, thus coarse particles with high velocity usually deposit here.

However, quiet breathing of particles 2-4 μm is sufficient to deliver the API to the alveolar region, and deposition in the upper respiratory tract is minimised (Gebhart *et al*., 1981; Ferron *et al*., 1988). Kim *et al.,* (1994) showed that deposition of 5 μm particles at a flow rate of 30 l min^{-1} was greatest in the upper airways, whereas sedimentation was greater in the lower airways. Maximum sedimentation was found to occur in the lower airways for particles between 3 and 5 μm and decreased with particle diameter due to the reduced settling velocity. Clark and Egan (1994) supported these findings, and found that 5 μm particles could not penetrate the respiratory zone (alveoli) effectively at flow rates higher than 40 l min^{-1}. Further work conducted by Martonen and Katz (1993) showed that particle residence time in the lungs was more influential than inspiratory flow rate on particle deposition.

1.4. Formulation Properties

The properties of DPI formulations are vital in controlling performance (Pell and Dunson, 1999). A range of particle and bulk powder properties influence the amount of fine particles that reach the target areas of treatment; this is often defined as the fine particle fraction (FPF) – the amount of fine drug particles reaching the lower airways (Hickey *et al*., 1994).

1.4.1. Forces Experienced by Formulation

Typical DPI formulations consist of adhesive mixtures where drug particles are distributed homogeneously over the total surface area of larger carrier crystals (Boerefjin *et al*., 1998). The work on the adhesive strengths of DPI formulations follows from that by Jones and Pilpel (1965), who were the first to observe the adhesion of particles smaller than 5 μm onto the surface of larger particles in an interactive powder mixture. Research on adhesive mixtures for inhalation requires the optimisation of homogeneity, stability, and drug-particle detachment during inhalation. This requires the balance of the adhesive forces in the mixture and the detachment forces experienced during inhalation; a "Force Distribution Concept" has explained the importance of this (de Boer *et al.,* 2003a; Frijlink and de Boer, 2004). Drug and carrier properties, carrier payload, mixing conditions and inhaler design all need consideration in this necessary balance.

The major forces which are relevant to the adhesion and separation of such particles include: van der Waals forces, which act between solid surfaces over distances

between 0.2 and 1 nm (Atkins, 1998); Coulombic (electrostatic) forces due to the insulating nature of the powder; capillary forces due to liquid bridges; mechanical forces caused by interlocking or irregularly shaped particles and surface asperities; and solid bridges (individual particles joined at point of contact by sintering, chemical reaction or re-crystallisation) - Visser, (1989); Hickey *et al.,* (1994) also affect adhesion.

Bulk-scale physical interactions due to surface roughness, shape, and size are major obstacles to overcome in particle dispersion. Temperature and humidity variations can lead to the formation of solid bridges through crystallisation/recrystallisation events at the particle surface (Crowder, 2003). Moisture can also induce the formation of capillary forces (Israelachvili, 1991). The strength of these forces is determined by the diameter of pores in which the moisture resides, and the tension experienced between surfaces due to hydrogen bonding between the water molecules. Changing the humidity of the environment that surrounds the formulation affects both capillary forces and the surface charge of the particles by different means: reducing humidity increases the electrostatic force but decreases capillary interactions whereas increasing humidity increases capillary forces but reduces the electrostatic force. Therefore, a careful control of humidity is vital in order to balance the capillary and electrostatic forces experienced by the formulation. Electrostatic charging can originate from atmospheric ionisation, chemical composition, contact with charged objects or tribocharging through motion. Since most pharmaceutical powders are good insulators, electrostatic charge plays an important role in their dispersion. One method of reducing the van der Waals forces is by using high-porosity, low-density particles (Edwards *et al.,* 1997). The forces of interaction between pharmaceutical powders are difficult to characterise and control due to the heterogeneous nature of the bulk powder, both in terms of composition and physicochemical properties.

Advances in characterisation and measurement techniques used to determine the adhesive and cohesive forces within DPI formulations increases knowledge of properties and behaviour of such products. Recent advances which have supplemented the traditional techniques include electrical low-pressure impaction for measuring electrostatic effects (Telko *et al*., 2007) and nano-indentation for characterisation of the effect of mechanical properties for individual properties (Taylor *et al*., 2004). In addition, focused-ion beam milling has been used in conjunction with SEM to observe

the interior of spray-dried particles for inhalation by removing outer layers of particles and imaging the cross-section (Heng *et al.*, 2007).

1.4.2. Powder and Aerosol Physics

An important process in the generation of a therapeutic aerosol by a DPI is the *fluidisation* and *entrainment* of the bulk powder (Telko and Hickey, 2005). The generation of an aerosol from a static powder bed defines the dispersion step shown in Fig. 1.2. Separate phases can be defined, including dilation, flow, and aerosol production (Dunbar *et al.*, 1998), however the influence and understanding of these mechanisms have often been overlooked, partly due to their transient nature and the fact that they typically occur simultaneously thus making them difficult to define and quantify (Daniher and Zhu, 2008). Recent work has studied the effects of fine particles on the "fluidisation and entrainment" behaviour of bulk DPI excipient (Shur *et al.*, 2008). However, the definition of fluidisation in their work is arguably more general than the traditional descriptions of fluidisation with respect to fluidised bed technology in chemical engineering applications. Regarding DPI formulations, fluidisation is defined as "the process by which a powder mass is disturbed by a stream of airflow resulting in the powder bed exhibiting 'fluid-like' properties" (Shur *et al.*, 2008). Following fluidisation, the powder removed from the device chamber is said to be entrained into the airflow (Castellanos, 2005) by the patient's inhalation (Telko and Hickey, 2005), where air is passed through the static bed creating a pressure differential causing powder to be pneumatically conveyed through the device. This differs to traditional fluidised bed applications in chemical engineering where gas is passed upwards through a bed of particles and the state of fluidisation is said to occur when the buoyant weight of the bed is supported by the upwards flow of gas (Seville *et al.*, 1997).

Following entrainment into an airstream, de-agglomeration or detachment of drug and carrier particles occurs via the forces generated by the pressure differential, or via particle-particle and particle-wall collisions within the device (Castellanos *et al.*, 1999; Zeng *et al.*, 2001). Detachment forces include: aerodynamic, centrifugal, inertial, shear and frictional forces, all of which attempt to overcome the adhesive forces described in section 1.4.1 (Timsina *et al.*, 1999; de Boer *et al.*, 2003a).

More recently, powder-packing properties have been linked to the aerosolisation ability of DPI formulations. Many previous studies have attempted to link the packing properties of such powders to their *in vitro* performance (Zeng *et al*., 2001; Concessio *et al*., 1999; Crowder and Hickey, 2006); however, Shur *et al*., (2008) take this concept further by attempting to relate the *in vitro* performance to the packing and tensile strength of formulations, but also consider the fluidisation ability of such powders.

Other work relating to the aerosolisation of DPI formulations includes that by Versteeg *et al*., (2005) who again investigate the aerosolisation of powders by a vertical jet of air, concluding that the initial mechanism of powder bed break-up is by shear fluidisation, where particles are entrained layer-by-layer producing a slow entrainment rate. Following this, the jet-flow penetrates the powder bed and aerates the entire bed from the centre – thus producing a fast entrainment rate. Although these qualitative results are conclusive, little quantitative data is produced.

1.4.3. Effect of Particle Size

Particle size is one of the most important design considerations to make regarding DPI formulations (Daniher and Zhu, 2008). Methods for determining the particle size distribution (PSD) of a formulation explore a range of geometric features and physicochemical properties (Snow *et al.,* 1999). Of these properties, aerodynamic diameter is the most important regarding drug delivery to the lung and hence, therapeutic effect. The aerodynamic diameter is defined as the diameter of an equivalent volume sphere of the same density with the same terminal velocity as the actual particle. Pharmaceutical powders are rarely spherical; however, various shape factors can define the deviation from sphericity. The dynamic shape factor is described as the ratio of the resistance force experienced by the non-spherical falling particle to the resistance force of a spherical particle of the same volume (Hinds, 1999). Thus, the aerodynamic diameter can be increased by increasing the particle size, increasing the particle density, or decreasing the dynamic shape factor.

As described in section 1.3.1, it is important to control particle size since it describes the crucial mechanisms of particle deposition in the lung via inertial impaction, sedimentation, and diffusion. To reach the lower airways, particles need to be in the 1-5 μm aerodynamic diameter range (Newman and Clarke, 1983; Zanen *et al.,* 1994), particles greater than this typically deposit in the oral cavity or pharynx; whilst

particles smaller than this are prone to not deposit at all. In addition, smaller particles are not as efficient at delivering dose to the lungs; a 0.5 μm particle will only deliver 0.1% of the mass a 5 μm particle is able to carry (Bates *et al.,* 1966).

There have been many techniques employed to produce particles in the preferred aerodynamic size range, such as fluid energy milling by Lai *et al*., (1981). Shekunov *et al.* (2003), and Schiavone *et al.* (2004), employed supercritical fluid crystallisation (SFC) to create drug particles not only of the desired size, but also with the desired surface characteristics, as opposed to the conventional jet milling process, which does not allow the control of such features. Their work claimed that drug particles manufactured by the SFC method yield increased FPF compared to standard micronised drug particles. Other particle techniques have been considered to produce drug particles for use in pulmonary treatments; these include spray-drying, supercritical drying and spray freeze-drying. These procedures can also be used to increase the ratio between geometric and aerodynamic particle size in order to reduce phagocytic clearance (Edwards *et al.,* 1997) or to increase the dispersibility compared to micronized particles (Vanbever *et al.,* 1999; Duddu *et al.,* 2002). In addition, nanospheres of hydroxyl-propyl-methylcellulose phathalate (Kawashima *et al.,* 1998b) have been considered, along with agglomerated drug crystals (Ikegami *et al.,* 2003) and salts of the same drug compound (Jashnani and Byron, 1996) to modify the physicochemical properties of the drug. The addition of salt compounds to the mixture affects the affinity of the drug to water, hence affecting its aerosolisation ability within the inhaler.

1.4.4. Crystallinity and Polymorphism

Most APIs and excipients are crystalline materials (Britain, 1995; 1999); however, non-crystalline materials are also common in DPI formulations, often as a result of the manufacturing process (Moulton *et al.,* 2001). In addition, the polymorphs of crystalline material can exhibit different physicochemical properties (density, solubility, melting point and hygroscopicity - Hancock *et al*., 1995); whilst the mechanical properties and vapour sorption ability of amorphous material may be significantly different from the crystalline material (Hancock and Zografi, 1997), and the chemical reactivity of amorphous substances may be significantly greater (Pikal *et al.,* 1977). In addition, crystallisation can also affect particle shape, since crystal growth

rates can vary independently of the crystal lattice and thus the morphology of the particles can be affected (Larhrib *et al*., 2003a). This in turn can affect the aerodynamic behaviour and consequentially, the lung deposition, due to changes caused by impurities during crystallisation, and processing variables such as temperature, pH, and viscosity (Wood, 2001; Rodriguez-Hornedo and Sinclair, 2002).

1.4.5. Moisture Content and Hygroscopicity

Hygroscopicity is the inclination of a material to uptake moisture from its surroundings, and is directly affected by both the crystallinity and morphology of the particles. Hygroscopic compounds are much more prone to chemical and physical instability, notably dissolution and recrystallisation. This can cause irreversible aggregation through solid bridge formation (Dunbar *et al.,* 1998) which adversely affects aerosol generation and subsequently lung deposition (Braun *et al.,* 1996; Chew and Chan, 2002). Hygroscopicity can also affect the adhesive and cohesive properties of formulations, along with significantly affecting PSDs (Hickey and Martonen, 1993; Maggi *et al.,* 1999). As aerosols enter the lungs, they approach a very high humidity environment (99.5% RH at 37°C); here susceptible particles may be subjected to hygroscopic growth that affects lung deposition (Martonen and Katz, 1993). Therefore, equilibrium moisture content of both drugs and excipients must be determined over a range of relative humidities in order to obtain suitable process and storage conditions. An example of such a study is shown by Zhu *et al*., (2008), who recognise the importance of relative humidity on the performance of salbutamol sulphate containing formulations in an airstream.

1.4.6. Effect of Shape and Surface Impurities

The surfaces of DPI formulation particles play important roles in the interactions, stability, and dispersion of such powders. Due to their low mass: surface area ratio, API particles have a greater potential for electrostatic charging and moisture uptake, in addition, their small size makes them more susceptible to the effects of van der Waals forces (Fults *et al.,* 1997; Young *et al.,* 2002).

Both drug and carrier particles can be modified to obtain desired surface characteristics in order to control lung deposition; ideally, the forces are balanced such that adhesion is strong enough to provide a stable formulation, but weak enough to allow separation during an inhalation event. The surface morphology of carrier and

drug particles has been shown to influence the FPF in several studies; Zeng *et al.,* (2000a) suggests that smooth surface lactose particles enhance FPF, whilst Zeng *et al.,* (2001) and Young *et al.,* (2002), contradict this claim, suggesting that rough carrier particles increased the FPF.

The majority of attempts to increase the amount of drug released from carrier particles during inhalation have involved the altering of the surface properties of the carrier particles (Podczeck, 1998a; Karhu *et al.,* 2000; Harjunen *et al.,* 2002) since surface features such as discontinuities (pores, clefts and cavities) - otherwise known as rugosity - and impurities are one of the dominant factors affecting interaction between drug and carrier particles. These carrier sites with high rugosity and number of impurities produce multiple contact points and allow an increase in the contact area. These are known as 'active sites' which have enhanced binding energies between carrier and drug; therefore, it is recommended to use smooth, clean particles which increase the ability for carrier and drug to detach during inhalation (Kassem and Ganderton, 1990; Kawashima *et al.,* 1998a; Podczeck, 1998a; Zeng *et al.,* 2000a; Zeng *et al.,* 2000b). However, different studies have found that there may be optimal carrier rugosities (Ganderton and Kassem, 1992, Vanderbist and Maes, 1998; Zeng *et al.,* 2000a; Young *et al.,* 2002), such that smooth carrier surfaces may exhibit lower (Zeng *et al.,* 2001a) and higher drug depositions (Kawashima *et al.,* 1998a).

Surface morphology measurements are often based on the amount of gas adsorbed to the powder surface at a given pressure. Inverse gas chromatography (IGC) is able to determine surface area (Grimsey *et al.,* 2002) and surface energy changes (Cline and Dalby, 2002), along with changes in surface characteristics due to processing (Ohta and Buckton, 2004). Scanning Electron Microscopy (SEM) and Atomic Force Microscopy (AFM) (Danesh *et al.,* 2000; Trojak *et al.,* 2001) are also used to describe the surface morphology of formulation particles.

In addition, the shape of the carrier particles is known to influence the drug particle detachment in inhalers due to turbulent shear forces (Zeng *et al.,* 2000a; Larhrib *et al.,* 2003b). However, these studies involved carrier particles specially prepared using crystallisation techniques that produced much smoother surfaces than the carrier particles in everyday use.

1.4.7. Excipients

Since excipients can typically make up in excess of 99% of the product by weight, they are crucial factors in the performance of a DPI formulation. Excipients improve the non-pharmacologic properties of a drug primarily through enhancement of the physicochemical stability of the API, its mechanical properties, or its pharmaceutical properties such as dissolution and permeation (Smyth and Hickey, 2005). In DPI formulations, their primary role is to act as a carrier particle. Typically, the drug dose required is only a few μg, therefore excipients provide bulk to improve the handling, dispensing and metering of the drug (Ashurst *et al.,* 2000). Unlike the GI tract, lungs have a low buffering capability, hence only a narrow range of mid-pH substances can be administered in order to prevent irritation. Therefore, potential excipients are limited to compounds that can be easily metabolised or cleared by aspiration.

Lactose is by far the most commonly used excipient in DPI formulations. It had long been used in oral dosage forms before being chosen for use in DPI formulations due to its established safety and stability profile, its rigid manufacturing process with strict controls on purity and physical properties, availability, and low cost. Lactose has the smooth surfaces and adequate flow properties desired in DPI carrier particles (Smyth and Hickey, 2005). It is less hygroscopic than other sugars and is relatively versatile, with various size distributions (Saint-Lorant *et al*., 2007), grades, and morphologies readily available. Its main drawbacks arrive from the fact it is a reducing sugar, thus making it incompatible with molecules with amine functional groups (Handbook of Pharmaceutical Excipients, American Pharmaceutical Association); and its problems associated with the lactose-intolerant population. Lactose is commonly found in four crystalline forms with α-lactose monohydrate used in DPI formulations, whilst the stable anhydrous form is used in MDIs and β-lactose used in tablets due to its preferential compaction properties (Hein *et al*., 2008).

Other sugars such as mannitol (Tee *et al.,* 2000), glucose (Braun *et al*., 1996; Steckel and Müller, 1997a), trehalose (Bosquillon *et al*., 2001a), sorbitol (Tee *et al*., 2000), sucrose (Naini *et al*., 1998) and phospholipids such as phosphatidyl choline and cholesterol have been shown to be viable alternatives to lactose, (Kawashima *et al.,* 1998b), however this study focuses on the use of α-lactose monohydrate.

The physicochemical properties, especially the size and morphology of the excipient particle will have significant effects on the performance of the DPI. Adhesive forces must be carefully considered, as inadequate separation of drug from carrier will cause major deposition problems. Excipients for DPIs are commonly in the mean geometric size range of 63-90 μm (Zeng *et al*., 1998), in order to facilitate accurate dosing from the device and improve flow properties into the lung (Crowder *et al*., 2001; Giry *et al*., 2006).

The size distribution of carrier particles affects drug-carrier detachment (Chew and Chan, 2002; Podczeck, 1999; Karhu *et al.,* 2000). Many studies have shown that the respirable (*in vitro*) fractions dramatically increase when *finer* carrier particles are used (Ganderton and Kassem, 1992; French *et al.,* 1996; Steckel and Müller, 1997b) due to the number and size of surface discontinuities and impurities increasing with mean diameter of crystals (de Boer *et al.,* 2002c; de Boer *et al.,* 2003b). On the other hand, the attachment forces between the carrier and drug produced during mixing increase (Podczeck, 1996b); coarser carrier particles produce much more friction and collision forces than fine particles.

An advantage of coarse carrier particles is their superior flow properties which increases the reproducibility of doses into capsules, blisters or metering devices, due to the ease at which they can be dispensed; however, there is a limit to the size of particles that can be entrained or pass through certain gaps in the device or capsule (Steckel *et al.,* 2004).

More recent studies have shown the importance of experimental design on the control of particle size during the manufacturing process (Guenette *et al*., 2009) in the development of DPI formulations.

1.4.8. Effect of Carrier Payload

The concentration of drug in the powder mixture is a vital parameter regarding drug-carrier interactions. As with carrier surface properties and size distribution, the role of the carrier payload may depend upon many other parameters. The drug concentration on the carrier surface can affect the bonding capacity of active sites on the carrier – and can be compounded if the active sites correspond to surface discontinuities as the drug particles may be sheltered from press-on forces experienced during mixing (Srichana *et al*., 1998). Therefore, the drug concentration needs to consider the sheltering

capacity of the surface discontinuities. A range of payloads has been studied in previous DPI literature; a list of examples is given in Table 1.2.

Table 1.2. Examples of carrier payloads used in other DPI studies.

Author	*Payload (% drug by weight)*
Schlimmer, 2002 Dubois *et al.*, 2003	0.05
Podczeck, 1998a, 1999	0.2
Harjunen *et al.*, 2003	0.6
Young *et al.*, 2005	0.8
Steckel and Müller, 1997a	1.0
Kassem and Ganderton, 1990 Timsina *et al.*, 1994 Srichana *et al.*, 1998 Zeng *et al.*, 1998 Larhrib *et al.*, 1999 Zeng *et al.*, 2000a Zeng *et al.*, 2001 Flament *et al.*, 2004 Flament *et al.*, 2006 Thi *et al.*, 2008	1.46
Heng *et al.*, 2000	2.0
Iida *et al.*, 2001 Iida *et al.*, 2003	2.5
Harjunen *et al.*, 2003	3.2
Steckel and Müller 1997b	5.0
Harjunen *et al.*, 2003	6.6
Steckel and Müller 1997b	9.0
Ikegami *et al.*, 2000 Ikegami *et al.*, 2003	10.0
Kawashima *et al.*, 1998a	11.1

1.4.9. Introduction of Ternary Components to Adhesive Mixtures

Typically, DPI formulations comprise micronised API and coarse lactose carrier (typically 63-70 μm size range). However, research has been conducted into the effect of adding ternary components to the mixture in order to enhance the performance of the formulation.

1.4.9.1. Lactose fines

Lactose fines generally less than 10 μm have been added to adhesive mixtures to influence the forces between API and excipient. Lactose fines are likely to be found in mixtures as a result of wear due to mixing and transport, from the selection of lactose blends with wide size distributions (Karhu *et al.,* 2000), or from the deliberate addition of lactose fines to coarse lactose fractions (Podczeck, 1998b; Zeng *et al.,* 1998). Zeng *et*

al., (2001) suggests that the addition of lactose fines to adhesive mixtures has a more dominant effect on drug dispersion than effects of carrier size and surface rugosity. It is also known that the amount of lactose fines added to the formulation influences the amount of drug that reaches the lower airways. A range of hypotheses has been proposed to describe this effect. These include: the possibility that lactose fines compete with API particles for "high energy" active sites on the carrier (Hersey, 1975; Staniforth, 1996); lactose fines form readily-dispersible "multiplets" with drug particles (Lucas *et al*., 1998); lactose fines create mono- or multi- layers between the drug and carrier particles, thus minimising the van der Waals forces between them (Zeng *et al*., 1998); or the fines act as a lubricant, preventing the build-up of electrostatic forces that affect adhesion between drug and carrier (Zeng *et al*., 1998).

1.4.9.2. Force control agents

Force control agents (FCAs) such as isoleucine and magnesium stearate have been added to the mixtures (Ganderton and Kassem, 1992; Colombo *et al.,* 2000; Young *et al.,* 2002; Begat *et al*., 2009) in order to decrease the interaction forces between the drug and carrier particle. The effect of van der Waals forces is reduced by forming a film around the excipient and/or drug particles; being hydrophilic, the capillary forces are also reduced. They also preferentially fill active sites on the carrier surface, thus reducing the ability of drug particles to occupy these strong attachment areas (Faqih *et al*., 2007). Louey *et al.,* (2003) also suggest that these ternary compounds may agglomerate with drug particles, which results in an increase in the detachment forces experienced during inhalation.

1.4.10. Formulation Processing (Blending and Storage)

Once drug and excipient have been manufactured into their desired physical form, they need to be combined to produce the working formulation. Understanding and control of this process has often been overlooked, despite the importance of obtaining optimal performance from a formulation (Sudah *et al.,* 2002a). When mixing powders with different properties, particle sizes and ratios, inadequate mixing can cause poor dose uniformity, something that may not be cured with increasing mixing time. Choice of mixer, rotation speed, capacity, and fill level all require optimisation, as they are likely to affect the blend homogeneity (Alexander *et al.,* 2004). In addition, blending conditions can also influence the interparticulate forces, which in turn determine the

FPF (Iida *et al.,* 2001). Different mixtures of drug and excipient along with different component ratios will affect the mixing conditions required (Staniforth *et al.,* 1981).

Increasing the mixing time of adhesive mixtures may increase the stability and homogeneity of the formulation. This is due to the prolonged period of time for which the adhesive forces are allowed to form which, in turn, increases the drug-carrier interaction. In addition, the extended mixing time allows for enhance distribution of drug over the carrier surface, thus allowing for an increase in occupation of active bonding sites (de Boer *et al.,* 2002c). However, as the drug-carrier interaction increases, it is likely that the drug detachment during inhalation will decrease – an undesirable effect from extending the mixing time. The strength of the adhesive and detachment forces needs to be controlled by modifying the drug concentration in the mixture in relation to the surface rugosity – hence the binding capacity of active sites. There have been relatively few studies determining the effect of mixing time on the drug-carrier interaction in adhesive mixtures for the use in DPIs (de Boer *et al*., 2002c).

This study focuses on *high shear* blending (HSB), a technique used primarily to overcome the cohesive forces found in micronised API, thus aiding dispersion of drug throughout the formulation in order to create a chemically homogenous mixture – a more detailed description of the uses of HSB is given by Wellm, (1997) and Knight *et al*., (2001). In this thesis, details of the HSB process and equipment can be found in section 4.2.3. This study differs from other work studying blending effects on DPI formulations in that low-shear tumbling methods are employed by Podczeck (1999), Zeng *et al*., (2000) and Dickhoff (2006). More recent work by Shur *et al*., (2008) focuses on two low shear blenders – the Turbula and Whirlimixer alongside a small-scale imitation high shear blender which was initially intended for use as a coffee grinder (Braun KSM2, Kronberg, Germany) which operated via a mechanism comparable to milling devices.

Following blending, the formulation is filled into capsules, blisters, or reservoirs ready for use with the inhaler device. Then, in order for the formulation to maintain its physicochemical integrity and dispersive properties, the product must be suitably stored. Storage conditions, primarily temperature and humidity profoundly affect DPI formulation stability (Podczeck 1996a; Podczeck *et al.,* 1997; Young *et al.,* 2004). The drug-carrier interaction in adhesive mixtures is susceptible to change over time and is

directly linked to the storage conditions, payload and carrier size fraction (Broadhead *et al.,* 1995; Harjunen *et al.,* 2003). Braun *et al.,* (1996) showed that the FPF of two strengths of disodium cromoglycate was increased when the formulation was stored for 27 days at 33% relative humidity rather than 55% relative humidity. In addition, it has been discovered that the relative humidity of the air during inhalation may influence the fraction of drug detached from the carrier particles (Vidgren *et al.,* 1987; Hindle *et al.,* 1995; Jashnani *et al.,* 1996) since the energy required to separate particles is directly influenced by humidity (Price *et al.,* 2002).

1.5. Measuring Drug-Carrier Adhesion

A good estimation of the force of drug-carrier adhesion can be made from the particle detachment force (Zimon, 1982), assuming that the two forces are equal in magnitude but act in opposite directions. There are two types of methods for interparticulate force analysis - bulk detachment, or single particle detachment. Bulk detachment methods include centrifugation (Podczeck and Newton, 1995; Podczeck, 1997), mechanical/air jet sieving (Staniforth *et al.,* 1981; Iida *et al.,* 2003, Flament *et al.,* 2004), or impact separation (Concessio *et al.,* 1999), whilst measurement of single particle adhesion force is usually performed via AFM. The varying performance of formulations containing different carriers can be attributed to the differences in the relative drug-carrier adhesive forces; this is the basis behind choice of drug. These have been quantified by colloidal AFM and utilised in an approach that measures the ratios of drug adhesion to cohesion – known as the cohesive-adhesive balance (CAB) (Begat *et al*., 2004) between both hydrophilic and hydrophobic drugs and excipient in DPI formulations.

This allows differences to be found in the relative affinities for the mimic drugs to each other compared to their affinity to lactose carriers – as described in the CAB work by Begat *et al*., (2004) and Jones *et al*., (2008). In addition, the use of shear test methods can allow differences to be found in flow properties that can be related to cohesivity of powder; this has been applied to salmeterol (hydrophilic drug) and salbutamol (hydrophobic drug) by Zhou *et al*., (2010).

A CAB <1 describes an adhesive formulation that forms a stable, ordered mixture on blending, whereas a CAB >1 describes a cohesive formulation where a less uniform mixture is produced, which is likely to contain agglomerates of active ingredient (de

Boer *et al*., 2002b). The work by Jones *et al*. (2008) used this approach to quantify the CAB for four carriers (lactose, glucose, mannitol, sorbitol) with four drugs possessing various physicochemical properties (fluticasone propionate, salmeterol xinafoate, budesonide and formoterol fumarate dihydrate) in an attempt to investigate the dispersion mechanisms of formulations containing fine excipient particles and relating them to the CAB properties of the formulation constituents. Results showed no relationship between the CAB ratio and homogeneity achieved during blending, and found that a formulation with greater CAB ratio resulted in enhanced *in vitro* fine particle delivery performance.

Images of drugs can be achieved using tapping mode AFM and numerous studies have been performed on the adhesive strength between drug and carrier (Louey *et al.,* 2001, Louey and Stewart, 2002; Eve *et al.,* 2002; Hooton *et al.,* 2003; Begat *et al.,* 2004). In addition, AFM can also be used to study the crystallisation of lactose (Price and Young, 2004) and the effect of mechanical processing on the powder surface (Begat *et al.,* 2003; Young *et al*., 2007b). Despite the advantages of AFM, it still has drawbacks, primarily in that statistically significant numbers of particle pairs cannot be easily analysed, along with the fact that results generated can vary strongly – up to 100x difference in some cases – thus rendering the relevance of such measurements questionable (Price *et al*., 2002; Tsukada *et al*., 2004; Schiewe and Zierenberg, 2004). Other findings concluded that the relative humidity in which the experiment was conducted affected the adhesive force between the drug and carrier particles (Podczeck *et al.,* 1996: Price *et al.,* 2002; Tsukada *et al.,* 2004); however, the extent to which the force increased was dependent upon the hygroscopicity of the drug.

1.5.1. In-vitro Methods to Assess Adhesion on a Bulk Scale

1.5.1.1. Air Jet Sieve

An air jet sieve (AJS) is a device in which a portion of powder in a sieve is fluidised by air passing upwards through it from a rotating slit. At the same time, a negative pressure is applied to the bottom of the sieve that removes the fine particles to a collecting device (vacuum with fine particle filter). A more detailed description of the working principles of an AJS is given in section 6.1.

AJS analyses have often been used to determine the rate of drug detachment from carrier crystals in an air stream. Dickhoff *et al.,* (2006) assess the rate of terbutaline

sulphate detachment from crystalline carriers exposed to differing surface treatments; Flament *et al.,* (2006) assess the adhesion between the APIs terbutaline sulphate and formoterol fumarate and four types of carrier, whilst Iida *et al.,* (2003) link surface properties of carriers to their adhesion with salbutamol sulphate. Each of the studies use comparable procedures for assessing detachment of API such that formulations are exposed to the air stream for varying lengths of time against a fixed pressure drop. The amount of drug not removed (still attached to the coarse carriers) is then assayed to determine the extent of fine drug particle removal through the sieve.

1.5.1.2. Cascade Impactors

Primarily a tool for determining the aerodynamic PSD, cascade impactors can also be used to determine the degree to which APIs separate from excipient, and are often used to asses the efficacy of DPI formulations by evaluating the *in vitro* FPF. The aerodynamic PSD of an aerosol cloud defines where the particles in that cloud are likely to deposit following inhalation (Hinds, 1999; de Boer *et al.,* 2002a). As stated in section 1.4.3, it is generally accepted that to be therapeutically effective, particles need an aerodynamic particle diameter between 1-5 μm to settle in the lung (Newman and Clarke, 1983), with the particle mass below 5 μm defined as the FPF (Marple *et al*., 2004).

The European Pharmacopoeia (Ph.Eur) Method, Chapter 2.9.18 specifies four impactors (one twin, and three multi-stage) for the aerodynamic assessment of inhaled particles from both MDIs and DPIs: Ph.Eur apparatus A – Glass Twin Impinger; apparatus C – Multi-stage liquid impinger; apparatus D – Andersen cascade impactor (ACI); apparatus E – Next generation impactor (NGI). However, only two impactors, the ACI and NGI, are recommended for use with MDIs and DPIs by both the European and United States Pharmacopoeias.

All inertial impactors operate using the same principle: the aerosol is passed through a nozzle and the output jet is directed against a flat (impaction) plate that directs the particles to form an abrupt 90° bend in the gas streamlines. The particles with inertia greater than a given value are unable to follow the streamlines and collide on the flat plate. Smaller particles follow the streamlines and avoid collision with the impact plate; they remain airborne and flow out of the impactor.

Therefore, each stage of the impactor separates aerosol particles into two size ranges: those that are greater than the aerodynamic size are removed from the airstream, and those with lower aerodynamic size, which pass through the impactor. Their main advantage over other methods is that they directly measure aerodynamic diameter of particles, rather than equivalent-volume diameter (from cross-sectional area data) (Marple *et al*., 2001). The use of several impactors in series is used such that the impactors are arranged in order of decreasing cut-off size, with the largest cut-off first. This is known a cascade impactor, and the cut-off size reduction at each stage is achieved by decreasing the nozzle size (Fig. 1.5). This increases the flow velocity and reduces the average size of particles passing through. Since the same volume of gas flows through each stage, the flow rate at just one nozzle needs to be controlled. Each stage is fitted with a removable impaction plate that needs to be removed with each experiment for gravimetric or chemical determination of the particles that are accumulated. The final action of the impactor is usually a filter that captures all particles less than the cut-off for the final stage (Mitchell and Nagel, 2003).

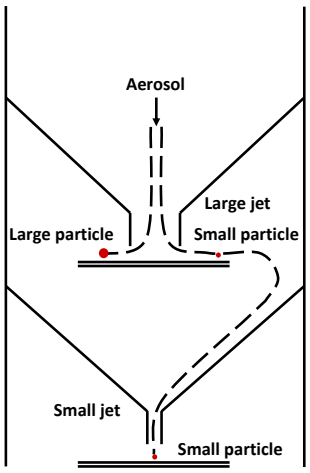

Fig. 1.5. Schematic of a typical cascade impactor

1.5.1.3. Centrifugal Techniques

Centrifugal techniques are based on the notion that force of adhesion is equal in magnitude, but opposite in direction to the centrifugal force required to dislodge fine particles from larger surfaces. This technique has been used extensively for both the separation of particles from flat surfaces (Podczeck *et al*., 1995) and drug particles from excipients (Podczeck, 1996a; Iida *et al*., 2003). A concise explanation of centrifugal adhesion measurements is given by Böhme *et al*., (1964).

1.6. Fluidised Beds

In this study, it was hypothesised that elutriation from fluidised beds could be used as a method to assess changes in physicochemical properties of DPI formulations that have been exposed to varying HSB regimes (chapters 5 and 7).

A fluidised bed forms by passing a fluid upwards through a bed of particles, as the velocity of the fluid is increased, the pressure drop across the bed increases until it equals the weight of the bed per unit area. At this point, the bed is said to be fluidised

(the corresponding gas velocity is known as the minimum fluidisation velocity, U_{mf}). At increasing fluid velocities, particles begin to *entrain* from the bed, and at sufficient velocity (greater than the terminal velocity of the particle), particles will *elutriate* out of the system.

Fluidised beds are commonly used in industry, primarily due to their ability to promote high levels of contact between solids and fluids (gases or liquids), and provide solids with a set of basic properties, including: extremely high surface area between solid and fluid per unit bed volume, high relative velocities between the dispersed solid and fluid phases, and high levels of intermixing and frequent particle-particle and particle-wall collisions.

Although more common in traditional chemical engineering industries, fluidised beds have been used in the pharmaceutical industry, notably for drying of pharmaceutical granules (including lactose) – Chaplin *et al*., (2005); and for the coating of pharmaceutical products – Fukumori *et al*., (1987).

Most fluidised bed applications in industry do not require separation of particles according to size – in fact, many applications consider the loss of fines (elutriation) to be a problem (Colakyan and Levenspiel, 1984), and as a result, utilise circulating beds that collect the fine particles and return them to the bed. However, due to elutriation, fluidised beds have the ability to act as air classifiers and separate particles according to their aerodynamic size by adjusting the flow rate of the incident fluid (Wu and Baeyens, 1998).

At gas velocities greater than U_{mf}, some of the fluidising gas passes through the bed in the form of bubbles, resembling a viscous fluid. Fig. 1.6 shows a typical pressure drop vs. superficial gas velocity (SGV) curve for readily fluidised material. The experimental U_{mf} can be approximately determined by the method described by Richardson (Richardson, 1971; Turki and Fatah, 2008), where the horizontal line representing fluidised bed operation, and the curve that exhibits packed bed operation intersect. The horizontal line and the curve are estimated with a regression analysis to approximately fit the SGV value. It is at the turning point of pressure drop that the maximum aerodynamic drag force is experienced by the powder bed (Valverde *et al.,* 1998).

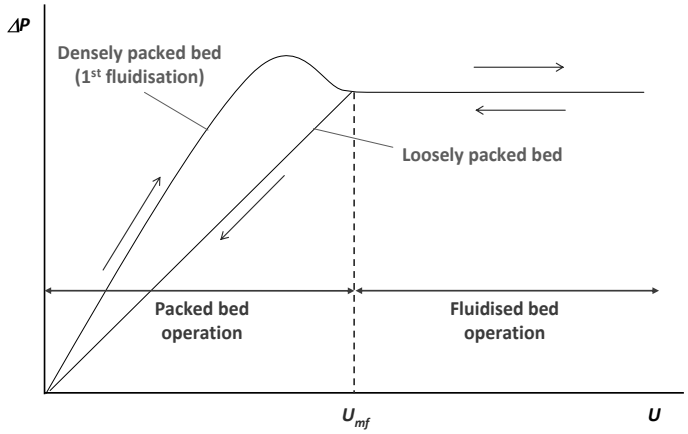

Fig. 1.6. Typical pressure drop (*ΔP*) vs. velocity (*U*) plot for fluidised beds. Initially if the bed is densely packed the pressure drop overshoots the fluidisation pressure until the particles separate and fluidise (Ganguly, 1993).

Material is held in a fluidised state by the action of gas flow through the distributor at the base of the column. In order to have sufficient carryover of material from the bed, the fluidising velocity needs to be several times greater than the U_{mf} (Gugnoni and Zenz, 1980). At high velocities, most of the fluidising gas forms bubbles which rise through the suspended solids phase and burst at the bed surface. The bursting action of the bubbles ejects large amounts of particulate solids of varying size into the freeboard above the bed surface (Ganguly, 1982).

Following fluidisation, particles are *entrained* (removed) from the system into the airstream (Castellanos, 2005), and subsequently *elutriated* from the device. Fluidisation is governed mainly by the bulk properties of the powder, primarily its packing, which in turn, is governed by the physicochemical properties of the particles and their interactions with each other and the bed apparatus (Valverde *et al.,* 1998).

This freeboard height is commonly referred to as the transport disengagement height (TDH) (Geldart, 1986). However, only the finest particles can be fully elutriated by the freeboard gas flow, the coarser particles fall back into the bed since their terminal velocity is greater than the upwards force produced by the gas (Geldart, 1986). This results in a decrease in solids density in the freeboard with height. If the freeboard height is sufficiently large, only fine particles that have a terminal velocity less than the freeboard gas velocity will be removed from the bed.

1.6.1. Geldart Classification of Powder

A key factor in considering the fluidisation ability of powders is the cohesivity of the material. Several attempts have been made to devise both theoretical and empirical classifications of powder behaviour; the most comprehensive attempt was made by Geldart, (1973) to describe the fluidising behaviour of powders according to their mean particle size and density difference between solid and fluidising gas (Fig. 1.7).

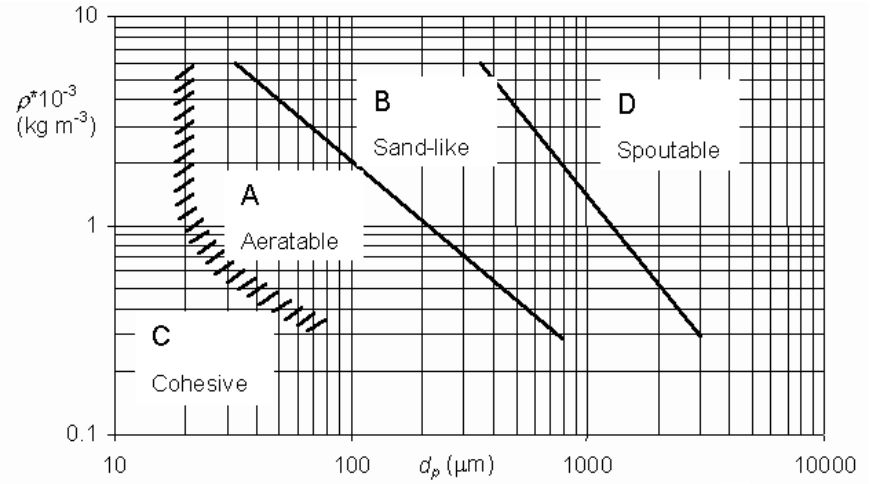

Fig. 1.7. Geldart Classification of Powder for Fluidisation Chart (Geldart, 1973). ρ^* is the density difference between fluidising gas and solid, whilst d_p is the average particle diameter.

Inhalation-grade lactose has previously been shown to be cohesive and notoriously difficult to fluidise (Zeng *et al*., 2001). As a natural product, it has inherent variability in its size, shape, and morphology; although its average particle size suggests it is a Geldart group A powder, its wide PSD includes a significant proportion of group C powder. Table 1.3 shows the characteristic features and examples of each of Geldart's powder groups.

Group C powders form stable channels from the distributor to the surface, and may lift as a cohesive plug, particularly if the apparatus is small, and there is a high surface-to-volume ratio. The pressure drop across the bed usually remains below the bed weight per unit area, and mixing and heat transfer are poor. Fluidisation can be improved by increasing the gas velocity to break up the cohesive structure, by mechanical stirring, or vibration. Electrostatic forces can be reduced by making the apparatus conducting, and by moderate humidification of the gas stream. Once group C powders become aerated, they generally take a long time to de-aerate.

When fluidising group A particles, bed expansion occurs above the U_{mf} but before bubbling occurs. Experimental evidence (Seville, 1987) suggests that group A particles are intermediate in cohesiveness between group C and B particles, and have the interparticle forces being the same order of magnitude as the particle weight.

Table 1.3. Characteristics of fluidisation behaviour (Geldart, 1973); adapted from Seville *et al.,* 1997.

	Group			
	C	***A***	***B***	***D***
Typical characteristics	Cohesive, difficult to fluidise	Bubble-free range of fluidisation	Starts bubbling at U_{mf}	Coarse solids
Examples	Cement, flour	Cracking catalysts	Sand, salt	Crushed limestone, coffee beans
Property				
1. Bed expansion	Low when bed channels; high when fluidisation occurs	High	Moderate	Low
2. Deaeration rate	Can be very slow	Slow	Fast	Fast
3. Bubble properties	Channels readily	Spitting and coalescence; limited bubble size; large wake fraction	Stable large size	Size limited by fluidising vessel; small wake fraction
4. Solids mixing	Very low	High	Moderate	Low
5. Gas back-mixing	Very low	High	Moderate	Low

Fluidisation engineers have attempted to reduce interparticle forces by various means, namely: mechanical vibration (Dutta and Dullea, 1991; Jaraiz *et al*., 1992; Mori *et al*., 1990), acoustic waves (Chirone and Massimilla, 1994; Chirone, *et al*., 1993; Montz *et al*., 1988; Morse, 1955; Nowak, *et al*., 1993; Russo, *et al*., 1995), mechanical stirring (Godard and Richardson, 1969; Nezzal *et al*., 1998; Reed and Fenske, 1955), and magnetic or electrical field disturbance (Hristov, 2000; Liu *et al*., 1991).

1.6.2. Air Classification Using Fluidised Beds

Particle size classification enables products to be removed from the fluidised bed (Gugnoni and Zenz, 1980). Classification can be achieved by various process equipment depending on the physical properties of the material, the required cut size, and the process economics (Perry and Green, 1997; Heath and Aconsky, 1963).

Air classifiers exploit the principles of drag, gravity, and particle inertia, which are all determined by particle size – and described by Stokes' equation (section 5.4). Small,

lighter particles are carried upwards in a gas stream with sufficient velocity, enough to overcome the terminal velocity of the particle (Seville *et al*., 1997; Perry and Green, 1997) whilst the bulk material remains in the bed in a loose, free-flowing state (Kunii and Levenspiel, 1991).

A recent study (Deng *et al*., 2010) has used the principles of fluidised bed elutriation (FBE) to mimic the air-induced segregation effects observed in direct compression pharmaceutical formulations as they are discharged from container to tablet press through a vertical chute. The segregation of API and excipient during the discharge event was studied and used a vertical column separated into seven vertical sections, which were sealed against airflow as the powder was loaded into the hopper above the column. A low SGV was applied to the system to initiate a bubbling regime before the powder was allowed to settle each stage was then assayed to determine API/excipient composition.

Elutriation from fluidised beds in the traditional sense has been extensively studied (Wen and Chen, 1982; Pemberton and Davidson, 1986; Chang *et al*., 2005) and in particular the effect of fine particles on the elutriation performance of systems with multi-modal size distributions (akin to the inhalation-grade lactose used in this thesis). Both Choi *et al*., (2001) and Li *et al*., (2004) explore the effects of fine cohesive powders on the elutriation of particles in fluidised beds, whilst Smolders and Baeyens, (1997) define the critical particle size at which interparticle adhesion forces become significant in fluidised beds. Baeyens *et al*., (1991) and Saleh *et al*., (2008) study the effect of adding fine, cohesive Group C powder (see section 1.6.1) to a readily fluidised Group A powder. Both Santana *et al*., (1999) and Mahmoud *et al*., (2004) employ this property and use fluidisation to deliberately separate fine particles (group C) from coarse (group A) bulk powder bed. Santana *et al*., show that fines in such systems exist as either free particles, small agglomerates with each other, or agglomerates with larger particles. Mahmoud *et al*., (2004) again showed that fines exist as different entities in such systems and also found that elutriation from these fluidised beds was strongly affected by interparticle adhesion forces. However, none of the above studies attempts to relate the HSB and storage conditions of DPI formulations to fluidisation and elutriation behaviour – the primary focus of this thesis.

PSD measurements of unprocessed lactose used in this study reveal a clear bimodal distribution (Fig. 1.8). Group C particles are extremely cohesive (section 1.6.1) and lift as a plug or channel badly. Thus, conventional fluidisation is difficult to achieve.

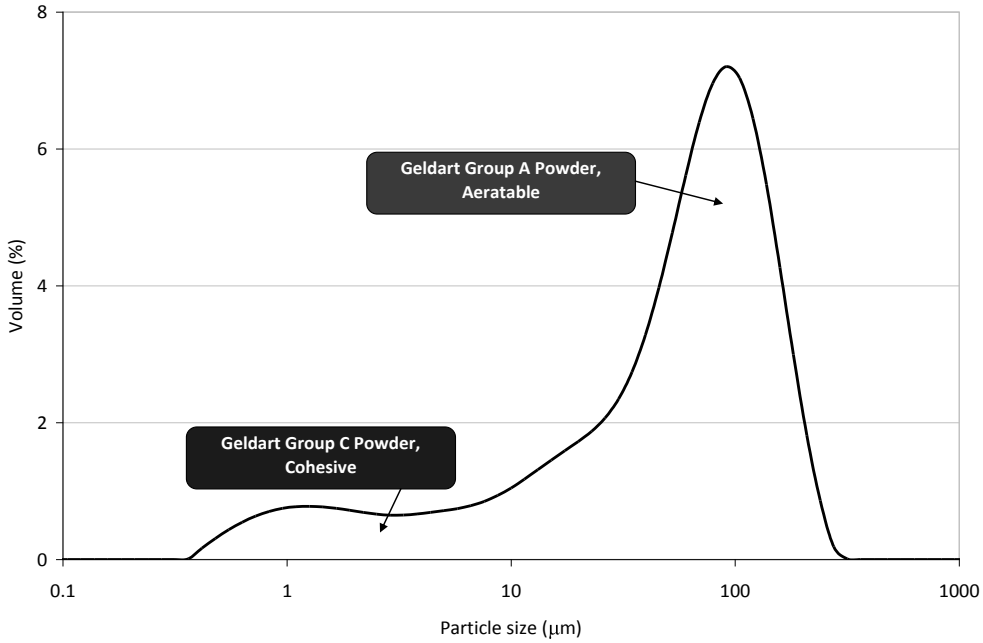

Fig. 1.8. PSD of unprocessed lactose (dry dispersion), clearly showing a bimodal population of fine, cohesive Group C powder and free flowing, aeratable Group A powder.

1.7. Motivation and Aims of Project

In 2002, the Food and Drug Administration (FDA) introduced a new initiative "Pharmaceutical cGMPs for the 21st Century" which proposed a risk-based approach to pharmaceutical manufacturing. This led to the creation of PATs (Process Analytical Technologies) – a framework for understanding and improving the processes involved in pharmaceutical development, manufacturing, and quality control. PAT operates on the premise that quality cannot be tested into products; instead, it should be built-in or should arise from design – QbD (Quality by Design). Therefore final product quality is achieved by understanding and controlling the processes involved in the manufacturing procedure.

One of the key areas for development in DPI formulation production is the understanding of the effect of blending on lactose-drug interactions. Previous work (Bridson *et al*., 2007) focused on the effect of blend parameters on formulations containing solely α-lactose monohydrate. In that study, a linear relationship between specific energy input (SEI) and number of "free" lactose fines was found; as the performance of DPI formulations is known to be affected by "free" lactose fines (see

section 1.4.9.1), it was proposed that this relationship could affect the FPF of drug particles. Other findings suggested that changes in the water sorption characteristics of lactose observed post-blending were indicative of changes in the lactose surface chemistry, potentially affecting lactose-drug adhesion. Storage conditions of α-lactose monohydrate prior to blending were also found to affect the blend behaviour.

At present, there is very little information relating blending regimes to DPI performance, and in particular, the critical fluidisation-like stage involved in generating an aerosol from a static powder bed. Recent work by Shur *et al*., (2008), and Tuley *et al*., (2008) began to investigate this, however this thesis will differ by using larger scale blenders with a distinct *high shear* mixing process and will investigate the classical fluidisation and elutriation ability of such formulations, rather than mimicking an inhalation event by employing large flow rates, much greater than the U_{mf} of inhalation-grade lactose.

The key aim of this work is to develop understanding of the relationships between blend (primarily SEI) and storage conditions to the *in vitro* formulation performance.

More specifically, the main aims of this work were to:

- Investigate the effects of SEI on the properties of model DPI excipient (α-lactose monohydrate) and compare results with previous literature.
- Investigate the effects of scale of HSB regimes on the properties of mimic DPI formulations, including PSD, SSA, and chemical homogeneity; this is to be used as a comparison against previous literature which investigated the effects of blending on the α-lactose monohydrate excipient used in DPI formulations.
- Explore the use of a classical FB to test DPI formulations and employ the principles of elutriation from a FB to separate fine particles from the bulk powder within the bed.
- Investigate the effects of HSB and storage regimes on the *in vitro* performance of mimic DPI formulations using the novel FBE technique, and compare to conventional AJS, NGI, and AFM separation techniques.
- Relate the *in vitro* performance of the mimic DPI formulation to the properties of the constituent mimic API.

2.0. Analytical Method Development

ABSTRACT

Particle characterisation is a vital part of understanding the behaviour of dry powder inhaler (DPI) formulations. Even slight changes in the physicochemical properties of the materials used in these products can have profound implications for the behaviour of the formulations that in turn, can significantly affect *in vivo* performance.
This chapter describes the development of methods frequently used throughout this thesis. Techniques such as laser diffraction (with various dispersion mechanisms) for exploring size distributions, scanning electron microscopy for surface morphology and size verification, and dynamic vapour sorption (DVS) methods for specific surface area and surface characterisation are explained, along with the rationale behind their use. In addition, bulk powder characterisation measurements were performed via a ring shear test method to determine the flow properties of excipients and mimic active pharmaceutical ingredients (APIs) – a property of powders known to affect the fine particle fraction (FPF) of DPI formulations.

2.1. Introduction

2.1.1. Particle Size Analysis by Laser Diffraction

The particle size distribution (PSD) of powders used in DPI formulations are known to have significant effects on the performance of the final product (Newman and Clarke, 1983; Zanen *et al.,* 1994; Ashurst *et al.,* 2000; Crowder *et al*., 2001; Giry *et al*., 2006; Daniher and Zhu, 2008;). Generally in the pharmaceutical industry, the particle size affects a range of attributes such as appearance, solubility, bioavailability, stability, processability, and content uniformity. In addition, particle size of APIs is a major parameter that can affect blending, flowability, compressibility, and segregation propensity. Therefore, the PSD of the powders should be measured using appropriate validated analytical methods, of which, laser diffraction is one of the most commonly used techniques. The method is popular since it is relatively quick and easy to use, is flexible, and can be adapted to measure samples in various physical forms; it is potentially seen as an alternative to impactor analyses for the study of fine particle fractions (FPFs) of DPI formulations (Marriott *et al*., 2006).

Fine powders such as those used throughout this study are notoriously difficult to handle due to their cohesive nature; in addition, such powders often contain agglomerates of "primary" particles held together by interactive forces (see section 1.4.1). Due to this cohesivity, effective de-agglomeration and particle detachment from surfaces is required to obtain size measurements of primary particles. Therefore, a well-defined degree of dispersion is required in order to both obtain these primary particles, and to prevent samples from re-agglomerating. In this particular study, determining the size of both primary particles and agglomerates was important, thus two separate dispersion techniques were employed.

Dry dispersion methods use pressurised air stream (Xu and Guida, 2003), whilst a wet method using solvents to disperse particles has been developed (Adi *et al*., 2007) for inhalation-grade lactose. Xu *et al*., (2009) emphasise the need for rigorous method development of particle size measurements since their work on spray-dried infant formula found that dispersion by large air pressures caused particle fracture, thus producing a smaller average particle size than wet dispersion in hexane.

The choice of method should primarily be made on the degree of dispersion required. In all cases, whether liquid or gas is used as the dispersion medium, irreversible changes to the particle size through dissolution, milling or aggregation should not occur (Merkus, 2009). In addition, the sample should be correctly mixed before a measurement is made. Dry powders will separate out when stored for a long time or vibrated - larger particles rise to the surface and smaller particles collect at the bottom of the container. A comparison between the dispersion methods used in this study is given in Table 2.1.

Table 2.1. Features of wet and dry dispersion systems for laser diffraction used in this study.

Wet dispersion	*Dry Dispersion*
Analysis time: minutes	Analysis time: seconds
Sample size: several mg	Sample size: several g
Interaction with dispersant	No chemical interactions
Liquid disposal	No liquid disposal required

However, it must also be considered that the different scattering theories applied to the data may also affect the results. The Fraunhofer theory (used by Sympatec) does not require optical information regarding the particles or dispersing medium, on the other hand, the Mie theory (used by Malvern) requires the refractive indices of both the dispersing medium and the particles to be measured. Incorrect prediction of the scattering efficiency has been shown to overestimate the fine particle fraction of pharmaceutical powders using the Fraunhofer theory (Malvern Application Notes), thus the particle size values quoted in this thesis are best used as a comparison between samples (Xu *et al*., 2000).

2.1.1.1. Wet Analysis

Wet analysis requires samples to be correctly dispersed in a liquid. The correct choice of dispersant prevents particles from agglomerating, floating on the surface, or even dissolving (Merkus, 2009). These events influence the particle size data due to their effect on the laser intensity reaching the detector. For example, dissolution of samples causes the obscuration to decrease over the course of the measurement. The dispersant should be free from impurities and should be degassed before use – especially if it has been stored at low temperatures or under high pressure. Bubbles can interfere with results as they can be mistaken for particles in the cell window

(typically appearing as a secondary peak around 100 μm). In addition, the dispersant and instrument should be at similar temperatures whilst performing the measurement to prevent condensation from forming on the cell window, which again could adversely affect results (Merkus, 2009).

In order to achieve suitable dispersion, the solids typically require wetting, the deagglomeration and stabilisation of the suspension (de Villiers, 1995). Mechanical methods used to enhance the stability of suspensions include stirring, shaking, and application of ultrasound. Various methods have been trialled to optimise the dispersion of inhalation-grade lactose for laser diffraction particle size analysis. Examples include: dispersion in chloroform with added sorbitan trioleate (Span 85) surfactant and 1 min sonication (Tee *et al*., 2000); dispersion in ethanol and sonication for 1 min (Louey and Stewart, 2002); dispersion in butan-1-ol with 3 min sonication (Islam *et al*., 2004). With cohesive powders, wetting of particles may not be sufficient to overcome the interparticle forces, therefore, further de-agglomeration may be required in order to obtain primary particles. Surfactants may be added to aid dispersion by reducing surface charge effects that can cause both agglomeration, and cause the sample to float on the surface of the liquid. Ultrasound may be applied to aid the dispersion if large particles or agglomerates are seen to sink to the bottom of the sample; however, fragile particles are susceptible to breakage with extended ultrasound application so care needs to be taken (Merkus, 2009).

Whilst performing PSD measurements, it is important to ensure that recordings are made when the laser obscuration is stable (Tinke *et al*., 2009). If the obscuration decreases over the course of the measurement, the particle size may be increasing because of agglomeration, or even swelling due to the dispersant. Other causes can be attributed to particles settling due to insufficient stirring or particles dissolving. Conversely, if the obscuration increases, particles could be attaching themselves to the cell window due to surface charges (Merkus, 2009; Tinke *et al*., 2009).

The dispersant should be a clear (at 633 nm wavelength), optically uniform liquid which does not interact with the sample causing it to change size (Lazghab *et al*., 2005). Critically, the dispersant should not dissolve the material under test during the measurement. As an initial check of the suitability of the dispersant, the particles are observed microscopically and by laser diffraction over the course of the measurement

to ensure they do not dissolve or agglomerate, and that dispersion stability is achieved (Chander *et al*., 2007; Tinke *et al*., 2009). In addition, the polarity of the dispersant should also be considered since preferential adhesion of particles to glass surfaces could occur due to inadequate dispersant selection (Merkus, 2009).

2.1.1.2. Dry Analysis

Dry powder dispersion has the advantages of measurements being performed on the powder in its original state and removing the need for additional chemicals to be used as dispersants. It is particularly suitable for formulations that comprise both hydrophilic and hydrophobic components, since finding a mutual dispersant can be difficult (Bosquillon *et al*., 2001b). To obtain suitable dispersion of powders, a steady flow of powders through the measuring zone is required; this is typically achieved by use of a vibratory feeder – a conical hopper connected to a chute that allows feed rate across the cell window to be controlled.

2.1.2. Dynamic Vapour Sorption

Dynamic vapour sorption (DVS) studies allow a range of applications to be investigated through the controlled exposure of samples to vapour sources. Precisely controlled concentrations of vapours flow over a sample suspended from an ultra-microbalance, which measures the change in mass caused by sorption or desorption of the vapour molecule. These dynamic flow conditions enable the sorption/desorption behaviour of samples to be investigated.

The interaction of organic solvents and water with pharmaceutical powders is highly important for the understanding of many processes that such products undergo. In particular, information about crystallisation, drying, and predictions of product stability and shelf life can be made using information gained from the shape of vapour sorption isotherms (Columbano *et al.,* 2002; Mackin *et al.,* 2002).

2.1.2.1. Water Sorption Studies

Water sorption studies allow a range of properties to be investigated including: moisture uptake and sorption of materials, stability, and degradation of powders, and the determination of amorphous content.

High-energy processing of pharmaceutical material, including the HSB and micronisation processes employed in this thesis, may induce particle surface changes,

an example of which is the development of amorphous material. Amorphous materials in pharmaceutical formulations produce complex and challenging problems that influence the performance, processing, and storage of these products. The presence of amorphous materials may or may not be beneficial, depending on the (un)desired, unique properties of the amorphous state.

Sorption isotherms describe the amount of vapour adsorbed (or desorbed) by a sample at different equilibrium concentrations in the gas phase. The shape of an adsorption isotherm is governed by the interaction between the vapour molecules and the solid; from this, the sorption mechanism can be determined. Isotherm shapes are described by the BDDT classification (Brunauer *et al.,* 1940), which suggests there are six types of isotherm (although only four are relevant to pharmaceutical powders). Monolayer adsorption is characterised by significant uptake of vapour at low and high partial pressures, with relatively low adsorption at intermediate vapour concentrations. Conversely, cluster adsorption is characterised by low uptake at low vapour concentrations, with greater adsorption at high vapour concentrations.

2.1.2.2. BET Surface Area Studies

The DVS instrument can be employed to calculate the surface area of powders available for adsorption of gas molecules. Historically, the Brunauer Emmet Teller (BET) method of adsorption of gases onto the surface of solids used inert gases such as nitrogen, krypton, and argon to form a monolayer on the surface of the particles (Brunauer *et al*., 1938). However, more recently developed methods use organic vapours as the probe molecules, thus eliminating the need to work at the low temperatures associated with the boiling points of gases mentioned above. Using organic vapours such as octane allows analysis to be performed at ambient temperatures (~300 K), rather than the very low boiling point of inert gases (the boiling point of nitrogen is ~77 K).

The BET equation,

$$\frac{1}{v\left[\left(P_0/P\right)-1\right]} = \frac{c-1}{v_m c}\left(\frac{P}{P_0}\right) + \frac{1}{v_m c} \qquad \textbf{Equation 2.1}$$

where, P and P_0 are the equilibrium and the saturation pressure of adsorbates at the temperature of adsorption (hence P/P_0 is the partial pressure of vapour), v is the

adsorbed gas quantity, and v_m is the monolayer adsorbed gas quantity. c is the BET constant, which is expressed by:

$$c = \exp\left(\frac{E_1 - E_L}{RT}\right) \qquad \textbf{Equation 2.2}$$

where, E_1 is the heat of adsorption for the first layer, and E_L is that for the second and higher layers and is equal to the heat of liquefaction. Plotting $1/[v([P_0/P]-1)]$ as the ordinate and P_0/P as the abscissa produces a straight line, with the gradient and y-intercept used to find v_m, the amount of gas adsorbed in the formation of a monolayer, and c, a constant used to describe the strength of the adsorbate-adsorbent interaction.

2.1.3. Scanning Electron Microscopy (SEM)

Electron microscopes were developed to overcome the limitations of light microscopes, which due to the wavelength of light, can only resolve images to 10^{-7} m. This limit was reached in the 1930s, however the demand to observe the structures of organic cells required magnifications greater than 10,000x, hence the need for a more powerful microscopy technique.

SEM allows various information to be determined regarding the specimen material, this includes: surface topography, which in turn allows material properties such as hardness and reflectivity to be understood; surface morphology, which allows information regarding ductility, strength and reactivity to be found; composition which has a direct relationship to melting point, reactivity, hardness of materials; and crystallographic information which allows electrical properties and strength to be inferred (Cosgrove, 2005). SEM images are extensively used in DPI literature to assess formulations, and (dis)prove hypotheses, however it remains a subjective assessment method and firm conclusions are difficult to make; therefore should always be treated with a degree of scepticism. Recent examples of the use of SEM in DPI literature include: Donovan and Smyth, (2010) who assessed the influence of size and surface roughness of large lactose particles in DPI formulations; Ógáin *et al.*, (2011) who observed spray-dried particles engineered from larger trehalose crystals; and Jones *et al.*, (2010) who tested the effect of blending regimes on the impact of drug-carrier interactions.

2.1.4. Shear Cell Analysis

It is widely known that particulate properties strongly influence the behaviour of bulk powders. Without adequate control of particulate properties, batch-to-batch variability of bulk powders and APIs can be large. Variations in raw materials can result in processing difficulties and produce large financial losses. The need for more consistent particulate properties of powder batches has resulted in tighter controls and the development of new grades of excipients to enhance flowability and dispersion (Crowder and Hickey, 2000). In addition, reliable and consistent flow from hoppers and feeders with minimal spillage and dust generation is required throughout the pharmaceutical industry.

Edwards *et al.,* (2009) investigated the relaxation effects on lactose/API blends produced using a high shear blender by comparing the flow functions of formulations stored over periods of time. Poor powder flow properties can result in reduced productivity and financial losses. A common approach used to improve the powder flow properties is to increase the size of the particles (i.e. granulation), although other methods involve increasing the powder density or altering the shape of the particle. It is known that more dense particles have improved flow properties, along with spherical particles rather than elongated, irregularly shaped particles (Danjo *et al.,* 1989; Popov *et al.,* 2003).

Shear cell tests of cohesivity compare *flow functions* (FF) of materials; the FF of a powder is the inverse of the gradient of the graph of unconfined yield stress (σ), against the consolidation stress (τ). A greater FF is indicative of superior bulk solid flow. Powders are often classified as being: *free flowing, easy flowing, cohesive, very cohesive,* or *non-flowing* (Table 2.2). Example plots of σ against τ with Mohr's circles are shown in the Appendix, pages 227 and 228.

With decreasing particle size, the gradient of the FF line should increase (Table 2.2), hence suggesting worsening flow conditions. If FF is plotted against particle size, i.e. d_{10}, d_{50}, and d_{90}, of the same material, then the slope of the FF will decrease with increasing particle size. The unconfined yield strength (f_c) represents the strength of the powder upon consolidation that needs to be overcome to initiate powder flow. Greater strength represents stronger particle-particle interactions, since the van der Waals forces and hydrogen bonds increase when the distance between particles

reduces. An increase in external stress consolidates powders and brings the particles close together. The closer arrangement and the increase in contact points between particles increases the strength of particle-particle interactions; and consequently the unconfined yield strength increases with increasing external stress. The stress required to induce particle-particle relative movement (i.e. shear failure in shear cell tests) is therefore higher if the powder bed is consolidated under a higher normal stress. This is comparable to the increase in friction forces when the normal stress is increased during the sliding of two touching surfaces; and is the reason behind the positive gradient of FF. If a powder is not subjected to significant consolidation by an external stress, the gradient of its FF line should be close to zero (Hou and Sun, 2008).

The overall strength of surface interactions amongst particles is governed by three main factors: the total area of contact; the chemical nature of the surfaces, and the separation between the particles.

Table 2.2. Classification of flow functions and their properties.

Flow function, FF	*Flow characteristic*
FF $\leq$ 1	Non-flowing
1 < FF $\leq$ 2	Very cohesive
2 < FF $\leq$ 4	Cohesive
4 < FF $\leq$ 10	Easy flowing
10 < FF	Free flowing

2.2. Materials and Methods

2.2.1. Lactose

Lactose (4-O-β-D-galactopyranosyl-D-glucose) is a disaccharide sugar consisting of galactose and glucose fragments which is most commonly found in milk. The grade of lactose used throughout this thesis is Lactohale (GSK Description: Lactose for MDPI Grade 5) (Friesland Foods, Zwolle, The Netherlands). It is commonly available in three forms: α-monohydrate, β-anhydrous and spray-dried; this study focuses on the α-monohydrate form since it is often the material of choice as a DPI excipient. Samples of this material used throughout the study were taken from batches stored in the original packaging (foil bag within a cardboard box) at 20°C and 40% RH in humidity-controlled cabinets (Binder, Germany).

2.2.2. Development of a Protocol For Laser Diffraction Particle Size Measurements (Wet Dispersion Systems)

The laser diffraction instrument used in this study was a Malvern Mastersizer 2000 connected to a Hydro SM small volume pump/stirrer dispersion unit (both Malvern Instruments, UK). This allows samples in suspension to be passed across the laser beam through a glass cell window. The setup of the pump and stirrer allows samples to be re-circulated, thus allowing multiple measurements to be made on the same sample to improve reliability of results. The lens used by this instrument had measurement range 0.02–20 000 μm.

In order to ensure consistency in results, the obscuration limits were set by the standard operating procedure (SOP) to be between 15 and 18% for lactose measurements and between 4 and 8% for micronised material, as recommended by the manufacturer's operating manual.

Prior to particle size measurements being made, a quality audit was performed to validate performance of the instrument. This involved dispersing glass beads (refractive index 1.52) of well-defined particle size in distilled water (refractive index 1.33); the theoretical defined limits and actual measurements from three independent tests are shown in Table 2.4.

2.2.2.1. Investigation Into Appropriate Dispersant

The method proposed by Adi *et al*., (2007) was investigated in order to determine the optimal method for dispersion of the lactose used throughout this study. In order to achieve this, propan-2-ol and ethanol (both analytical reagent grade, Fisher Scientific, Loughborough, UK) were used as dispersants to test the stability of results over time. This test involved the dispersion of approximately 500 mg lactose in 5 ml of each solvent and gently shaking by hand before adding drop-wise to the dispersion unit (filled with approximately 200 ml solvent) until an obscuration between 15 and 18% was achieved. The stirrer speed was set at 1500 rpm for each experiment with measurements taken at regular intervals to determine the stability of results over time. Each time-course experiment was performed three times. Reference refractive indices of lactose (1.533), propan-2-ol (1.378), and ethanol (1.361) were used, with an estimated imaginary refractive index of lactose of 0.1 (Adi *et al*., 2007).

2.2.2.2. Use of Sonication to Aid Dispersion

Samples were prepared and measured using the method described in section 2.2.2.1, using propan-2-ol as dispersant before being placed in an ultrasonic bath for 2, 5, 10, 15, 20, 30, 40, 50 and 60 minutes to aid dispersion. Following sonication, samples were measured immediately to determine the effects of sonication on particle size. A further test was performed to describe the relaxation of the effects on lactose particle caused by sonication, this involved exposing a sample to ultrasound for 30 min then measuring the particle size at: 10 s, 30 s, 1 min, 5 min, 10 min, 20 min, 30 min, 60 min, 2 hr, 3 hr, 4 hr and 5 hr following this.

2.2.3. Development of a Protocol for Laser Diffraction Particle Size Measurements (Dry Systems)

The instrument used for this method was the Sympatec HELOS laser diffraction system, with RODOS dispersion unit and VIBRI vibrational feeder used in this study (all Sympatec, Germany).

2.2.3.1. Effect of Pressure

The major drawback using dry dispersion systems - in particular the compressed air that produces the dispersion - is the possibility of particle breakage or fracture (Merkus, 2009). In order to determine the degree of fracture, a simple pressure titration experiment was performed to test the effect of pressure on the PSD of unprocessed lactose carrier (Fig. 2.6).

Unprocessed lactose was measured using the R3 lens with a focal length of 100 mm and 0.5-175 μm detection range – suitable for the finest particles within the excipient PSD, at a range of pressures to determine the ability to disperse agglomerates. Approx 1 g of material is typically required to obtain a recommended laser obscuration of 5-8% (recommended by manufacturer).

2.2.4. Dynamic Vapour Sorption

Water sorption and specific surface area (SSA) measurements made throughout this study were performed using a DVS Advantage II (Surface Measurement Systems, UK) using previously well-developed methods (Bridson *et al*., 2007). Results from these analyses can be found in chapters 3, 4, and 5.

2.2.4.1. Calibration

In order to validate the mass flow controller, salt validation trials allowed partial pressures to be accurately generated. These calibrations were based on the principle that the vapour pressure above a saturated salt solution in equilibrium with its environment is constant at fixed temperature. Several salts were used for validation covering a range of partial pressures (Table 2.3), with the saturated salt solution (~50 mg) made with distilled water and placed in the sample pan.

To perform validations, the temperature was held at the temperature required for standard experiments, and then the partial pressure set at approximately 5% above the salt solution partial pressure (P/P_0) before being subsequently reduced to 5% below the salt solution partial pressure over a period of five hours. Finally, the partial pressure was returned back to the starting pressure, over a three-hour period. By plotting (Fig. 2.1) the target $\%P/P_0$ against $\mathrm{dm/d}(\%P/P_0)$, and finding when $\mathrm{dm/d}(\%P/P_0) = 0$, the generated $\%P/P_0$ was calibrated against the actual partial pressure above the saturated salt solution at this temperature – therefore ensuring the partial pressure accuracy of the system.

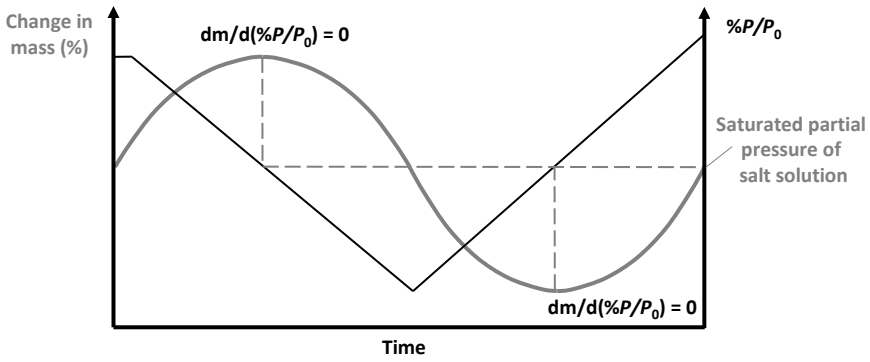

Fig. 2.1. Change in mass and partial pressure generated by DVS system as a function of time. The points at which dm/d(%P/P_0) = 0 correspond to the saturated partial pressure of the salt solution.

Table 2.3. Saturated salt deliquescence points (Greenspan, 1977).

Salt	*Water%P/P_0 at 25°C*	*Water%P/P_0 at 40°C*
Lithium chloride	11.3	11.2
Magnesium chloride	32.8	31.6
Magnesium nitrate	52.9	48.4
Sodium chloride	75.3	74.7
Potassium nitrate	93.7	89.0

2.2.4.2. Water Sorption Studies

120 ± 1 mg samples were dried for 4 hours using oxygen-free nitrogen (BOC, UK) before being subjected to increasing humidity steps from 0-90% in 10% increments whilst being kept at constant 25°C ± 0.1°C. Samples were allowed to reach a near-equilibrium state ($\%^{dm}/_{dt}$ = 0.0002% min^{-1}) at each humidity step before progressing to the next stage.

2.2.4.3. BET Surface Area Analysis

Application of the Brunauer Emmet Teller (BET) equation was performed using octane (HPLC grade, Fisher Scientific, UK) as the probe molecule that allowed the SSA of lactose samples to be determined. For these experiments, dry, oxygen-free nitrogen (BOC, UK) was purged over the 120 mg ± 5 mg sample for four hours. The partial pressure was then sequentially increased from 0 to 96% in 3% increments, with the sample being allowed to reach a near-equilibrium ($\%^{dm}/_{dt}$ = 0.0002% min^{-1}) at each partial pressure stage before progressing to the next. All stages of the experiment were performed at 25°C ± 0.1°C and were repeated three consecutive times on each sample.

2.2.5. Scanning Electron Microscopy

PSD and particle morphology were investigated throughout this study using SEM to produce images of material before and after processing. Images of the surface morphology and uniformity of material were taken using a JEOL 6060 Scanning Electron Microscope (JEOL, Japan) at 10 keV accelerating voltage. Each sample was mounted on a carbon sticky tab (carbon is used since it absorbs electrons rather than re-emitting electrons, hence reducing background noise) and gold coated (10 nm thickness), prior to analysis (Young *et al*., 2007a). Gold sputter coating was performed using an Emscope SC 500, Elexience, Paris, France. SEM images of mimic formulations can be found in chapters 4, 5 and 6.

2.2.6. Shear Cell Method

Cohesivity of materials was determined using a Ring Shear Tester, (RST-XS, Dr. Dietmar Schulze, Wolfenbüttel, Germany). A small volume of material (~30 cm^3) was loaded into a shear cell with the excess powder scraped off by a spatula, ensuring that no force was applied to the powder surface; the powder was then weighed before a lid was placed on top of the bed and a loading rod inserted to apply the normal stress to

the bed. Two tie rods were then used to apply a shear stress and are attached to two load cells. To test the cohesivity of materials used in this study, a preshear stress of 20 kPa was applied before consolidation stresses of 2, 3, 5, 10, 15 kPa to determine at which points the bed fails. These values were chosen to correspond to consolidation stresses experienced by pharmaceutical formulations during handling and device filling (Schulze, 2005).

Tests of the cohesivity of materials are employed throughout this study. Chapter 3 utilises the shear test method to compare the cohesivity of materials prior to blending, and the mimic APIs post-micronisation used in this study. Chapter 4 describes the effect of specific energy input (SEI) during HSB on the cohesivity of α-lactose monohydrate, whilst chapter 5 assesses the cohesivity of mimic API-containing formulations exposed to different blending and storage regimes.

2.3. Results

2.3.1. Wet Dispersion Results

The calibration of the instrument was performed on a regular basis to ensure consistent performance. Table 2.4 shows an example of such a test.

Table 2.4. Quality audit of Mastersizer 2000 using glass beads as standards. Values are averaged from three independent measurements ± SD.

	d_{10} (μm)	d_{50} (μm)	d_{90} (μm)
Manufacturer's Lower limit	27.58	45.86	74.69
Manufacturer's Median	28.43	46.8	77
Manufacturer's Upper limit	29.28	47.74	79.31
Measured value	28.61 ± 0.03	47.04 ± 0.05	76.69 ± 0.09

2.3.1.1. Appropriate Dispersant Selection

Fig. 2.2 shows the differences in d_{10} (used to describe the FPF of the PSD) and d_{50} particle size measurements using ethanol and propan-2-ol as dispersants. It can be shown that the use of propan-2-ol as dispersant produced more stable results over time than ethanol, despite the two producing similar results during the initial measurement. Since the particle size measurements performed throughout this study required stability over time, propan-2-ol was the preferred option for lactose, in agreement with the work by Adi *et al.*, (2007).

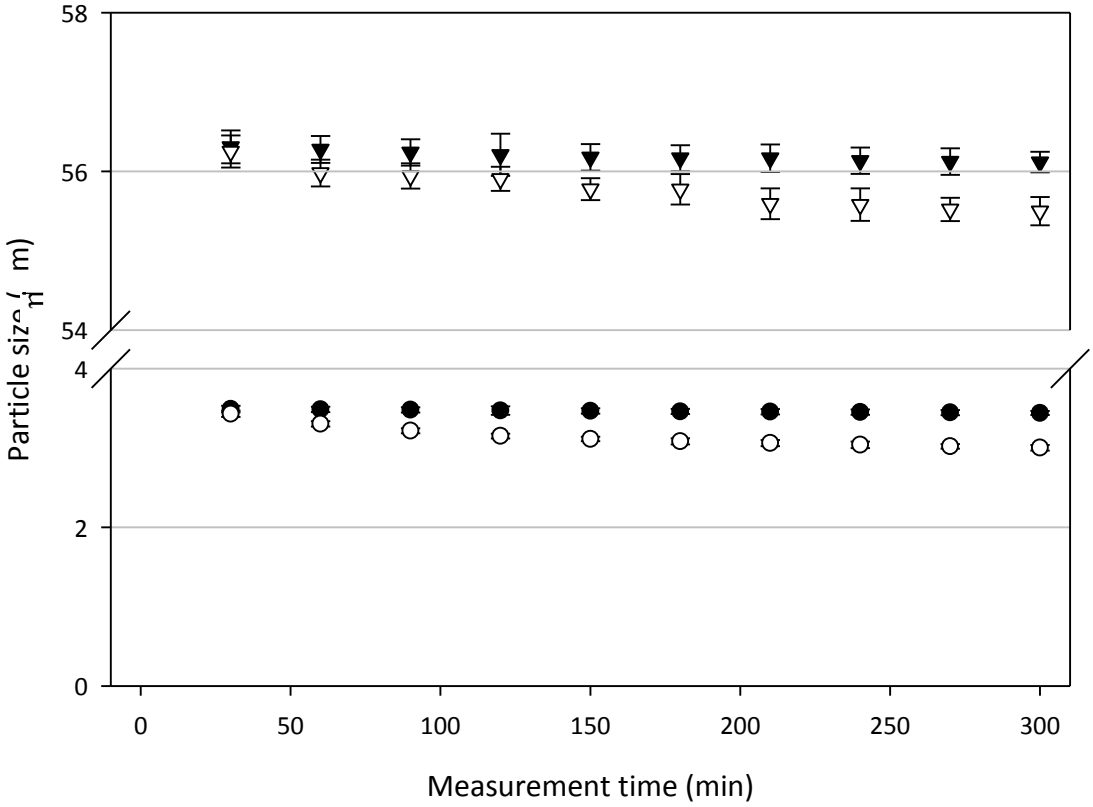

Fig. 2.2. Comparison between ethanol and propan-2-ol for particle size measurements of unprocessed lactose. Results show the change in d_{10} and d_{50} particle size as a function of measurement time from three samples ± SD. ○ - d_{10}, ▽ - d_{50} (ethanol); ● - d_{10}, ▼ - d_{50} (propan-2-ol).

2.3.1.2. Sonication Results

Fig. 2.3 shows the effect of sonication on lactose in propan-2-ol suspensions; such that sonication aids dispersion of particles and creates a homogeneous suspension more suitable for size analysis.

Fig. 2.4 shows the effect of sonication on the d_{10} and d_{50} particle size of unprocessed lactose – the results show that application of ultrasound significantly reduces the particle size of the material, however, does not provide information on the mechanism that causes this. Either particles may be fracturing, or de-agglomeration is being enhanced by ultrasound, thus producing smaller free particles than by simply wetting the material.

Fig. 2.3. Lactose in propan-2-ol suspensions; without sonication (left); 1 min after sonication for 3 min (right).

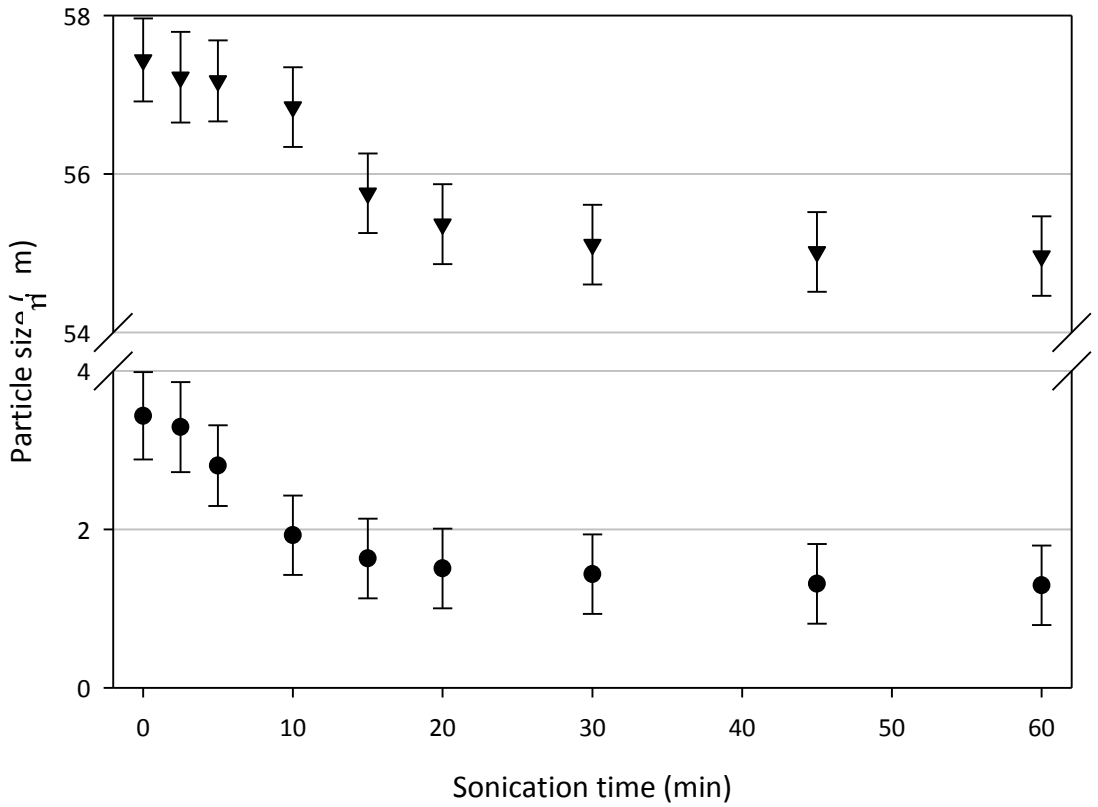

Fig. 2.4. Effect of sonication time on the d_{10} - ● and d_{50} - ▼ particle size of unprocessed lactose. These results suggest that either agglomerates are being broken up, or particles are fracturing due to sonication. Results shown are averaged from three independent batches of unprocessed lactose ± SD.

In order to check which mechanism occurs, the relaxation of the suspended lactose particle size was determined by PSD measurements at time intervals following sonication (Fig. 2.5). This shows that the particle size returns to the original size after several hours, thus suggesting that particles are not being fractured and that sonication simply improves the de-agglomeration of particles in suspension. Should particle fracture occur, it is unlikely that the size distribution would return to its original state. It is important to note that application of ultrasound is only intended as a dispersion aid for measurement and not to be used in the production of micronised drug particles (Kinnarinen *et al*., 2003). Re-agglomeration of particles is initiated through particulate collisions caused by settling and mixing within the dispersion unit (Adi *et al*., 2007).

These results correlate with those found in a previous study by Adi *et al*., (2007), who reviewed several dispersion mechanisms and their effect on PSD of fine lactose in order to develop a suitable methodology for size measurements using laser diffraction. The results found dispersion in propan-2-ol combined with 3 min sonication was

suitable for fine lactose particle size measurements. Sonication was required to achieve suitable de-agglomeration and detachment of fines from larger carrier particles, however, extended sonication was found to potentially cause particle fracture, whilst dispersion in both ethanol and butan-1-ol caused time-dependent changes in particle properties that were attributed to possible dissolution and recrystallisation.

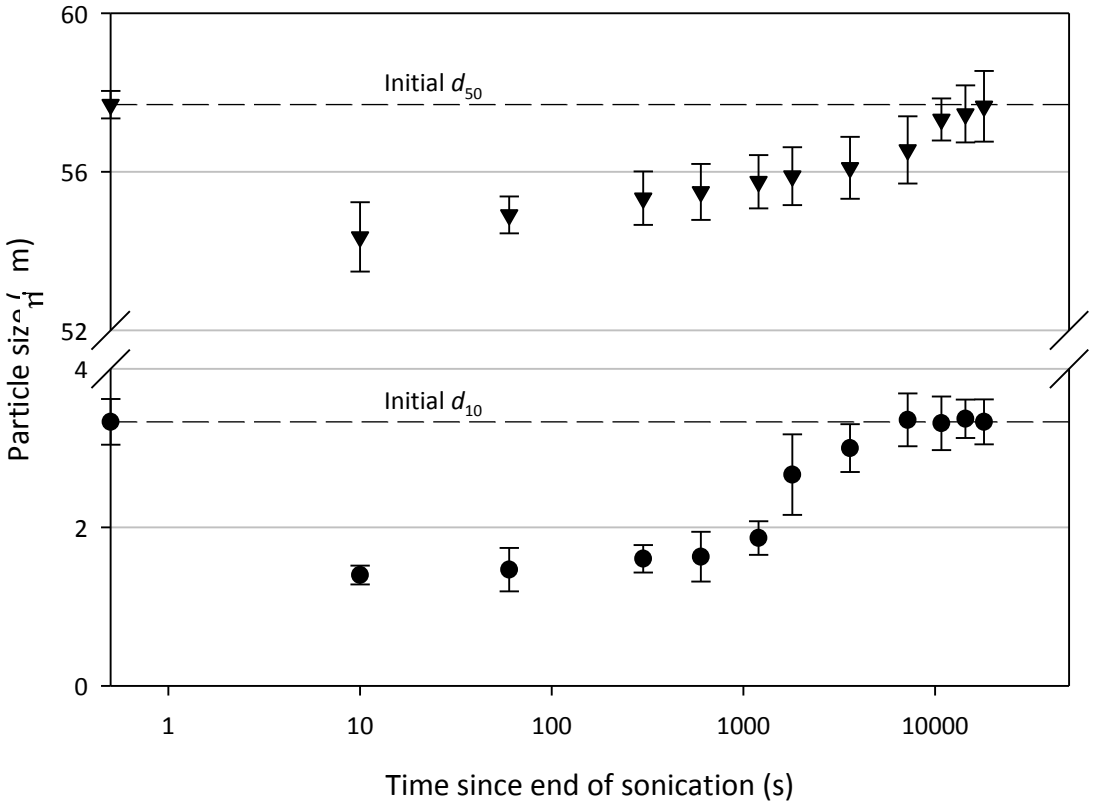

Fig. 2.5. Time dependent relaxation of unprocessed lactose to its original size following sonication for 30 min. Results are averaged from three independent experiments ± SD. d_{10} - ●, d_{50} - ▼.

2.3.1.3. Wet Dispersion Conclusion

As a result of the experiments performed above, the experimental conditions used in determining the PSD of lactose were suspension in propan-2-ol followed by 15 min sonication and immediate measurement post-sonication. The stirrer speed was set at 1500 rpm and obscuration settings were dependent on the material being analysed. Based on manufacturer's specifications, obscuration of 12-20% is suitable for particles <50 μm, whilst an obscuration of 3-5% is suitable for particles <10 μm.

2.3.2. Dry Dispersion Results

Regular quality audits of the detector were performed using silicon carbide reference material (P600, Sympatec, Germany). The theoretical defined limits and an example of actual measurements from three independent tests are shown in Table 2.5.

Table 2.5. Quality audit of Sympatec HELOS using silicon carbide reference material (R3 lens). Values are averaged from three independent measurements ± SD.

	d_{10} (μm)	d_{16} (μm)	d_{50} (μm)	d_{84} (μm)	d_{90} (μm)
Lower limit	16.54	18.62	27.23	38.72	41.74
Median	17.05	19.19	28.08	39.91	43.03
Upper limit	17.56	19.77	28.92	41.11	44.32
Measured value	17.21 ± 0.29	19.49 ± 0.28	28.49 ± 0.27	39.23 ± 0.07	42.15 ± 0.19

2.3.2.1. Effect of Pressure on Particle Size of α-Lactose Monohydrate

Fig. 2.6 shows that dispersion of particles is enhanced with increasing pressure up to 2 bar, at which point further de-agglomeration is not observed. This is particularly noticeable at the fine end of the size distribution, suggesting that unprocessed lactose consists of a number of fine particle agglomerates and fines attached to larger carriers.

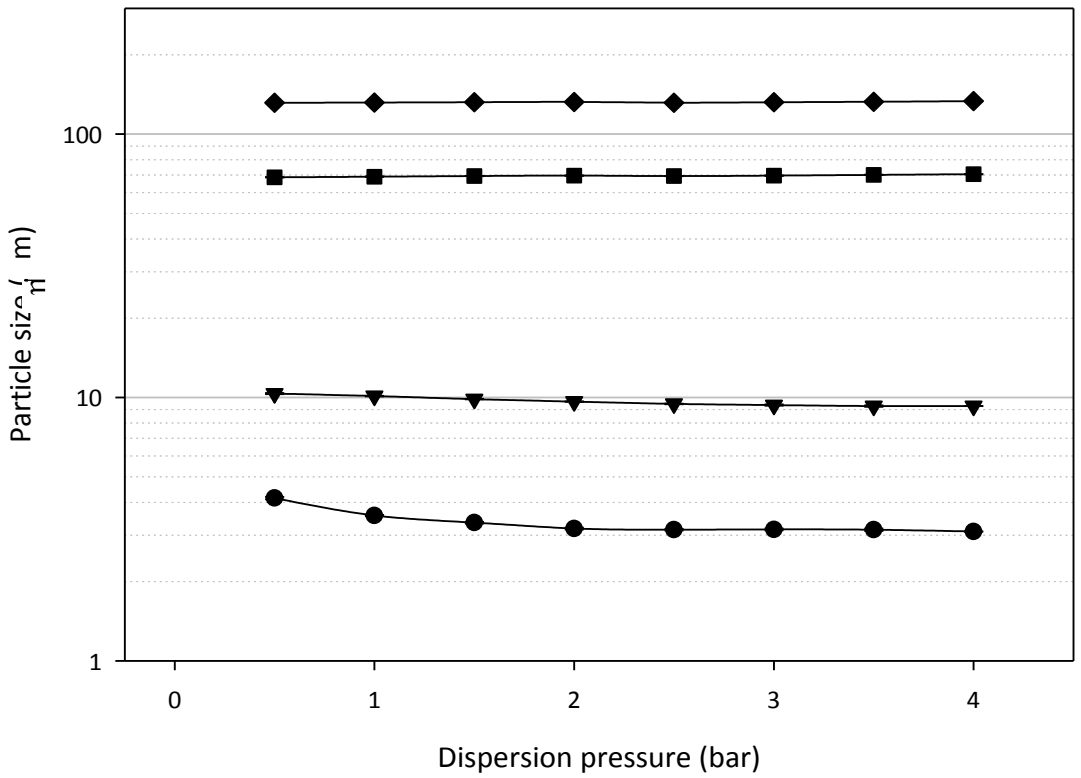

Fig. 2.6. Pressure titration test to determine the effect of increasing pressure on the d_5 - ●, d_{10} - ▼, d_{50} - ■, and d_{90} - ◆ particle size of unprocessed lactose using RODOS/L dispersion unit with HELOS sensor.

This pressure titration experiment showed that the PSD of lactose is not adversely affected by the range of dispersion pressures obtainable by the system. Differences were observed at the fine particle region of the distribution, suggesting that pressures lower than ~2 bar were not as efficient at de-agglomeration or removing fines adhered to larger particles, hence a d_5 particle size of 4.15 μm is achieved at 0.5 bar dispersion pressure compared to 3.15 μm at 2 bar.

As a result of this pressure titration test described above, dry dispersion measurements were performed using a dispersion pressure of 2 bar, as used previously by Bridson *et al.*, (2007).

2.4. Conclusion

Throughout this thesis, particle size data will be reported using measurements from both wet and dry dispersion laser diffraction devices. The choice of device was dependent primarily on the degree of dispersion required. When enhanced dispersion was required (for particularly cohesive powders), and knowledge of primary particle sizes desired, wet dispersion was used, whereas dry dispersion allowed more accurate representation of particles in their natural (often agglomerated) state. The sample size to be analysed was also considered. When the amount of material was not limited, dry dispersion was used as this is the most common technique used in literature (for ease of comparison), two such examples include Bridson *et al.*, (2007) and Deng *et al.*, (2010) and allowed for more rapid analysis.

Table 2.6 shows a comparison between the d_{10}, d_{50} and d_{90} particle sizes produced by dry and wet dispersion laser diffraction techniques of unprocessed lactose taken from 20 samples throughout the batch of powder used in this study. The results show that the wet dispersion method with suspension in propan-2-ol and 5 min of sonication offers greater dispersion efficiency than 2-bar compressed air,

Table 2.6. Comparison of wet and dry dispersion techniques on particle size values of unprocessed lactose.

	Sympatec dry dispersion (2 bar)	***Mastersizer wet dispersion (propan-2-ol)***
d_{10}	9.55 ± 0.57 μm	3.43 ± 0.21 μm
d_{50}	68.46 ± 0.89 μm	56.05 ± 0.34 μm
d_{90}	134.40 ± 1.42 μm	132.81 ± 0.78 μm

3.0. Mimic API and Formulation Production and Characterisation

ABSTRACT

A key requirement for the delivery of therapeutic drugs to the lower airways is an aerodynamic diameter of 1-5 μm. Producing this size of particles is often a difficult process, typically involving the high energy micronisation of larger particles. This chapter describes the production and characterisation of two compounds with different physicochemical properties, cholesterol and vitamin C, along with the rationale behind their choice as mimic active pharmaceutical ingredients (APIs) throughout this study.

This work focuses on the use of a planetary ball mill to micronise the compounds, and describes the characterisation techniques used to ensure the micronised material behaves consistently throughout the course of the experiments.

The final part of this chapter describes the production of formulations using high shear blending (HSB) and the characterisation of these formulations, including the test used to determine if, and when, blend content uniformity had been achieved.

Results showed that micronised cholesterol and vitamin C were stable (in terms of particle size, chemical composition, and crystallinity) over the course of a typical long-term storage study (5 months) when stored at 40% RH and 20°C. Since their physicochemical properties were not affected by controlled long-term storage, they were deemed suitable for use in tests to determine the effects of blending and storage regimes on the adhesion between API and carrier (chapter 7).

3.1. Introduction

3.1.1. Mimic API selection

The drugs used in DPIs can broadly be split into two groups: corticosteroids used to treat diseases of the bronchi and lungs, and β_2 adrenergic agonists – either long acting or short acting – used to cause smooth muscle relaxation, resulting in the dilation of blood vessels and bronchial passages. These drugs may be administered solely, or in combination, providing both relief and symptom control to the patient. APIs have a wide range of physicochemical properties, for example, different APIs are known to exhibit a range of affinities to moisture. Salbutamol sulphate is a common short-acting β_2 adrenergic agonist which exhibits hydrophilic nature (Brodka-Pfeiffer *et al*., 2003), whilst the long-acting salmeterol xinafoate (Murnane *et al*., 2008) and the corticosteroid triamcinolone acetonide (Williams *et al*., 1999) possess hydrophobic properties.

Inhaled corticosteroids (ICSs) such as budesonide, fluticasone propionate, and beclomethasone dipropionate belong to the steroidal group of organic compounds that comprise four carbon rings joined together, as shown in Fig. 3.1. The sterane core comprises seventeen carbon atoms bonded together to form four rings – three cyclohexane rings and one cyclopentane ring. The differences between the steroids arise from the functional groups attached to the four rings, and their oxidation states. Due to their similar sterane cores, cholesterol was proposed as a suitable choice for mimic steroid-based API.

Cholesterol (3β-cholest-5-en-3-ol) is a waxy steroid metabolite found in the cell membranes and blood plasma of all animals. It is an important component for the manufacture of steroid hormones and fat-soluble vitamins. It was chosen as a mimic drug due to its hydrophobicity and steroidal core (Fig. 3.1) similar to drugs used in DPI formulations, particularly the corticosteroids such as budesonide and salmeterol. The chemical structure of cholesterol is given in Fig. 3.2.

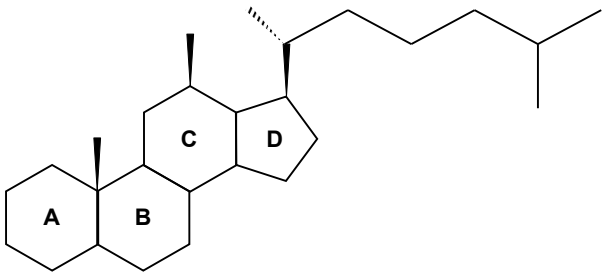

Fig. 3.1. Steroid core skeleton found in budesonide and other inhaled corticosteroids.

Vitamin C (L-ascorbic acid) is an antioxidant required for a range of essential metabolic reactions in plants and animals. It is a water-soluble vitamin naturally present in some foods; it is however also added to other foods and used as a dietary supplement. It was proposed as a mimic drug due to its water solubility in contrast to the hydrophobicity of cholesterol. The chemical structure of vitamin C is given in Fig. 3.3.

Other mimic drugs used in inhalation studies include: bovine albumin serum (Adi *et al*., 2008), salicylic acid (El-Hagrasy *et al*., 2006); ethenzamide (Takano *et al*., 2003); and disodium cromoglycate (Braun *et al.,* 1996; Young *et al*., 2007a).

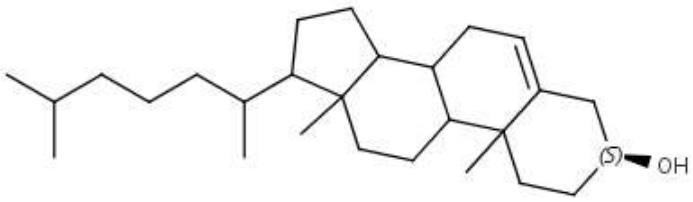

Fig. 3.2. Chemical structure of cholesterol

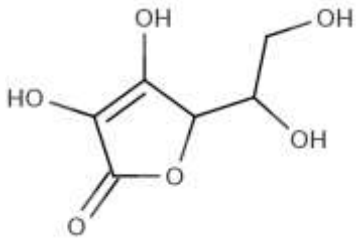

Fig. 3.3. Chemical structure of vitamin C

3.1.2. Micronisation

Micronisation of API particle size is achieved through either top-down processes, in which particle size is reduced, or bottom-up processes where particles are produced by increasing droplets of the API to the desired size (Ennis and Litster, 1997; Hu *et al*., 2004).

3.1.2.1. Top-down processes

Milling is a frequent choice of mechanical reduction (Merisko-Liversidge *et al.,* 2003; Müller *et al.,* 2000), of which there are several alternative methods, typically consisting of fluid-energy (jet) mills (Bentham *et al*., 2004), high-peripheral-speed mills (Nakach *et al*., (2004), and ball mills (Snow *et al.,* 1999). These high-energy processes often

generate forces that are likely to induce lattice defects, weaken intermolecular bonds, and alter the physicochemical stability of crystalline materials (Ticehurst *et al*., 2000).

Planetary ball mills are commonly used in laboratory-scale applications for ultra-fine milling (defined as milling to <10 μm). Milling is primarily achieved through the high-energy impact of the grinding balls and chamber. Within the grinding bowl, the grinding media and feed material rotate around its own axis on a main disc, which rapidly rotates in the opposite direction (Fig. 3.5). At a certain speeds, the centrifugal force causes the ground sample material and grinding balls to separate from the inner wall of the grinding bowl and cross the bowl at high speed to further grind the material by impact against the opposite bowl wall. An impact between the balls themselves also adds to the size reduction process. Milling conditions to be considered include, grinding media size, grinding time and grinding speed (Dudognon *et al*., 2006).

Ball mills consist of a cylindrical tube into which the grinding media and material to be ground are filled. Size reduction occurs when the loose media slides and rolls about in a parabolic arc within the rotating cylinder (Müller *et al.,* 2001). Some of the grinding balls are pushed to the outside of the chamber by the centrifugal force and are raised upward in the cylinder. When these particles fall, they impact on the feed material. During slower rotation, the balls mainly roll against each other. The balance between rolling and tumbling is a function of operating speed, and the amount of media present. Decisive factors affecting the success of size reduction include correct choice of media, size of media, and mix ratio of media according to size (Merisko-Liversidge *et al.,* 2003).

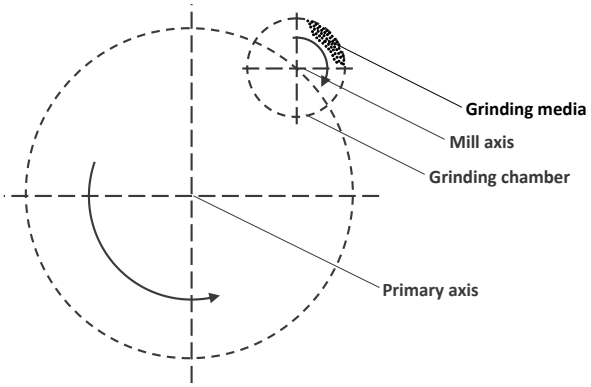

Fig. 3.4. Operating principles of planetary ball mill (Fisher, 2007).

The desired PSD of the feed material is dependent on the grinding media size. A coarse end product requires larger grinding media, whilst a fine end product requires small grinding media. Wet size reduction is preferential for size reduction to <30 μm, since shear forces of the surrounding medium assist the size reduction between two solid surfaces and the deagglomeration of compacted particles. This enhances the fineness of particles that can be achieved, prevents dust formation and is suitable for suspended

feed materials or if the end product is required as a suspension for downstream processing (Merisko-Liversidge *et al.,* 2003). Approximately 30% less energy is required for wet processing, and wear to the milling equipment is 3-5 times less than dry processes. This has several advantages over dry milling methods in that heat-sensitive materials can be milled conveniently, since the slurry removes heat generated by the friction generated in the milling process (Fisher, 2007). Despite being a slow method and difficult to scale up, ball milling is efficient at producing small-scale batches for laboratory purposes (Hu *et al.,* 2001).

Generally, harder materials have a greater grindability (i.e. a finer particle size can be achieved) – Fisher, (2007). Particle toughness affects the size reduction of particles by resisting the propagation of cracks through the material. In tough materials, excess strain energy induces plastic deformation, rather than the production of new cracks. Mechanical size reduction is difficult for very ductile materials, whilst brittle materials are readily reduced; the point at which plastic and brittle transformations is recognised as important by Shariare *et al*., (2011) in their work on lactose micronisation. The size reduction of tough materials can be enhanced by reducing the temperature of the material, hence reducing its ability to flow plastically and rendering the particle more brittle (Fisher, 2007).

3.1.2.2. Bottom-up processes

Two commonly used bottom-up processes include spray-drying and supercritical fluid crystallisation (Rogers *et al.,* 2001). Spray drying involves drug dissolved in solvent being sprayed as a fine mist into a heated expansion chamber (Chawla *et al.,* 1994; Sarkari *et al*., 2002). The droplets dry, leaving tiny particles of drug that are collected at the bottom of the chamber. Spray-drying produces particles with greater sphericity than milling; however, the particles are mostly amorphous (Vidgren *et al.,* 1987). Supercritical fluid crystallisation employs the liquid-like density and gas-like transport properties of supercritical fluids to recrystallise drugs. They allow the solubility to be controlled by altering the pressure of the (anti)solvent (typically carbon dioxide or propane) to produce small particles (Schiavone *et al.,* 2004).

3.2. Materials

Cholesterol was obtained from Sigma Aldrich, UK, and stored below 0°C prior to micronisation and blending. Granulated vitamin C was also obtained from Sigma Aldrich, UK and stored in ambient conditions prior to micronisation and blending.

3.3. Methods

3.3.1. Characterisation

Individual batches of both cholesterol and vitamin C were combined and gently shaken to produce a single batch to be used throughout the study in order to normalise the characteristics of the mimic API, since controlling the particle size of several batches is known to be difficult during micronisation (Ticehurst *et al*., 2000). Particle size data of combined batches is given in Table 3.2.

3.3.1.1. Particle size

PSDs were obtained using the Mastersizer 2000 with Hydro SM small volume dispersion unit (section 2.2.2). This was chosen over the dry dispersion technique due to its greater ability to disperse cohesive materials. Vitamin C was suspended in the non-polar isooctane (Analytical Reagent Grade – Fisher Scientific, Loughborough, UK), whilst cholesterol was suspended in distilled water (Chen *et al*., 2009).

In order to stabilise suspensions and aid de-agglomeration for measurement, surfactants were added to the micronised mimic APIs. Cholesterol particles were measured via the addition of polysorbate 20 surfactant whilst vitamin C particles were measured via the addition of sorbitan trioleate (both in 1% w/w ratios) (Tee *et al*., 2000). Each sample was resuspended in the dispersant/surfactant and sonicated to enhance de-agglomeration, mixing was performed via a vortex mixer (Vortex Genie 2, Scientific Industries) for 30 s prior to measurement[1]. Table 3.2 shows particle size statistics for cholesterol and vitamin C before and after micronisation. Results are averaged from three individual experiments on combined micronised batches.

Images of milled mimic drug particles were obtained in order to confirm PSD data. Images were obtained by placing a small drop of drug suspension on a clean

[1] Surfactant was added to samples for measurement purposes only, no surfactant was used on the batches used in formulations due to surface adhesion effects.

microscope slide and using an Olympus BX50 light microscope in conjunction with a Leica Q500IW camera attached to a PC. Images were taken at 1000× magnification.

3.3.1.2. FTIR chemical composition analysis

Infrared spectroscopy utilises the property of molecules that makes them vibrate or rotate depending on the specific frequencies linked to their discrete energy levels (vibrational modes). These resonant frequencies are determined by the shape of the molecular potential energy surfaces, the masses of the atoms and, by the associated vibrational coupling. In addition, resonant frequencies can be related to the strength of the bond, and the mass of the atoms at either end of it. Thus, the frequency of the vibrations can be associated with a particular bond type (Paradkar and Irudayaraj, 2002).

FTIR analysis was employed to determine if the micronisation process required to reduce the particle size of vitamin C and cholesterol affected the chemical composition. The FTIR instrument used in this study was the Nicolet 380, Thermo Electron Corporation. The wavenumber range for cholesterol was based on that used by Kleiner *et al*., (2002) and Schafmayer *et al*., (2006); whilst the wavenumber range used for vitamin C followed that used by Chen *et al*., (2006). 400-4000 cm^{-1} with resolution of 4 cm^{-1} was the wavenumber range used in both cases. Measurements required approx 100 mg sample and were performed in triplicate.

3.3.1.3. Water sorption studies

Water sorption studies were performed on micronised cholesterol and vitamin C post milling and after prolonged storage at 40% RH and 20°C, and compared to the water sorption profiles of the unprocessed material to detect changes in surface characteristics. This method was also used to determine whether amorphous material was created due to the milling process, especially during increased milling times (Young *et al*., 2007b). Even relatively low levels of amorphous material (<10%), may have a detrimental impact on the stability, dissolution and adhesive characteristics of the formulated drug product. The water sorption study performed on these samples matched that used for lactose, as described in section 2.2.4.2.

3.3.1.4. Cohesivity of Micronised Mimic APIs

The cohesivity of APIs is an important consideration in the design of DPI formulations. Cohesive and adhesive compounds differ in their behaviour both during manufacture and on their fluidisation, entrainment, and deposition performance.

Many studies have shown that the flowability of powders can be linked to their cohesiveness (Kawashima *et al*., 1998a,b; Kumon *et al*., 2006; Zhou *et al*., 2009), however, only Zhou *et al*., (2010) have linked the aerosolisation performance of powders to their intrinsic cohesion. In their work, salbutamol sulphate, salmeterol xinafoate, triamcinolone acetonide were used based on their differing physicochemical properties, with cohesion being measured by an established shear cell method, and aerosolisation performance analysed by a twin-staged impinger.

The method used to test the cohesivity of micronised mimic actives is described in section 2.2.6.

3.3.2. Micronisation

Size reduction was performed using a planetary ball mill (Pulverisette 6, Fritsch, Germany) described in section 3.1.2.1. A 45 ml grinding bowl was half filled with 1 mm grinding media, based on recommendation by Fisher, (2007) in order to achieve a product size of ~1 μm. A 1:3 w/w cholesterol:water ratio was used with the bowl filled to the top to minimise the "foaming" of material caused by insufficient wetting of the material (Czekai and Seaman, 1999) and enhance the efficiency of the milling procedure. Without filling the bowl, particles rise to the surface and escape the impaction events that cause fracture, and hence size reduction. The procedure lasted ~2 hours (Fig. 3.7) with intermittent breaks to avoid the product and equipment overheating (Choi *et al*., 2004), rotation was set at 400 rpm.

Following milling, water was removed by a Büchner funnel, using 0.4 μm filter paper (Whatman, UK) before drying. Particle size was verified by laser diffraction and light microscopy (section 3.3.1.1).

Isooctane was used as dispersant medium for vitamin C to fulfil the criteria of being non-dissolving and for safety reasons, having relatively high boiling and flash points; it also has low viscosity, enabling shear forces to be imparted on the material. The same grinding media were employed as in the wet milling of cholesterol since the same

product size was desired. The length of milling time required was explored by checking the particle size of the product at regular intervals (Fig. 3.7). Following milling, solids were filtered and dried using a rotary evaporator. Particle size was verified by laser diffraction using the method described in section 3.3.1.1.

3.4. Results

3.4.1. Particle Size Data

Initial PSD data (Fig. 3.6) showed that unprocessed cholesterol contained ~10% material in the desired size range of 1-5 μm (Newman and Clarke, 1983). It was found that cholesterol suspensions separated on storage – larger particles floated on the surface of the liquid, whilst the smaller particles formed a suspension with the liquid (Fig. 3.5).

Fig. 3.6 and Table 3.1 show PSD data of unprocessed cholesterol, a sample of the particles that form the foam, particles in suspension and a homogenised sample (5 min at 10,000 rpm – IKA® T25 digital homogeniser, Ultra Turrax, UK). Particle size measurements were performed following 10 min sonication to aid de-agglomeration. It is clear from Fig. 3.6 that size reduction is required to produce a significant amount of particles in the desired size range. Homogenisation is not sufficient to reduce the PSD and although it removes the distinction of foam and suspension, the particles soon re-separate.

Table 3.1. Cholesterol PSD post milling, following filtration, drying and resuspension, after 5 min sonication.

	Particle size (μm)		
	d_{10}	d_{50}	d_{90}
Unprocessed	4.11	29.60	103.58
Suspension	0.45	1.51	67.66
"Foam"	11.53	98.75	252.94
"Homogenised"	6.24	63.49	221.26

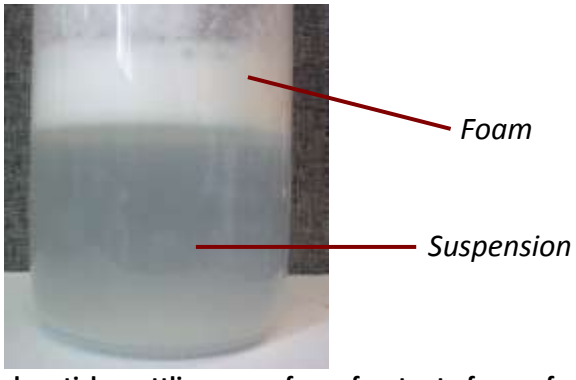

Fig. 3.5. Cholesterol particles settling on surface of water to form a foam and suspension.

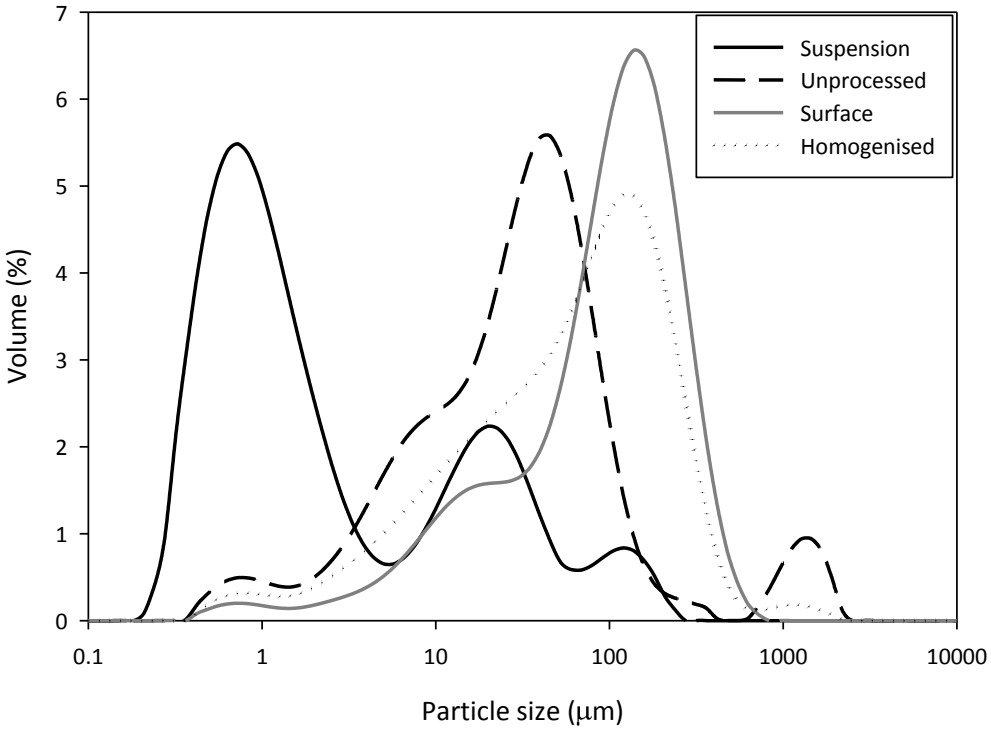

Fig. 3.6. PSDs of unprocessed cholesterol, homogenised cholesterol, material held in suspension, and material found in the foam on the surface of the suspension.

3.4.2. Micronisation

Fig. 3.7 shows that the optimum particle size for vitamin C could be achieved after just ~30 min compared to ~2 hours for cholesterol, possibly due to the hardness of vitamin C with respect to cholesterol, thus making the material more susceptible to fracture. Particle failure is the aim of size reduction; the particles are subjected to contact forces, between both themselves and the grinding media (Hennart *et al*., 2010). Contact forces deform particles and generate stress, which, if sufficient can produce fractures and cracks in the particle. The number and direction of these fractures determine the size and the form of the fragments and the surface of the particles (Chen *et al*., 2004). The type of deformation that occurs depends on the strain exerted on the particle; hence, either inelastic deformation or fracture may occur. Splits and cracks in the material are the source of inelastic deformation and fracture, with decreasing particle size, the elastic behaviour decreases as the plastic behaviour increases. This is the limit of the grindability and is dependent on the hardness of the material. Generally, harder materials have a greater grindability (i.e. a finer particle size can be achieved) – Fisher, (2007).

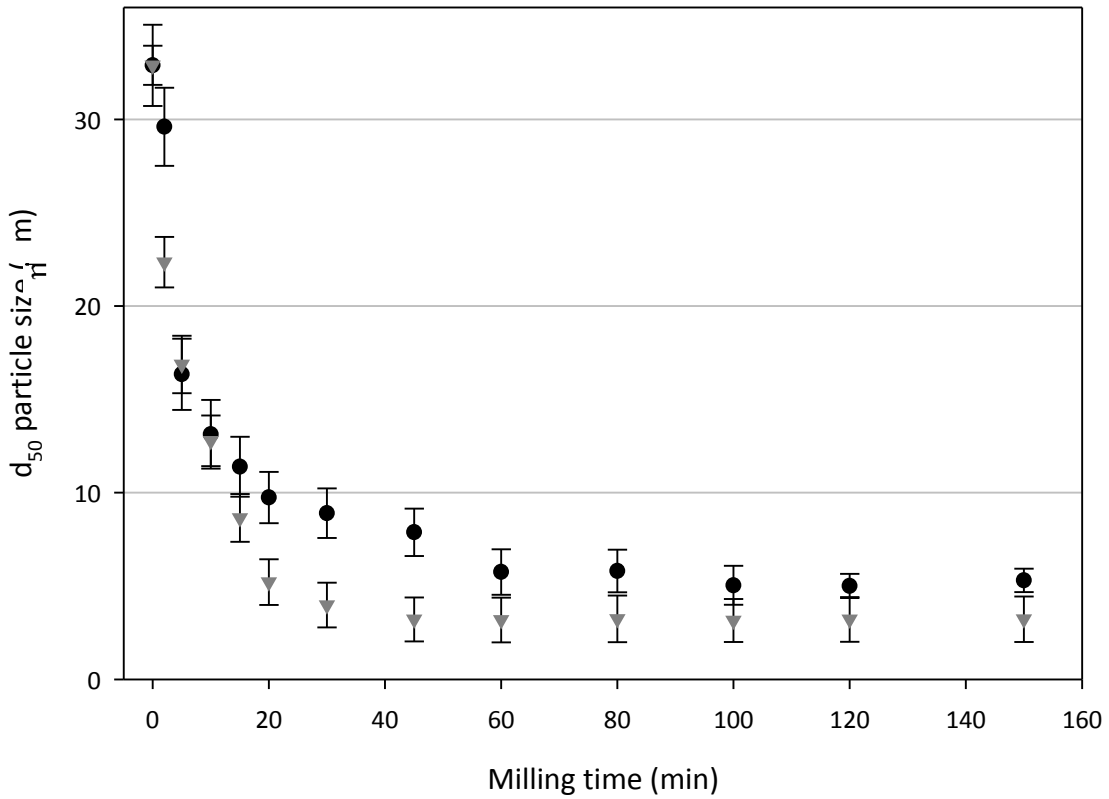

Fig. 3.7. Effect of milling time on the d_{50} particle size of cholesterol (●) and vitamin C (▼). Graph shows a plateau of particle size >120 min for cholesterol, and >30 min for Vitamin C, thus showing the maximum milling time required for each material.

The initial and final particle sizes of the combined batch of cholesterol and vitamin C is given in Table 3.2. Both batches fall within the limits of 1-5 μm for average particle size for APIs in DPI formulations defined by Newman and Clarke, (1983) and Zanen *et al.,* (1994). Light microscope images are shown in Fig. 3.8 and verify the laser diffraction PSDs.

Table 3.2. Cholesterol and vitamin C PSD post milling, following filtration, drying and resuspension with surfactant, after 5 min sonication.

		Particle size (μm)		
		d_{10}	d_{50}	d_{90}
Cholesterol	***Average***	1.51 ± 0.19	4.45 ± 0.29	11.47 ± 3.39
	Unprocessed	4.11	29.60	103.58
Vitamin C	***Average***	1.13 ± 0.21	3.21 ± 0.18	7.59 ± 0.75
	Unprocessed	1.50	32.90	99.51

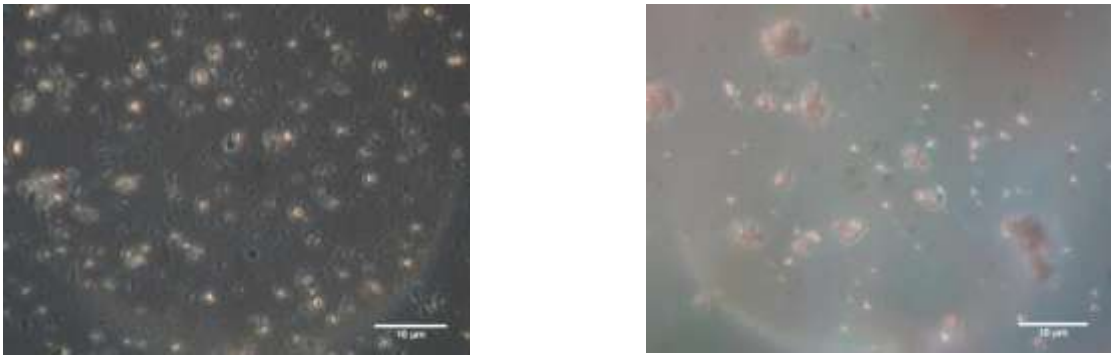

Fig. 3.8. Light microscope image of milled cholesterol (left), suspended in 1% w/w polysorbate 20:water solution, and milled vitamin C (right) suspended in 1% w/w sorbitan trioleate:isooctane solution.

3.4.3. FTIR analysis

Fig. 3.9 (cholesterol) and Fig. 3.10 (vitamin C) show FTIR spectra of micronised and non-micronised mimic drugs along with a description of the structural features that produce characteristic shape for each compound. FTIR analysis of both cholesterol and vitamin C showed that the micronisation process did not affect the chemical composition of either compound, with the absorbance spectra showing similar shapes and intensities across the wavenumber range for unprocessed material, material immediately post micronisation, and material stored under controlled conditions over the duration of this study (5 months).

Had any changes in the chemical composition of the micronised drug occurred from the micronisation process, this could have affected adhesion between drug and lactose particles, hence affecting the ability to relate changes in the adhesive properties to blending and storage regimes. The use of these micronised drugs is described in chapter 7.

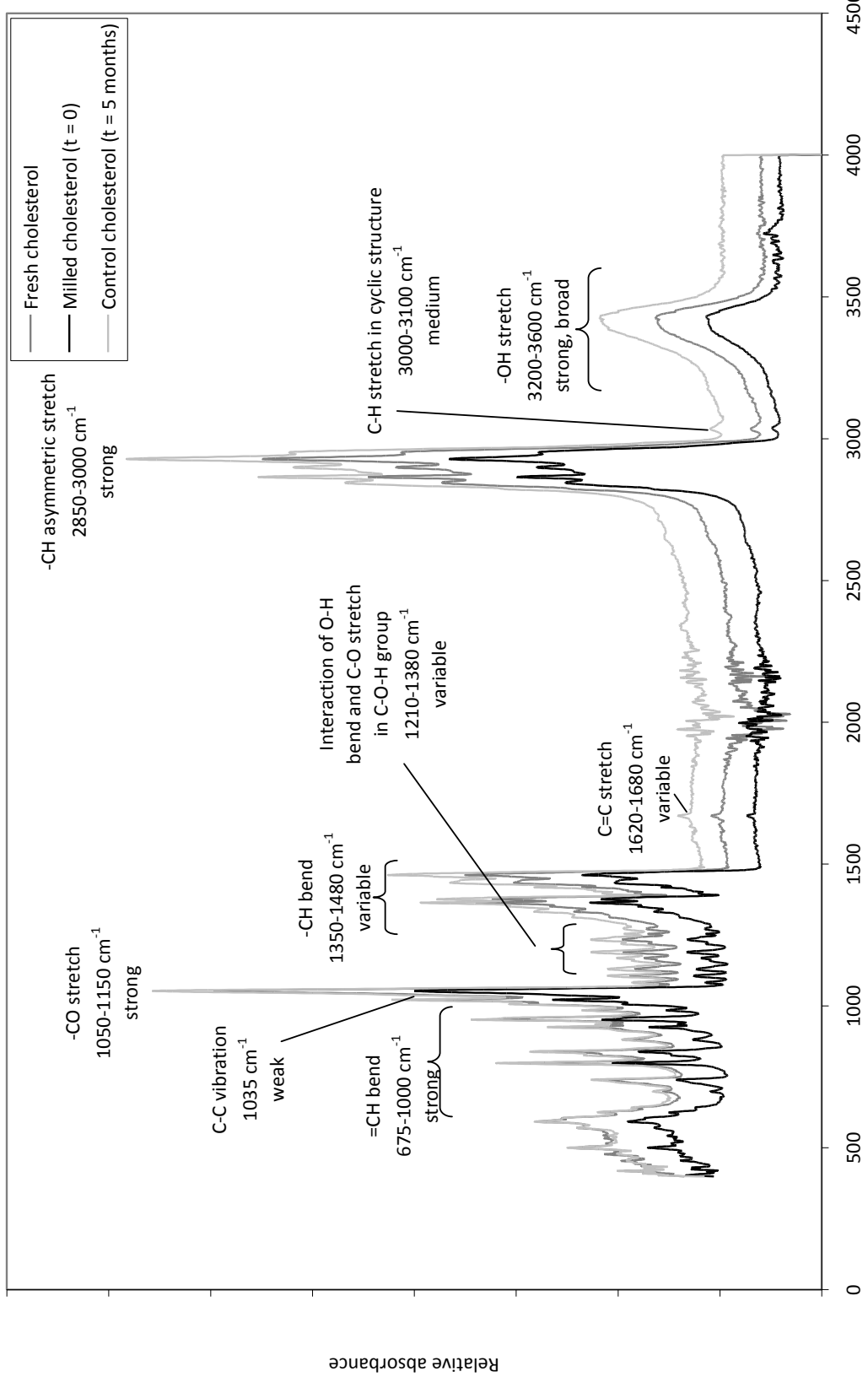

Fig. 3.9. FTIR spectrum of unprocessed and milled cholesterol. Plots have been shifted on x-axis to allow for easy comparison.

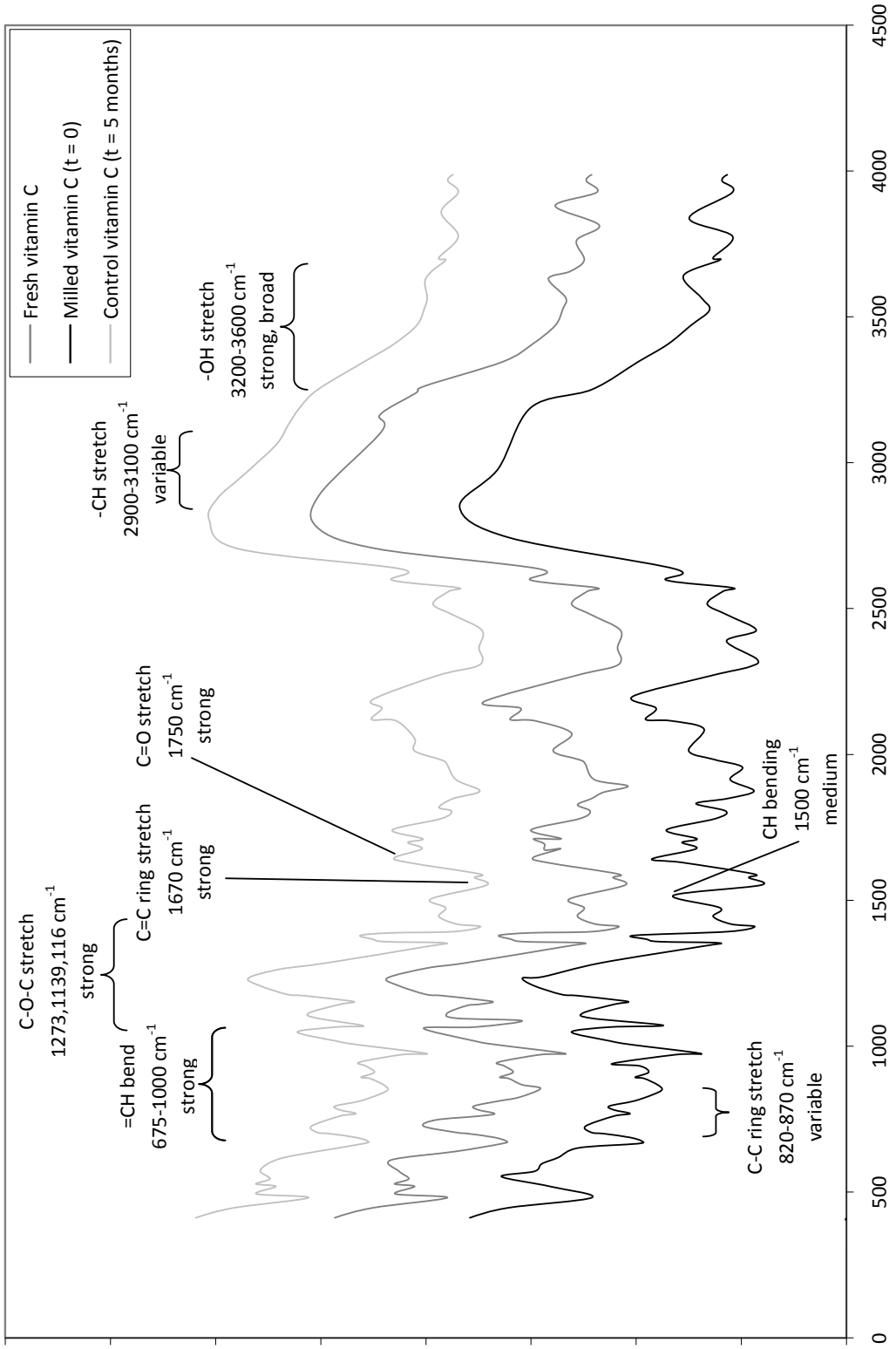

Fig. 3.10. FTIR spectrum of unprocessed and milled vitamin C. Plot s have been shifted on x-axis for easy comparison.

3.4.4. Water Sorption Studies

Water sorption isotherms for cholesterol are shown in Fig. 3.11. These isotherms show classic type II isotherm behaviour according to the BDDT classification (Brunauer *et al.,* 1940), where a significant uptake of vapour occurs at low partial pressures, followed by relatively low uptake at intermediate vapour concentrations, and then a further relatively large uptake at high partial pressures.

Micronised cholesterol shows a greater water sorption profile (greater uptake of water) than unprocessed cholesterol. The most likely explanation is an increase in surface area due to the reduction in particle size, or possibly the formation of amorphous regions on the particle surfaces (Ahlneck and Zografi, 1990). However, the formation of amorphous material was not detected via this method, unlike the work by Mackin *et al*., (2002) (Fig. 3.13), as no apparent collapse of isotherm due to any recrystallisation event was observed (Saleki-Gerhard *et al*., 1994; Buckton, 1995).

It can also be seen from Fig. 3.11 that no changes in the shape or magnitude of the isotherms can be observed due to storage at 40% RH and 20°C for five months, suggesting that the material is stable over this time period.

As with cholesterol, neither micronisation nor controlled storage of vitamin C appeared to induce any major changes in the crystallinity of the powder. The increased mass change of the micronised powder compared to the unprocessed vitamin C can again be attributed to the increased SSA (Bridson *et al*., 2007).

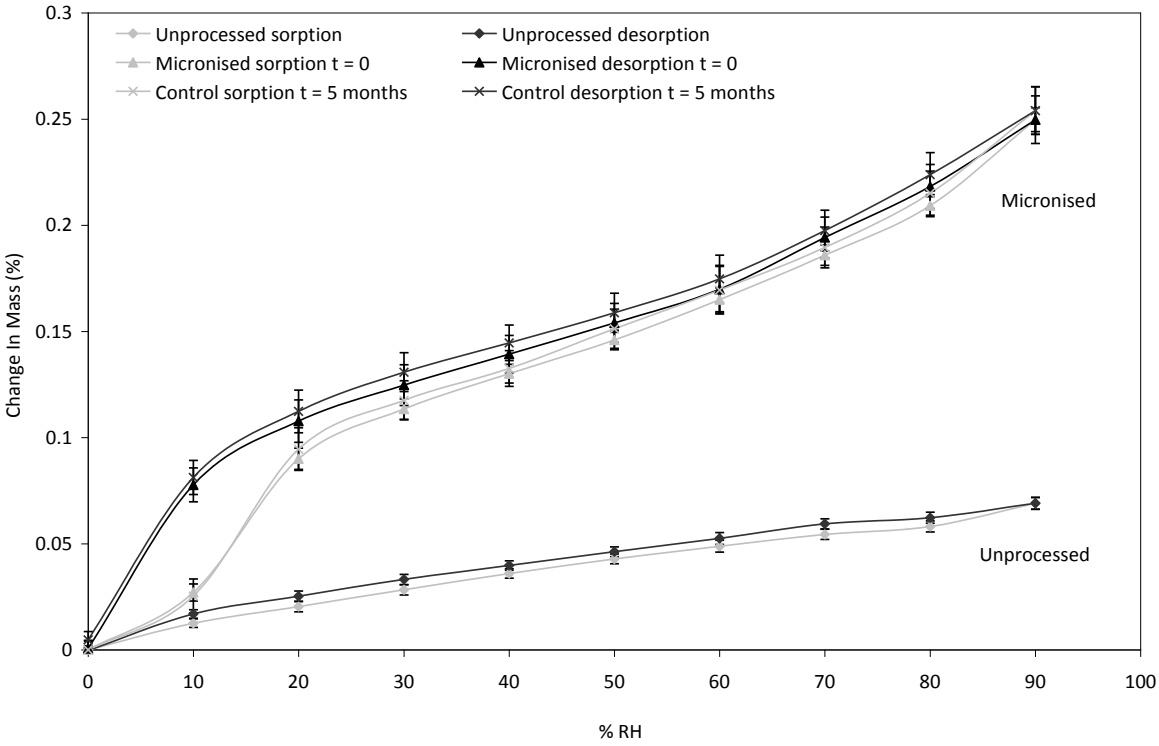

Fig. 3.11. Water sorption isotherms for unprocessed and micronised cholesterol – post micronisation and following five months storage at 20°C and 40% RH (control). Results show the average from three independent experiments ± SD.

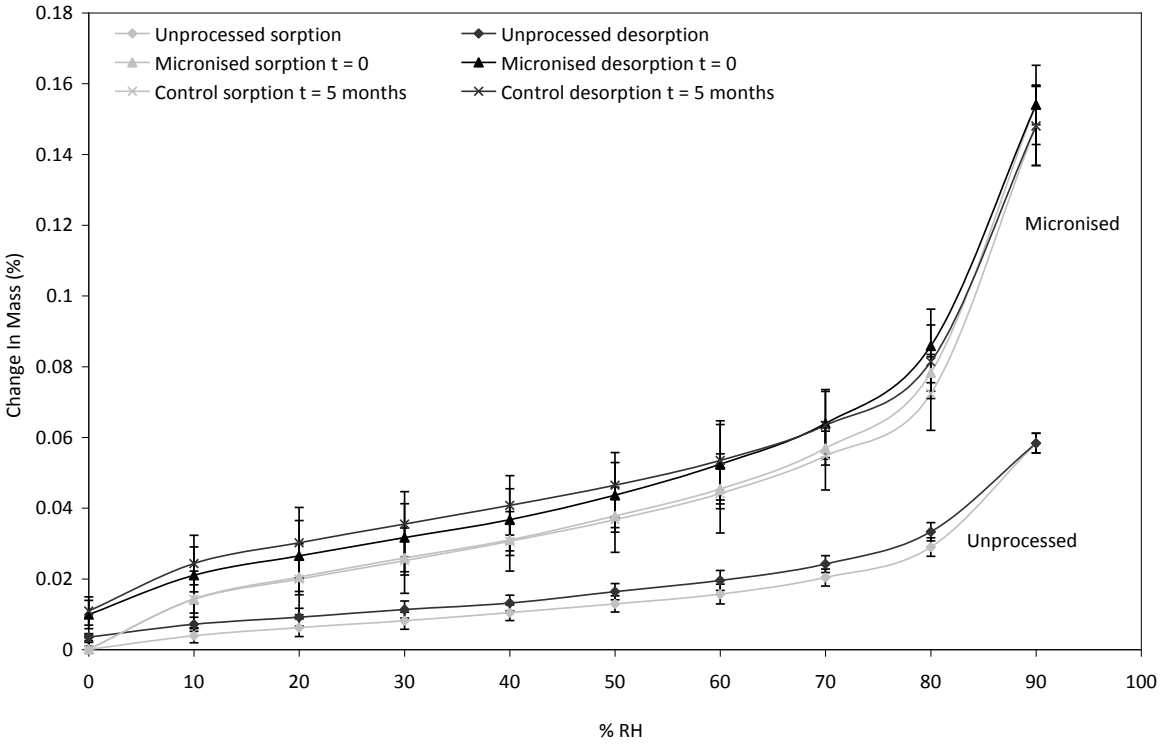

Fig. 3.12. Water sorption isotherms for unprocessed and micronised \vitamin C– post micronisation and following five months storage at 20°C and 40% RH (control). Results show the average from three independent experiments ± SD.

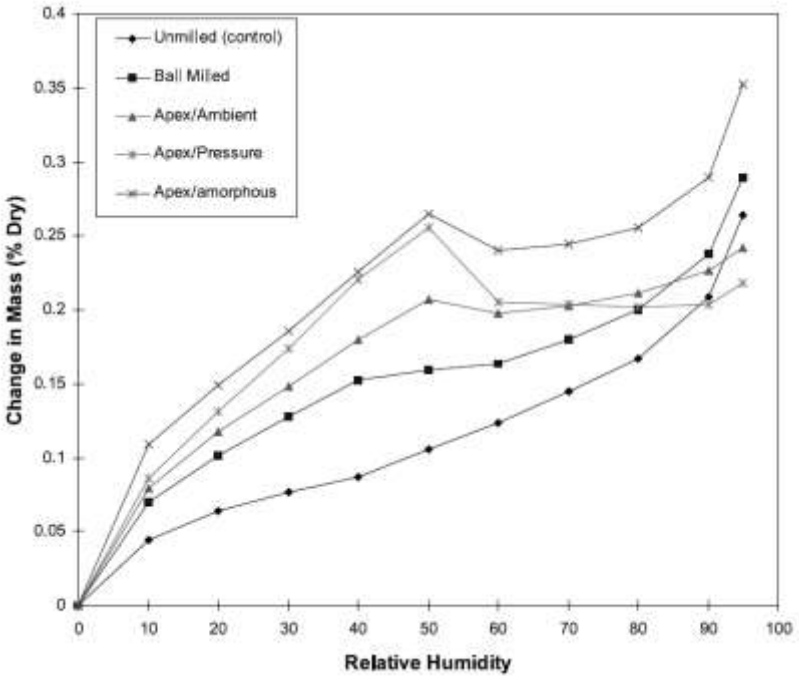

Fig. 3.13. Comparison of the moisture sorption profiles of milled xemilofiban active batches immediately after milling (taken from Mackin *et al.*, 2002). This shows the "collapse" in isotherms above 50% RH due to the introduction of amorphous material caused by the high energy milling process.

3.4.5. Cohesivity

Fig. 3.14 shows the normal stress vs. shear stress measurements for all powders used in this study in their original state, and - in the case of the mimic active ingredients cholesterol and vitamin C - following micronisation.

3.4.5.1. Deliberately coarsened samples

For comparison, deliberately coarsened samples of lactose were prepared by removing fine particles less than 25 and 71 μm by use of an air jet sieve (AJS). This provided samples had noticeably different flow properties. Many examples exist of previous work that employ an AJS to produce samples of lactose of a specific size fraction; Flament *et al.*, (2004) and Dickhoff *et al.*, (2006) are two such examples.

To produce these samples, 10 g of unprocessed lactose was sieved for 30 min at the maximum backpressure (3400 Pa) available, using the 25 μm and 71 μm sieves.

3.4.5.2. Results

Table 3.3 shows the calculated flow functions from the shear tests performed in order to compare cohesivity of powder used in this study. The materials used in this thesis have FFs that compare with materials used in previous DPI literature.

Zhou *et al.*, (2010) used micronised salbutamol sulphate and salmeterol xinafoate in their study and found flow function values of 1.91 and 1.27 respectively for the untreated powder.

Edwards *et al.*, (2009) found the flow function of a 25:75 fine (d_{50} = 8 μm):coarse (d_{50} = 61 μm) lactose mixture to be 3.10 (2.50 following four weeks of storage at ambient conditions).

Tuley *et al.*, (2008) found a flow function of 7.30 for lactose with 6% fines <15 μm (d_{50} = 80 μm), and a flow function of 2.45 for lactose with 16% fines <15 μm (d_{50} = 70 μm) – the latter being more akin to the unprocessed lactose used throughout this study.

Mullarney and Leyva, (2009) find flow functions between 1.2-28.5 for APIs, excipients and blends of the two with volume mean diameters between 2-457 μm.

All results found in the literature described above fit with the typical ranges described for powdered bulk materials (Jenike, 1964).

Differences in flow functions of micronised cholesterol and vitamin C can be attributed to differences in particle size and cohesivity. The flow functions of micronised cholesterol and vitamin C cannot be affected by particle size alone since cholesterol shows inferior flow properties despite being a coarser material. Therefore, particle shape and chemistry must play a role in the cohesivity of these materials. However, for the purpose of this study, they have notably different cohesivities, which should affect the behaviour of their constituent formulations in the physical tests described in the following chapters.

Table 3.3. Flow functions (f_c) of powders used in this study. Results show average from three independent experiments on each material with error the SD of the mean and are rounded to two decimal places.

Material	*Symbol (Fig. 3.14)*	*Gradient*	*Flow function, f_c*
Unprocessed lactose	◆	0.23	3.92 ± 0.44
25 μm lactose	●	0.06	17.86 ± 2.02
71 μm lactose	○	0.03	33.22 ± 2.22
Unprocessed vitamin C	□	0.03	32.26 ± 4.44
Unprocessed cholesterol	△	0.20	5.05 ± 0.58
Micronised vitamin C	■	0.51	1.94 ± 0.34
Micronised cholesterol	▲	0.72	1.39 ± 0.23

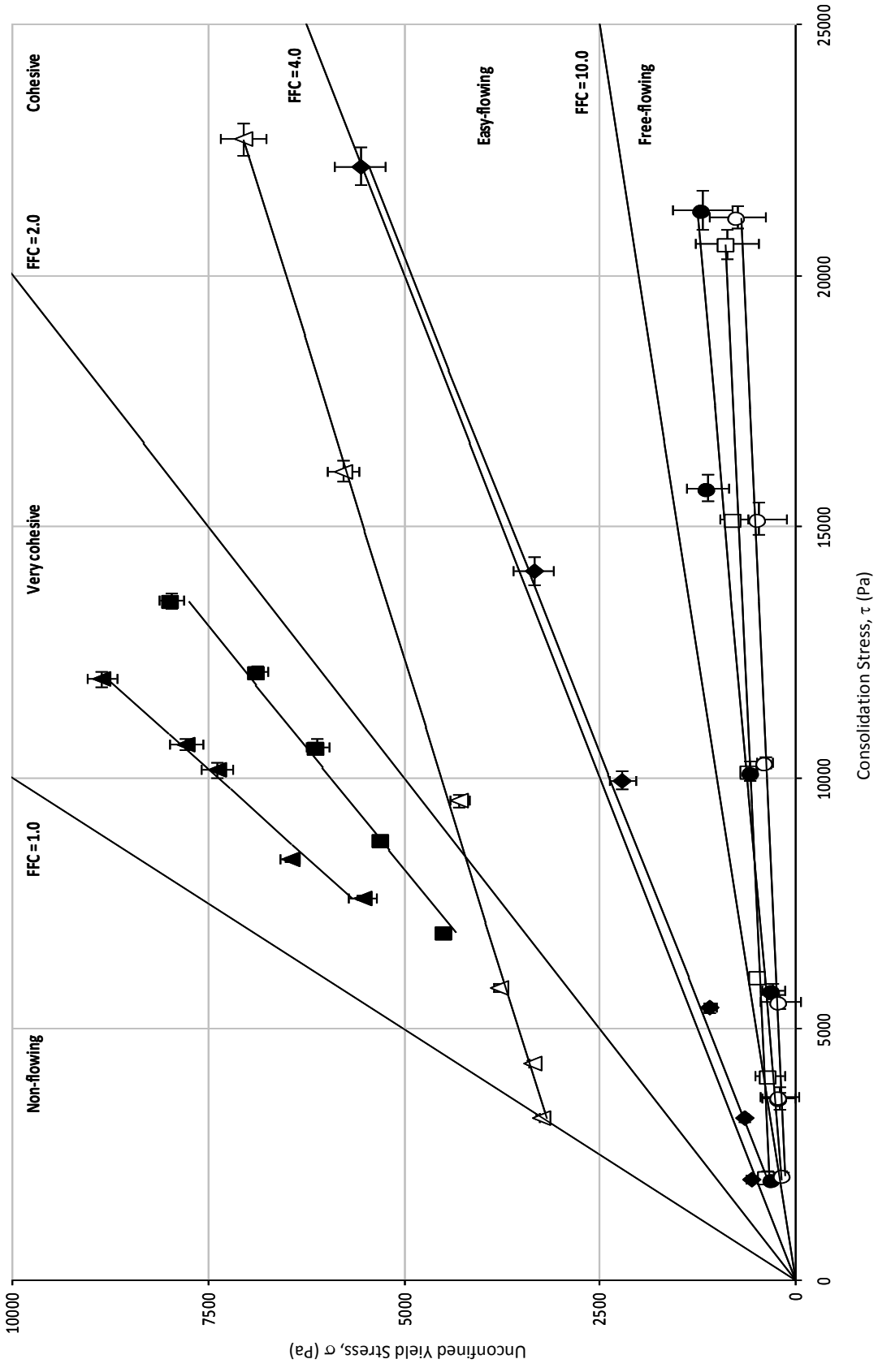

Fig. 3.14. Unconfined yield stress (σ) vs. consolidation stress (τ) measurements of powders used in this study. ◆- Unprocessed lactose; ● - 25 μm lactose; ○ - 71 μm lactose; □ - Unprocessed vitamin C; △ - unprocessed cholesterol; ■ - micronised vitamin C; ▲ - micronised cholesterol.

3.5. Blend Homogeneity

A key objective of any blending process is to achieve a uniform mixture of all ingredients including both active and excipient(s); homogeneity is a key property of high quality formulations (El-Hagrasy *et al*., 2001). A lack of content uniformity often leads to product recall by the FDA for sub- or super-potency. Recalls for sub-potency represented the second most common reason for drug recalls in 1999[1].

Formulation homogeneity is often defined to be achieved when the coefficient of variance (CV) value is <6% (Crooks and Ho, 1976). Recent literature CV values for DPI formulations are shown in Table 3.4 and have been used as a basis to assess the formulations produced throughout this study.

CV is defined as the normalised measure of dispersion within a probability distribution, calculated as the ratio of the standard deviation (σ), to the mean (μ) (Equation 3.1).

$$CV = \frac{\sigma}{\mu} \qquad \textbf{Equation 3.1}$$

Table 3.4 shows a selection of recent publications and typical CVs produced by their blending regimes.

Table 3.4. Typical blend homogeneity results from previous work, showing coefficients of variation and mean recovery related to the nominal dose to describe the homogeneity of the blend (TBS = terbutaline sulphate).

Paper	*Carrier/drug blend*	*Average content of drug (μg)*	*Mean recovery related to the nominal dose*
Thi et al., (2008)	Inhalac 120/spray-dried TBS	499.47 (CV = 1.84%)	99.9%
	Inhalac 230/spray-dried TBS	488.56 (CV = 0.92%)	97.7%
	Lactohale 100/spray-dried TBS	477.49 (CV = 0.77%)	95.5%
	Lactohale 200/spray-dried TBS	482.74 (CV = 1.30%)	96.5%
Flament et al., (2004)	Lactose A (63–90 μm)	491.25 (CV = 4.5%)	98.2%
	Surface Roughness 3605 ± 657		
	Lactose B (63–90 μm)	492.5 (CV = 14.33%)	98.5%
	Surface Roughness 2691 ± 462		
	Lactose C (63–90 μm)	500.5 (CV = 7.35%)	100.1%
	Surface Roughness 3135 ± 742		
Flament et al., (2006)	Pearlitol 100 SD/terbutaline sulphate	483.45 (CV = 2.25%)	96.69%
	Pearlitol 110 C/terbutaline sulphate	478.00 (CV = 4.79%)	95.6%
	Lactose 250 SD/terbutaline sulphate	504.57 (CV = 0.76%)	100.9%

[1] http://www.fda.gov/cder/reports/ rtn00-3.htm

3.5.1. UV Spectroscopy

Ultraviolet (UV) spectroscopy was used to determine average drug content in formulations. The mimic drug compounds both exhibit UV absorbance at specific wavelengths, on the other hand, lactose does not possess a UV absorbing chromaphore in its structure. Therefore, the presence of lactose does not affect the UV absorbance of the mimic drug compounds (Hegedüs *et al*., 1999; Ganesh *et al*., 2009; Shahi *et al*., 2008). Drug content methodologies were important to this project as they were required for two separate measures of formulation performance – the homogeneity of the formulation post-blending, and determination of the average drug content during drug detachment studies - FBE (chapter 5), AJS (chapter 6), and cascade impactor (chapter 7).

3.5.2. Cholesterol Assay Method

The average content of cholesterol in a blend was determined by UV spectroscopy at 205 nm (Brown, 1986; Hoving, 1995; Choudari *et al*., 1996; Mazalli *et al*., 2006). Being hydrophobic, a non-polar solvent is required, Choudari *et al*., (1996) used methanol, which proved to be the best solvent for this application. Acetone, propan-2-ol and ethanol were also investigated; however, they either produced excessive absorbance at the desired wavelength (acetone), or gave unstable measurements (propan-2-ol and ethanol). As a non-polar solvent, methanol does not dissolve lactose; hence, the lactose particles remain in suspension and will adversely affect the UV absorbance by physically blocking the light. To remove the lactose particles, the use of solvent mixtures were investigated (water and methanol/propan-2-ol/acetone/ethanol), however, despite being miscible, the UV absorbency remained unstable and repeatable results could not be obtained.

As an alternative, the lactose particles were removed by a centrifuge in a method similar to that used by Waites and Morgan, (2001), de Boer *et al*., (2004) and Dickhoff *et al*., (2006).

The methanol/cholesterol solution and suspended lactose particles were centrifuged for five minutes at 3000 rpm (de Boer *et al*., 2004; Dickhoff *et al*., 2006) and the supernatant was removed using a pipette. Cholesterol concentrations were analysed using a UV spectrophotometer (Jasco, UK) at a wavelength of 205 nm. A linear

calibration curve was produced for cholesterol concentrations below 100 μg ml^{-1}, and is shown in Fig. 3.15.

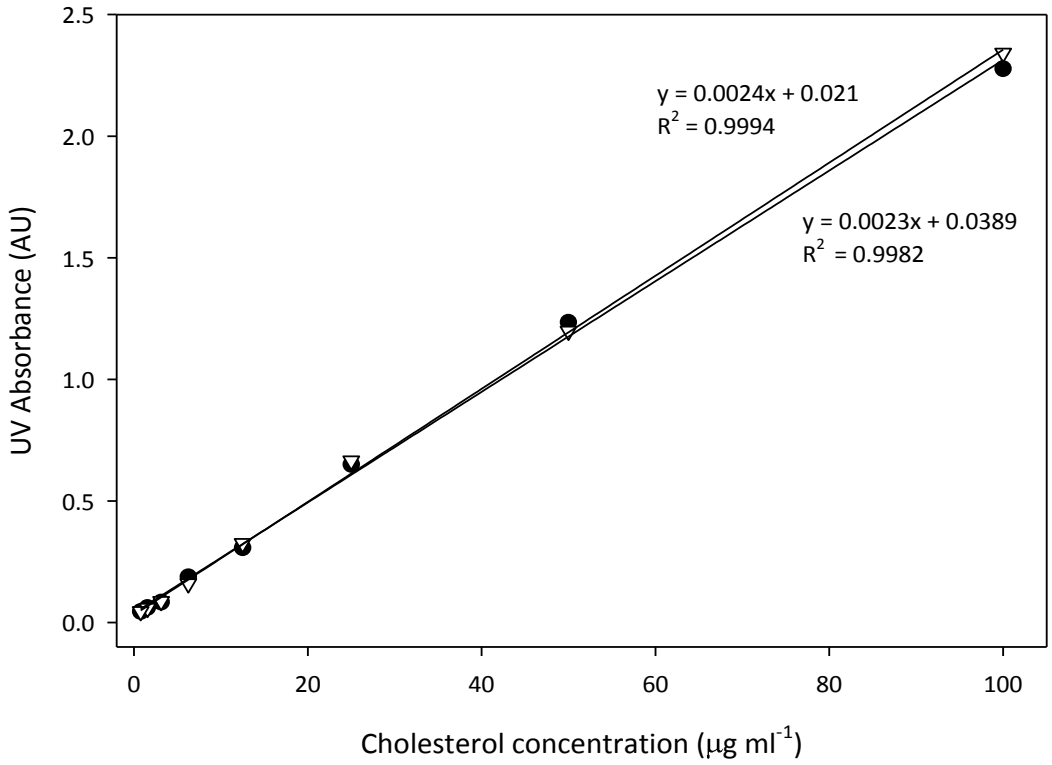

Fig. 3.15. Calibration curve for cholesterol/methanol solution, after centrifugation to remove suspended, non-dissolved lactose particles. The different drug:lactose ratios of 1.5% (▽) and 15% (●) show that the presence of lactose does not have an effect on UV absorbance (measured at 205 nm).

3.5.3. Vitamin C Assay Method

The average content of vitamin C in a blend was determined by UV spectroscopy at 225 nm following a wavelength scan between 200 and 300 nm that showed peak absorbance at 225 nm. Many studies report peak UV absorbance of vitamin C across a range of wavelengths; hence, a spectrum scan was required. The use of UV spectroscopy for vitamin C assays is difficult due to its instability in aqueous solutions (Kwakye, 1997, 2000) due to its reversible oxidation to dehydroascorbic acid, and subsequent, irreversible oxidation to 2,3-diketo-L-gulonic acid. Antioxidants can be added to these solutions to inhibit these reactions by providing a hydrogen atom or electron (Lachman *et al*., 1976), thus, sodium phosphate (0.5% w/w) was added to the water as a buffer solution in order to stabilize the UV absorbance. Unlike the cholesterol assay, the solvent dissolves both lactose and vitamin C, thus centrifugation is not required to separate suspended particles.

A linear calibration curve was produced for vitamin C concentrations below 100 μg ml^{-1} with the presence of lactose shown to have no effect on UV absorbance at this wavelength. A linear calibration curve was produced for cholesterol concentrations below 100 μg ml^{-1}, and is shown in Fig. 3.16.

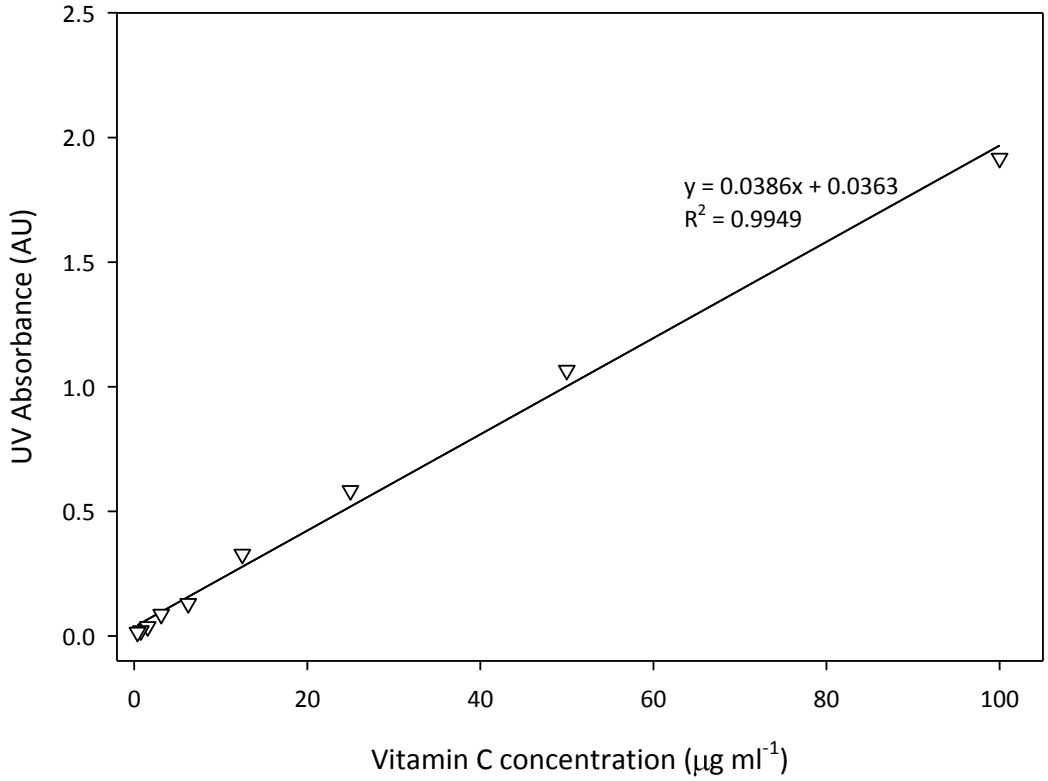

Fig. 3.16. Vitamin C calibration curve for 1.5% vitamin C:lactose solution in 0.5% w/w sodium phosphate buffer solution. UV absorbance measured at 225 nm.

3.6. Conclusion

This chapter has described the production and characterisation of the mimic APIs to be used throughout this study. Both cholesterol and vitamin C have been micronised such that their average particle size is within the 1-6 μm size range, as recommended throughout DPI literature. Tests have shown that the cohesivity of these drugs is noticeably different, and coupled with their different affinities to water, their adhesive behaviour with respect to lactose is likely to be different. In addition, the stability of the micronised compounds is not affected by long term storage at controlled conditions (40% RH and 20°C), therefore these mimic actives are suitable for use in the final chapter, which assesses the effect of blending and storage on fine particle adhesion.

4.0. Effects of High Shear Blending on α-Lactose Monohydrate

ABSTRACT

α-lactose monohydrate is an important excipient used in dry powder inhaler (DPI) formulations. It is commonly blended with active ingredients in a high shear blending (HSB) process – required to disperse effectively the cohesive, micronised drug particles. This study explores the effect of HSB on some of the physicochemical properties of α-lactose monohydrate such as particle size distribution (PSD), surface area and morphology.

Experiments were carried out using laboratory-scale HSB equipment with initial trials performed to determine optimal blending regimes characterised by good powder turnover and bowl stability. A series of formulations were produced using a range of blending conditions with the sampling of powder performed at regular intervals in order to determine the effects of specific energy input (SEI) on the physicochemical properties of lactose. The final part of the study involved the production of formulations containing mimic API in order to determine the SEI required to achieve chemical homogeneity.

Results showed that lactose exposed to low SEIs underwent de-agglomeration, which then reversed, subsequently increasing the particle size by agglomeration with additional energy input. This effect was observed across all scales, although the rate at which this phenomenon occurred varied, with larger equipment showing a more rapid increase of particle size with respect to SEI.

4.1. Introduction

The key secondary manufacturing step in the production of dry powder inhaler (DPI) formulations is the blending of excipient with active pharmaceutical ingredient (API). This is commonly achieved through use of high shear mixing – primarily to facilitate the dispersion of the extremely cohesive, micronised, API in order to achieve a homogenous, well-ordered product. This chapter will investigate the effect of specific energy input (SEI) on PSD of inhalation-grade α-lactose monohydrate and covers the blending scale-up effect produced by different equipment geometries.

Blade shape, size, and height is known to affect the torque generated by a blade impeller (Equation 4.1), but these blade variations are not studied in the current work. In the experiments described throughout this study, fixed impeller geometry was used for each scale to determine the effect on energy addition due to changes in the impeller speed and blending time (Knight *et al*., 2001).

Blade geometry and speed are considered the primary factors that determine the shear rate and, consequentially, the power imparted to the powder, one of the factors that may influence the particulate cohesive/adhesive strength (Wagner *et al*., 2009). Specific energy input is then dependant on the time for which the particular power is delivered (Equation 4.2).

4.1.1. Secondary Manufacturing of DPI Formulations

Pharmaceutical powder blending is a key process in the manufacture of DPI formulations. HSB is used when the effects of impaction are desired to produce an ordered mixture, which is difficult to create using low shear blending which produces more random outcomes (Wagner *et al*., 2009). HSB exposes powders to a variety of forces, both attractive (van der Waals forces, electrical forces and – during granulation – liquid bridges) and dispersive (rotation, shear and gravitational). These forces are strongly influenced by a range of blending parameters (Knight *et al*., 2001), thus studies to characterise and understand the effects of blending on the formulation and the impact on powder properties are necessary. Blend parameters are carefully monitored in order to control the critical quality attributes of the final inhaled formulation, such as emitted dose, chemical homogeneity, and fine particle fraction (FPF) (Pilcer and Amighi, 2010).

Bridson *et al*., (2007) showed that total energy input in the blending process could have profound consequences on the final product. The primary effect observed was an agglomeration of powder with increased SEI; it was proposed that this could lead to decreased FPF and poorer particulate dispersion. The power supplied to the impeller in a high shear blender is considered the primary source of this energy input into the material (Equation 4.1 and Equation 4.2, section 4.2.3).

High-shear processing of pharmaceutical powders can potentially cause changes in the physicochemical properties of the active ingredient, the excipient, and the interactions between the two. HSB processes have been preferred over low shear processes due to its ability to improve dispersion of fine materials, and hence can produce a beneficial effect on dose content uniformity (Malcolmson and Embleton, 1998). Conversely, HSB processes may damage particles thus generating intrinsic fines and/or induce high-energy biding sites on the surface that can affect the formulation properties. In addition, blends manufactured using a high shear process are likely to change over time with varying storage conditions as material "relaxation" occurs, potentially causing inconsistent formulation performance (Edwards *et al*., 2009).

As described throughout chapter 1, slight changes in the properties of these materials can have profound implications on the performance of DPI formulations, thus careful consideration needs to be made regarding the magnitude of these effects caused by the blending procedure.

4.1.1.1. Importance

Powder blends can be classified into two main types: free-flowing and cohesive. Free-flowing powders comprise particles that do not tend to agglomerate and are not strongly affected by interparticle forces. On the other hand, cohesive powders do not flow readily due to the strong interparticle forces between the particles, causing agglomeration of multiple particles. The type of cohesive force (electrostatic, van der Waals, etc.) determines the overall cohesiveness of the material; this is influenced by surface charge, moisture, and particle size and particle shape (Muzzio and Alexander, 2005). Cohesive nature increases as the particle size decreases, and this generally occurs during micronisation of drug substances. Micronisation of drug substances can result in an increased risk of segregation within the blend, reducing chemical homogeneity; thus, shear forces are often used to improve the dispersion of the drug

substance and overcome the cohesiveness of the formulation. The importance of blend homogeneity is described in section 3.5.

4.1.1.2. Scale-up of blending procedures

Systems that are geometrically-similar have constant ratios of linear dimensions. Kinematic scale up enables systems of different size to have similar ratios of velocities between two points in the systems. However, equipment of different sizes are geometrically similar if, in addition to being geometrically and kinematically similar, the ratios between corresponding points in the systems are equal (Wang and Fan, 1974). During dynamic scale-up, as the batch size is increased, the forces experienced by the powder are also increased, partly due to the increase in formulation mass, but also due to the increased impeller tip speeds. Cohesive forces between particles have been shown to reduce as the blender size is increased and a result of the greater shear forces experienced. This study will explore the effect of changing equipment geometry on the characteristics of lactose. Using different equipment geometries allows factors such as *Fr* and tip speed to be investigated at different scales.

To improve mixing, it is preferable to have equally dispersed ingredients throughout the blender. Layering or "sandwiching" the small amounts of active ingredients between excipient (Fig. 4.6) has been shown to be useful in producing a uniform blend (Sudah *et al*., 2002b). Since the mixing of cohesive powders is primarily influenced by shear rate (dependent on material and equipment) and blender speed (dependent on equipment only) (Muzzio and Alexander, 2005), intensifier bars have been shown to enhance the shear forces experienced, whilst strategically-placed baffles introduce asymmetry into the mixing regime which has also increased the mixing efficiency (Brone and Muzzio, 2000).

A "blending window" can be found by experimental design to determine the optimum conditions for producing a homogeneous blend. Blade speed, blender fill volume, blend time and blender geometry all influence blend uniformity (Alexander and Muzzio, 2005). The Froude number (*Fr*) has been suggested for use in scale-up processes, along with the tangential (linear) velocity of the impeller, especially when similar geometries are considered (Fig. 4.1). The linear velocity remains constant if the rotational speed is adjusted in line with the size of the bowl (inversely proportional). Deviations from predictions using *Fr* can often be experienced if scale-up is between blenders with different geometries of if different fill volumes are used (Alexander and Muzzio, 2005).

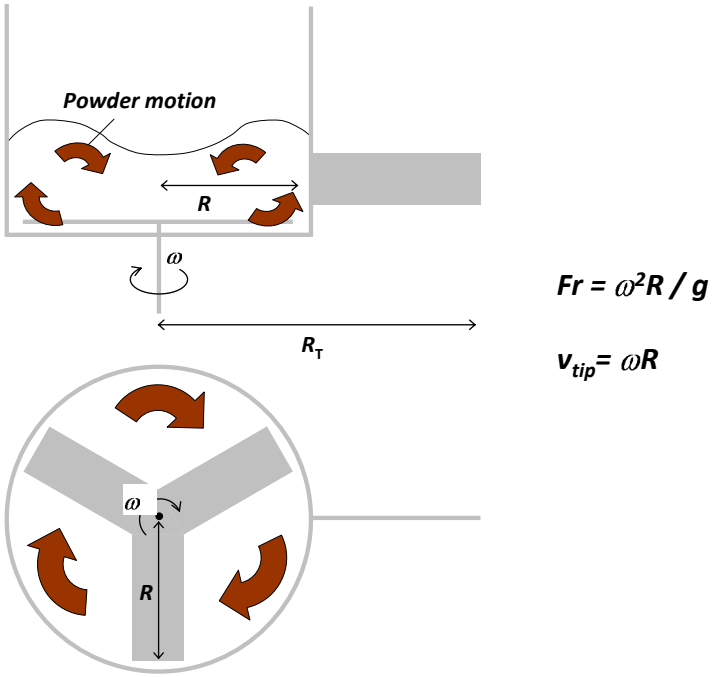

Fig. 4.1. Definition of Froude number (*Fr*) with respect to the equipment used throughout this study. ω is the angular velocity of the impeller, *g* is the acceleration due to gravity, *R* is the impeller radius, and R_T is the distance between the centre of the bowl and the force transducer.

An understanding of the impact of changes that occur during scale-up is vital in maintaining optimum mixing efficiency. Blend uniformity sampling is an important step in this process since the homogeneity of the final powder blend will correlate to the uniformity of the final drug product (although significant post-blend processing may also affect the distribution) (Kraemer *et al.*, 1995). Problems with the sample thief method for measuring blend uniformity have been discussed (Kreamer *et al.*, 1999; Garcia *et al.*, 2001) and recent developments have proposed alternatives. Process Analytical Technologies (PAT) (see section 1.7) such as near infrared (NIR) methods have enhanced the way in which blend uniformity and scale-up effects have been monitored (Liew *et al.*, 2010). PAT enables a more rigorous, scientific approach to scale-up to be performed, whilst NIR can be used to produce instant results to control variability in blend homogeneity (Hailey *et al.*, 1996; El-Hagrasy *et al.*, 2001).

4.2. Materials and Methods

4.2.1. Lactose

As the most frequently used excipient in DPI formulations, this study uses the inhalation-grade lactose described in section 2.2.1. As APIs typically comprise less than 2% of the formulation by weight, effects of blending on pure lactose should not be

significantly affected by the absence of drug. The initial particle size data for lactose used in this chapter is: d_5 = 3.10 ± 0.02 μm; d_{10} = 9.32 ± 0.10 μm; d_{50} = 68.65 ± 0.01 μm.

4.2.2. Micronised Mimic APIs

Tests were performed using cholesterol and vitamin C (Sigma Aldrich, UK) as mimic APIs (section 3.2), the methods for micronisation and characterisation of these materials is described in section 3.3. The d_{50} particle size of these mimic actives lay within the 1-5 μm aerodynamic diameter specifications defined by Newman and Clarke (1983): d_{50} (cholesterol) = 4.45 ± 0.29 μm; d_{50} (vitamin C) = 3.21 ± 0.18 μm. 500 g blends containing 1:67.5 w/w (common payload used in previous literature - Table 1.2) mimic actives were prepared using the method described in section 4.2.4 using the small bowl with impeller speed 500 rpm. Samples of formulation were taken at regular intervals using the method described in section 4.2.5, and assayed via the methods described in section 3.5.1.

4.2.3. High Shear Blending Equipment

Cylindrical, stainless steel bowls, with a flat base, vertical side walls and internal diameter 0.13, 0.16 and 0.21 m (Fig. 4.2) were mounted on bearings supporting them and allowing free rotation in the horizontal plane.

Fig. 4.2. Three bowls used throughout the study.

In order to measure the torque generated, rotation was prevented by an arm attached to the bowl that rested against a load cell that was fixed to the apparatus structure. The torque was calculated from the measured load. The drive shaft was projected into the centre of the bowl, and was driven by a 7.5 kW three-phase DC motor (Fig. 4.3), which allowed rotational speeds of 30-1100 ± 5 rpm to be achieved. Instantaneous torque

measurements were recorded at regular intervals (5 min) and averaged over the duration of the blend (Knight *et al.*, 2001).

Fig. 4.3. Small bowl with lid shown resting on bearings driven by the 7.5 kW motor.

Fig. 4.4. Three-blade impellers for the small and large bowls used in study.

Three-blade impellers were used (Fig. 4.4) with a constant width in the horizontal plane of 50 mm, and 10 mm depth. Blades with bevelled with 11° angle with 1 mm of the leading edge left vertical, so that the blades were not sharp. Both the blades and bowls were finished with a machined surface.

The power input P (W) into the powder during blending can be given by the equation:

$$P = \frac{2\pi R_T FN}{60} \qquad \textbf{Equation 4.1}$$

where, R_T is the radial distance from the axis of rotation to the force transducer (m), F is the force measured by the transducer (N), and N is the rotational speed of the impeller in (rpm). The force applied to the powder formula is dependent upon the impeller speed and the mass of powder used. The greater the mass or rotational speed, the greater the force applied to the system.

Since power is defined as the work done in unit time, the energy applied to the blend can be given by:

$$E = \int_0^t P dt \qquad \textbf{Equation 4.2}$$

where, t is the period of time for which the force is applied to the system.

The impeller speed and mass loadings were in line with other HSB work on lactose using similar equipment (Bridson *et al.*, 2007; Wagner *et al.*, 2009). Bridson *et al.*, (2007) employed the same equipment (0.13 m diameter bowl) used in this study with impeller speeds between 200 – 600 rpm and mass fills in the range 300 g – 700 g. Wagner *et al.*, (2009) used 0.75 kg and 1.2 kg mass fills in 1-litre and 2-litre vessels, with a constant impeller speed (400 rpm or 700 rpm) and constant vessel fill volume (50% or 80% fill volume). The mass loadings used in this study are described in the experimental procedure section below.

In order to calibrate the load cell, the transducer was removed from its horizontal location on the apparatus frame and placed in an upright position and subjected to various weight forces from known masses. Three calibration curves (the calibration was repeated at regular intervals throughout the study and showed the load cell response was consistent) used to determine the force applied to the load cell during blending experiments are shown in Fig. 4.5.

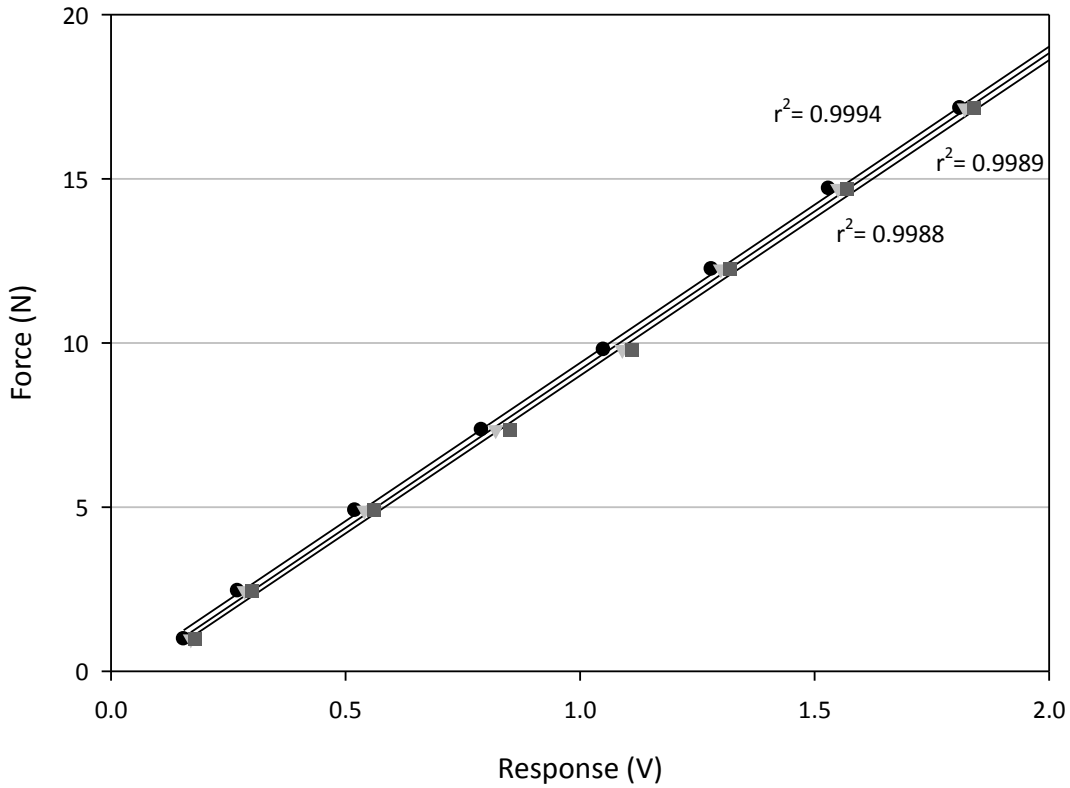

Fig. 4.5. Three separate load cell calibration curves used in determining the force produced during blending.

4.2.4. Bowl Filling

Formulations containing mimic API were prepared by filling the bowl in a stratified manner (Popo *et al.*, 2002), with three equal layers of drug sandwiched between four equal layers of lactose (Fig. 4.6). As each successive level was added, the powder was

levelled by gently shaking the bowl, with sampling performed via a powder thief at vertically and radially different locations throughout the bowl.

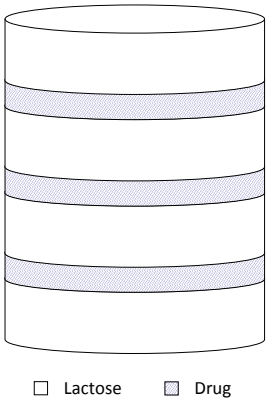

Fig. 4.6. Stratified filling of lactose and drug in bowl (Not to scale).

4.2.5. Sampling Procedures

Powders can be defined as free-flowing or cohesive. Free-flowing powders are prone to segregation during handling and storage, and individual samples are rarely representative. Cohesive powders are more likely to retain their bulk characteristics during handling, but are still prone to segregation during manufacture or packaging.

Handling of free-flowing powders can result in size segregation, thus the size distribution of particles in a powder is influenced by its previous history. Free-flowing powder poured into a heap will show a tendency for the fine particles to percolate through the powder and allow the coarse particles to roll on the fines – this even occurs if the larger particles are denser than their smaller particles. This results in an abundance of fine particles in the centre of the mound, with proportionally more large particles on the outside Fig. 4.7.

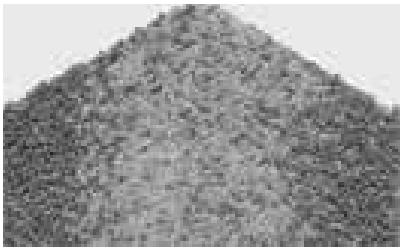

Fig. 4.7. Segregation of fine (light grey) and coarse (dark grey) particles.

Surface sampling of cohesive powder can be performed if the bulk material had been mixed prior to storage. Accuracy can be increased by taking multiple measurements from different regions throughout the batch. For this, a sampling spear (thief) can be used (Fig. 4.8); this consists of a sampling chamber at the end of the spear that generates a spot sample for compacted powders. Several samples can be extracted at different depths, which can then be blended to from a composite sample. The spear is inserted into the powder with the inner chamber closed off, and when in the desired position, the outer tube is rotated, to

allow the powder to fall into the inner chamber. When the chamber is full, the inner tube is again turned to the closed position, and the spear is withdrawn. The International Standards Organisation (ISO) recommends several samples from differing depths be taken from the front and rear of the batch (Barber, 2000).

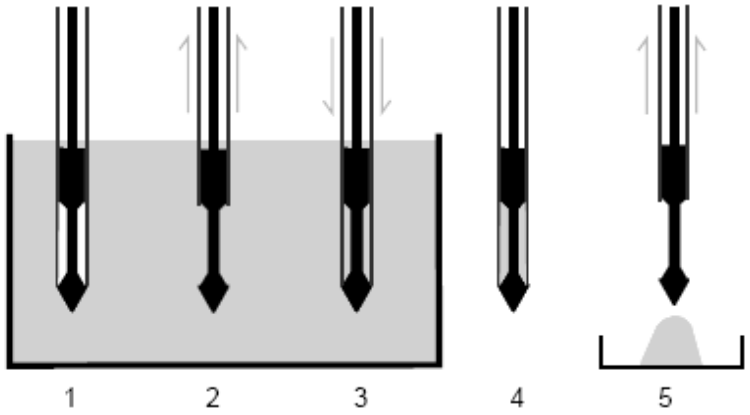

Fig. 4.8. Principle of operation of powder thief used for sampling bulk formulations. 1 - Closed powder thief is inserted into bulk powder; 2 – Outer sleeve is removed allowing powder to enter chamber; 3 – Sleeve is lowered to enclose powder sample; 4 – Powder thief is removed from bulk powder; 5 – Outer sleeve is raised allowing powder sample to be removed.

4.2.6. Particle Size Measurements

Particle size measurements were performed using laser diffraction. Both wet and dry dispersion techniques were used as described in sections 2.2.2 and 2.2.3. The propan-2-ol used in wet particle size analysis was analytical reagent grade, obtained from Fisher Scientific, Loughborough, UK.

4.2.7. Surface Area and Characteristics

Specific surface area was measured using a DVS Advantage II (Surface Measurement Systems, UK) using octane as probe molecule whilst water sorption studies were performed using the same instrument to identify changes in surface characteristics (see sections 2.2.4.2 and 2.2.4.3 for respective methods). Both the octane and water used in these studies were HPLC grade, obtained from Fisher Scientific, Loughborough, UK. Before analysis samples were dried in order to remove moisture from the powder surfaces, this was achieved by purging oxygen-free nitrogen (BOC, UK) over the sample for four hours.

4.2.8. Scanning Electron Microscopy

Scanning electron microscopy was used to verify particle size measurements, and as an indicator of changes in the population of particles that comprised the size distribution.

The microscope employed was a JEOL 6060 SEM (JEOL, Japan) with accelerating voltage 10 keV (section 2.2.5).

4.2.9. Cohesivity of Blends

The cohesivity of blends produced in this chapter was determined by a shear cell test method described in section 2.2.6.

4.2.10. Blend Content Uniformity

Content uniformity was measured using UV spectroscopy with the assay for cholesterol being described in section 3.5.2, and the method for vitamin C described in section 3.5.3. For each method, a 34.25 mg sample of formulation was taken which corresponded to a nominal drug dose of 500 μg. The final study incorporated micronised mimic hydrophobic (cholesterol) and hydrophilic (vitamin C) drugs to create "active" formulations. A key quality and one of the indicators of performance of active formulations is the chemical homogeneity of the product (Pilcer and Amighi, 2010), thus the relationship between homogeneity and SEI was investigated using common, previously-studied parameters, namely: 0.13 m diameter bowl, 500 rpm impeller speed and 160 kg m^{-3} mass fill ratio.

4.2.11. Experimental Procedure

Initial experiments were performed to identify suitable blending regimes in which good mixing can be achieved. These principles overlap with those utilised in wet granulation procedures, focusing on the importance of good bed turnover in order to maximise the API/excipient interactions. "Regime maps" are commonly used when predicting granule growth in equipment such as rotating drums and HSB for granulation (Tu *et al*., 2009). It is important for both granulation and HSB processes to occur in good blending regimes to ensure suitable turnover and mixing of powders (Litster *et al*., 2002). Good blending regimes were determined by two methods. Firstly, visual inspection of powder movement within the bowls, and secondly, the fluctuation of torque at given impeller speeds and mass loadings. Large torque fluctuations give rise to unstable mixing conditions, and make accurate calculations of SEI difficult, thus need to be avoided whilst producing formulations. For the purposes of this experiment, low torque fluctuations were considered to be <5% (from trial experiments) over a fixed time period between removal of samples (typically 10 min). A longer period of time is difficult to interpret as the torque imparted on the powder can be affected by

the removal of samples for analysis, thus it is necessary to monitor using constant mass. Percentage torque variations were chosen rather than absolute variations in order to compare across geometric scales (larger mass fills produce larger torque values).

Once good blending regimes had been identified, the second part of this study involved producing lactose-only blends using a range of parameters including bowl size (internal diameters 0.13, 0.16 and 0.21 m; impeller speed (300-700 rpm) and mass fill ratios (120-250 kg m^{-3}). The impact on physicochemical properties of lactose due to these changes was studied at regular intervals described by the SEI applied to the system.

4.3. Results and Discussion

4.3.1. Regime Maps

For this study, good mixing conditions have been described by "regime maps" for each bowl (Fig. 4.10); these contour plots from torque fluctuation measurements have been overlaid with regions corresponding to visual observations of blending conditions described in Fig. 4.9.

In vertical shaft mixers, two flow regimes are observed (Fig. 4.9). At low impeller speeds, the powder is vertically displaced as the impeller blade passes underneath, this causes slow, bumpy powder motion in the vertical direction. There is very little vertical turnover of the powder bed in this "bumping" regime.

Good blending conditions can be clearly identified in the regime maps since areas where both visual observations of good "roping" behaviour and low torque fluctuations clearly overlap. These regions showed good bed turnover and hence suitable mixing conditions. Toroidal motion, where the centrifugal acceleration of particles overcomes their gravitational force can be observed during the blending in these regions – as identified by Plank *et al.*, (2002) and Ng *et al.*, (2008).

It can also be seen from the regime maps in Fig. 4.10 that both bowl instability and poor powder movement are associated with high torque fluctuations. At low impeller speeds and low mass loadings, torque fluctuations were often low, but turnover of material was poor and bumping was observed, indicating poor blending conditions (Chandratilleke *et al.*, 2010).

On the other hand, at high impeller speeds and insufficient mass loadings, the bowl became unstable, leading to large torque fluctuations and often causing the equipment to shake vigorously. This was clearly unsuitable for controlled blending conditions. Another problem encountered by insufficient powder and excessive impeller speed was the aeration of powder, causing material to be entrained into the headspace above the bulk powder – similar findings were recognised by Sebti *et al*., (2007). Although a lid was used to contain material within the bowl, aeration of powder is still undesirable as it could affect the quality of the formulation by reducing either the fine particle fraction or chemical homogeneity.

Regions of poor blending conditions were also observed when the impeller speed was low and mass loadings were high – these produced large torque variations and powder movement and turnover was clearly restricted. In this operating region the impeller was unable to lift the mass of powder in the bowl sufficiently, thus only the powder immediately above the impeller experiences shear forces thus likely to cause a heterogeneous mixture of powders (Litster *et al*., 2002).

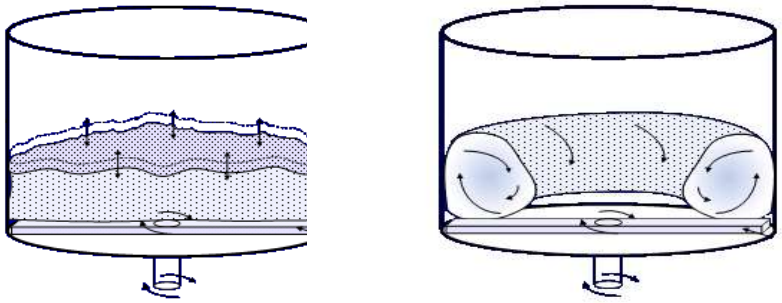

Fig. 4.9. "Bumping" and "roping" powder regimes during HSB. Taken from Litster *et al*., (2002).

At higher impeller speeds, a transition to "roping" behaviour occurs – this is where material from the bottom of the powder bed is forced up the vessel wall and tumbles down the angle of the bed surface towards the centre of the bowl. In this regime, there is good rotation of the bed and good vertical powder turnover.

In the bumping flow regime, the powder surface velocity increases proportionally with the impeller speed, however in the roping regime; the surface velocity stabilises and becomes less sensitive to impeller speed (Litster *et al*., 2002). The transition from bumping to roping is attributed to the change in balance between the powder's rotational inertia, which pushes the powder to the outside of the bowl, and gravity.

Similar patterns of bumping and roping were observed across all scales, there was no apparent propensity for a particular scale to show more or less bumping or roping at a particular mass fill or impeller speed.

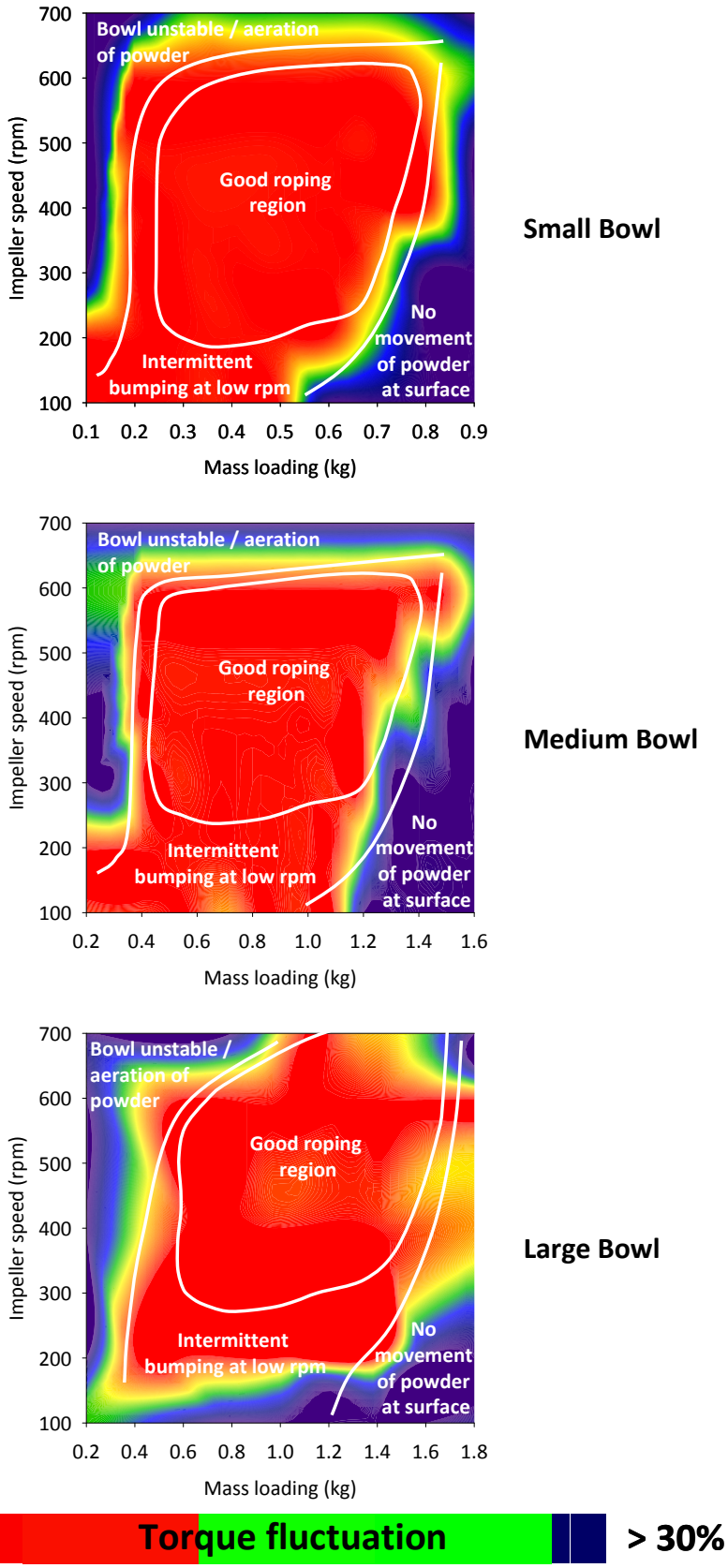

Fig. 4.10. Blending regime maps for small bowl (top), medium bowl (centre) and large bowl (bottom).

4.3.2. Blending Conditions

In order to explore the impact of bowl size, impeller speed and overall SEI on (primarily) the PSD of inhalation-grade lactose, a range of blending experiments were carried out using conditions that fell within the "good" blending regimes described in Fig. 4.10.

Table 4.1. Blend conditions used in this study.

Blend code	*Bowl size*	*Mass fill* (g)	*Fill ratio* (kg m^{-3})	*Impeller speed* (rpm)
A	Small	370	120	300
B	Small	370	120	500
C	Small	520	170	300
D	Small	520	170	500
E	Small	680	220	300
F	Small	680	220	500
G	Small	750	250	600
H	Small	750	250	600
I	Small	600	200	400
J	Small	500	160	600
K	Small	500	160	600
L	Small	500	160	600
M	Small	400	120	500
N	Small	500	160	600
O	Medium	500	120	600
P	Medium	600	140	600
Q	Medium	800	190	600
R	Medium	500	120	450
S	Medium	800	190	450
T	Large	900	120	600
U	Large	1300	190	600
V	Large	1300	190	600
W	Large	1600	220	700
X	Large	1200	160	700

These particular blend conditions were chosen to investigate a range of mass loadings and impeller speeds across the three geometric scales employed. For example, blends A and B, C and D, E and F, G and H, and J and K compare different impeller speeds whilst maintaining a similar mass fill ratio for the small bowl. Repeat experiments were performed to examine the variation within the process (blends J, K, L; blends O and R; and blends U and V are all repeats).

4.3.3. Effect of Specific Energy Input on Particle Size

The results presented in this section describe the effects of SEI - calculated by Equation 4.1 and Equation 4.2 - on the particle size of α-lactose monohydrate. Primarily, the results are described by d_5 particle size – the size below which 5% of all particles in the distribution reside. This is a particularly useful indicator of fines content within the

powder, and since the roles of fine particles in DPI formulations has been widely acknowledged as an important factor in performance (Hersey *et al*., 1975; Staniforth, 1996; Lucas *et al*., 1998; Zeng *et al*., 1998), it is useful to describe particle size changes by this measurement. Previous work has recognised the importance of this statistic in size distribution descriptions; Bridson *et al*., (2007) uses d_5 to describe the effects of blending on α-lactose monohydrate, whilst Watling *et al*., (2010) reports findings regarding entrainment mechanisms of DPI formulations in terms of the percentage number of particles below 5 μm – again recognising the importance of the fine portion of the size distribution.

4.3.3.1. Small (0.13 m Diameter) Bowl

Fig. 4.11 shows the change in d_5 particle size as a function of SEI using the small (0.13 m diameter) bowl for a series of blends described in Table 4.1.

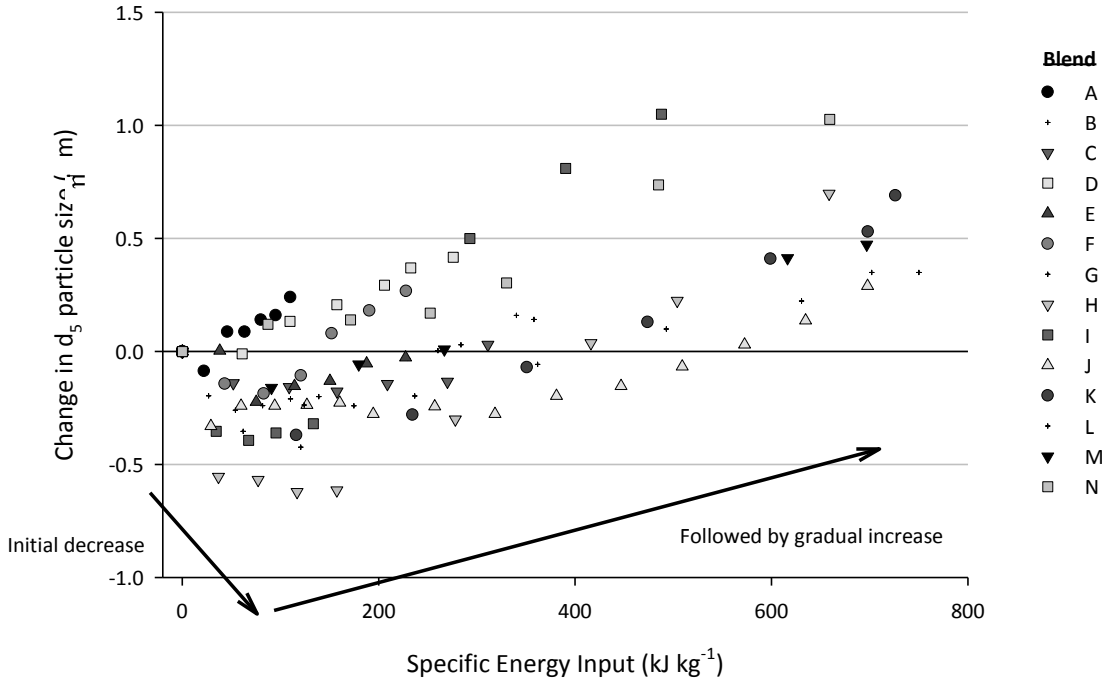

Fig. 4.11. Change in d_5 particle size as a function of SEI using the small (0.13 m diameter) bowl.

SEI is seen to have a pronounced effect on the d_5 particle size of lactose. Generally, results show that the d_5 particle size initially decreases following the onset of blending, and then subsequently increases with additional SEI.

The degree of change in particle size values varies with different mass fills and impeller speeds, and the total SEI (Fig. 4.11). The greatest reduction of particle size is

observed in blend H with a reduction in d_5 of 0.62 μm following an energy input of 117 kJ kg^{-1}. In comparison, the greatest reduction in d_5 for blend D is just 0.01 μm (achieved at 60.8 kJ kg^{-1}). On the other hand, the greatest increase in d_5 is observed in blend I (1.05 μm after 487 kJ kg^{-1} input), whereas blend L achieves just a 0.35 μm increase in d_5 following an energy input of 750 kJ kg^{-1}. Comparable energies also produce widely different results, for example blends A and B at 62 kJ kg^{-1} produce show d_5 changes of 0.09 and -0.35 μm respectively, whereas blends D and G at 109 kJ kg^{-1} show d_5 changes of 0.13 and -0.21 μm respectively. At greater SEIs, the d_5 changes between blends E and F at 227 kJ kg^{-1} are -0.02 and 0.27 μm, and the d_5 changes for blends H and N at 659 kJ kg^{-1} are 0.70 and 1.03 μm.

Blends produced using the same experimental parameters, i.e. mass loading and impeller speed (for example, blends J, K, and L) show the extent of the differences in particle size produced by HSB. The reduction in d_5 particle size at ~125 kJ kg^{-1} (127, 125 and 124 kJ kg^{-1}) is -0.24, -0.37 and -0.33 μm for blends J, K and L respectively. At the other end of the scale, the increase in d_5 particle size at ~700 kJ kg^{-1} (698, 698 and 702 kJ kg^{-1}) is 0.29, 0.53 and 0.35 μm. This highlights the inherent, variable nature of the HSB process, hence the need to characterise powders both before and after blending.

4.3.3.2. Medium (0.16 m Diameter) Bowl

Fig. 4.12 shows the change in d_5 particle size as a function of SEI using the medium (0.16 m diameter) bowl for a series of blends described in Table 4.1.

d_5 particle size data using the medium (0.16 diameter) bowl (Fig. 4.12) follows a similar trend as the data for the small bowl described above such that an initial decrease in particle size is observed at low SEIs, which, with additional energy input produces an increase in particle size. The greatest reduction in d_5 is observed in blend O (-0.34 kJ kg^{-1} at 36 kJ kg^{-1}), however blend Q shows similar reductions (-0.33 μm) at energy inputs of 31.3 and 53.6 kJ kg^{-1}. Blend S clearly displays the greatest increase in d_5 particle size – the two greatest changes in d_5 (1.35 and 1.52 μm) are produced by SEIs of 386 and 447 kJ kg^{-1} respectively. In comparison, blend O produces a change in d_5 of just 0.73 μm at an energy input of 622 kJ kg^{-1}.

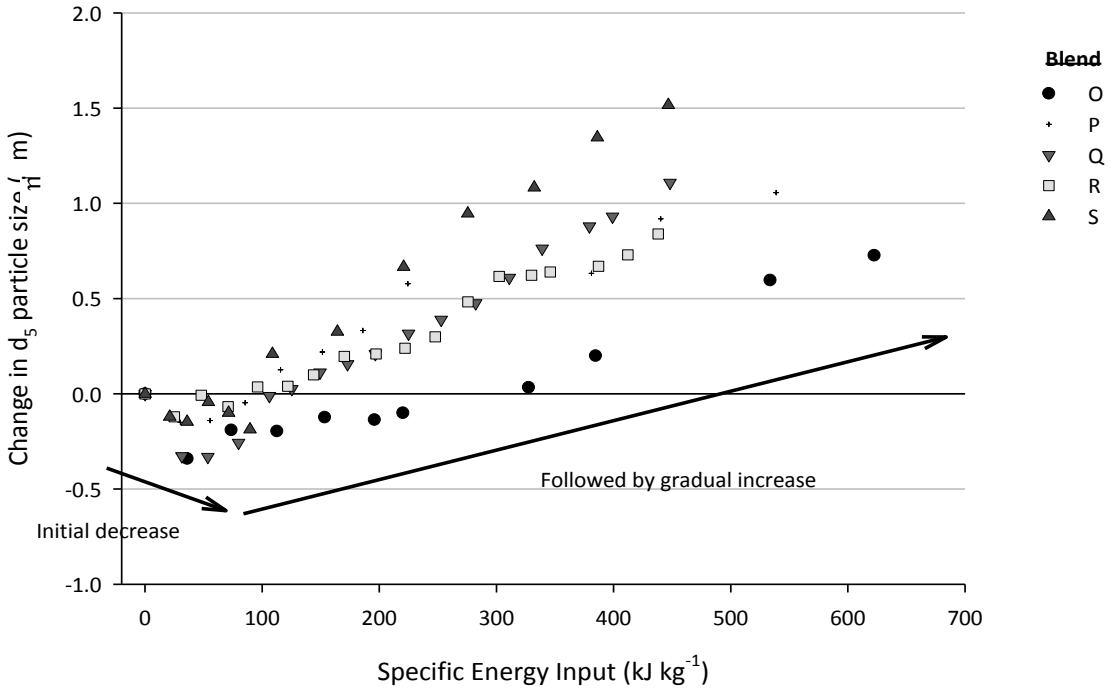

Fig. 4.12. Change in d_5 particle size as a function of SEI. Medium (0.16 m diameter) bowl.

4.3.3.3. Large (0.21 m Diameter) Bowl

Fig. 4.13 shows the change in d_5 particle size as a function of SEI using the large (0.21 m diameter) bowl for a series of blends described in Table 4.1.

Studies using the large (0.21 m diameter) bowl again showed similar trends to the small and medium bowls in that d_5 particle size appeared to decrease at low SEIs, which was then followed by a gradual increase to larger particle sizes. The changes in particle size (both reduction and increase) were more pronounced using the larger bowl (the greatest reduction was -0.785 μm (blend V, 83 kJ kg^{-1}), compared to -0.62 μm for the small bowl and -0.34 μm for the medium bowl. In addition, an increase of 2.05 μm was observed using the large bowl (blend X) with just 460 kJ kg^{-1} SEI; this compares to the maximum increases for the small bowl of 1.05 μm (487 kJ kg^{-1} input – blend I) and 1.52 μm for the medium bowl (447 kJ kg^{-1} – blend S). As identified at the other scales there is a degree of scatter amongst change in d_5 at comparable energy inputs. For example, Table 4.2 highlights the differences at selected SEIs; particularly large differences are experienced at ~320 kJ kg^{-1} – blend V shows a d_5 change of -0.28 μm, yet blends W and X show changes in d_5 of 1.68 and 1.66 μm respectively.

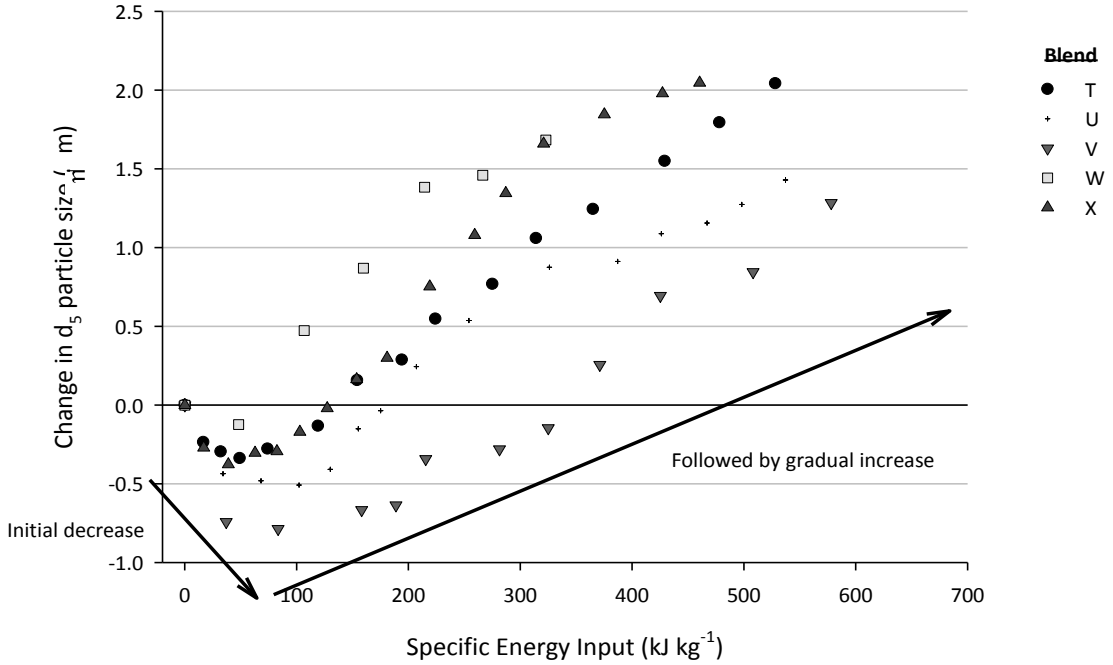

Fig. 4.13. Change in d_5 particle size as a function of SEI. Large (0.21 m diameter) bowl.

Table 4.2. Examples of change in d_5 particle size at comparable SEIs using medium (0.16 m diameter) bowl.

Specific energy input	*Blend*				
	T	***U***	***V***	***W***	***X***
~155 kJ kg^{-1}	0.16 μm (154 kJ kg^{-1})	-0.15 μm (155 kJ kg^{-1})	-0.67 μm (158 kJ kg^{-1})	0.87 μm (160 kJ kg^{-1})	-0.16 μm (153 kJ kg^{-1})
~215 kJ kg^{-1}	0.55 μm (224 kJ kg^{-1})	-0.04 μm (207 kJ kg^{-1})	-0.64 μm (215 kJ kg^{-1})	1.38 μm (214 kJ kg^{-1})	0.75 μm (219 kJ kg^{-1})
~320 kJ kg^{-1}	1.06 μm (314 kJ kg^{-1})	0.54 μm (326 kJ kg^{-1})	-0.28 (325 kJ kg^{-1})	1.68 μm (323 kJ kg^{-1})	1.66 μm (321 kJ kg^{-1})

4.3.4. Effect of Mass Fill Ratio on Particle Size

The effect of mass fill ratio of the rate of change of d_5 particle size does not show any trends across any of the geometric scales studied. As can be seen from Fig. 4.11, blends that were produced using the same impeller speed but with varying mass fill ratios did not follow any trend in terms of change in particle size. For example, blends B, D and F were produced using impeller speed of 500 rpm and mass fill ratios of 120, 170 and 220 kg m^{-3} respectively. However, their d_5 particle sizes at ~120 kJ kg^{-1} showed changes of -0.42, 0.13, and -0.1 μm respectively. In addition, their d_5 particle sizes at ~230 kJ kg^{-1} (specifically 230, 233 and 228 kJ kg^{-1}) showed changes of -0.03, 0.37 and 0.27 μm – indicating no definite trend with respect to mass fill ratio.

This is also observed for the medium bowl (Fig. 4.12) where blends O, P and Q were produced using a fixed impeller speed (600 rpm) but with mass fill ratios of 120, 140 and 170 kg m^{-3} respectively. Their d_5 particle size following ~50 kJ kg^{-1} (specifically 46,

55 and 54 kJ kg^{-1}) SEI showed changes of -0.34 μm, -0.14 μm and -0.33 μm respectively, whereas at ~220 kJ kg^{-1} (specifically 220, 225 and 225 kJ kg^{-1}), the changes were 0.1 μm, 0.58 μm and 0.32 μm respectively. In addition, the changes at ~380 kJ kg^{-1} (384, 381 and 379 kJ kg^{-1}) were 0.2 μm, 0.63 μm and 0.88 μm respectively.

4.3.5. Effect of Bowl Size on Particle Size Distribution

It can be shown from Fig. 4.15 and Table 4.3 that the rate of change of d_5 is greater as the bowl size is increased. Fig. 4.15 shows the same data as Fig. 4.17, however, trendlines have been added for the maximum and minimum "agglomeration gradients" for each bowl size. These agglomeration gradients are simply trendlines that describe the overall rate of increase of d_5 particle size as a function of SEI.

It is clear that the greater rate of change of d_5 can be seen with the larger bowl than the smaller bowls whilst an overlap is found between the large and medium bowls, and the medium and small bowls. However, the average gradients for each bowl follow the trend that as the bowl size increases, so does the rate at which d_5 increases with respect to SEI. A possible explanation for this would be the greater tip speed (linked to Froude number) of the larger bowl impeller creates more energetic collisions between particles towards the outside of the bowl, thus increasing the d_5 particle size more rapidly. This has implications for scale-up of blending processes in order to be able to control the properties of the final product.

4.3.6. Effect of Impeller Speed on Particle Size

Fig. 4.14 describes the effect of a fixed impeller speed (600 rpm) on the d_5 particle size across three geometric scales. Comparison of impeller speeds over different geometric scales shows a noticeable increase in the rate of change of d_5 particle size with respect to SEI as bowl diameter is increased. For example, blend J (small bowl) shows an increase of just 0.29 μm following application of 698 kJ kg^{-1}, whereas blend O (medium bowl) shows an increase of 0.73 μm following application of 622 kJ kg^{-1}, and blend T shows an increase of 2.04 μm after being subjected to just 528 kJ kg^{-1} SEI. Since the impeller speed is fixed, this cannot be the sole factor in causing the trend observed in Fig. 4.14.

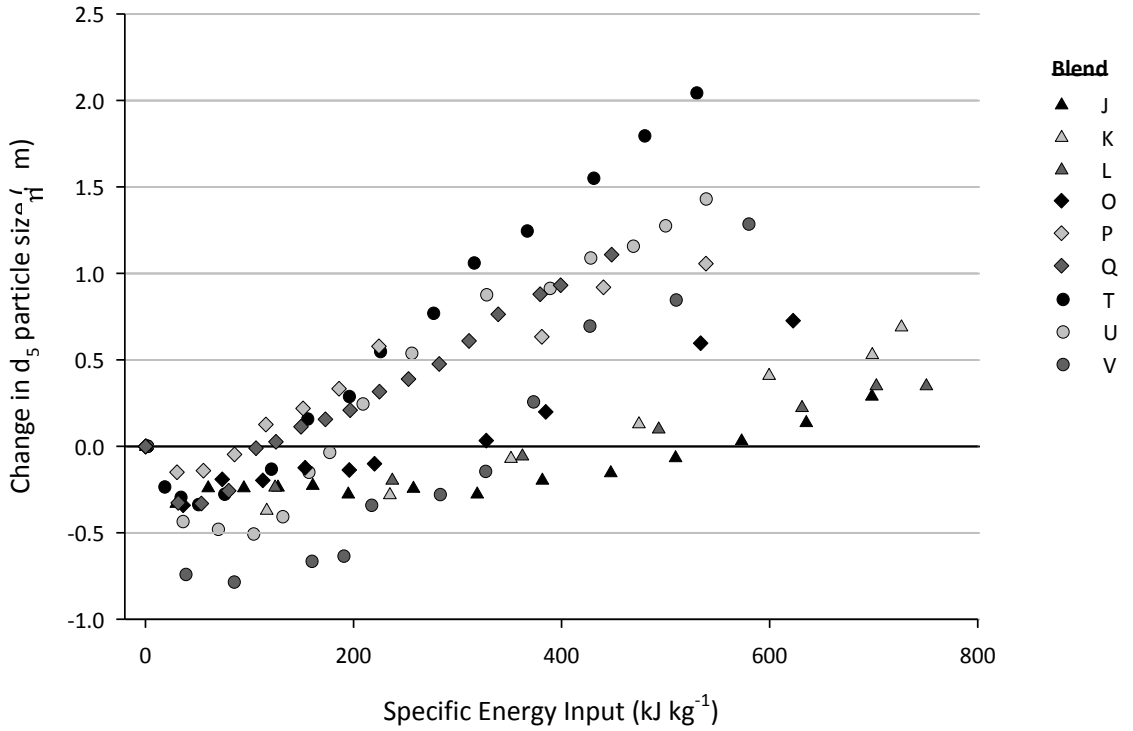

Fig. 4.14. Effect of impeller speed on d_5 particle size across three geometric scales with fixed impeller speed (600 rpm). Triangles represent small bowl, diamonds represent medium bowl, and circles represent large bowl.

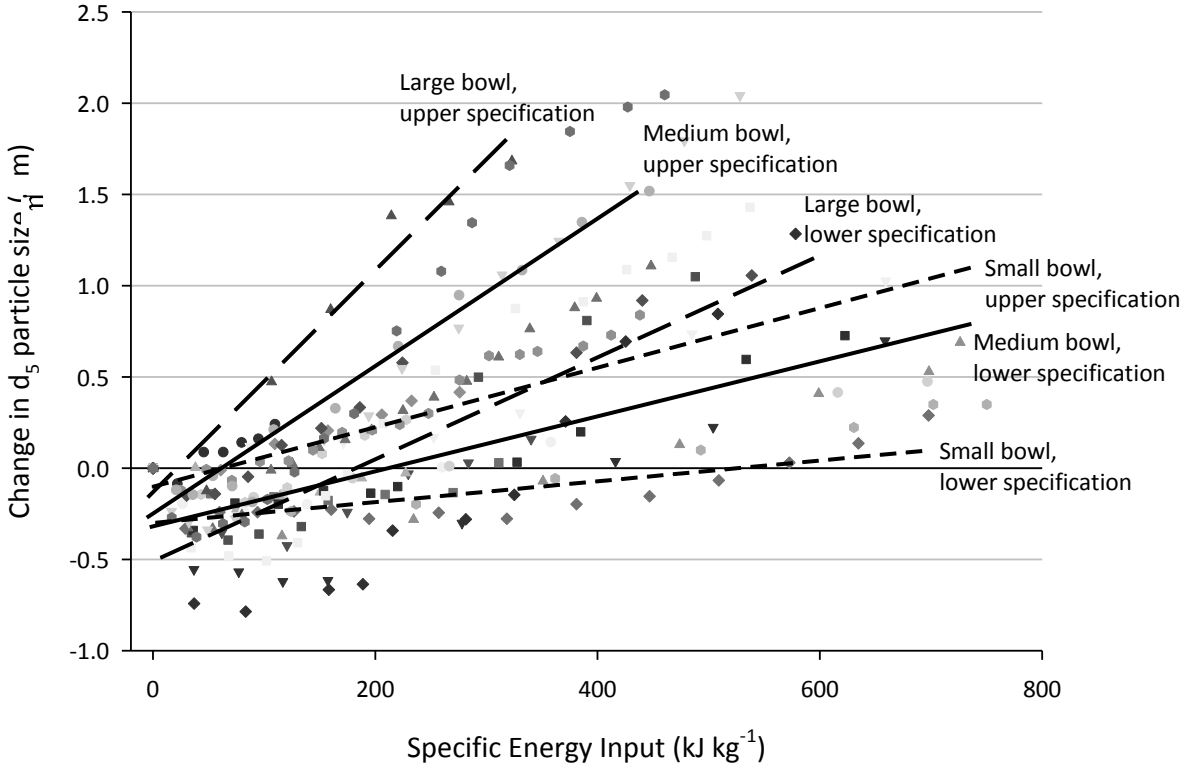

Fig. 4.15. All data, with trendlines showing the maximum and minimum rates of change of d_5 with respect to SEI for each bowl. Small bowl – short dashes; medium bowl – solid line; large bowl – large dashes.

Table 4.3. Range and average gradients of the trendlines in Fig. 4.14.

Bowl	*Gradient*	
	Range	*Average*
Small	0.0010-0.0033	0.00203 ± 0.0010
Medium	0.0017-0.0045	0.00340 ± 0.0013
Large	0.0034-0.0066	0.00508 ± 0.0014

4.3.7. Comparison With Previous Literature

The results throughout this study - summarised in Fig. 4.17 - differ from those seen in previous work, (Bridson *et al*., 2007), in that a noticeable reduction in d_5 particle size is observed at low SEI – a phenomenon that was apparent using all bowls, mass loadings and impeller speeds. This contrasts to the previous study that found a steady, linear increase in d_5 particle size as a function of SEI and no apparent reduction in particle size at the initial stages of blending (Fig. 4.16). This marked difference in results proved interesting since they occurred despite the experimental, measurement and characterisation conditions and instruments being constant across the two studies.

However, it was noticed that the characteristics of the starting material used in each study were different – despite being inhalation-grade lactose from the same manufacturer, the lactose used in the current study was significantly finer than the lactose used in the previous study (as observed by the d_{10}, d_{16} and d_{50} values in particular (Fig. 4.16). This highlights the importance of characterising starting materials in order to predict and control behaviour of the final formulation – even slight changes in the starting material may have considerable effects on the performance and characteristics of the final product.

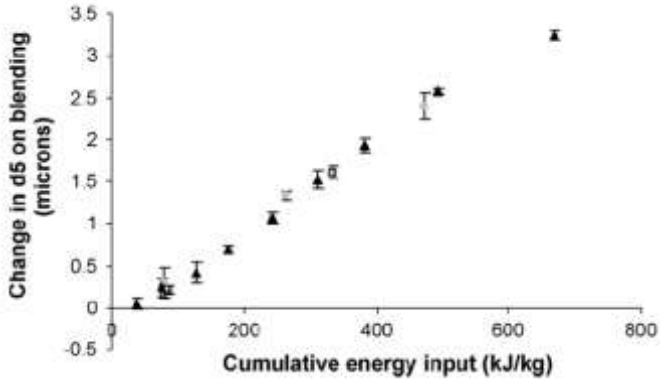

	Particle size (μm)	
	Bridson et al., (2007)	***Current study***
d_5	3.04 ± 0.04	3.10 ± 0.02
d_{10}	15.47 ± 0.03	9.32 ± 0.10
d_{16}	27.15 ± 0.05	18.92 ± 0.12
d_{50}	79.14 ± 0.10	68.65 ± 0.01
d_{84}	127.80 ± 0.11	118.20 ± 0.06

Fig. 4.16. Results and starting material particle size statistics from previous work (Bridson *et al*., 2007) and those found in the current study (Fig. 4.17), using identical experimental conditions.

Fig. 4.17 and Fig. 4.18 show the change in d_5 and d_{50} particle size respectively as a function of SEI. Both measurements show the same trend in that an initial reduction in particle size at low SEIs is followed by an increase at greater energy inputs. Both measurements show similar-sized changes overall; the typical reduction in both d_5 and d_{50} being around 0.5-1 μm. However, d_5 increases at ~400 kJ kg^{-1} range from -0.15 μm (blend J – 447 kJ kg^{-1}) to 1.98 μm (blend X – 427 kJ kg^{-1}), compared to typical d_{50}

increases ranging from 0.32 μm (blend I – 390 kJ kg^{-1}) to 1.73 μm (blend Q – 399 kJ kg^{-1}). Thus, the spread of d_5 increase is far more pronounced than d_{50} that shows less variation in change in d_{50} particle size at higher SEIs than d_5.

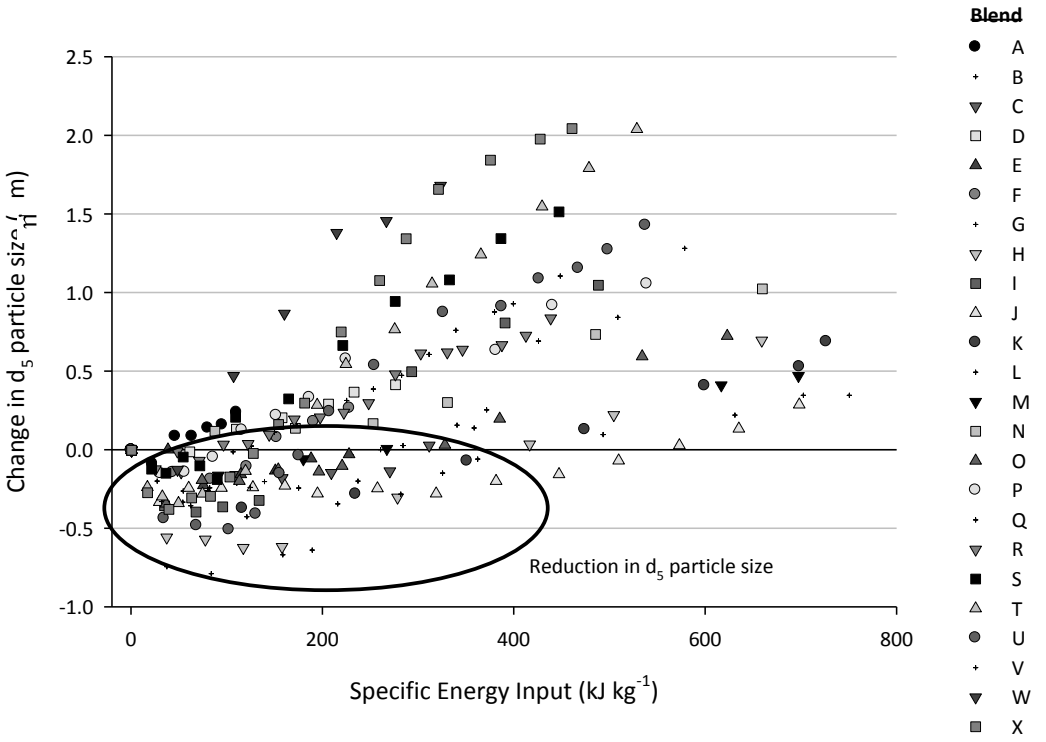

Fig. 4.17. Change in d_5 particle size at low SEIs (all data).

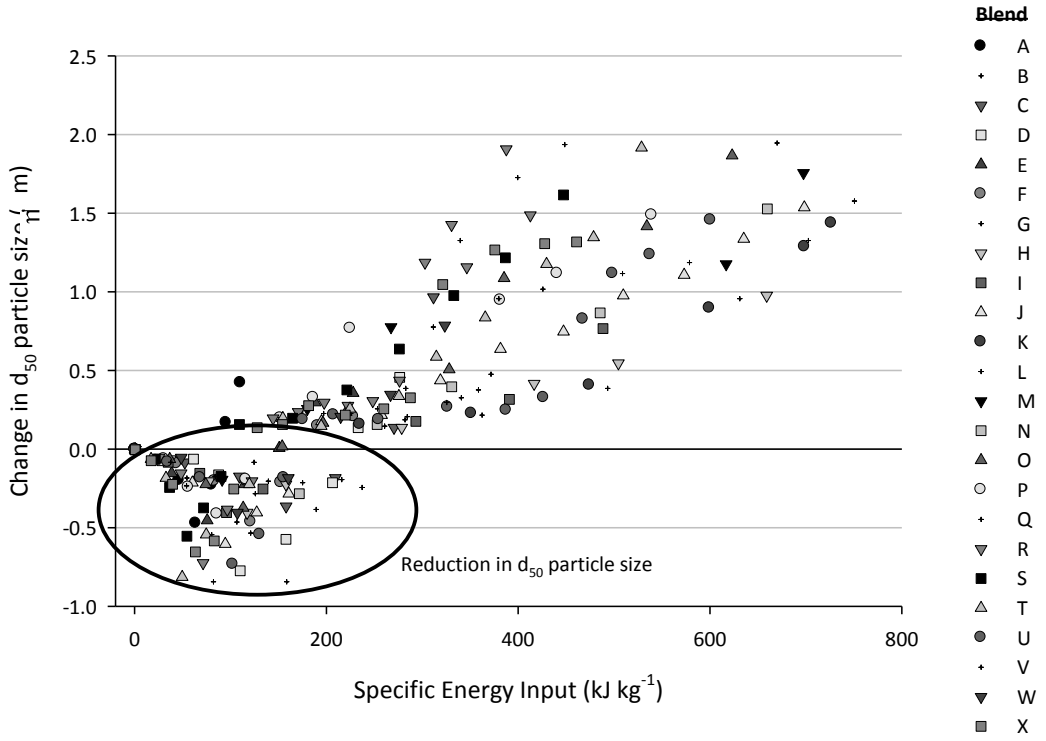

Fig. 4.18. Change in d_{50} particle size at low SEIs (all data).

Max reduction of d_{50} = -0.84 μm (blends G and V – 81.7 and 158 kJ kg^{-1} respectively), whereas the max reduction of d_5 was -0.79 μm (blend V – 83.3 kJ kg^{-1}). The maximum increase of d_{50} was found to be 1.95 μm (blend V – 669 kJ kg^{-1}), compared to the maximum d_5 increase of 2.05 μm (blend X – 460 kJ kg^{-1}). It is also noticeable that following the initial reduction, the return to original d_{50} particle size occurs at lower SEI than the d_5 particle size.

4.3.8. Effect of Blending on Cohesivity of α-Lactose Monohydrate

The effects of HSB on the cohesivity of lactose was studied by analysing the flow functions of samples taken from blends exposed to various SEIs. Fig. 4.19 and Table 4.4 show example results from blend K (chosen due to the wide SEI range and average trend observed) with samples taken at low, intermediate and high SEIs, incorporating material which had shown a reduction in particle size, similarity to original particle size, and an increase in particle size. Results from other blends showed similar results, such that no statistically significant (Kruskal-Wallis non-parametric hypothesis test for multiple samples, with chosen level of significance, $\alpha = 0.05$) differences could be observed between blends exposed to varying SEIs across the geometric scales, impeller speeds and mass loadings used. As seen in the initial characterisation of starting materials (Fig. 3.14), the Schulze shear cell test method is able to discriminate between samples with clear differences in cohesivity (namely AJS-coarsened lactose with fine particles <25 and <71 μm removed). However, despite differences in the PSD observed by laser diffraction (Fig. 4.17 and Fig. 4.18), and differences in the specific surface area observed by BET analysis (Fig. 4.21), cohesivity differences could not be observed using the shear cell test method.

Table 4.4. Flow functions (f_c) of samples from blend K. Results show average from three independent experiments ± SD. Results are rounded to two decimal places.

Material	*Energy Input* (kJ kg^{-1})	*Symbol (Fig. 3.14)*	*Gradient*	*Flow function, f_c*
Unprocessed lactose	0	◆	0.23	3.92 ± 0.44
Low energy blended 1	115	◇	0.23	4.44 ± 0.51
Low energy blended 2	234	■	0.25	4.03 ± 0.53
Mid energy blended	474	○	0.23	4.31 ± 0.37
High energy blended	726	△	0.24	4.14 ± 0.35
25 μm lactose	N/A	□	0.06	17.86 ± 2.02
71 μm lactose	N/A	▲	0.03	33.22 ± 2.22

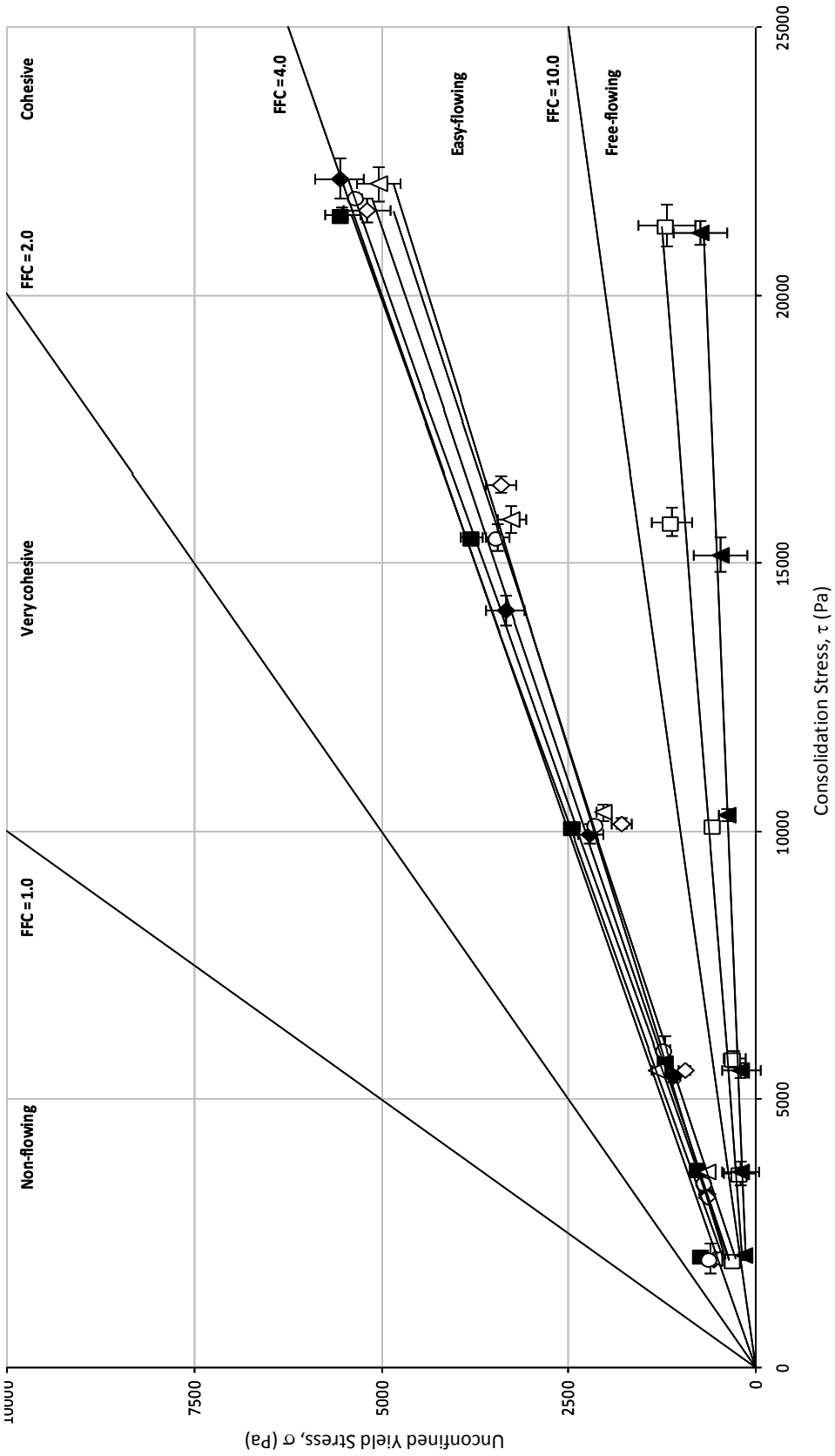

Fig. 4.19. Unconfined yield stress (σ) vs. consolidation stress (τ) measurements of powders used in this study.
◆ - Unprocessed lactose; ◇ - Low energy input 1 (115 kJ kg^{-1}); ■ - Low energy input 2 (234 kJ kg^{-1}); ○ - Mid energy input (474 kJ kg^{-1}); △ - High energy input (726 kJ kg^{-1}); □ - 25μm lactose; ▲ - 71 μm lactose.

4.3.9. Mechanisms for Particle Size Distribution Change

The mechanism behind the initial decrease and subsequent increase in particle size with increasing SEI cannot be determined by dry laser diffraction alone. There are several possible mechanisms to describe these events. Firstly, the reduction in particle size could be attributed to de-agglomeration, or particle fracture – producing more fine particles and hence reducing the fine portion of the PSD. The increase in PSD could be attributed to agglomeration or re-agglomeration (if de-agglomeration had previously occurred) or loss of fines from the system. The following sections attempt to explain the mechanisms behind the observed change in PSD due to increasing SEI.

4.3.9.1. Particle Size Distribution of Primary Particles – "De-agglomerated" and "Agglomerated" Lactose

Further verification of these results can be achieved through use of wet dispersion laser diffraction. Preliminary studies (section 2.3), showed that wet dispersion produces a finer PSD than dry dispersion (even at the maximum dispersion pressure). Therefore, wet dispersion is likely to give a stronger indication of the primary particle sizes in each sample, as opposed to dry dispersion that may not fully de-agglomerate.

Fig. 4.20 shows the d_{10} and d_{50} particle size data of unprocessed lactose and "de-agglomerated" and "agglomerated" lactose exposed to varying SEIs. In this thesis, the terms "agglomerated" and "de-agglomerated" particles refer to the particles displaying a reduced PSD and increased PSD respectively. Until the true mechniasm behind the increase/decrease can be determined, these terms will be used. Following application of the Kruskal-Wallis test (page 119), it can be shown that there are no statistically significant differences between samples exposed to differing SEIs. As shown in section 2.2.2, the use of propan-2-ol and sonication is suitable for adequate dispersion of particles, thus it can be assumed that the particles measured are "primary" particles and no agglomerates are being measured. Fig. 4.20 shows that there are no differences between the samples with regards the distribution of primary particles; this suggests that particles are not being lost from the system, and HSB causes a redistribution of particles which can be identified using dry dispersion, however is not detectable using wet dispersion.

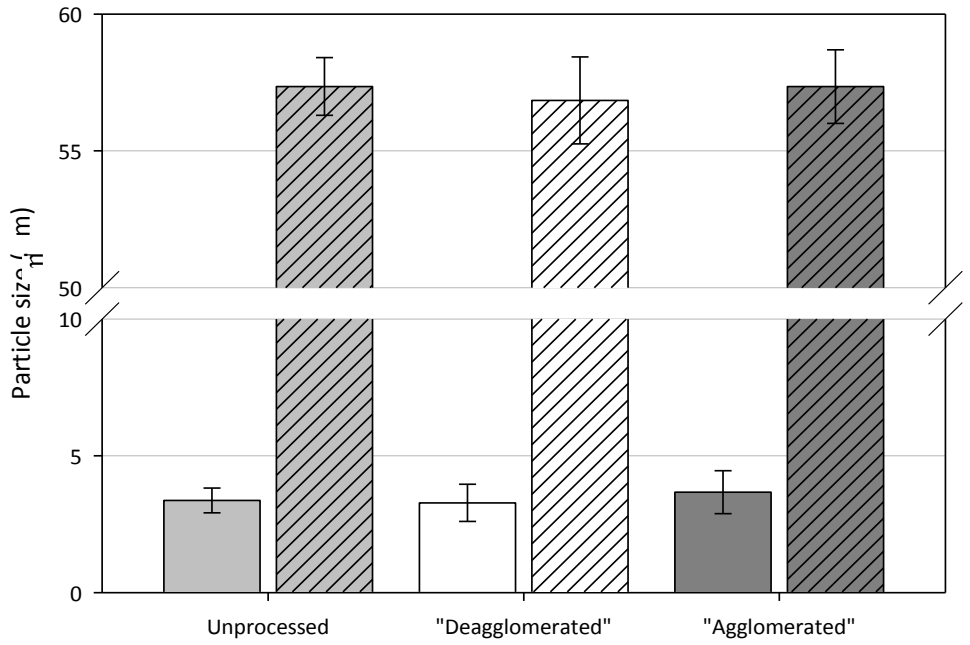

Fig. 4.20. Particle size analysis (wet dispersion) of unprocessed, "de-agglomerated" and "agglomerated" material. d_{10} - solid; d_{50} - hatched. Results shown are the average values from three independent experiments of six blends (B, H, I, O, Q, S - Table 4.1), with error bars showing the standard error of the mean. These blends were chosen as they displayed distinct de-agglomeration and agglomeration of particles with increasing SEI.

4.3.9.2. Specific Surface Area Studies

BET surface area analysis of "de-agglomerated" material was performed along with analysis of unprocessed lactose and "agglomerated" material in order to gain more insight into the mechanism behind the increase and decrease in particle size observed during blending. Fig. 4.21 shows the results of this surface area analysis and it can be shown that there are no statistically significant differences (using the Kruskal-Wallis test - page 119) between the unprocessed and the "de-agglomerated" material, however, significant differences exist between these, and "agglomerated" material. These samples reported were chosen as they represented a blend with distinct de-agglomeration and agglomeration of particles with increasing SEI; however, the trend is applicable to all blends used in the study.

This suggests that initially, fine particles are weakly attached to the surface of coarse particles (unprocessed lactose), and low SEIs simply de-agglomerate these particles. Hence, the octane molecules employed in BET analysis are able to "see" these weak agglomerates as discrete particles and thus once they do become separate entities, the combined surface area is not significantly affected. However, following high SEIs, these fine particles become strongly bound due to the press-on forces caused by the blending process, forming multiplets with other fine particles (Lucas *et al*., 1998), or adhering to

the surface of larger particles. These attractions are likely to be sufficiently strong that neither octane molecules are able to identify the individual particles, nor dry dispersion is able to separate the particles – thus coarsening the PSD.

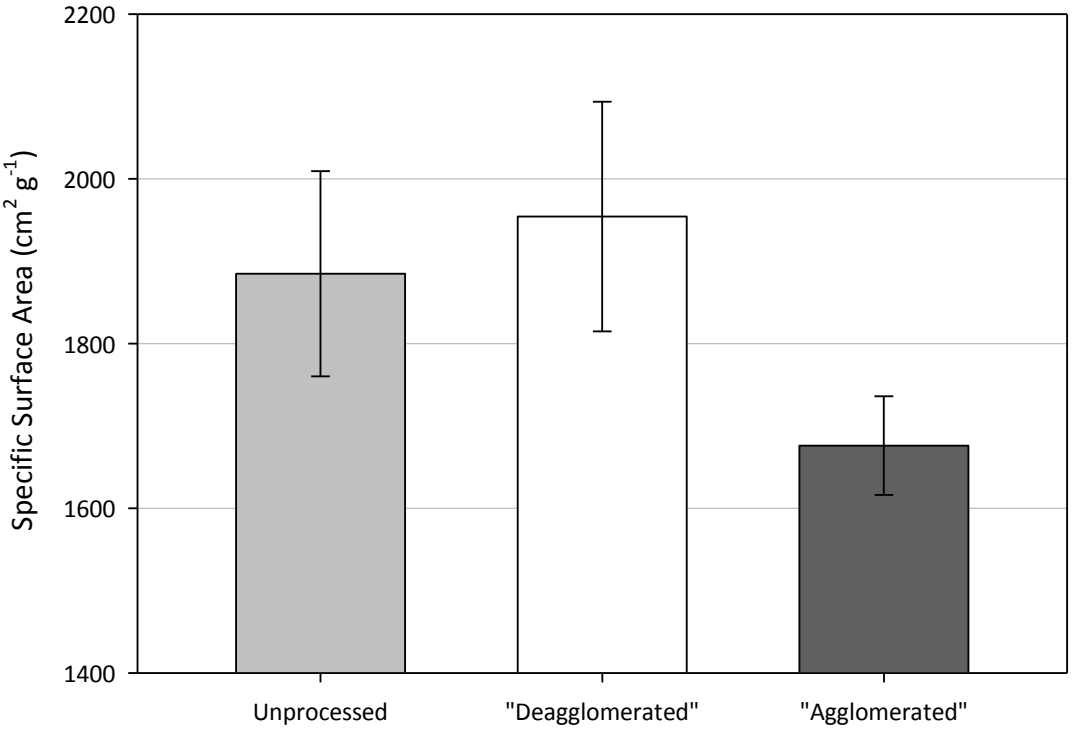

Fig. 4.21. BET surface area analysis of unprocessed, "de-agglomerated", and "agglomerated" material produced from HSB. Results shown are the average values from three independent experiments of six blends (B, H, I, O, Q, S - Table 4.1), with error bars showing the standard error of the mean. As with Fig. 4.20, these blends were chosen as they displayed distinct de-agglomeration and agglomeration of particles with increasing SEI.

4.3.9.3. Loss of Fines

Further evidence to show that lactose particles were being redistributed rather than fine particles being lost was gained by analysing particles that adhered to the bowl or impeller surfaces during HSB. Since a lid was placed on the bowl during blending, fines were not lost via the headspace (no particles were observed coating the lid); however, there was the possibility that fine particles were preferentially adhering to the impeller and bowl surfaces, thus affecting the PSD of the bulk lactose. Fig. 4.22 compares the d_{10} and d_{50} sizes of unprocessed lactose with lactose subjected to a large SEI (660 kJ kg^{-1} – blend N) that had adhered to the impeller and bowl and the bulk powder. It can be shown that no statistically significant differences (Kruskal-Wallis test - page 119) can be observed between the PSDs of material adhered to the side of the bowl or impeller, and that in the bulk material, thus suggesting that the change in

particle size due to HSB is attributed to agglomeration and not loss of fines from the system.

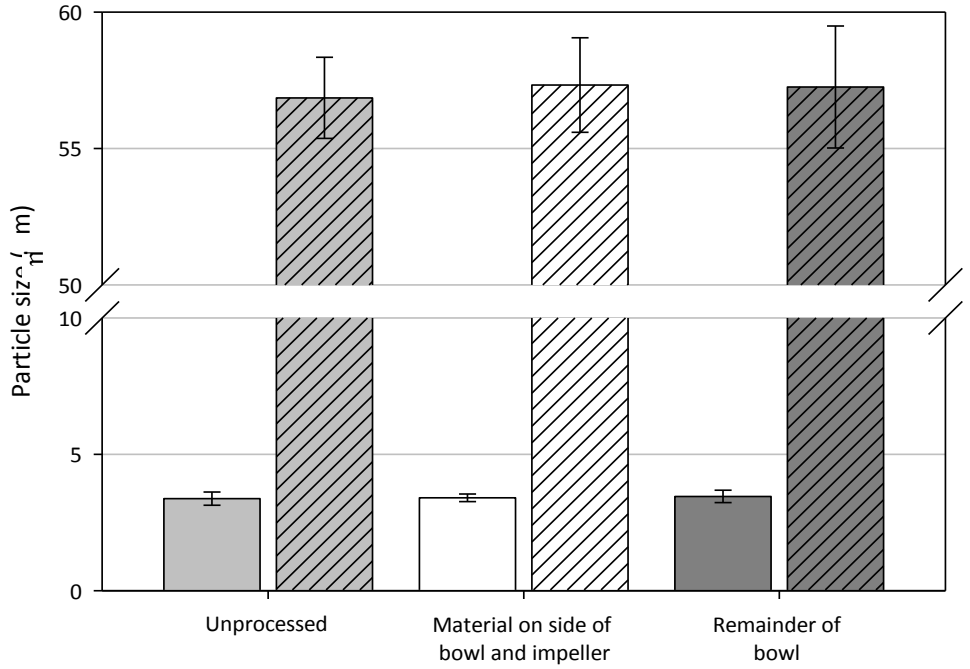

Fig. 4.22. PSD of the bulk formulation, those adhered to the sides of the bowl and the impeller compared to unprocessed lactose. Solid bars - d_{10}; hatched bars - d_{50}.

4.3.9.4. Water Sorption Profiles

It is well-known that high energy processing of pharmaceutical material can induce changes in the surface characteristics, notably the introduction of amorphous regions (Waltersson and Lundgre, 1985; Mackin *et al*., 2002). Water sorption isotherms were produced in order to determine if any changes in the crystal structure had occurred during the blending process. As can be seen from Fig. 4.23, the shape of the water isotherm does not change due to blending; the inflection points of the curve appear at the same partial pressures, thus suggesting that any changes in crystallinity had not occurred. In addition, there are no statistically significant (Kruskal-Wallis test - page 119) differences in the overall water adsorption (at all humidity stages) with respect to SEI, also indicating that changes in the crystal structure could not be detected.

Work done by Mackin *et al*., (2002), identified changes in the crystallinity of xemilofiban and a benzyl ether derivative pharmaceutical compound by changes in the water sorption profiles, such that the percentage change in mass due to increased exposure to humidity was greater for amorphous material when compared to crystalline material. Therefore, if HSB created amorphous regions on the surface of the lactose particles, it is likely that the water sorption isotherms would show a decrease

in percentage mass change with increased humidity for material exposed to greater SEI.

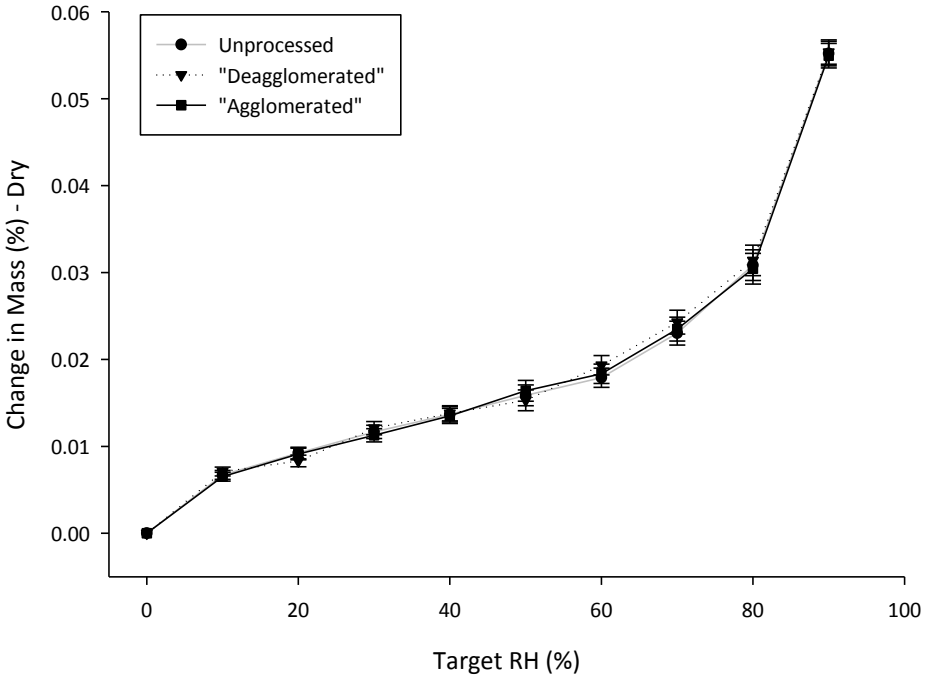

Fig. 4.23. Example moisture sorption profiles representative of unprocessed, "de-agglomerated" and "agglomerated" lactose subjected to differing SEIs. Error bars represent the SD from three independent experiments of sample from blend N.

4.3.9.5. Surface Morphology Studies

Finally, SEM images were produced of representative unprocessed, "de-agglomerated" and "agglomerated" material to determine if the subtle changes in PSD could be detected visually (Fig. 4.24). The images show that slight differences in the population of particles can be observed – the key feature is that more "free" fines can be observed in the "de-agglomerated" sample than in the unprocessed and "agglomerated" samples. The "agglomerated" sample shows a different distribution of particles than the unprocessed sample in that small multiplets of fines appear to have been formed and the number of free fines appears to have reduced. With greater magnification, Fig. 4.25 shows the formation of a fine particle multiplet from extended HSB. It is possible that this multiplet is bound by strong interparticle forces that cannot be separated by dry dispersion sizing techniques (RODOS), hence the coarsening of PSD and reduction in specific surface area measured by BET analysis. However, the dispersion caused by propan-2-ol in wet size analysis allows this multiplet to de-agglomerate and the primary particles are observed – as in the case of both unprocessed and de-agglomerated lactose. Whilst SEM images are a powerful tool in qualitatively assessing surface morphology and other particle characteristics, it remains a subjective

assessment method. Firm conclusions are difficult to make and should always be treated with a degree of scepticism.

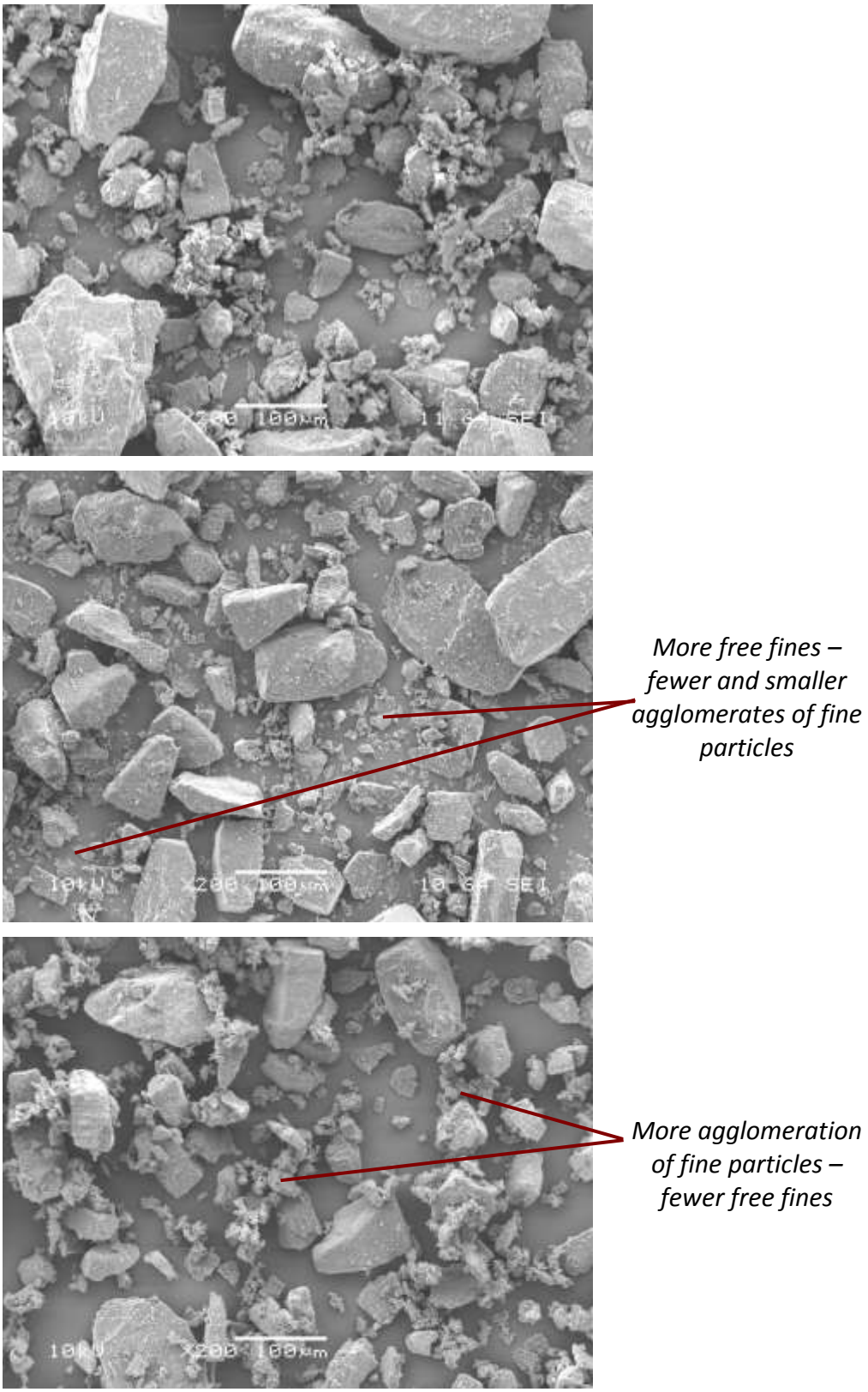

Fig. 4.24. Representative SEM images of unprocessed (top), "de-agglomerated" (middle), and "agglomerated" (bottom) material. Samples taken from blend N, with x200 magnification and 10kV potential.

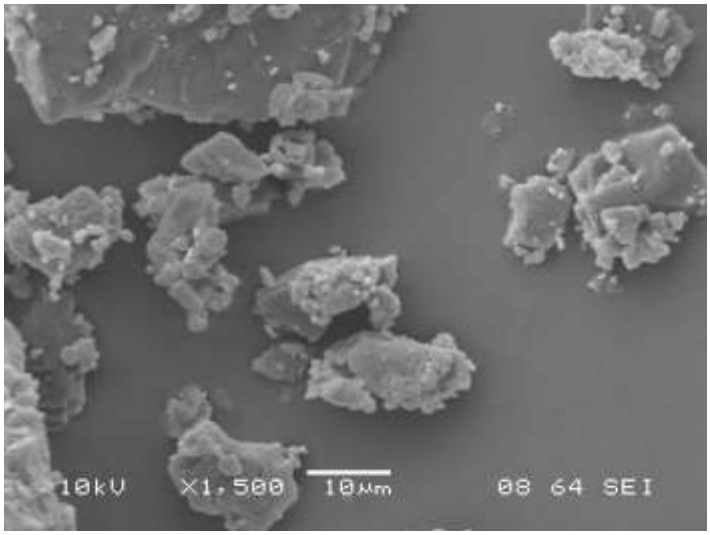

Fig. 4.25. Representative SEM image of "agglomerated" lactose. Sample taken from blend N, with x1500 magnification and 10kV potential.

4.3.10. Blend Homogeneity Studies

The blend homogeneity results as a function of SEI from three independent experiments using each mimic API are shown in Fig. 4.26 (cholesterol) and Fig. 4.27 (vitamin C).

As seen during lactose-only tests, the initial de-agglomeration of particles is observed, before an increase in particle size with increased SEI (Fig. 4.17). As expected, the addition of mimic drugs did not alter the impact of SEI on the PSD of the formulation since they comprise less than two percent (by mass) of the mixture. In addition, there are no significant differences between the PSD of the cholesterol formulations and the vitamin C formulations – compare Fig. 4.26 and Fig. 4.27 at corresponding SEIs.

However, results show that the onset of homogeneity is achieved following a SEI of approximately 200 kJ kg^{-1} in the case of cholesterol, and 150 kJ kg^{-1} in the case of vitamin C (these results are obtained through analysis of three independent experiments of each mimic drug). It is clear that changes in the PSD of the formulation continue to occur with increasing energy input, despite there being no impact on the drug homogeneity. Since no improvement on the formulation homogeneity can be identified, the importance of applying further energy to the formulation depends on the effect produced regarding aerosolisation and deposition efficiency. This work led to tests to determine the significance of SEI on the *in vitro* performance of mimic API formulations – the results from these tests are described in chapter 7.

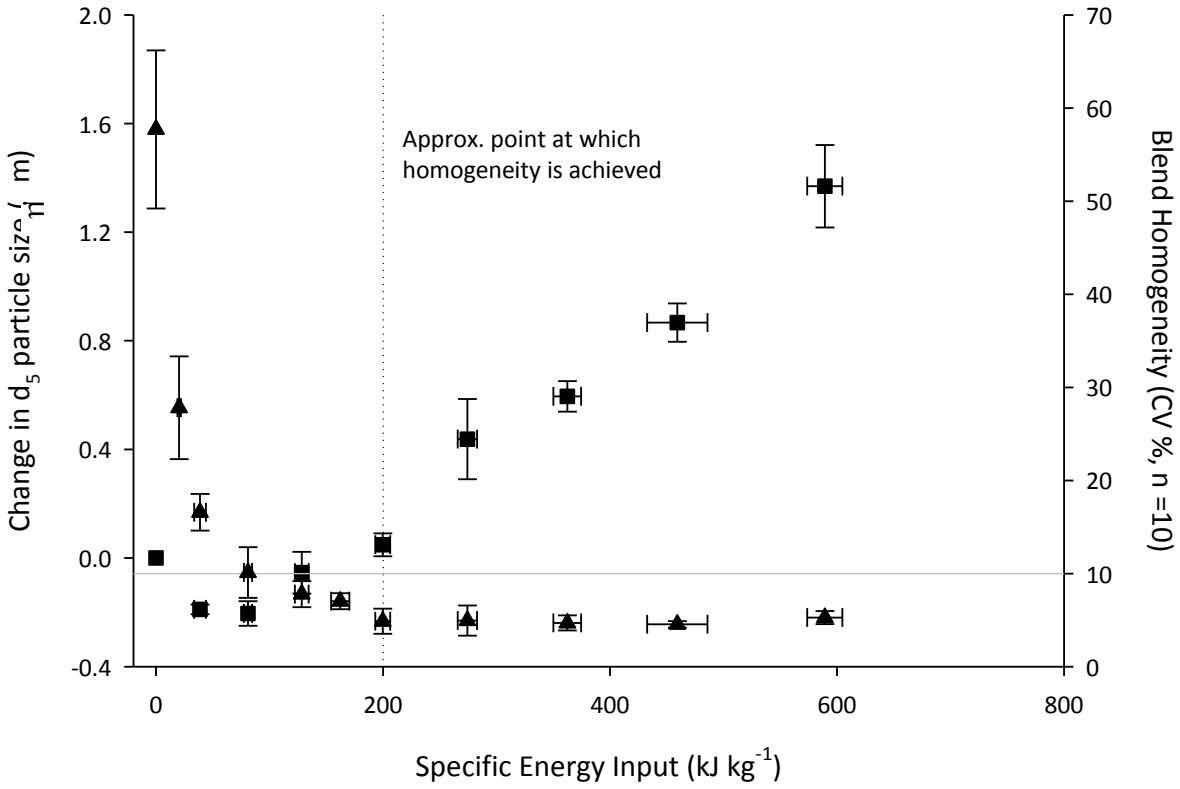

Fig. 4.26. Blend homogeneity (▲) and change in d_5 particle size (■) with respect to SEI for three independent 1:67.5 w/w cholesterol:lactose blends ± SD.

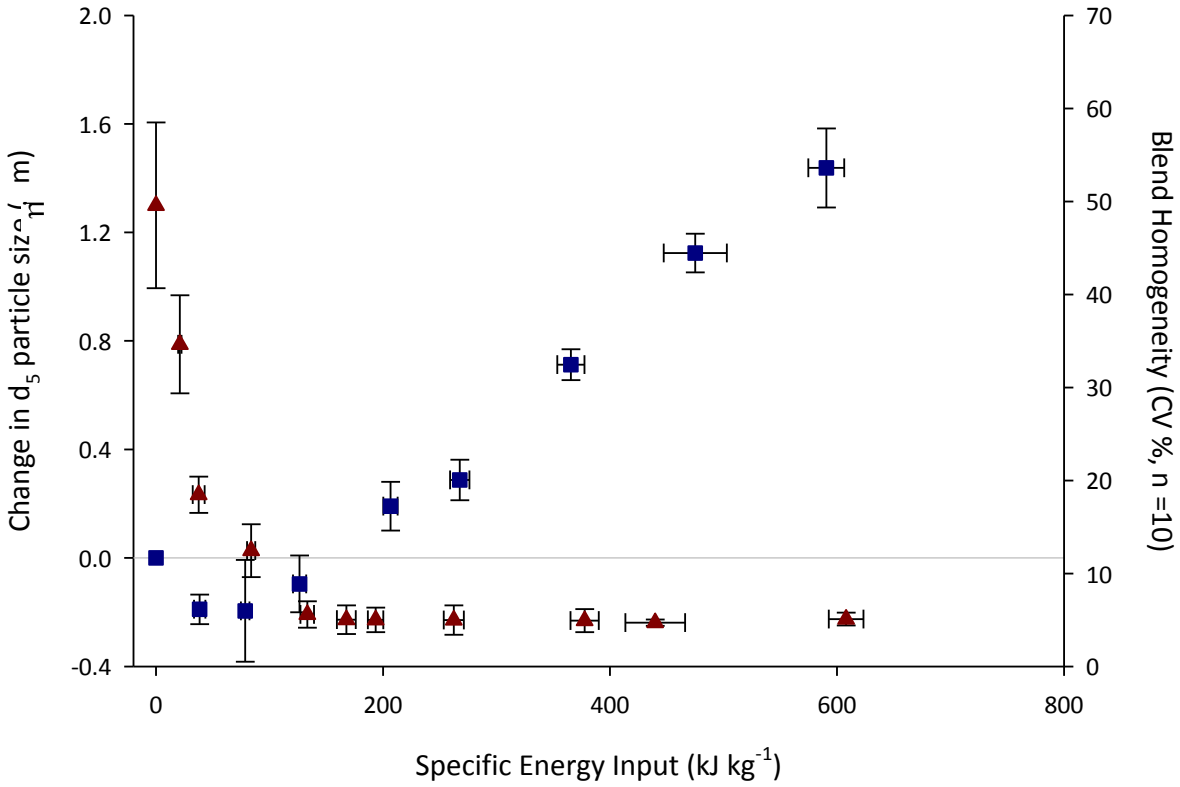

Fig. 4.27. Blend homogeneity (▲) and change in d_5 particle size (■) with respect to SEI for three independent 1:67.5 w/w vitamin C:lactose blends ± SD.

4.4. Conclusions

It has been shown that extended HSB has a noticeable and consistent effect on the PSD of inhalation-grade lactose (Bridson *et al*., 2007; Tu *et al*., 2009). This occurs across a range of laboratory-scale bowl sizes, albeit at different rates. However, the importance of changing the size distribution of lactose particles regarding the performance of DPI formulations is uncertain. Blending is primarily required to form a stable, homogeneous mixture of drug and carrier - in particular, HSB is used to obtain an ordered mix of two fine powders (Yip and Hersey, 1977). However, the extent to which this process is required remains uncertain.

Several conclusions can be drawn from the results presented in this chapter. Firstly, it is clear that when using HSB as a means to produce DPI formulations, SEI is the dominant factor regarding PSD; trends across the several laboratory scales employed in this study are similar, such that an increase in SEI results in an overall reduction in fines particle content (characterised by an increase in d_5 particle size), although absolute changes may increase with scale. It remains to be seen if this effect occurs beyond the laboratory-scale sizes used in this study, or even if it has implications for the manufacture of DPI formulations. It is recognised that an effective DPI formulation can be characterised by its emitted dose, chemical homogeneity, and FPF (Pilcer and Amighi, 2010), thus this study has shown that the point at which a homogeneous mixture has been achieved does not correspond to an end-point regarding changes in excipient PSD. Whilst the aerodynamic properties of the formulation (emitted dose and FPF) are considered in chapter 1, the results in this chapter potentially show that unnecessary powder changes are implicated by continuation of the blending process beyond the point at which chemical homogeneity is achieved.

Tests have been performed to eliminate or substantiate hypotheses relating to the cause of the reduction in fines content. One possibility was the loss of fines from the system – either by entrainment through the headspace of the bowl or by adherence to blending equipment – this has been eliminated by confirmation of the primary PSD of material adhered to the blending equipment and the bulk powder.

Finally, it is clear that lactose is a variable material – rigorous characterisation prior to blending is essential, as it has been shown that even slight changes in the starting properties of the input material can have significant effects on the performance of the formulation during blending. The differences in behaviour observed between the

material used in this study and a previous study (Bridson *et al.*, 2007) – notably the reduction in d_5 particle size at low SEI - was found to likely be caused by de-agglomeration, rather than particle fracture.

There is currently a paucity of information regarding the impact of this secondary manufacturing process on the performance of DPI formulations, thus chapters 5 and 6 will follow on from this work and detail the development of tests to assess the impact of blending on DPI formulations and use mimic formulations to test the effects different blending and storage regimes have on mimic DPI formulations.

5.0. Design and Use of a Novel Fluidised Bed Elutriation Technique to Assess the Changes in DPI Formulation Properties due to High Shear Blending

ABSTRACT

High shear blending (HSB) has been shown to affect the properties of dry powder inhaler (DPI) formulations. These changes may have adverse effects on the performance of such formulations, and thus a greater understanding of such effects will help enhance quality and efficacy of the product. A small-scale bulk method to assess the detachment of fine API particles from coarse excipient and to detect changes that arise from blending and storage of formulations was desired, with the use of a novel fluidised bed elutriation (FBE) technique proposed for development and use.

This chapter is split into two sections – the design considerations and initial trials forming a proof-of-concept study are described in section A, whilst tests on lactose-only formulations exposed to various blending regimes are reported in section B.

The FBE method involved consideration of the cohesivity of the material causing poor fluidisation conditions that were improved by control of fluidising gas humidity and bed vibration to reduce interparticulate forces. Consideration was also made regarding the bed dimensions and the superficial gas velocity (SGV) as this influenced the particle size that could be elutriated from the bed.

Although no apparent differences were observed in the bulk fluidisation behaviour of lactose exposed to different HSB regimes (or unprocessed lactose), the method showed that it could distinguish between grades of lactose that had been deliberately conditioned. In addition, this method showed that by subjecting inhalation-grade lactose excipient to various HSB specific energy inputs (SEIs), subtle differences could be observed in the elutriated powder, from which properties of formulations can be inferred, thus having possible implications for the production of such products.

5.1. Introduction

Based on the characteristics and operating principles of fluidised beds - in particular the elutriation of fine particles from the top of the column - it was proposed that a fluidised bed could be utilised to study the ability of fine particles (including APIs) to separate from the coarse carriers in DPI formulations. The first part of the chapter describes the considerations made in designing apparatus to study FBE of DPI formulations, whilst the second part uses this method to study the elutriation characteristics of lactose-only blends subjected to various specific energy inputs (SEIs) during HSB. Although fluidisation has been recently suggested as an important mechanism in the generation of an aerosol during an inhalation event (Tuley *et al*., 2008; Shur *et al*., 2008), no previous literature has utilised FBE performance as an indicator of DPI performance.

5.2. Materials and Methods

5.2.1. Lactose

Inhalation-grade lactose was provided by Friesland Foods Domo, Netherlands (section 2.2.1). Samples of this material used throughout the study were taken from batches stored in the original foil packaging (foil bag within cardboard box) at 20°C and 40% RH in humidity-controlled cabinets (Binder, Germany).

5.2.2. Particle Size Distribution

PSDs were determined using both wet and dry dispersion laser diffraction methods (see sections 2.3.1 and 2.3.2).

5.2.3. Dynamic Vapour Sorption

BET SSA analyses were performed using a DVS Advantage II (Surface Measurement Systems, UK) instrument following the methods described in section 2.2.4.3.

5.2.4. Scanning Electron Microscopy

SEM images were produced using the method described in section 2.2.5.

Section A
Development of a Fluidised Bed Elutriation Technique

5.3. General Fluidised Bed Design

Fig. 5.1 shows the final design and setup of the fluidised bed used in this study. The glass column was of circular internal diameter 25 mm and height 400 mm. This section will describe key features of the equipment, along with the experimental and theoretical considerations behind their use.

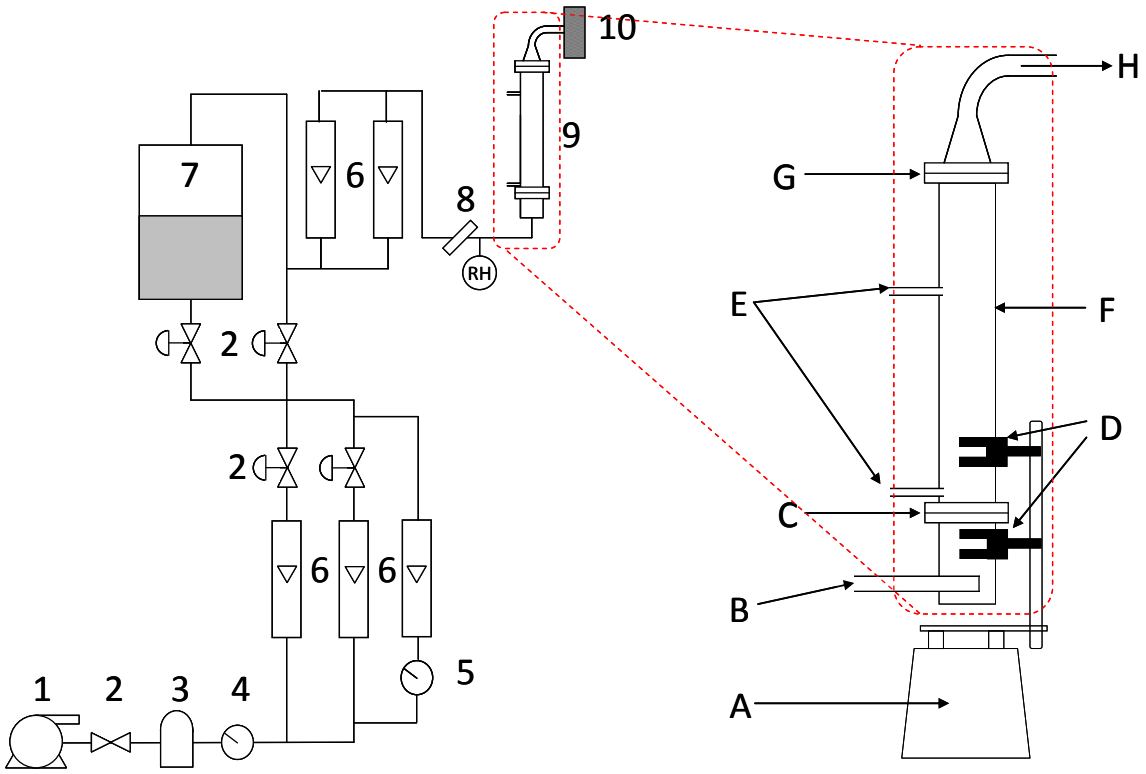

Fig. 5.1. Setup of humidifying rig and fluidised bed equipment. 1. Central compressor; 2. Valves; 3. Oil filter; 4. Pressure regulator; 5. Pressure gauge; 6. Rotameters; 7. Humidifying tank; 8. Temperature / humidity probe; 9. Fluidised bed; 10. Particulate filter; A. Vibrational feeder; B. Air inlet; C. Distributor; D. Clamps; E. Pressure taps; F. Fluidised bed column; G. Flanges to fill bed; H. Elutriated material to filter.

5.4. Transport Disengagement Height

In order to design the column height, the terminal velocity, U_t of particles was considered to determine a suitable transport disengagement height (TDH) for the column.

In order to elutriate particles of a given size, first the terminal velocity of particles needed to be estimated to give an indication of the fluidising gas velocity required. Application of Stokes' Law (Equation 5.1), allows the terminal velocity of particles to be approximated for systems with low Reynolds number (Re <1).

$$U_t = d_p^2(\rho_p - \rho_g)g/18\mu \qquad \textbf{Equation 5.1}$$

Here, U_t is the terminal velocity (m s^{-1}), g is the acceleration due to gravity (m s^{-2}) d_p is the particle diameter (m), ρ_p and ρ_g are the densities of the particle and gas respectively (kg m^{-3}), and μ is the gas viscosity (kg m^{-1} s^{-1}). This calculation allows the SGV to be set according to the desired particle cut size, since elutriation will only occur when the terminal velocity is smaller than the SGV (Saxena and Jadav, 1983). For a cut size of 25 μm, the minimum required gas velocity was found to be ≈ 2.5 cm s^{-1} therefore, based on the recommendation that during air classification by FBE, the fluidising velocity should be at least twice the terminal velocity of the fines cut size (Heath and Aconsky, 1963), a gas velocity corresponding to a volumetric flow rate of 2 l min^{-1} was chosen (6.27 cm s^{-1}).

When the SGV exceeds the terminal velocity of the particle, it is able to entrain from the bed. Often the terms *elutriation* and *entrainment* are used to describe the same phenomenon, however they have similar meanings and are often confused. Entrainment describes the flux of solids carried away from the powder bed by the gas and is related to the cross-sectional area of the bed, elutriation describes the classifying effect of the fluidised bed entrainment – it characterises the selective removal of particles of individual sizes from the system (Hartge and Werther, 2003). Leva, 1951 measured elutriation from a bed of particles with a bimodal size distribution and found that:

i) when the column height is small, elutriation rate is high, but if the height exceeds a minimum size, the elutriation rate is a constant, minimum value. This is due to small particles, which have a high velocity, and hence require greater distance to slow down and return to bed, being expelled, and:

ii) elutriation causes a decrease in particle concentration.

An estimation for the TDH was made by Zenz and Weil (1958), and Kunii and Levenspiel (1991), who relate TDH to column diameter, d_t and superficial gas velocity, U_{SGV}:

$$\frac{TDH}{d_t} = 3.171\frac{U_{sgv}^2}{d_t g} \qquad \textbf{Equation 5.2}$$

this could be rearranged to give:

$$\frac{U_{sgv}^2}{TDHg} = 0.0432 \qquad \textbf{Equation 5.3}$$

The constant in Equation 5.3 is dependent on the properties of the material. Fournol *et al*., (1973) determined that for fine catalyst with average particle size 58 μm (similar particle size to the material used in this study);

$$\frac{U_{sgv}^2}{TDHg} = 1.001 \qquad \textbf{Equation 5.4}$$

Based on a SGV of 6.27 cm s^{-1}, the TDH necessary from Equation 5.4 is approximately 37 cm.

5.5. Vibration

Visual observations of channelling and general poor fluidisation were made whilst performing initial fluidisation trials. The cohesivity of the powder prevented good fluidisation; channelling cannot be described as good fluidisation since the individual particles within the bed cannot be entirely supported by the pressure drop. Therefore, a method was required to enhance the fluidisation performance.

Various methods have been described in literature to improve the fluidisation regime of cohesive powders. These primarily focus on the reduction of the strong interparticle forces that predominate in cohesive powders. Park *et al*., (2002) explore methods for reduction of electrostatic charges in gas-solid fluidised beds; whilst Ma and Kato (1997) and Li and Kato (2001) study the effect these forces have on elutriation of fines.

Zhou and Li, (1999), describe the effect of adding different sized particles on the fluidisation of cohesive powders and relate them to the interparticle forces that affect gas fluidisation of fine powders in several ways. Micron-sized particles in the Geldart group C class form channels and spouts, rather than the bubbling regime associated with larger group A particles. The fluidisation of unprocessed lactose is difficult to predict due to its wide PSD, with its considerable fine particle fraction making the powder cohesive in nature. Dutta and Dullea, (1991); Jaraiz *et al*., (1992); Mawatari *et al*., (2000); Mori *et al*., (1990); and Wang *et al*., (2000) have all explored the possibility of applying both horizontal and vertical mechanical vibrations to the powder bed in order to enhance fluidisation performance.

5.5.1. Method

Based on the work by Mawatari *et al*., (2003), and Levy and Celeste, (2006) apparatus was built to apply vibrations to the fluidised bed to enhance the fluidisation ability of the cohesive lactose formulations. For this, a small vibrational feeder (Retsch Vibratory

Feeder DR 100, Newtown, PA, USA) was modified by removing the chute and attaching a stand with clamps to hold the fluidised bed column; vibrations were applied with oscillations in the range of 30-45 Hz, and amplitudes of 0.5-1.5 mm.

To test the ability of the bed to fluidise Group A powders, the fine particle population of particles were removed by air jet sieving unprocessed lactose for 30 min using 25 μm and 71 μm sieves. A standard pressure drop vs. SGV experiment using 20 g ± 0.1 g was performed without vibration to compare the performance of cohesive powder against more free-flowing material. 20 g was used as the initial mass based on work by Kim *et al*., (1999) who suggest that the bed length:diameter ratio should be greater than 2 to ensure good aeration of the bed. As bed height increases in comparison to diameter, wall effects are more prominent and it becomes more difficult to fluidise powder (Rao *et al*., 2010), thus, based on the 25 mm diameter column, a mass of 20 g unprocessed lactose provided a bed height of approximately 70 mm– thus allowing good aeration of the bed.

5.5.2. Results

Fig. 5.2 shows pressure drop vs. SGV curves for samples of unprocessed lactose both with, and without the aid of vibration. Results show that even with the aid of vibration, a good fluidisation regime is difficult to achieve with the cohesive unprocessed inhalation-grade lactose used in this study. However, vibration allows a more stable bed to form by reducing the channelling which causes pressure drop to be both unstable and much lower than for a packed bed; this is consistent with results found by Xu and Zhu, (2006) who found that vibration of cohesive powders reduced their propensity to channel and lift as a plug. Vibrating the powder bed also produced a fluidisation curve more akin to the theoretical curve shown in Fig. 1.6, due to the additional energy applied to overcome the interparticle forces. The large error bars are indicative of channelling since the pressure drop is erratic and uncontrolled, leading to large variations both during an individual experiment, and across several experiments.

On the other hand, it can be seen from Fig. 5.3 that "25 μm" and "71 μm" grades of lactose do not require vibration of the bed to improve their fluidisation performance. Both grades of lactose are readily-fluidised, and their U_{mf} correlate closely with those determined theoretically (Fig. 5.9 and Table 5.3).

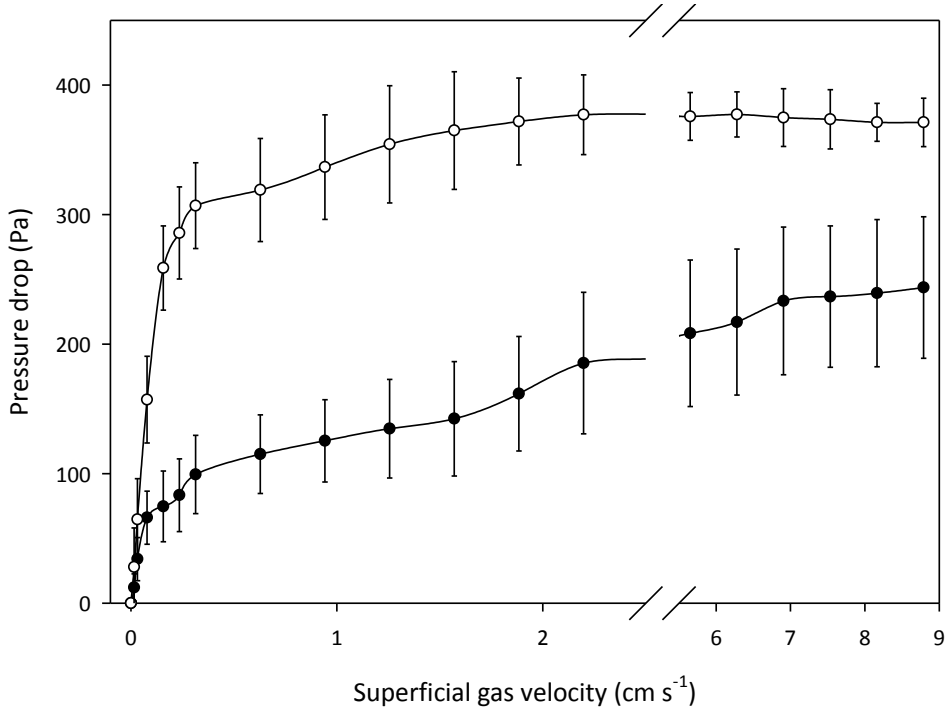

Fig. 5.2. Effect of vibration on the fluidisation performance of 20 g ± 0.1 g unprocessed lactose. Results are averaged from three independent experiments ± SD. ○ - With vibration, ● - without vibration.

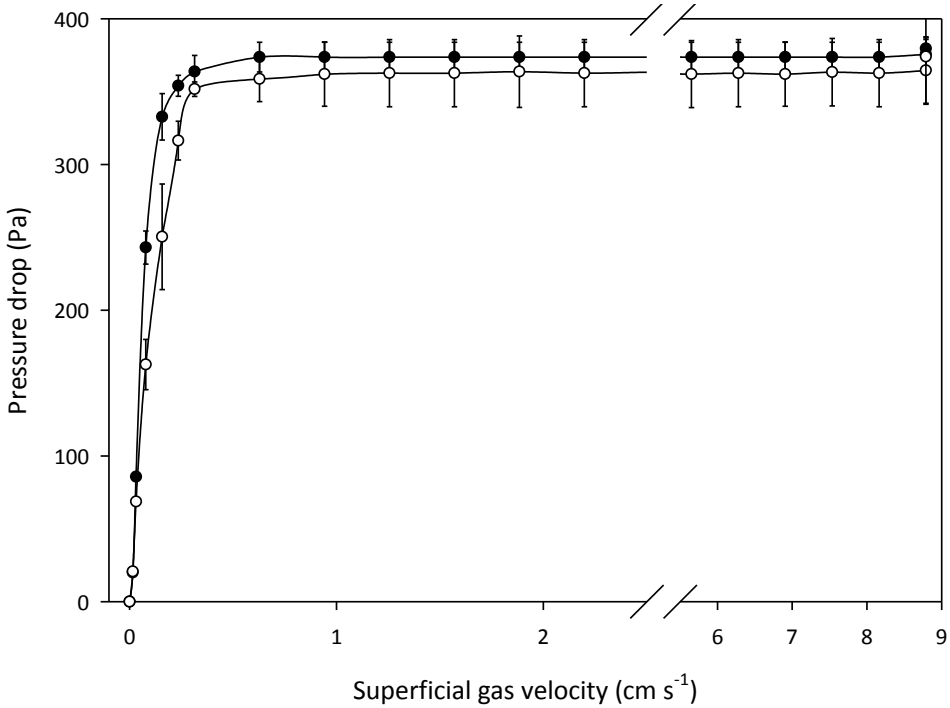

Fig. 5.3. Pressure drop vs. SGV for "25 μm" (●) and "71 μm" (○) grades of lactose, without vibration. Results are averaged from three independent experiments ± SD.

5.6. Superficial Gas Velocity

The elutriation of fine particles is dependent on the balance between the particles' terminal velocity and the SGV (section 1.6). To determine the effect on the fluidised bed used in this study, a simple experiment was performed to describe the extent to which SGV affects the mass of fine particles that can be removed from the bed. This

experiment also allowed a test of sampling time to be performed, as due to the limited size of the particulate filter (section Fig. 5.8), a suitable sampling time needed to be found to prevent the filter clogging, and producing adverse backpressure to the system.

5.6.1. Method

Two flow rates were used (2 l min^{-1} and 8 l min^{-1}) corresponding to SGVs of 6.27 and 25.08 cm s^{-1} respectively. These were chosen as they equated (approximately) to terminal velocities of 25 and 50 μm particles (Equation 5.1). 20 g ± 0.1 g unprocessed lactose was exposed to the SGV in the vibrating bed for 10 min with elutriated samples taken at 1, 2, 5 and 10 min intervals, and filter emptied. Following this, the samples were left to fluidise until all possible material was elutriated. Samples were then weighed and sized using the wet dispersion laser diffraction method described in section 2.3.1.3. This experiment was performed in triplicate.

5.6.2. Results

Fig. 5.4 shows the cumulative mass elutriated at different SGVs. It can be shown that a greater SGV will remove more material more rapidly than a lower SGV. It takes approximately 1 hour to remove all available material at 25.08 cm s^{-1}, whereas it takes over two hours to remove all material at 6.27 cm s^{-1}.

Table 5.1 describes the particle size and surface area of unprocessed lactose elutriated at different SGVs, highlighting the ability of the fluidised bed to act as an air classifier and its ability to separate particles by altering the SGV.

Fig. 5.5 shows that, as expected, a greater SGV elutriates more material than a lower SGV. Following 10 min elutriation time, an average of 789 mg of lactose is removed by 25.08 cm s^{-1}, whereas just 253 mg is removed by a SGV of 6.27 cm s^{-1}. The total amount of material elutriated (Fig. 5.4) was 1743 ± 102 mg (8.7% initial material) when exposed to a SGV of 6.27 cm s^{-1}, whereas when exposed to 25.08 cm s^{-1}, the total elutriated material was 4855 ± 239 mg (24.3% initial mass). Hence, these results suggest that 8.7% of particles are below 25 μm Stokes' diameter, whilst 24.3% are below 50 μm; this compares to laser diffraction data (dry dispersion) suggesting 17.5% particles are below 25 μm, whilst 35% are below 50 μm. It should be considered that the laser diffraction method used to size the elutriated fraction is known to cause de-agglomeration, thus producing a finer distribution, which does not

entirely represent this material. In addition, the elutriation method is much more subtle, operating at lower pressures than the RODOS device, thus de-agglomeration is unlikely, and agglomerates greater than the cut-off diameter will not be elutriated, hence their constituent particles do not appear in the distribution.

Fig. 5.5 also shows that at the higher SGV, the sampling time needs to be shorter due to particulate filter filling up with the amount of material elutriated. It can be shown that the amount of material removed after 5 min was similar to that removed after 10 min, thus suggesting (and confirmed by observation) that the filter was full. However, this was not the case at the lower SGV since the cumulative amount of material elutriated after 10 min was similar regardless of the sampling intervals.

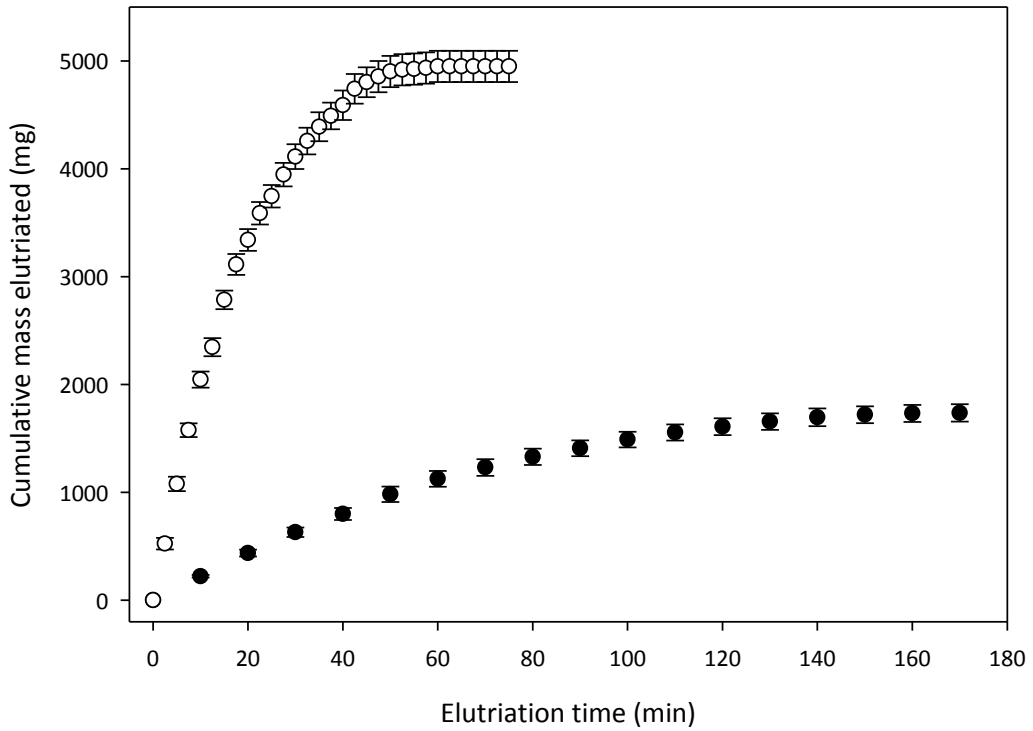

Fig. 5.4. Effect of fluidisation time on cumulative mass elutriated at different SGVs. Results are averaged from three independent experiments ± SD. 25.08 cm s^{-1} (○), 6.27 cm s^{-1} (●). The difference in sampling time was due to the filling of the particulate filter at higher SGV, therefore requiring more frequent emptying.

Table 5.1. Comparison of SSA and PSD for unprocessed lactose elutriated by different SGVs.

Superficial gas velocity (cm s^{-1})	*Specific surface area* (cm^2 g^{-1})	Particle size (μm)		
		d_{10}	d_{50}	d_{90}
6.27	6768 ± 453	1.05 ± 0.08	10.92 ± 1.09	27.51 ± 2.27
25.08	4410 ± 67	1.23 ± 0.11	15.25 ± 2.74	46.91 ± 5.86

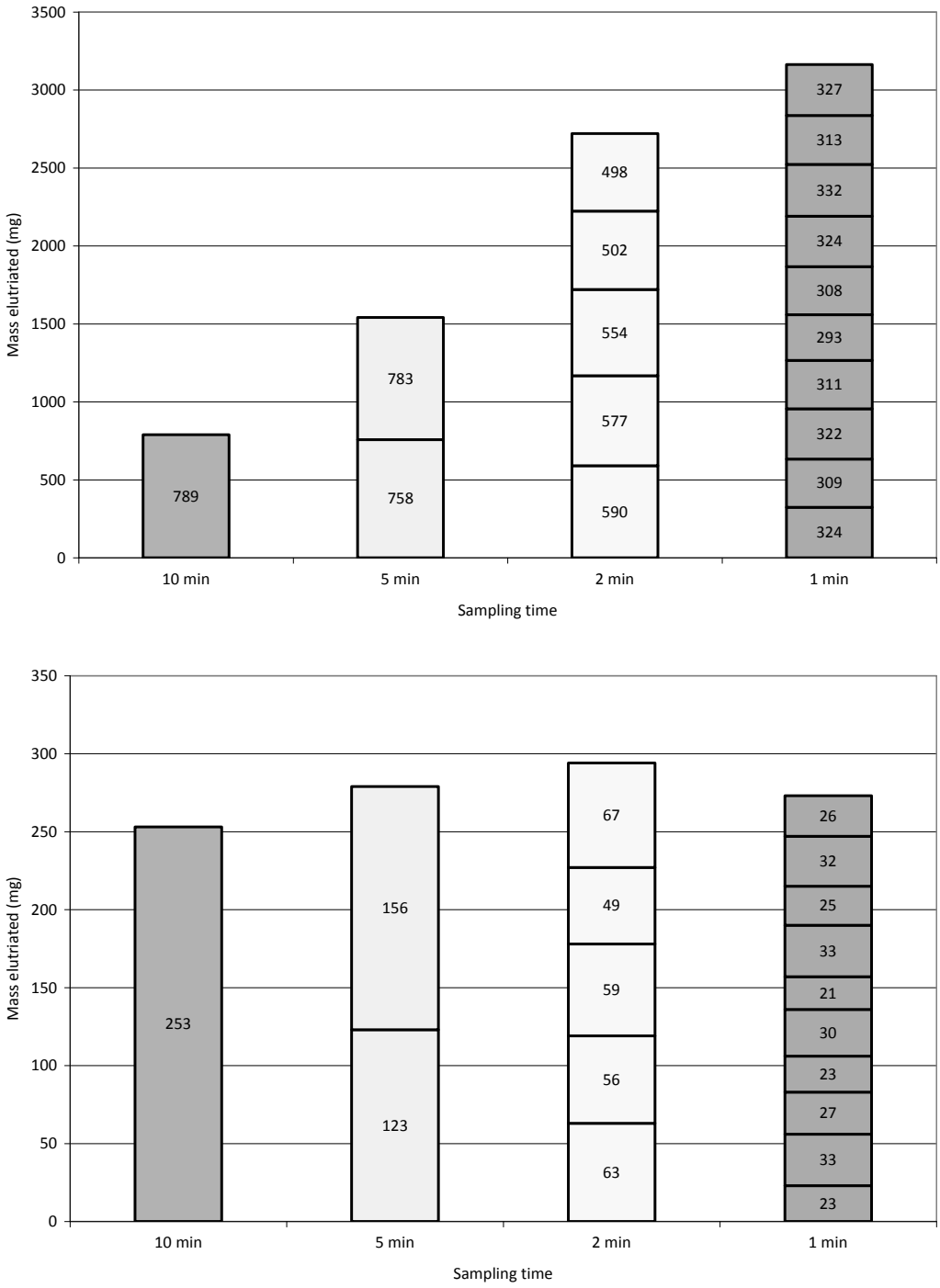

Fig. 5.5. Mass elutriated from fluidised bed as a function of sampling time at different SGVs. Top (25.08 cm s^{-1}), bottom (6.27 cm s^{-1}).

5.7. Relative Humidity

Relative humidity (RH) is known to affect the performance of DPI formulations (Chew and Chan, 2002; Young *et al*., 2007b; Guenette *et al*., 2009); therefore, control of the airstream RH is vital. In order to achieve this, a humidifying rig was used consisting of a series of valves and pipes in conjunction with a water tank to provide moisture (Fig. 5.1). The air humidity was controlled by a valve situated on a bypass line across a humidifying tank of water. With the bypass valve open, the air is dry, as it chooses the

path of least resistance. When the bypass valve is closed, the air is forced through the water, thus picking up moisture en route. Humidity measurements were made to ±2% RH accuracy with a HumidiProbe temperature and humidity sensor and data logging software (PicoLog, Pico Technology Ltd. UK).

The sensitivity of the system was determined by varying the position of the valve on the bypass line to alter the amount of air flowing through the water tank. Fig. 5.6 shows that humidity could be varied in 10% intervals with stability of approximately ±2%.

Initial trials using fluidising gas of varying humidities showed that air with low moisture content produced strong electrostatic charging effects, causing particles to adhere to the column (Fig. 5.7), whereas using moist air, channelling readily occurred through the bed, and good fluidisation was difficult to achieve.

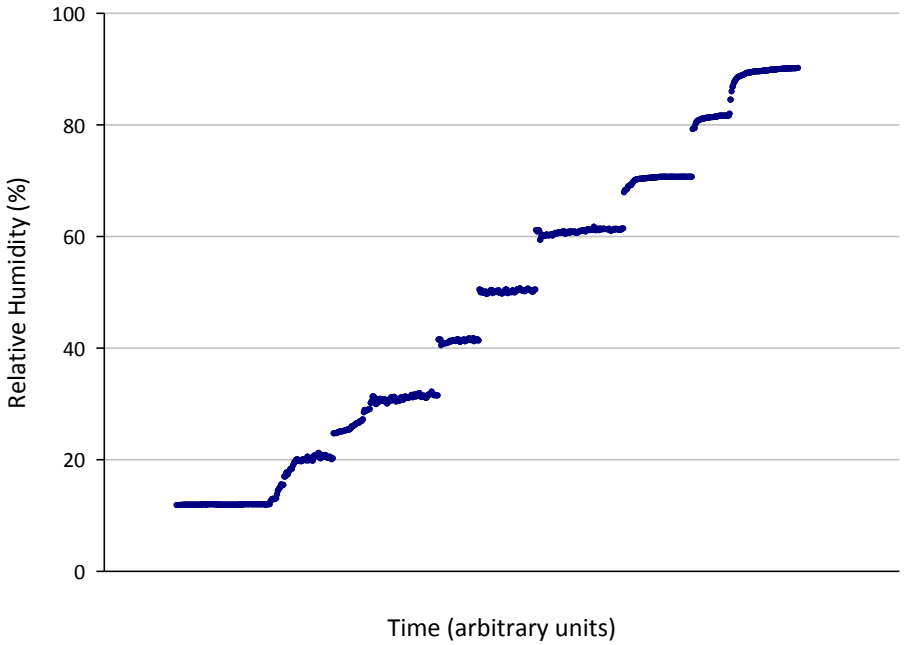

Fig. 5.6. Ability to manually control airstream humidity.

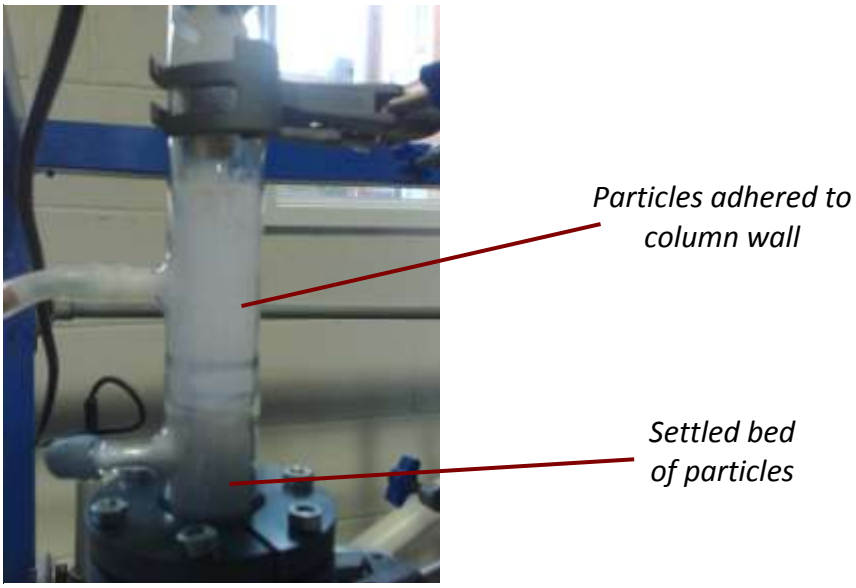

Fig. 5.7. Particles adhered to column wall following exposure to 10% RH fluidising gas for 30 min.

5.8. Device to Collect Fines

Cyclones are often used to collect fines elutriated from fluidised beds, in order to return them to the bed in circulating systems.

Fig. 5.8. Swagelok particulate filter

Other methods: Callen *et al*., (2007) describe the use of charged parallel plates to collect elutriated fine particles from a fluidised bed. Since no recirculation of fines is required, and the fraction of particles likely to be entrained is small, a cyclone would be cumbersome and inefficient given the relatively small scale of the fluidised bed used. As relatively low flow rates and SGVs are to be employed, a 12 mm stainless steel tee-type particulate filter, with 0.5 μm pore size was chosen to collect elutriated material (Swagelok, UK) (Fig. 5.8).

5.9. Distributor

A fluidised bed distributor serves two purposes: Firstly, it must support weight of non-fluidised material, and facilitate effective distribution of fluidising gas over the cross-sectional area. The gas must be distributed uniformly into the fluidised bed without causing attrition of the bed material (Pell, 1990; Perry and Green, 1997; Seville *et al*., 1997). There needs to be a sufficient number of holes to ensure local uniformity across the cross-sectional area. Key considerations made included: correct sealing between distributor and wall (flanges were incorporated into design to "clamp" distributor and

seal with PTFE), and plenum design – a tube entered the plenum from the side wall and was bent downwards at the centre to ensure adequate dispersion of gas (Pell, 1990; Perry and Green, 1997).

Since the powder, fluidising gas and operating conditions (temperature, humidity, pH, etc.) were mild and only small masses, SGVs and pressure drops were experienced, Whatman Grade 1 Qualitative Cellulose Filter Paper (Whatman, UK) was cut to size and employed as gas distributor. In, addition, although the filter paper distributor produces a relatively large pressure drop (and hence energy loss) compared to that across the bed, the resultant energy loss is not important in this application, unlike industrial processes where minimising energy losses is vital.

5.10.Temperature

Wu and Baeyens (1991) and more recently, Xu and Zhu (2006) recognise the importance of controlling gas and powder temperature during fluidisation and describe the effects of gas temperature on the fluidisation ability of cohesive powders. All fluidising experiments in this study were performed at ambient temperatures.

5.11.Flow Rate and Pressure Drop Measurements

A rotameter is a device that measures the flow rate of a liquid or gas in a closed tube. The rotameters used in this study were made from tapered glass tubes with a float inside which are lifted by the force of the moving gas, against the gravitational force. The rotameters used in this study had optimal flow rate working ranges between 0-0.2 and 0-5 l min^{-1} (Platon Series Rotameters, Muis Controls, Alberta, Canada).

Differential pressure drop measurements across the powder bed were performed using a digital manometer (FC0510 Micromanometer, Furness Controls Limited, UK).

5.12.Summary of Experimental Conditions Used

Based on the findings above, tests of the effect of SEI on the elutriation and fluidisation performance of lactose blends were performed using a SGV of 6.27 cm s^{-1} (to correspond to particles with Stokes' diameter of 25 μm). Since fine particles are known to play an important role in the performance of DPI formulations (section 1.4.9.1), it was sensible to study the separation of the finest possible particles. Lower SGVs were difficult to use since the amount of material that could be removed was insufficient for size analysis.

Section B
Use of Fluidised Bed Elutriation Technique to Explore Blending-Induced Changes in α-Lactose Monohydrate

5.13. Materials

The following study employed use of unprocessed lactose, and lactose exposed to differing blending regimes (obtained by varying the SEI – section 4.2.3). Formulations were prepared using the HSB equipment described in section 4.2.3 with sampling of powders performed using the method described in section 4.2.5. For this study, the small bowl with internal diameter 130 mm was employed with an initial mass loading of 500 g and rotational speed 500 rpm (a good blending regime – section 4.3, Fig. 4.10). Table 5.2 details the particle size data and SEI of lactose-only blends used in this study, along with a deliberately agglomerated sample conditioned through exposure to high humidity (70%) for two weeks.

Table 5.2. Selected samples for FBE and AJS study. Particle size values are mean values of three measurements (dry dispersion) taken from at least three samples from the blended batch.

	Sample	*Specific energy input* (kJ kg^{-1})	*Particle size* (μm)		
			d_5	d_{10}	d_{50}
Unblended	A	0	2.97	9.72	68.72
	B	0	3.03	9.59	69.54
	C	0	3.06	9.93	69.04
Low energy input 1	A	24	2.80	8.79	70.14
	B	31	2.79	8.46	68.19
	C	35	2.84	8.76	68.7
Low energy input 2	A	56	2.65	8.22	67.52
	B	82	2.77	8.42	67.92
	C	68	2.71	8.30	67.68
Medium energy input	A	189	3.06	9.93	69.16
	B	210	3.18	10.04	70.11
	C	223	3.29	10.25	70.24
High energy input	A	538	4.35	11.45	70.92
	B	622	4.86	11.84	71.3
	C	460	4.33	11.57	71.68
Deliberately agglomerated	A	N/A	5.14	13.33	75.28
	B	N/A	5.20	13.47	75.44
	C	N/A	5.11	13.30	75.21

5.14. Determination of Minimum Fluidisation Velocity and Pressure Drop

For a settled bed, there is a point at which, as the gas velocity is increased, the drag force on the particles becomes equal to the buoyant weight of the bed. The bed is then supported by the gas flow and subsequently exhibits fluid-like properties; flowing easily, and showing an apparent viscosity. Since the drag force on the particles due to the gas flow is equal to the manometric pressure drop across the bed, then the manometric pressure drop (ΔP) is equal to the buoyant weight of the bed, or:

$$\frac{\Delta}{L} = 1 - \varepsilon_f)(\rho_p - \rho_g)g \qquad \textbf{Equation 5.5}$$

where, L is the bed height, ε_{mf} is the voidage at minimum fluidisation, and ρ_p and ρ_g are the gas and particle densities respectively. When combined with the Ergun (1952) equation (Equation 5.6) for the pressure drop through a settled bed of solids with particle diameter d_p,

$$\frac{\Delta}{L} = 150\frac{(1-\varepsilon_f)^2}{\varepsilon^3}\frac{\mu U}{d_p^2} + 1.75\frac{(1-\varepsilon_f)}{\varepsilon^3}\frac{\rho_g U^2}{d_p} \qquad \textbf{Equation 5.6}$$

where, μ and U are the gas viscosity and velocity respectively. It can be shown that:

$$\frac{\rho_g d_p^3(\rho_p - \rho_g)g}{\mu^2} = 150\frac{(1-\varepsilon_{mf})}{\varepsilon_{mf}^3}\frac{\rho_g d_p}{\mu}U_f + 1.75\frac{\rho_g d_p^2}{\varepsilon_{mf}^3\mu}U_{mf}^2 \qquad \textbf{Equation 5.7}$$

The left hand side of Equation 5.7 is dimensionless and is known as the Archimedes number, Ar. This equation is difficult to use since there are no prescribed values for ε_{mf}. Therefore, Wen and Yu (1966) described a simplified equation:

$$Ar = 1650Re_{mf} + 24.5Re_{mf}^2 \qquad \textbf{Equation 5.8}$$

where, Re_{mf} is the Reynolds' number of the system at minimum fluidisation – dependent on gas density, U_{mf}, particle diameter and gas viscosity, μ,

$$Re_{mf} = \rho_g U_{mf} d_p / \mu \qquad \textbf{Equation 5.9}$$

thus, U_{mf} can be more easily calculated. For particles smaller than around 100 μm, and Re_{mf} << 0.5, the second term on the right hand side of Equation 5.8 can often be neglected, thus,

$$U_{mf} = \frac{d_p^2(\rho_p - \rho_g)g}{1650\mu} \qquad \textbf{Equation 5.10}$$

This leads to a description of how the pressure drop across the bed increases with increasing SGV up to the U_{mf} (Fig. 1.6). This pressure drop cannot exceed the buoyant weight of the particles, therefore, the bed voidage must increase in order to maintain pressure drop at or below this level. For comparison, Walker *et al*., (2007) estimate a U_{mf} for lactose particles with average size of 50 μm of 6.6×10^{-4} m s^{-1} in their work on the fluidised bed granulation of pharmaceutical powders. With a bimodal distribution of powders, especially over such a wide span of sizes, it is difficult to apply Equation 5.10 accurately to the lactose used in this study; instead, it is more useful to determine the U_{mf} experimentally.

5.14.1. Method

20 g ± 0.1 g was exposed to increasing SGV with pressure drop recorded at each interval. Unprocessed lactose, low energy input (68 ± 13 kJ kg^{-1}), high energy input (540 ± 81 kJ kg^{-1}), deliberately agglomerated lactose (unprocessed lactose stored at 70% RH for two weeks), "71 μm" lactose, "25 μm" lactose (both obtained through air jet sieve (AJS) removal of fines) were used to give materials with a range of cohesivity. See Table 5.3 for particle size data of these samples.

5.14.2. Results

As can be seen from Equation 5.10, the U_{mf} across the bed is a function of particle size, thus a bed consisting of larger particle sizes theoretically produces a greater U_{mf}.

However, this only holds true for readily-fluidised material comprising non-cohesive, near-spherical particles, and is difficult to predict when powders with bimodal distributions and intrinsic cohesive fines are present, as is the case with the unprocessed and blended lactose used in this study (Perry and Green, 1997; Pell, 1990). This occurs since the fine particles in the voids between the larger particles will fluidise before the larger particles as the SGV increases. This partial fluidisation will occur at a smaller velocity than the average U_{mf}, thus making comparisons between theory and experiment difficult.

The apparent U_{mf} of lactose used in this study was determined approximately by the standardized method of Richardson (Richardson, 1971; Turki and Fatah, 2008), which corresponds to the intersection with the horizontal line representing fluidised bed operation, and the curve that exhibits packed bed operation (Fig. 1.6). The horizontal line and the curve are estimated to approximately fit the SGV value. Experimental values for "71 μm" and "25 μm" lactose are approximately 0.35 cm s^{-1} and 0.25 cm s^{-1} respectively (Fig. 5.9). These results follow the predicted trends, with the theoretical values of U_{mf} shown in Table 5.3 for "71 μm" and "25 μm" lactose such that the coarser material displays a greater U_{mf} than the finer material. Since these grades of lactose have a monomodal distribution and are not particularly cohesive, a reasonable estimate of their U_{mf} can be made, however this is not the case for unprocessed and blended lactose due to the cohesivity of the powder and bimodal distribution of powder.

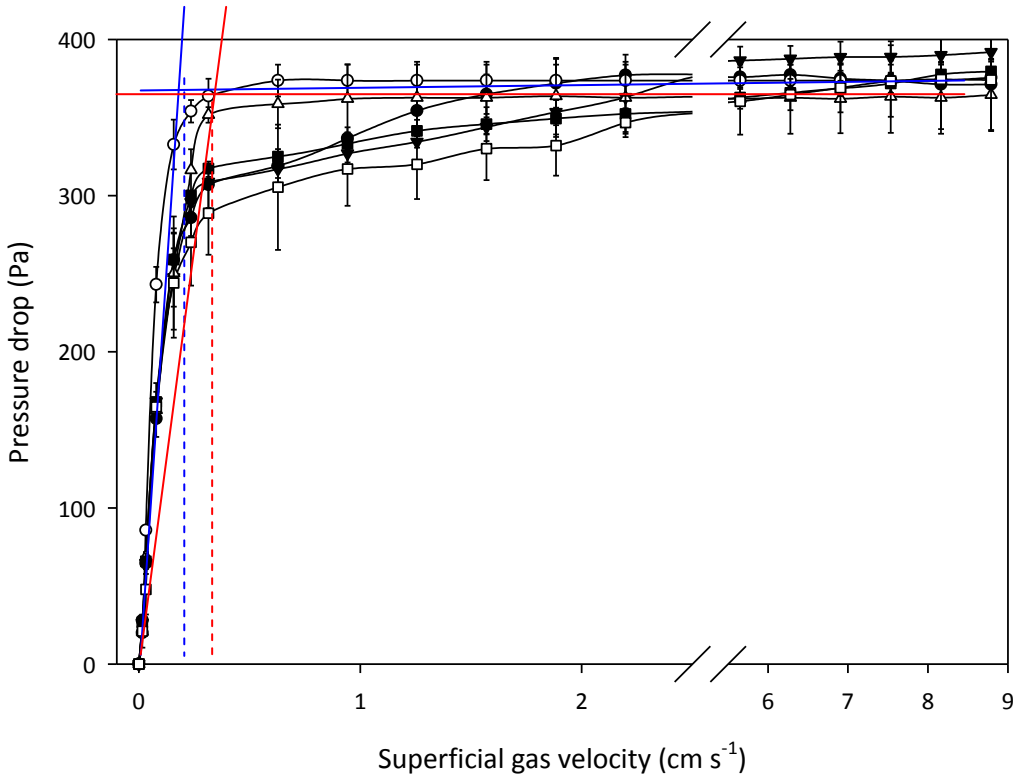

Fig. 5.9. Pressure drop across bed as a function of SGV for various lactose samples. ● - Unprocessed lactose, ■ - Low energy input (68 ± 13 kJ kg^{-1}), ▼ - High energy input (540 ± 81 kJ kg^{-1}), □ - Deliberately agglomerated lactose, △ - "71 μm" lactose, ○ - "25 μm" lactose. Blue and red lines represent approximate determination of U_{mf} of 25 and 71 μm lactose respectively. Results shown are the SEM of three samples for each energy input/grade of lactose, with measurements performed in triplicate.

Despite its smaller average particle size, reliable estimates of U_{mf} for unprocessed and blended lactose are difficult to make. An increase in the interparticulate forces results in the finer, unprocessed and blended lactose showing a greater U_{mf} than the 25 μm and 71 μm lactoses with fines removed.

The change in bed height was also greater for this material than the coarser lactose due to the greater voidage of the bulk powder. This is supported by Räsänen *et al.,* (2003) who found an increase in poor fluidisation behaviour and higher than expected U_{mf} (from theory) due to the increased interactions and interparticulate forces of fine paracetamol particles. In addition, the sphericity of particles and the degree of agglomeration can cause differences between theoretical and experimental results (Turki and Fatah, 2008). As with both the blended (all energy inputs) and unprocessed lactose, the deliberately agglomerated lactose shows poor fluidisation behaviour due to the cohesivity of the material and propensity for channelling, despite vibration of the bed.

Table 5.3. Theoretical calculations of U_{mf} based on mean particle size using Equation 5.10.

	Mean particle size (μm)	U_{mf} (cm s^{-1})
"71 μm lactose"	96	0.463
"25 μm lactose"	75	0.282
Unprocessed lactose*	68	0.233

* **difficult assumption to make due to wide, bimodal PSD and large proportion of fine material**

Pressure drops of the 71 μm, 25 μm, unprocessed, blended, and deliberately agglomerated lactoses show that a maximum value of ~375 Pa is achieved when all materials can be considered to be in the fluidised state, where the pressure drop is equal to the buoyant weight of the bed. However, the equation to estimate pressure drops (Equation 5.5) cannot be adequately applied to the systems used in this study as both the ε_{mf} and L terms (representing the bed voidage and height at the point of minimum fluidisation respectively) were very difficult to accurately measure during operation. Instead, the pressure drop can be estimated by multiplying the bed mass by g (the acceleration due to gravity – 9.81 ms^{-2}) and dividing by the bed area, this gives a value of approximately 400 Pa.

The pressure drop vs. SGV curves shown in Fig. 5.9 show a noticeable difference to the curve described by Shur *et al.*, (2008), where an argument is made that the tensile strength of a fixed bed needs to be overcome before the bed is fluidised. This "hump" at the top of the pressure drop curve is shown in the theoretical plot in Fig. 1.6, however was not observed in any of the experimental data shown above.

To investigate the absence of the tensile strength "hump", the hysteresis of the pressure drop was measured at both increasing and decreasing SGV. Fig. 5.10 shows this hysteresis effect on the pressure drop across a bed of unprocessed lactose (similar trends were observed for blended lactose and deliberately agglomerated lactose). It was found that the bed behaviour differs when reducing the SGV compared to increasing the SGV, such that the fluidisation state operates at lower gas velocities and channelling was less likely. In this type of regime, the bed is said to be acting in a dynamic state, where the interparticle forces and initial packing history have been reduced. This work supports the theory suggested by Shur *et al.*, (2008), suggesting that the tensile strength of DPI powders, needs to be overcome in order to aerosolise the formulation for delivery to the lungs. However, due to the channelling observed in the powders in this study, the static and dynamic states have switched, with the static state operating at lower pressure drops for cohesive powders.

Features of unprocessed lactose fluidisation curves (Fig. 5.10):

1. Channelling causes poor fluidisation state, the bed weight is not fully supported and the bed is prone to fracture with unstable pressure drops resulting in large error bars.

2. High SGV allows "good" fluidisation – high level of mixing and good bed circulation.

3. Reduction of SGV - fluidisation regime continues at lower SGV due to rearrangement of particles - less disruption by channelling.

4. Difference in pressure drops at early fluidisation stage caused by removal of packing history - related to the tensile strength of the powder bed described by Shur *et al.*, (2008).

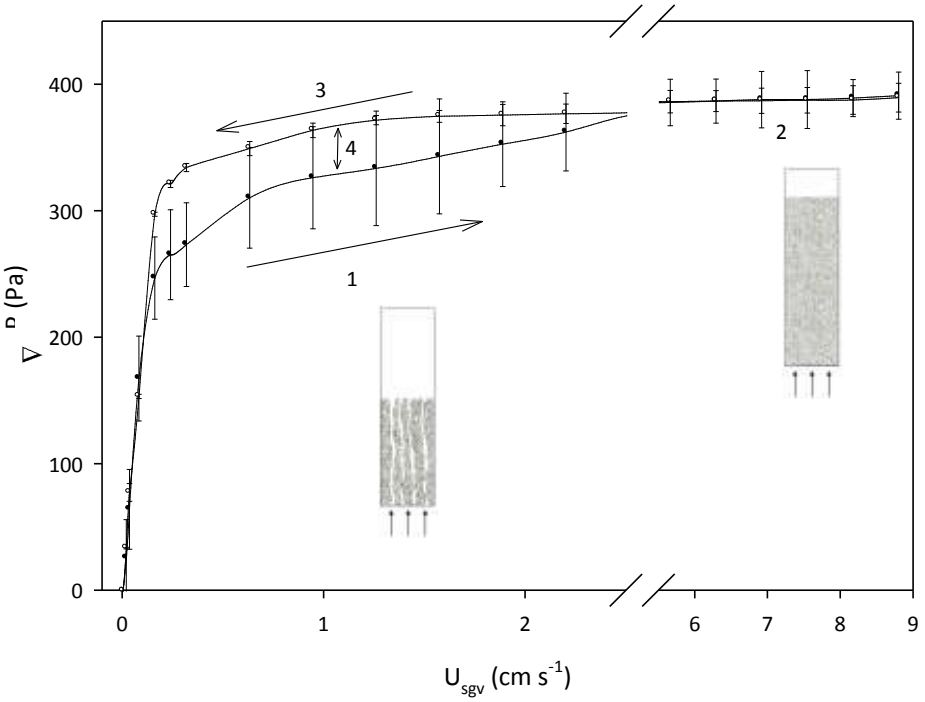

Fig. 5.10. Increasing and decreasing pressure drop vs. SGV curves for three independent unprocessed lactose samples. Curves show hysteresis effect caused by removing the tensile strength of the bed during the initial fluidisation stage. ● - increasing SGV, ○ - decreasing SGV.

The absence of the tensile strength "hump" can be attributed to the wide size distribution of lactose and its irregularity in shape and hence packing ability. Much of the theoretical fluidisation curves showing the "hump" which characterises the tensile strength of the powder is based on fluidisation of powders with well-defined particle size and shapes that are often readily-fluidised. Saleh *et al.*, (2006) conducted fluidisation tests on similar-sized group A and C powders to those used in this study

and the curves produced again showed a lack of "hump" without distinct packed bed and fluidised bed operations, similar to the unprocessed, blended, and deliberately agglomerated lactose.

As a comparison, Fig. 5.11 shows a typical fluidisation hysteresis curve for 71 μm lactose, which shows a more conventional pattern of fluidisation, as described by Shur *et al*., (2008) and in Fig. 1.6. On increasing the SGV, distinct packed bed and fluidised bed regimes are observed. Pressure drop increases linearly with SGV whilst the powder bed remains static (1), whilst at sufficiently large SGV, pressure drop during the fluidisation state is steady and fully supports the bed weight (2). The decreasing SGV curve falls *below* the increasing curve (3) due to the lack of channelling experienced on initial fluidisation, hence the greatly reduced experimental error with respect to unprocessed lactose. Although no tensile strength "hump" is observed, there is a clear difference in the pressure drop values (4) caused by hysteresis of the bed.

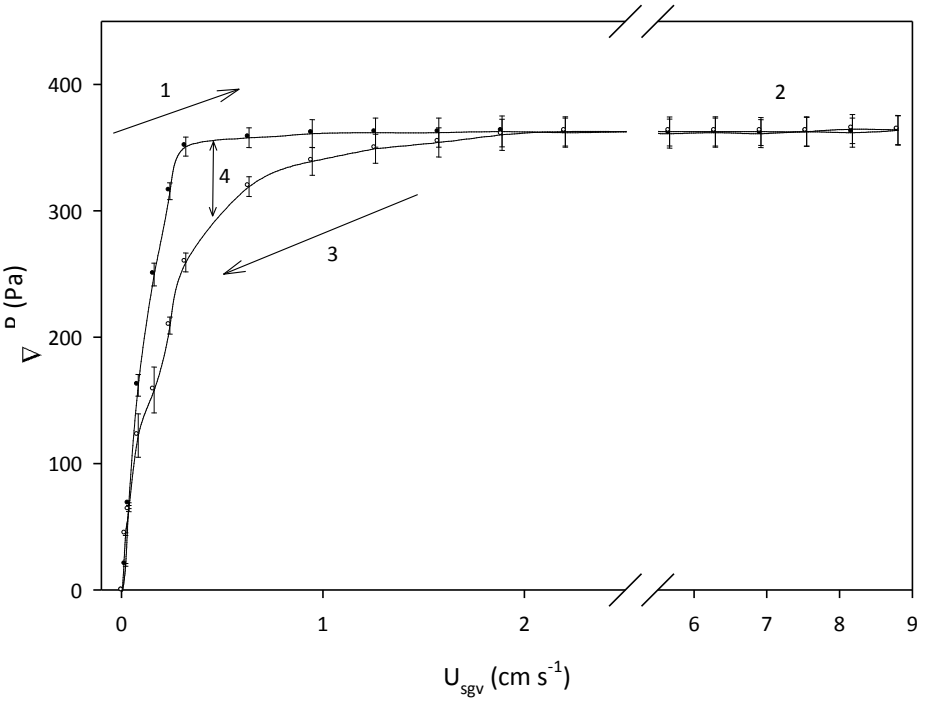

Fig. 5.11. Increasing and decreasing pressure drop vs. SGV curves for three independent 71 μm lactose samples. ● - increasing SGV, ○ - decreasing SGV.

The work by Shur *et al*., (2008), Tuley *et al*., (2008) and Watling *et al*., (2010), suggested that the more cohesive formulations were more susceptible to fluidise following fracture of the powder bed, whilst less cohesive formulations were subject to a "layer-by-layer" erosion mechanism of fluidisation. This work shows a similar occurrence, however has been performed quantitatively, with the unprocessed and

blended formulations showing fracture (channelling), and the 25 μm and 71 μm lactose grades showing the erosion fluidisation representative of readily-fluidised materials.

5.15.Effect of Specific Energy Input on Elutriation of Lactose Fines

This section describes the effect of SEI applied through HSB on the elutriation characteristics of lactose.

5.15.1. Method

Samples from blends described in Table 5.2 were used in this experiment. 20 g ± 0.1 g of each powder was fluidised at 6.27 cm s^{-1} with elutriated material collected at 10 minute intervals. This material was subsequently weighed, sized using the wet dispersion laser diffraction method described in section 2.3.1.3, and analysed for SSA using the BET technique described in section 2.2.4.3. A MATLAB code was written to find the particle size corresponding to the peak height of PSD curve. Six points around the peak of the curve were fitted to a 5^{th} order polynomial, the peak of which was determined by differentiation.

5.15.2. Results

Fig. 5.12 shows the cumulative mass elutriated for unprocessed lactose, and lactose subjected to a range of SEIs through HSB. It is clear that applying energy and altering the PSD (as seen throughout chapter 4 and in Table 5.2) does not affect the amount of material that can be elutriated from a fluidised bed. There are no statistically significant differences between any of the blends in terms of total mass elutriated (Kruskal-Wallis test - page 119), although a small difference was found between "low energy input 2" lactose and the other samples at elutriation times 50-100 min (found by application of Nemenyi's *post-hoc* statistical test). Should a trend have been observed with respect to the samples from other SEIs, a conclusion could have been made, however this appears to be an experimental anomaly.

As a comparison, deliberately agglomerated lactose was subjected to the same experiment and a clear reduction in material elutriated was observed. This material had been exposed to a high (70%) humidity environment for several days before fluidisation, thus liquid bridges and capillary forces are likely to have created agglomerates between the particles, thus reducing their ability to be lifted from the bed.

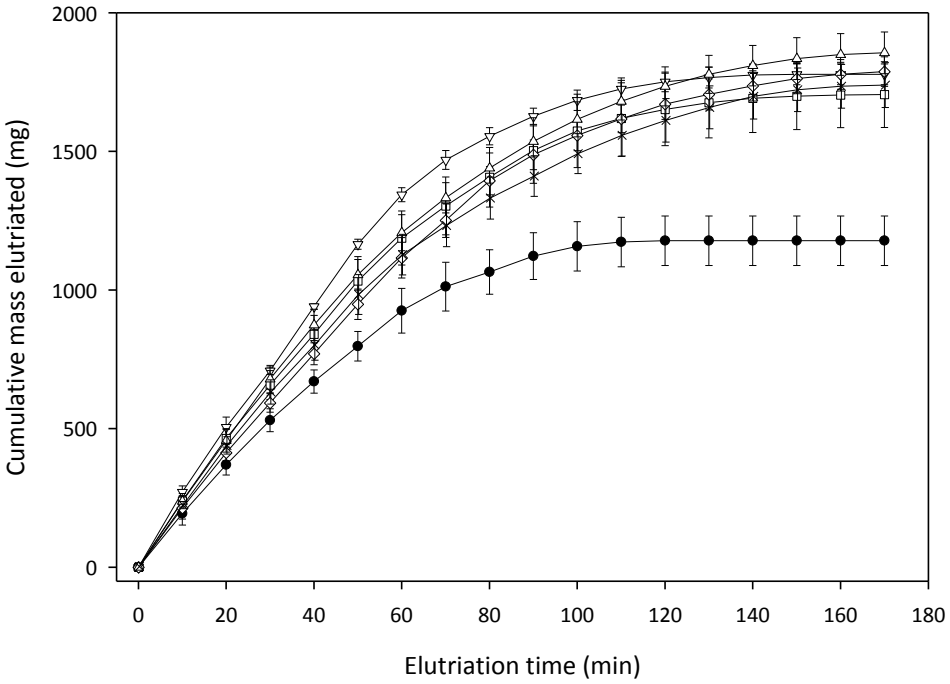

Fig. 5.12. Cumulative mass elutriated as a function of time for lactose subjected to various specific blend energy inputs, and deliberately agglomerated lactose. △ - Unprocessed lactose, ◇ - Low energy input 1 (30 ± 5.5 kJ kg^{-1}), ▽ - Low energy input 2 (68 ± 13 kJ kg^{-1}), □ - Mid energy input (207 ± 17 kJ kg^{-1}), × - High energy input (540 ± 81 kJ kg^{-1}), ● - Deliberately agglomerated lactose. Results shown are averaged from three independent experiments on each sample described in Table 5.2, ± SEM.

Results from FBE suggest that there are subtle differences in the particle population of unblended and blended lactose. Despite there being no statistically significant difference between the total mass that can be elutriated from a bed, the PSDs of such material show slight differences.

This is supported by the PSDs of elutriated material, Fig. 5.14, Table 5.4, and Table 5.5 show the differences in the PSDs of the elutriated material from samples subjected to varying SEIs. It can be shown that the secondary peaks (see Fig. 5.13 for definition) of the elutriated material PSDs have a greater variation for unprocessed lactose than lactose that has been subjected to significant energy inputs. Blended material shows a very tight distribution of peak particle size, a possible hypothesis suggests that the elutriated material belongs to a small group of particle sizes (small, free agglomerates). Conversely, unblended material shows a range of size distributions, thus suggesting that there is a range of fine particle sizes elutriated – some individual particles and some small agglomerates. This could suggest there are different populations of particles that are present within the system, and that they are removed from the fluidised bed at different times.

The particle size of peak 2 elutriated size distributions have increasingly wide spread of values with increasing SEI. For example, unprocessed lactose has peak 2 values of its elutriated material ranging from 17.8 μm to 25.6 μm, whereas the range of values for lactose subjected to higher energy inputs ranges from just 23.72 μm to 25.75 μm. This suggests that the blending process has subtle but noticeable effects on the population of particles in this mid-size range, not just on the very fine particles. These particles have been affected in a way that prevents them from elutriating out of the fluidised bed system, i.e. forming agglomerates that have aerodynamic size greater than 25 μm.

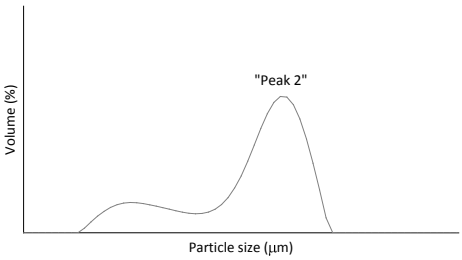

Fig. 5.13. PSD peak used in analysis of elutriated material

Table 5.4. "Peak 2" values from PSD data of elutriated material taken at various time points from samples subjected to varying energy inputs. Values represent mean peak heights from three independent blends at each energy, and three samples taken from each batch.

	"Peak 2" Particle size values (μm)				
Elutriation time	***Unblended (0 kJ kg^{-1})***	***Low energy input 1 (30±5.5 kJ kg^{-1})***	***Low energy input 2 (68±13 kJ kg^{-1})***	***Mid energy input (207±17 kJ kg^{-1})***	***High energy input (540±81 kJ kg^{-1})***
Non-fluidised	87.23 ± 0.60	85.68 ± 1.30	88.78 ± 0.89	86.71 ± 0.35	86.21 ± 1.78
10 min	17.80 ± 0.27	20.89 ± 0.83	18.63 ± 0.83	23.72 ± 1.22	24.63 ± 0.73
20 min	18.86 ± 1.00	19.08 ± 1.48	19.99 ± 0.59	25.31 ± 1.66	23.98 ± 1.55
30 min	18.09 ± 0.78	20.32 ± 0.71	19.31 ± 2.57	24.86 ± 1.26	23.72 ± 0.73
50 min	18.39 ± 1.44	20.78 ± 0.66	21.52 ± 0.98	25.01 ± 0.62	25.16 ± 0.69
110 min	19.20 ± 1.01	24.86 ± 1.36	24.24 ± 0.60	23.98 ± 1.92	25.75 ± 0.79
120 min	22.56 ± 0.66	24.71 ± 0.60	24.11 ± 0.93	23.59 ± 0.38	24.86 ± 0.97
130 min	25.60 ± 0.82	24.79 ± 0.84	24.05 ± 0.91	23.08 ± 1.02	24.37 ± 0.70
Average	20.07 ± 2.91	22.21 ± 2.49	21.69 ± 2.46	24.22 ± 0.84	24.64 ± 0.70
Non-elutriated	105.48 ± 0.83	103.36 ± 0.71	104.89 ± 1.12	106.21 ± 0.53	105.76 ± 0.88

It is interesting to note that the point at which chemical homogeneity of formulations is achieved roughly corresponds to the specific energy input point described above where the elutriation particle size characteristics become more consistent with elutriation time. Along with the homogeneity results of the previous chapter (Fig. 4.26 and Fig. 4.27) this suggests that increasing the specific energy input beyond this point ~200 kJ kg^{-1} in both cases only has the effect of redistributing the population of lactose particles, rather than further dispersing of drug particles, an effect which may not necessarily affect formulation performance.

Table 5.5. Specific surface area (SSA) data of elutriated material taken at various time points from samples subjected to varying energy inputs. Values represent mean peak heights from three independent blends at each energy, and three samples taken from each batch.

Elutriation time	*SSA ($cm^2 g^{-1}$)*	*R^2 (%)*	*SSA ($cm^2 g^{-1}$)*	*R^2 (%)*
	Unblended (0 kJ kg^{-1})		*High energy input (540 $\pm$ 81 kJ kg^{-1})*	
Non-fluidised	1593 $\pm$ 63	99.49	1556 $\pm$ 100	99.52
10 min	4283 $\pm$ 97	99.79	4030 $\pm$ 139	99.82
20 min	4159 $\pm$ 93	99.95	4008 $\pm$ 96	99.93
30 min	4096 $\pm$ 106	99.91	3796 $\pm$ 110	99.93
50 min	4278 $\pm$ 87	99.28	4003 $\pm$ 143	99.91
110 min	3910 $\pm$ 141	99.88	3923 $\pm$ 130	99.66
120 min	3873 $\pm$ 74	99.87	3752 $\pm$ 102	99.94
130 min	3872 $\pm$ 116	99.90	3895 $\pm$ 74	99.94
Average	4067 $\pm$ 183	99.78	3915 $\pm$ 109	99.88
Non-elutriated	834 $\pm$ 23	99.75	864 $\pm$ 34	99.64

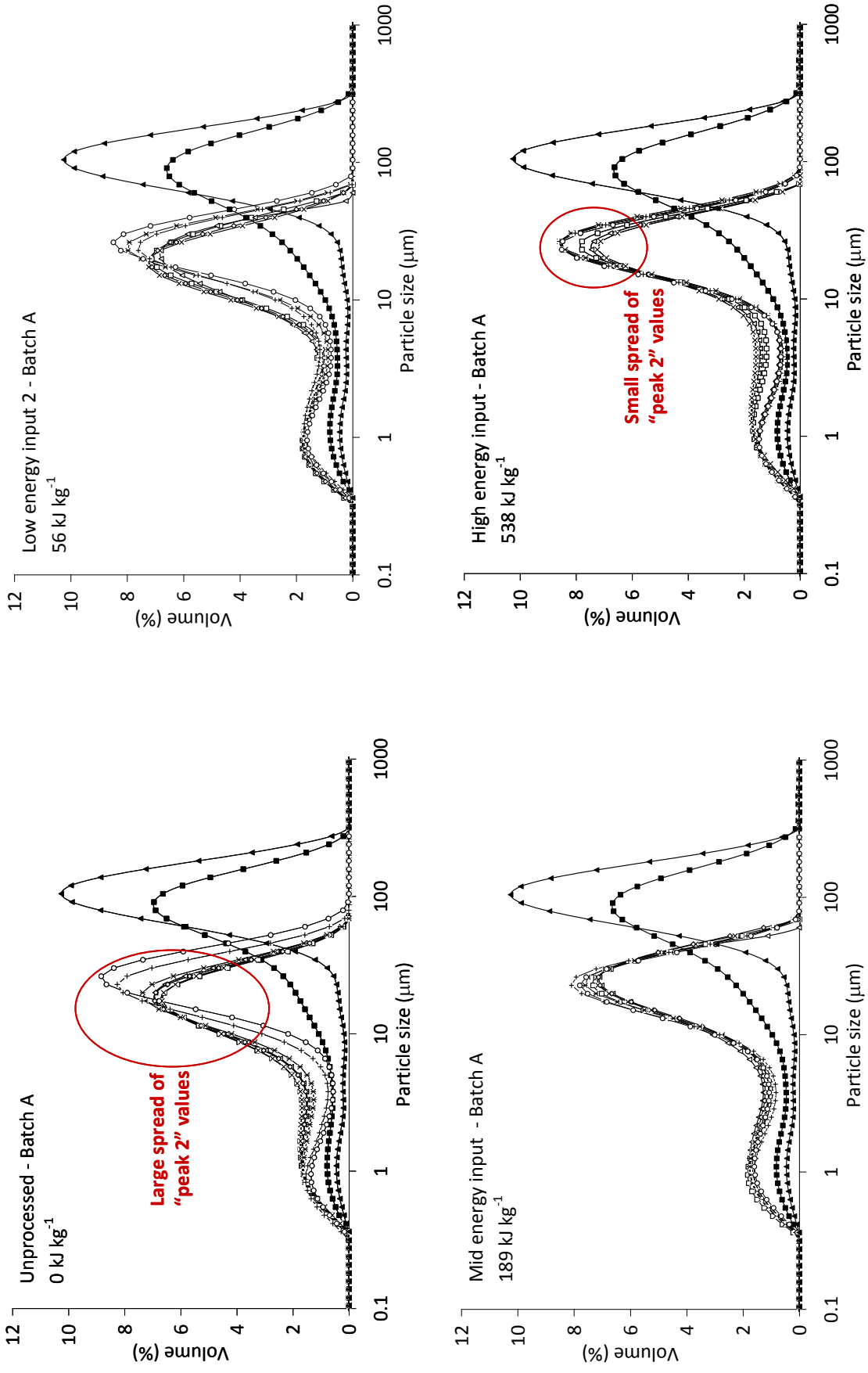

Fig. 5.14. Typical PSD of elutriated material as a function of time for a range of energy inputs. ■ - Non-fluidised, □ - 10 min elutriation, △ - 20 min elutriation, × - 30 min elutriation, ◇ - 50 min elutriation, ✳ - 110 min elutriation, + - 120 min elutriation, ○ - 130 min elutriation, ▲ - Non elutriated.

Fig. 5.15 shows representative SEM images of unprocessed lactose that has been elutriated from the fluidised bed by a SGV of 6.27 cm s^{-1}. It can be shown that elutriated material contains both individual particles and agglomerates of fine particles, however it appears that each entity (whether single particle or agglomerate) has a diameter <25 μm. However due to the cohesivity of such fine material, discrete particles cannot be identified, thus the images produced show agglomeration that is likely to have occurred post-fluidisation.

Fig. 5.16 shows representative SEM images of non-elutriated lactose that remained in the fluidised bed following two hours of fluidisation at a SGV of 6.27 cm s^{-1}. It can be shown that the non-elutriated material comprises both agglomerates of fine particles and coarse particles, both of which possess an aerodynamic diameter sufficiently large that their terminal velocity is greater than the SGV. Such images are evidence that the forces experienced in the fluidised bed are not sufficient to overcome all the interparticle forces of each agglomerate, thus only the most loosely attached and free fine particles can be elutriated from the system.

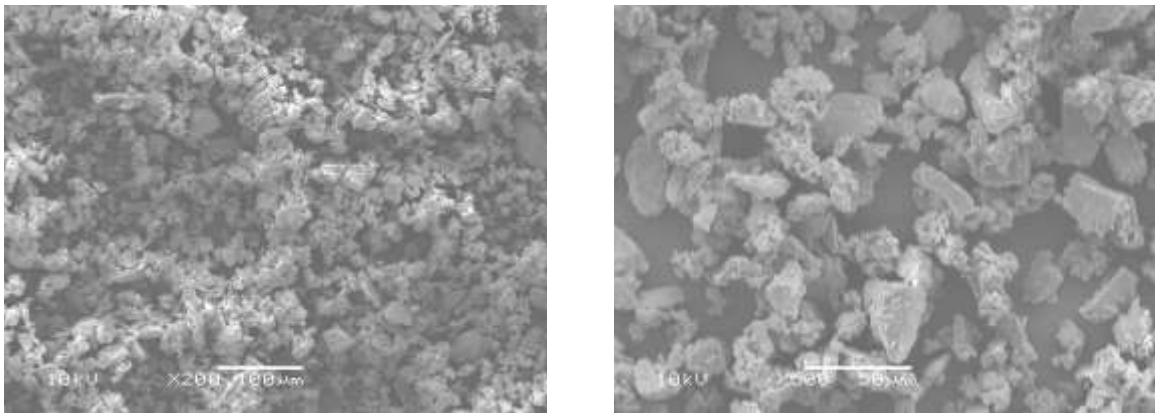

Fig. 5.15. Representative SEM images of elutriated (unprocessed) lactose following fluidisation at 6.27 cm s^{-1} for two hours. x200 (left) and x500 (right) magnification and 10kV potential.

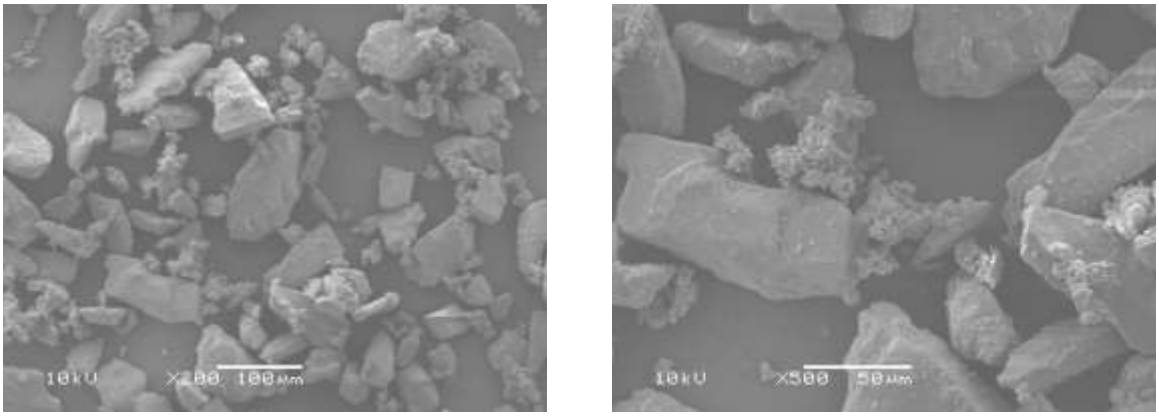

Fig. 5.16. Representative SEM images of non-elutriated (unprocessed) lactose following fluidisation at 6.27 cm s^{-1} for two hours. x200 (left) and x500 (right) magnification and 10kV potential.

No differences could be observed between images from unprocessed, de-agglomerated, or agglomerated lactose. In addition, no differences could be observed between the lactose elutriated at different time intervals. For example, the SEM images of lactose elutriated initially appeared similar to that at the end of the fluidisation period. As expected, the images of non-elutriated lactose following short periods of elutriation contained significantly more fine particles than non-elutriated lactose taken from the bed after longer periods of fluidisation.

The fine-particle agglomerates present in the non-elutriated material may have been formed from several processes. They may have been present in the initial unprocessed lactose, produced by the blending process, or formed from free fines liberated by the fluidisation process. Previous observations of fine particles generated by attrition during fluidisation have been shown to affect the elutriation of particles from mixtures of fine and coarse particles (Santana *et al.*, 2005).

5.16. Conclusion

This chapter has shown that a small-scale fluidised bed has been shown to discriminate between samples of inhalation-grade lactose that had been deliberately conditioned (section 3.4.5.1) to show different performance on fluidisation (in terms of pressure drop as a function of SGV). However, it has been shown that this method cannot adequately differentiate between inhalation-grade samples exposed to various HSB SEIs. This is caused by the level of fines present in these powders that causes their cohesivity and poor fluidisation performance. Fig. 5.17 highlights the difference in fluidisation performance of readily fluidised powders (such as those deliberately coarsened by AJS in this study) to that suggested in the work by Shur *et al.*, (2008), and the cohesive lactose powders used in this study.

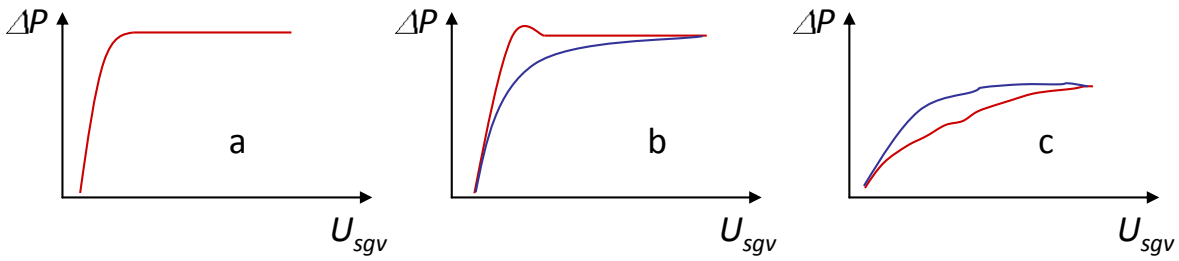

Fig. 5.17. Sketches of pressure drop vs. SGV curves: red line – increasing SGV, blue line – decreasing SGV. a) idealised response; b) semi-ideal response showing tensile strength of bed and hysteresis effect when reducing SGV; c) inhalation-grade lactose used in this study showing channelling and reversed hysteresis effect.

This work has shown that a FBE method has been able to detect subtle changes in the behaviour of inhalation-grade lactose exposed to various blending regimes. The method was not designed to mimic an inhalation event; indeed the flow rates used are significantly lower than a typical inhalation event (~60 l min^{-1} is commonly used for inhalation studies (Harris, 2007; de Koning *et al*., 2002), whereas flow rates of ~2 l min^{-1} are used in this study). Other differences to previous work studying the effects of fluidisation on the performance of DPI formulations include the quantity of powder tested and both the geometry and orientation of analysis equipment. Shur *et al*., (2008) use airflow applied below DPI formulations to observe the cohesivity through use of a powder rheometer, although no qualitative measures of pressure drop across the bed for various gas velocities are given, and the pressure drops calculated were measured with an external normal load applied to the system, causing the bed to consolidate.

Shur *et al*. also use high speed imaging to analyse the fluidisation and entrainment mechanics of 33 mg DPI formulation. This qualitative approach allowed the fracture mechanisms to be explored of formulations exposed to different blending conditions; Tuley *et al*., (2008) also employ high-speed imaging to assess the differences in fluidisation behaviour for different powders (including lactose with various fines content). That study used airflows with a range of pressure gradients, applied to powder beds residing in a series of geometries, experiments were performed over a typical inhalation event timescale of 0.2 s.

The FBE test is a novel tool that uses the principle of air classification to determine the amount of material in a formulation that is below a certain aerodynamic diameter. A similar study (Deng *et al*., 2010) uses the same principal to study the flow of a tablet formulation from a hopper; however, this study uses a SGV that is greater than the U_{mf} of the formulation, whereas the previous study deliberately works in a sub-U_{mf} regime.

Chapter 7 will follow from this chapter and use the principles of air classification to determine the effects of HSB and storage on the separation of fine mimic drug particles from lactose carrier particles.

6.0. Design and Use of an Air Jet Sieve Technique to Assess the Changes in DPI Formulation Properties due to High Shear Blending

ABSTRACT

High shear blending (HSB) has been shown to affect the properties of DPI formulations, in particular the particle size distribution (PSD) of particles, which consequentially may affect performance of such formulations. Therefore, a greater understanding of these effects may help enhance quality and efficacy of the product. A small-scale bulk method to assess the detachment of fine API particles from coarse excipient particles was desired, with the use of an air jet sieve (AJS) method proposed for development and use. This chapter is spilt into two sections, with the first section detailing the method development, whilst the second section tests differences in behaviour on sieving of lactose-only formulations exposed to different blending regimes.

The AJS method described in this chapter evaluated the initial mass, sieve aperture size, and both sieving pressure and time as factors affecting the separation of fine and coarse particles.

Results showed that by subjecting the lactose excipient used in DPI formulations to various specific energy inputs (SEIs) by HSB, subtle differences were observed in the behaviour of the powder. In particular, the amount of fine material removed from the bulk powder varied depending on the amount of SEI imparted to the formulation during HSB.

6.1. Introduction

An air jet sieve (AJS) is an analysis device for determining the particle size distribution (PSD) of bulk materials (Fig. 6.1). The sieving chamber is exposed to vacuum with the incoming air entering through a rotating nozzle where it disperses the bulk powder. The fine particles are conveyed through the apertures of the sieve by an underpressure determined by the amount of material and aperture size of the sieve. Coarse material remains on the sieve and can be further classified using larger sieves. Many applications exist for the use of AJSs in the pharmaceutical industry, notably for the assessment of drug-carrier adhesion (Iida *et al*., 2003; Flament *et al*., 2006; Dickhoff *et al*., 2006) or for the preparation of grades of lactose with certain fractions of particles removed in order to produce a consistent and coarse grade of powder (Lucas *et al*., 1998; Zijlstra *et al*., 2004; Nguyen *et al*., 2010). The work in this chapter was based on the methods used in these previous studies such that the amount of material removed by the AJS was used to describe the formulation behaviour. However, the novelty of this study lay with designing optimal experimental AJS conditions for identifying blending-induced changes in lactose-based formulations.

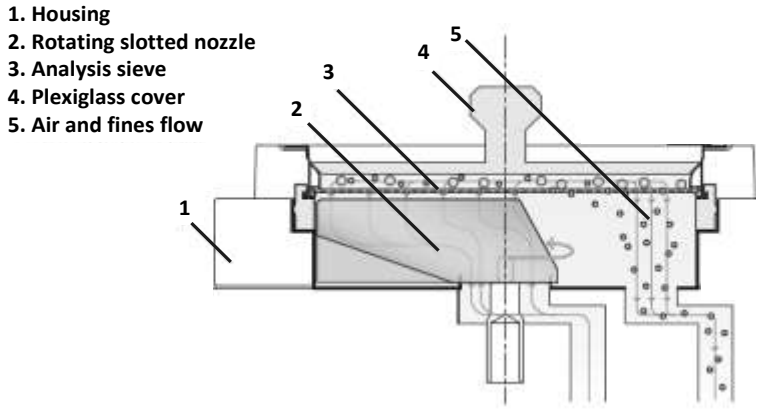

Fig. 6.1. Sketch of an Alpine Air Jet Sieve (Hosakawa Micron, Japan).

6.2. Materials and Methods

6.2.1. Lactose

Inhalation-grade lactose was provided by Friesland Foods Domo, Netherlands (section 2.2.1). Samples of this material used throughout the study were taken from batches stored in the original foil packaging (foil bag within cardboard box) at 20°C and 40% RH in humidity-controlled cabinets (Binder, Germany).

The lactose-only formulations used in this study match those used in chapter 5 and are listed in Table 5.2. All results shown are averaged from three independent experiments on each sample.

6.2.2. Particle Size Measurements

Particle size measurements were performed using laser diffraction. The dry dispersion technique used is described in section 2.2.3.

6.3. Factors Affecting Mass Removed on Air Jet Sieve

Key factors that affect the mass removed from an AJS consist mainly of the backpressure applied across the system, sieving time and initial mass to be sieved. The backpressure is application specific, whereas the sieving time and initial mass have a range of recommended values according to the manufacturer's manual.

Sources in the literature (Iida *et al*., 2003; Flament *et al*., 2004, 2006; Dickhoff *et al*., 2006) use backpressures between 3.5 and 4 kPa – the upper limit of the Alpine AJS used in this study. However, there is no reported literature regarding the influence of backpressure on the amount of fines removed from formulations.

The effect of sieving time varies according to the material to be analysed. Materials that are more cohesive lose mass less rapidly than free-flowing materials that consist of well-defined independent particles. The sieving time is the parameter that has the greatest influence on the result according to the manufacturer's manual and can only be determined experimentally as there are no theoretical predictions that suggest when analysis would be complete for given powders.

The mass of sample to be analysed is dependent on the sieve to be used, powder cohesivity, and the availability of sample. The amount of sample needs to be sufficient to perform suitable analyses, however cannot overload the system since this may reduce the pressure drop across the sieve, limiting the amount of fines that can be removed, and prolonging sieving time.

6.3.1. Effect of Pressure on Mass Removed

A study was performed to assess the ability of the AJS to remove fines at different backpressures. The initial mass of formulations exposed to different SEIs was kept constant (10g $\pm$ 0.1 g, as specified by manufacturer's manual), along with the maximum sieving time (see section 6.3.2) of 30 min (1800 s).

6.3.2. Effect of Sieving time on Mass Removed

The effect of sieving time on the amount of material removed on the sieve was tested by controlling the initial mass and pressure applied to the sieve and recording the residue mass at various time intervals.

6.3.3. Effect of Initial Mass on Mass Removed

Various initial masses were loaded onto the sieves over the range recommended by the manufacturer (10, 20 and 30 g $\pm$ 0.1 g) and exposed to 3400 Pa backpressure with the mass removed on the sieve determined at each time interval.

6.3.4. Results

6.3.4.1. Effect of Pressure on Mass Removed

Fig. 6.2 shows the effect of sieve backpressure on the removal of fine particles smaller than 25 μm from three independent batches of unprocessed lactose, lactose subjected to low SEI (~68 kJ kg^{-1}) and lactose subjected to high SEI (~540 kJ kg^{-1}). The purpose of this experiment was to determine the backpressure at which the greatest differences could be observed amongst the different batches of lactose. Sieving time was set at 30 min in order to remove all possible fines (Fig. 6.4).

The results show that the greatest difference in mass removed between lactose subjected to varying SEIs can be found at low backpressure (600 Pa). At this pressure, it can be shown that the greatest mass can be removed from lactose subjected to low SEI; whilst the least amount of mass could be removed from lactose subjected to large SEIs. This appears to support the PSD data from dry dispersion laser diffraction results, which show a coarsening of particles with increasing SEI. However, it is important to consider that the RODOS dry dispersion system operates at 2 bar (200 kPa), a substantially-greater pressure than the AJS, thus agglomerates are far more likely to be broken up into individual particles during size measurements. HSB may cause mid-size agglomerates to form which are greater than 25 μm and thus, due to the relatively low dispersion efficiency of 600 Pa, these agglomerates are not removed as readily as smaller agglomerates and the free fines present in unprocessed lactose.

Fig. 6.3 shows SEM images of unprocessed lactose residue taken from the same batch subjected to just 10 s of sieving at 600 Pa and 3400 Pa to highlight the effect pressure has on removal of material. The greater sieving pressure clearly removes more fines,

and is therefore likely to remove any information held within the PSD of the residue regarding the effect of blending on lactose.

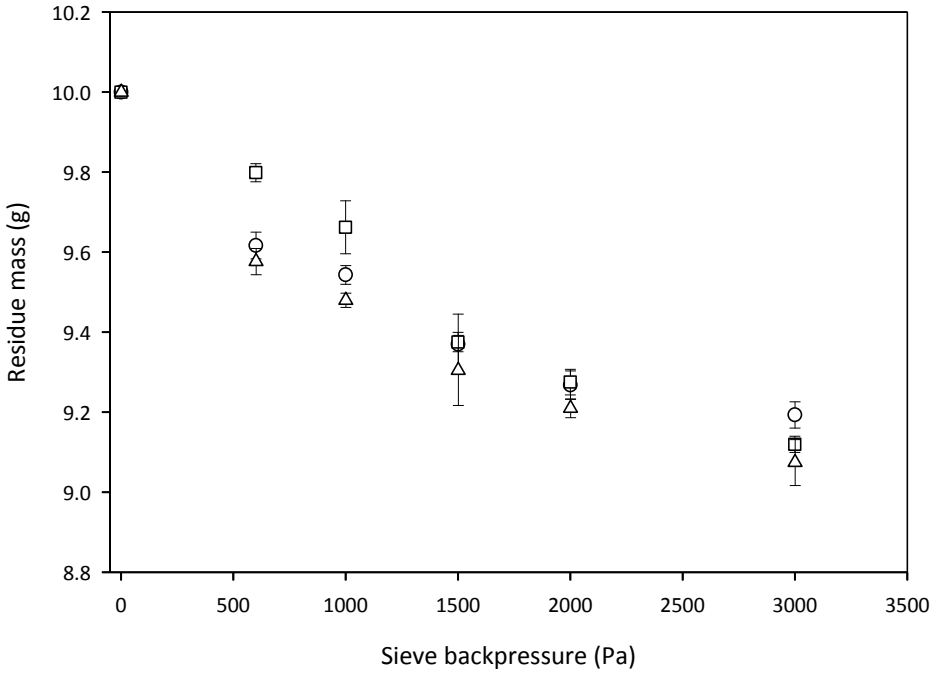

Fig. 6.2. Effect of sieve backpressure on the amount of fines removed from a 10 g ± 0.01g initial sample, expressed as residue mass. 25 μm sieve, 30 min sieving time. Results shown represent the mean from three samples from each of three independent batches ± SEM.
○ - Unprocessed lactose, △- low energy input (68 ± 13 kJ kg^{-1}), □ - high energy input (540 ± 81 kJ kg^{-1}).

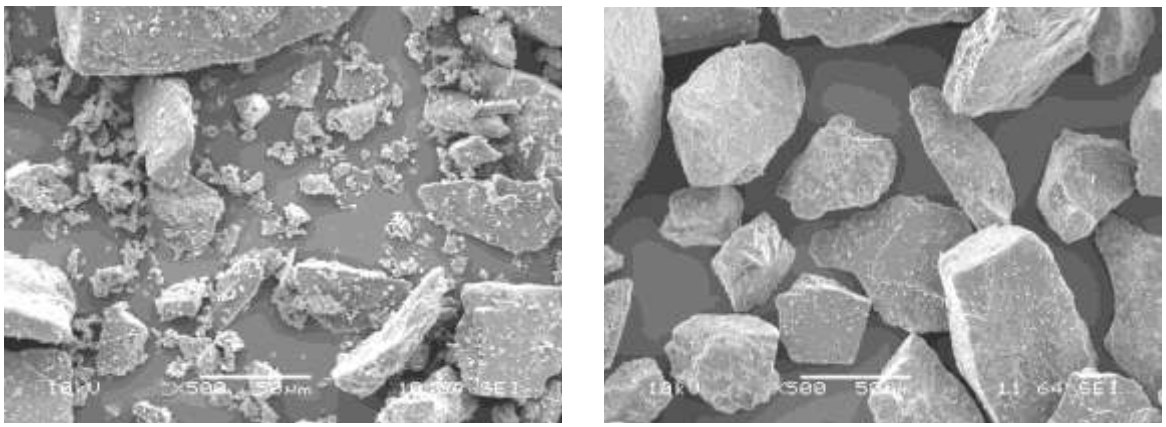

Fig. 6.3. SEM images of unprocessed lactose subjected to 600 Pa (left) and 3400 Pa (right) for 10 s using 25 μm AJS.

6.3.4.2. Effect of Sieving time on Mass Removed

Fig. 6.4 shows that a plateau of residue mass has been reached for the 71 μm sieve soon after sieving begins. This suggests that it is relatively easy to remove particles <71 μm, and that few particles undergo de-agglomeration in order to pass through the sieve apertures. Conversely, the 25 μm sieve shows a more gradual reduction in residual mass (Fig. 6.5) as a function of sieving time. This suggests those particles

around 25 μm consist of both individual particles and agglomerates, with the primary particles <25 μm passing through readily, and the agglomerates taking time to de-agglomerate in order to pass through the sieve apertures. Residue mass plateaus at sieving times >15 min for the 25 μm sieve, thus suggesting that all de-agglomeration occurs before this point.

Fig. 6.6 highlights the difference between residual unprocessed lactose following exposure to an AJS backpressure of 3400 Pa with 25 μm sieve for varying periods of time (10 s and 30 min). It can be shown that sieving for just 10 s removes the majority of fine particles; however, there are still some "free" fines and agglomerates that can be removed by extending the sieving time.

Fig. 6.7 highlights the ability of extended sieving times to remove fine particles adhered to coarser particles. Both individual and agglomerated fine particles are situated on the surface of carriers exposed to just 10 s of sieving, however the material exposed to 30 min sieving shows far fewer fine particles still adhered to the surface, and an absence of agglomerates.

It is interesting to note the coarse AJS residue shows only single particles (Fig. 6.6) and an absence of fines or agglomerates. However, the analogous non-elutriated material from the FBE method shows the presence of agglomerates that were not elutriated from the bed (Fig. 5.16). Thus, despite the shear forces and frequent particle collisions experienced during fluidisation, the energy of such events was not sufficient to de-agglomerate the whole bulk material. However, the AJS method appears to remove all agglomerates from the bulk material, suggesting that the FBE method is a more subtle technique for analysing size distributions of formulation particles.

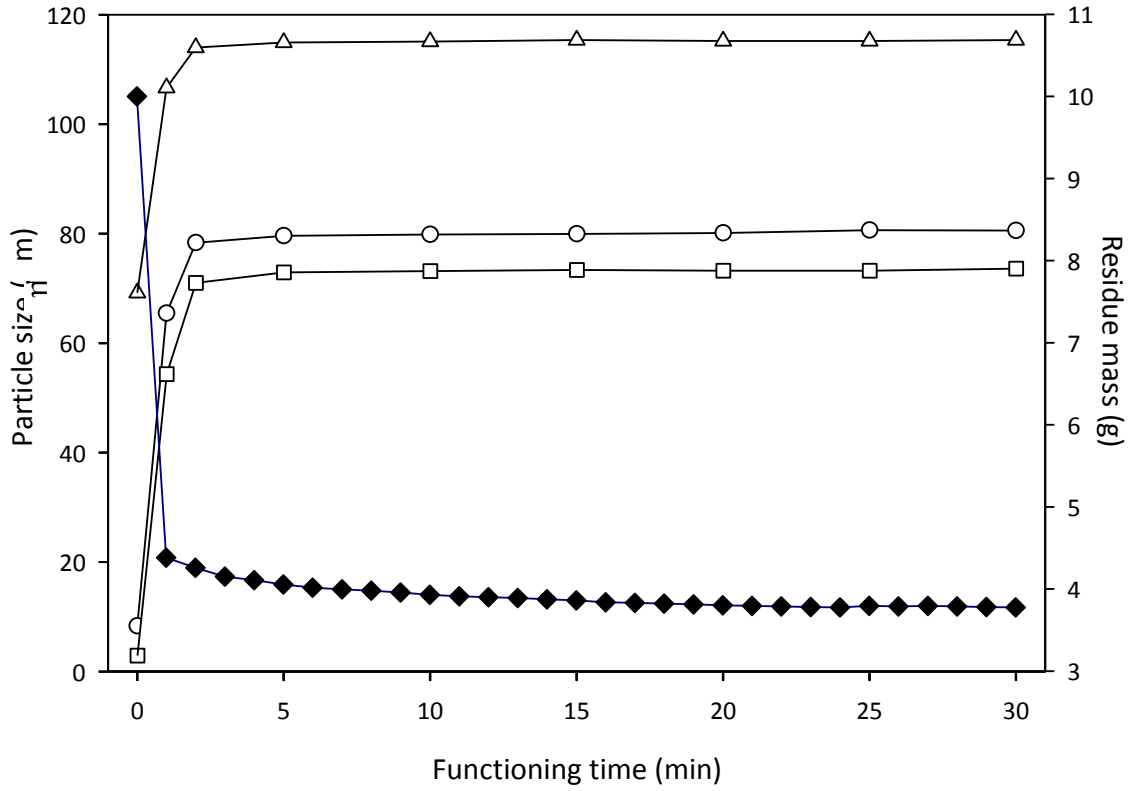

Fig. 6.4. Effect of sieving time on the amount of fines removed from a 10 g ± 0.01g initial sample of unprocessed lactose expressed as residue mass, along with particle size data. Results shown represent the average from three samples using 71 μm sieve at 3400 Pa (max operating pressure).
□ - d_5 particle size; ○ - d_{10} particle size, △ - d_{50} particle size, ◆ - residue mass.

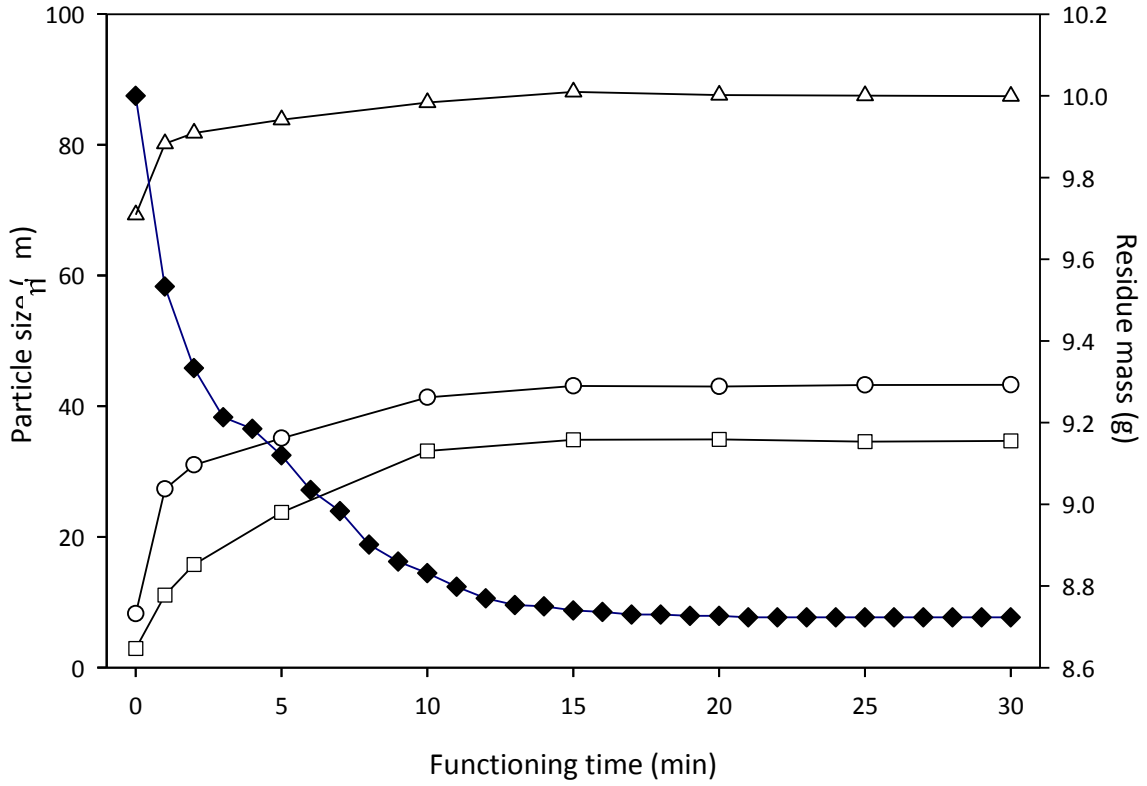

Fig. 6.5. Effect of sieving time on the amount of fines removed from a 10 g ± 0.01g initial sample of unprocessed lactose expressed as residue mass, along with particle size data. Results shown represent the average from three samples using 25 μm sieve at 3400 Pa (max operating pressure).
□ - d_5 particle size; ○ - d_{10} particle size, △ - d_{50} particle size, ◆ - residue mass.

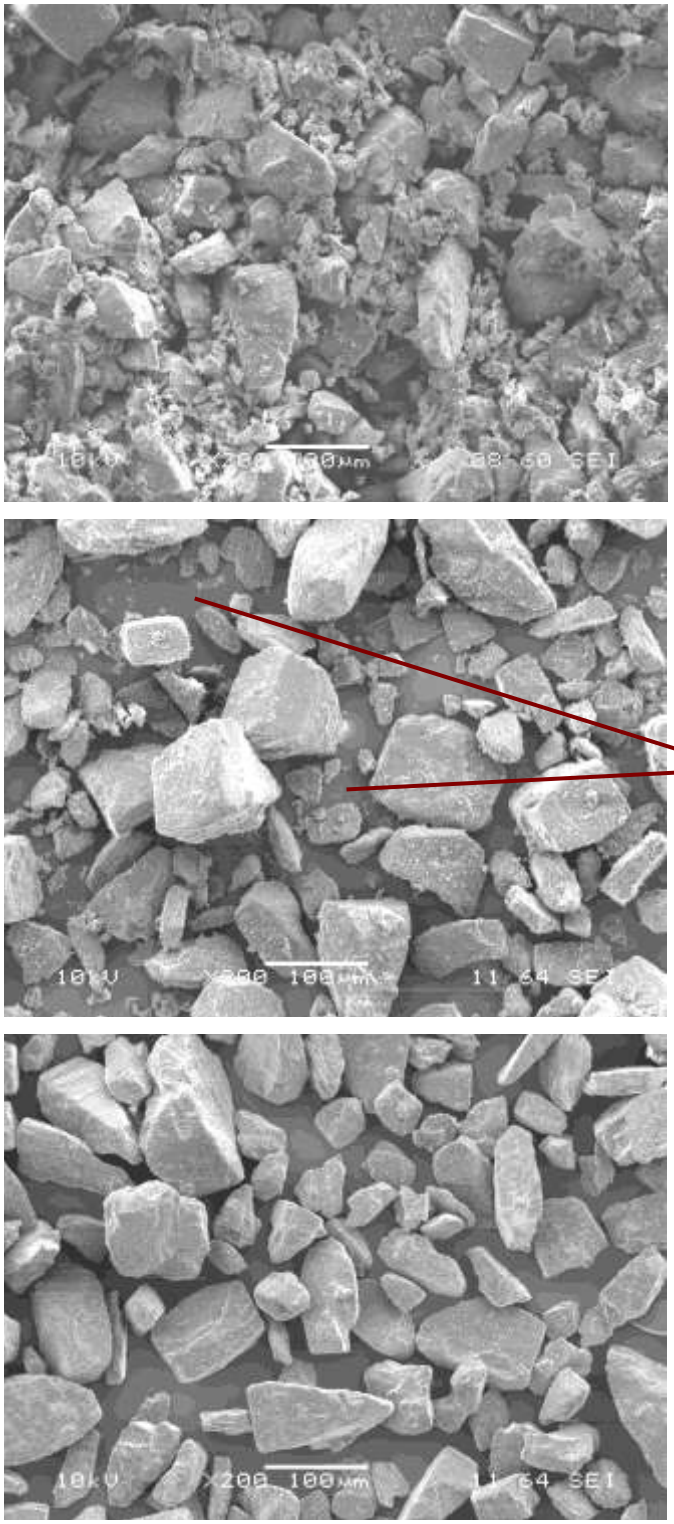

Wide PSD; presence of agglomerates and individual particles.

Greatly reduced number of fine particles and agglomerates, still some fine particles present.

Complete absence of fine (<25 μm) particles.

Fig. 6.6 Representative SEM images of unprocessed lactose exposed to AJS with 25 μm sieve and 3400 Pa backpressure for 0 min (top), 10 s (middle), and 30 min (bottom), (x200 magnification and 10kV potential).

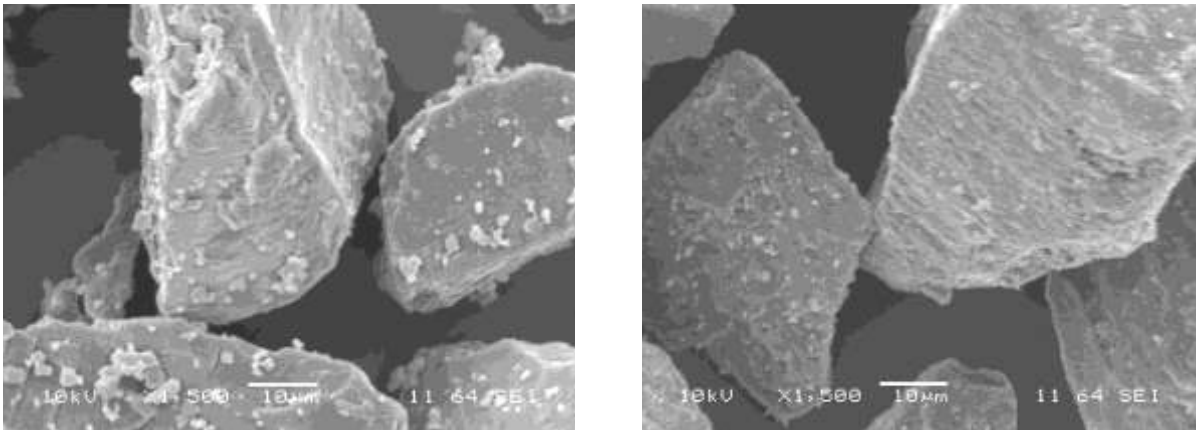

Fig. 6.7 Representative SEM images of unprocessed lactose exposed to AJS with 25 µm sieve and 3400 Pa backpressure for 0 min, (left), and 30 min (right)., with x1500 magnification and 10kV potential.

6.3.4.3. Effect of Initial Mass on Mass Removed

Fig. 6.8 shows that the percentage mass removed from initial samples between 10 and 30 g does not differ significantly, thus the mass used would not affect the results generated. The initial sample mass does not affect percentage mass removed providing samples mass is between 10 and 30 g, therefore, 10 g was chosen to limit the amount of material used for this analysis.

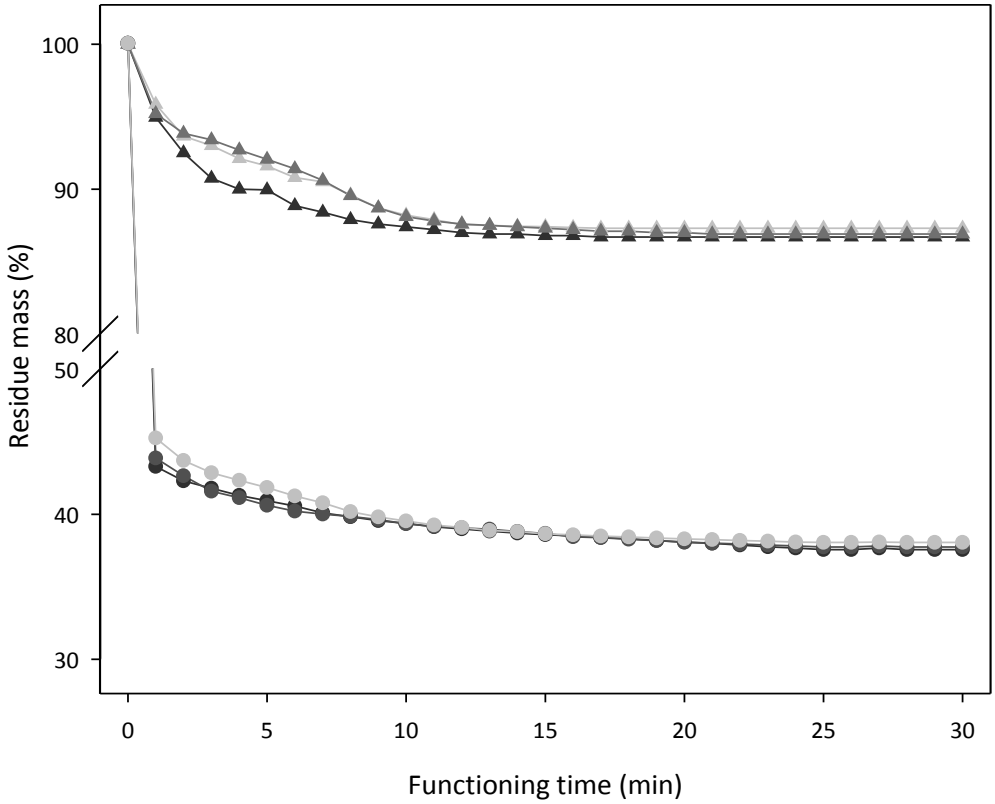

Fig. 6.8. Effect of sample size on the% mass removed using a backpressure of 3400 Pa. Results shown represent the average from three samples of unprocessed lactose using both 71 µm and 25 µm sieves.
▲ - 10g, 71 µm sieve; ▲ - 20g, 71 µm sieve; ▲ - 30g, 71 µm sieve;
● - 10g, 25 µm sieve; ● - 20g, 25 µm sieve; ● - 30g, 25 µm sieve.

6.4. Summary of Experimental Conditions Used

As can be seen in sections 6.3.4.1 and 6.3.4.2, the AJS is most able to discriminate between samples exposed to different blending regimes at low sieving pressure, and that sieving time >15 min are required to remove all possible material. In line with previous AJS experiments (Flament *et al*., 2004; Saint-Lorant *et al*., 2006, Dickhoff *et al*., 2006) on lactose-based formulations, a short sieving time of 10 s was used, along with an intermediate 5 min sieving, and long 30 minute sieving time to ensure all available material was removed. These sieving times matched those used in the previous studies named above. Since the results in section 6.3.3 show that the initial mass loading did not measurably influence the amount of fines removed, 10 g was chosen to conserve samples. The 25 μm sieve was chosen for analysis as this gave the strongest indication of the behaviour of fines in the formulation following HSB. It also coincided with the cut size of particles determined by SGV in the FBE tests (section 5.12).

6.5. Effect of Specific Energy Input on Air Jet Sieve Removal of Fines from Lactose Only Formulations

6.5.1. Method

The method used to determine the amount of fines removed from formulations exposed to different SEIs is described in section 6.4.

The lactose-only formulations used in this study match those used in chapter 5 and are listed in Table 5.2. All results shown are averaged from three independent experiments on each sample.

6.5.2. Results

The effect of SEI on the amount of fines <25 μm removed by the AJS is shown in Fig. 6.9. These results show that at low pressure (600 Pa), at short sieving times, more material is removed from lactose subjected to low energy inputs than the lactose subjected to high energy inputs. This supports the theory that upon blending, lactose fines combine either with each other or with larger particles such that the AJS cannot easily remove them. On the other hand, unprocessed lactose and that subjected to just low SEI, contains free fine particles (or only weakly-attached) particles that are readily removed by the AJS.

Fig. 6.9 also shows that during extended sieving times, these results normalise, and the differences seen at short sieving times can no longer be observed. Prolonged sieving allows sufficient disturbances of particles to occur which removes all available particles, rather than just the weakly attached particles that are preferentially removed during short sieving times. No statistically significant differences can be observed between the amounts of fines removed from blends exposed to different SEIs (Kruskal-Wallis test - page 119), when sieved for 30 minutes.

However, when using the more discriminating shorter sieving times, a trend appears that is similar to the trend observed in the PSD of lactose with increasing SEI. Particle size data showed an initial decrease with low SEIs, followed by a subsequent increase (reagglomeration) with greater SEIs. These low SEIs corresponded to a reduction in the mass remaining (increase in mass removed) on the 25 μm sieve after short sieving times, again suggesting that the powder was de-agglomerating, since more particles were able to pass through the sieve. This effect was not observed at higher sieving times as the AJS was able to break up loose agglomerates over a prolonged period, and any changes caused by blending were normalised by the sieve.

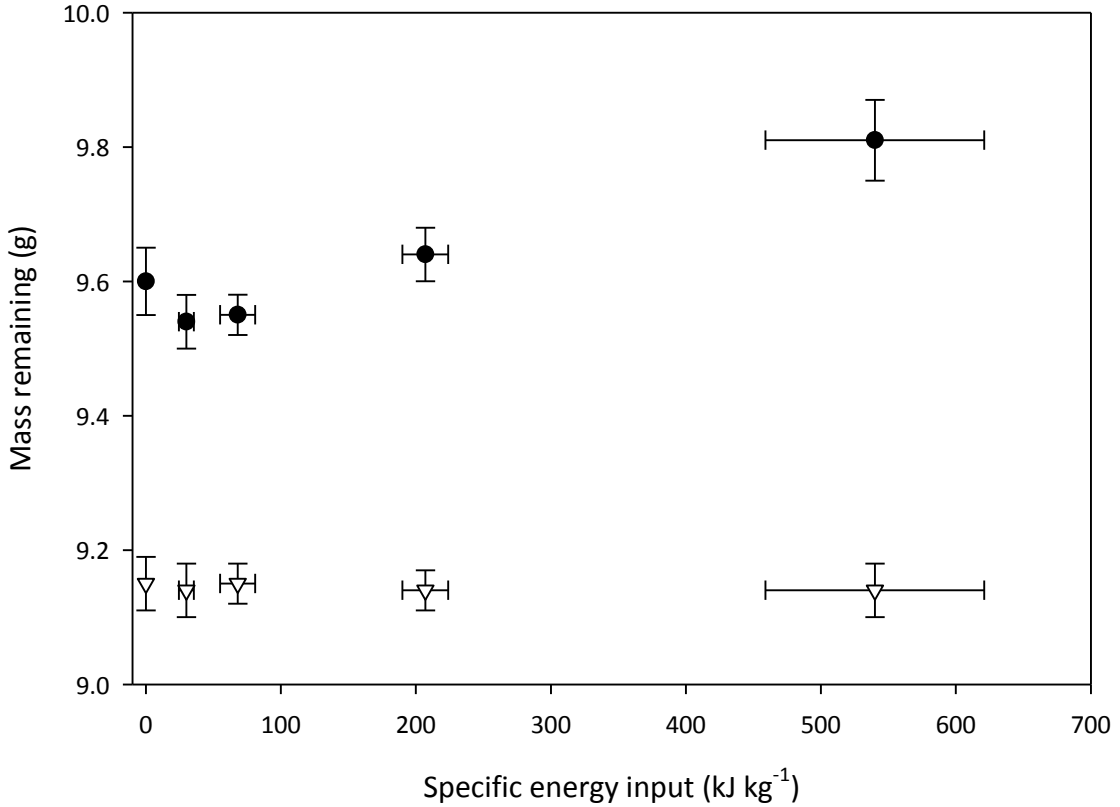

Fig. 6.9. Effect of SEI on the amount of fines removed and particle size using the 25 μm sieve at 600 Pa for 10 s (●) and 30 min (▽). Results are averaged from three independent experiments from three samples at each energy input described in Table 5.2. Horizontal error bars represent SD of SEI from three samples, whereas vertical error bars represent SEM of residual mass.

6.6. Conclusion

AJS analyses of lactose-only formulations have showed differences between blends exposed to various SEIs through HSB. This chapter has found that the optimal conditions for observing the subtle differences between different blends requires short sieving times and low pressures, as extended times and high pressures normalise the blends and remove all possible material from the bulk powder. The more subtle technique only removes the most weakly bound fines and agglomerates, thus allowing more distinct differences to be observed.

This chapter has also investigated the effects of SEI on the removal of fine lactose particles from lactose-only formulations. This is a novel feature of this work as previous literature focuses on removal of drug particles from carriers with various surface roughness (Flament *et al*., 2004; Iida *et al*., 2003); and separation of different drugs from different carriers (Saint-Lorant *et al*., 2006).

However, the measurement of adhesion forces cannot be made by an AJS, since the turbulent, chaotic nature of the airflow that separates drug from carrier is difficult to control and measure effectively. The work above, which assesses drug-carrier adhesion, uses an AJS to empirically determine the adhesion between different drugs and grades of excipients, by calculating the mass of drug removed by the AJS system for various sieving regimes.

The following chapter will describe the effects of HSB on the AJS removal of mimic actives from such formulations and explores the effect of energy input and storage regimes on formulation behaviour.

7.0. Effects of Blending and Storage on Fine Particle Behaviour

ABSTRACT

This chapter describes the effects of both high shear blending (HSB) and storage regimes on the properties of mimic DPI formulations containing mimic APIs. Specific energy input (SEI) is known to be the major factor that influences formulation characteristics during HSB, whereas different storage regimes (temperature and humidity) have been shown in previous studies to significantly affect the physicochemical properties of α-lactose monohydrate – the excipient commonly used in such products. This chapter extends previous studies to examine the effect of SEI on the properties of such formulations using existing cascade impactor techniques and novel fluidised bed elutriation (FBE) and air jet sieve (AJS) tests developed and described earlier in this thesis.

Blending of lactose with two mimic APIs (cholesterol and vitamin C) was performed using a laboratory-scale high shear blender, whilst formulations were stored post-blending in controlled-climate chambers at 40% and 60% RH. Tests were performed via the FBE and AJS methods developed in chapters 5 and 6, along with a conventional Next Generation Impactor (NGI) method to assess the formulations' fine particle fraction (FPF).

Results showed no evidence of the behaviour of fine drug particles being affected by blending regimes, specifically, the SEI during blending was not observed to alter the ability of fine particles to separate from coarse carrier via any of the test methods. On the other hand, storage regimes were observed to induce subtle changes in the ability of fines to separate from coarse particles. In particular, storage of mimic formulations at 60% RH was seen to reduce the amount of vitamin C and cholesterol elutriated from the fluidised bed. In addition, fine particle deposition was seen to decrease with prolonged storage in the case of vitamin C using NGI analyses, with the effect of capillary forces being suggested as the mechanism responsible for this effect. Storage of formulations at 40% RH was not observed to have any effect on the fine particle delivery of drug using any of the methods developed in this thesis.

7.1. Introduction

Following from the work in chapter 4, and by Bridson *et al.*, (2007), an energy-dependent loss of free lactose fines was shown to occur during the high shear blending (HSB) of inhalation-grade lactose. It was proposed that these blending-induced, energy-dependent changes observed might affect the fine particle fraction (FPF) associated with drug-containing active formulations.

In addition to the effect of HSB, post-blending storage regimes are known to affect the fine particle fraction (FPF) (Young *et al.*, 2007b; Kwok and Chan, 2007), and hence, formulation performance. The interaction between drug and carrier in various environments has been extensively studied, particularly via the cohesive-adhesive balance (CAB) method initially developed by Begat *et al.*, (2004) and described in more detail in section 1.5. Despite this, relatively few methods have been used to assess the effect of blending and storage regimes on the bulk separation of drug from carrier.

Three test methods were used in this chapter to assess the amount of fine (drug and lactose) particles that could be removed from mimic dry powder inhaler (DPI) formulations exposed to various blending and storage regimes; the fluidised bed elutriation (FBE) and air jet sieve (AJS) methods developed in chapters 5 and 6 respectively, along with a conventional Next Generation Impactor (NGI) method commonly used to assess the FPF deposition following aerosolisation of a DPI formulation.

7.2. Materials and Method

7.2.1. Lactose

Inhalation-grade lactose was provided by Friesland Foods Domo, Netherlands (section 2.2.1).

7.2.2. Mimic APIs

Tests were performed using cholesterol and vitamin C (Sigma Aldrich, UK) as mimic APIs (section 3.1.1), the methods for micronisation and characterisation of these materials is described in section 3.4.2. The d_{50} particle size of these mimic actives lay within the 1-5 μm aerodynamic diameter specification for DPI formulations defined by Newman and Clarke (1983): d_{50} (cholesterol) = 4.45 $\pm$ 0.29 μm; d_{50} (vitamin C) =

3.21 ± 0.18 μm. The aerodynamic diameter of particles is given by the equation $d_a = d_e\left(\frac{\rho_p}{\rho_0}\chi\right)^{1}$, where d_a is the aerodynamic diameter, d_e is the equivalent volume diameter (value measured by laser diffraction), ρ_0 is the standard particle density (1 g cm^{-3}), ρ_p is the particle material density, and χ, is the shape factor of the particles. It is the diameter of a spherical particle of density 1000 kg m^{-3} with the same settling velocity as the particle in question (related to Stokes' diameter). 500 g blends containing 1:67.5 w/w (common payload used in previous literature - Table 1.2) mimic active were prepared using the method described in section 4.2.4 using the 0.13 diameter bowl with impeller speed 500 rpm. Samples of formulation were taken at regular intervals using the method described in section 3.5.1.

7.2.3. Particle Size Distribution

Measurement of particle size distributions (PSDs) were performed using both wet and dry dispersion laser diffraction systems (see sections 2.3.1 and 2.3.2 respectively).

7.2.4. Chemical Assays

Drug content and blend uniformity was measured using UV spectroscopy, with the assay for cholesterol being described in section 3.5.2, and the method for vitamin C described in section 3.5.3. For each method, a 34.25 mg sample of formulation was taken which corresponded to a nominal drug dose of 500 μg.

7.2.5. High Shear Blending

Formulations were prepared using the HSB equipment described in section 4.2.3 with sampling of powders performed using the method described in section 4.2.5. For this study, the small bowl with internal diameter 130 mm was employed with an initial mass loading of 500 g and rotational speed 500 rpm (a good blending regime – section 4.3, Fig. 4.10). Blends were performed based on data from Fig. 4.26 and Fig. 4.27 since these show the onset of homogeneity for each mimic API. Samples taken from lower SEIs were not used, as these will not be suitably homogeneous. Blends were performed in triplicate with SEI approximately 200, 400 and 600 kJ kg^{-1}.

Fig. 7.1 shows representative SEM images of vitamin C and cholesterol containing formulations blended with ~400 kJ kg^{-1} SEI. Although unable to distinguish between mimic drug and lactose, an even distribution of fine particles can be observed over the

surface of the larger carrier particles for both vitamin C and cholesterol containing formulations.

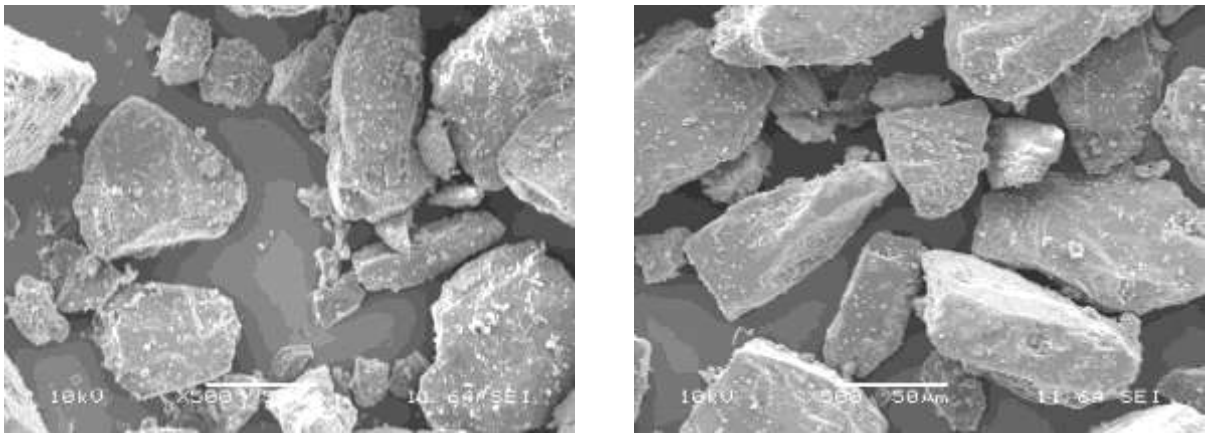

Fig. 7.1 Representative SEM images of cholesterol/lactose (left) and vitamin C/lactose (right) formulations at ~400 kJ kg^{-1} SEI with x1500 magnification and 10kV potential.

7.2.6. Storage Conditions

The effects of storage on the physicochemical properties and consequential performance of formulations are vitally important to the pharmaceutical industry (Callahan *et al*., 1982; Melveger and Huynh-Ba, 2008). Bridson *et al*., (2007) and Das *et al*., (2009) describe work conducted to investigate the effects of prolonged storage on the properties of lactose carrier and salmeterol xinafoate drug respectively; the study by Bridson *et al*., (2007) was performed over 21 weeks, whilst the study by Das *et al*., (2009) lasted three months - both typical of the timescales the pharmaceutical industry employs for storage of their products. The most common factors that need to be controlled in storage studies are temperature, and more importantly, relative humidity (RH) (Callahan *et al*., 1982; Melveger and Huynh-Ba, 2008).

Storage studies post-blending were carried out in two humidity-controlled cabinets (Binder, Germany), with temperature maintained at 20°C, and humidity controlled at two separate values - 40% RH and 60% RH (as requested by project sponsoring company GSK). Formulations were stored at these conditions for twelve weeks, based on other similar storage studies on pharmaceutical ingredients by Ng *et al*., (2007).

7.2.7. Fluidised Bed Elutriation Testing

As described in chapter 5, a FBE method was shown to be successful in separating fine and coarse particles of inhalation-grade lactose. For this test, 20 g $\pm$ 0.1 g formulation

was placed in the column described in chapter 5, and exposed to a superficial gas velocity (SGV) of 6.27 cm s^{-1}, which corresponded to a terminal velocity of approximately 25 μm diameter lactose particles. Fluidisation was performed until all removable material was elutriated; this was subsequently weighed gravimetrically and assayed for drug content.

7.2.8. Air Jet Sieve Testing

An AJS method as described in section 6.4 was used to assess the amount of drug removed at various sieving times (10 s, 5 min, 30 min) using a back pressure of 600 Pa. 10 g ± 0.1 g was used per sample, and drug assays were performed on coarse residue once sieving was complete to determine the amount of material removed by the sieve.

7.2.9. Next Generation Impactor Testing

Cascade impactors operate using the principle of inertial impaction. Each stage of the impactor comprises a single or multiple nozzles or jets through which the particles entrained in the air stream pass. Whether a particle impacts on a particular stage is dependent on its aerodynamic diameter. Particles with sufficient inertia will impact on that particular stage collection plate, whilst smaller particles with insufficient inertia remain in the air stream and pass to the next, smaller stage where the process is repeated. Since the stages are ordered in decreasing jet size, the air velocity increases and finer particles are collected.

The Next Generation Impactor (NGI - Copley Scientific, Nottingham, UK) was launched in 2000 and accepted into the European Pharmacopoeia as Apparatus E and into the United States Pharmacopoeia as Apparatus 5 and 6 in 2005. At a volumetric flow rate of 60 l min^{-1} the cut-off points for stages 1-7 (Fig. 7.2) are 8.06, 4.46, 2.82, 1.66, 0.94, 0.55, and 0.34 μm respectively. The airflow passes through the impactor in a saw tooth pattern with particle sizing achieved by successively increasing the air velocity by passing through successively smaller jets. NGIs are becoming increasingly common tool for aerodynamic particle size analysis – Pitchayajittipong *et al*., (2010) and Taki *et al*., (2010) both highlight recent examples of NGI use for assessing DPI formulations.

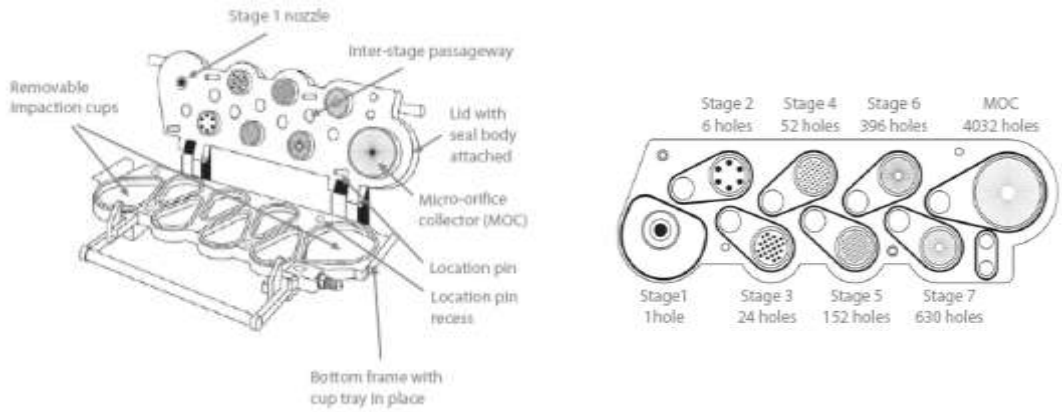

Fig. 7.2. Next Generation Impactor stages and collection plates

Aerosolisation testing was performed on a NGI with preseparator that was connected to a vacuum pump (Copley HCP5, Copley Scientific, Nottingham, UK). Prior to testing, the preseparator was filled with 15 ml solvent, as were the NGI cups to eliminate particle bounce upon deposition. 25 ± 1 mg of each blend was accurately weighed into size three hydroxypropylmethyl cellulose capsules (HPMC, ShionogiQualicaps, UK). For each experiment, two individual capsules of the same formulation were discharged into the NGI at 60 l min^{-1} for two bursts of 1.5 s in order to fully discharge the formulation from device. Formulations were discharged via two separate devices; a generic sample holder made from stainless steel (Steckel and Bolzen, 2004), and a Cyclohaler® (TEVA Pharmaceuticals, The Netherlands) - Pitchayajittipong *et al.*, (2010). Following aerosolisation, each part of the NGI was washed with known volumes of solvent and the mass of drug deposited on each stage was determined by UV spectroscopy. For this study, the FPF was defined as particles which deposited in stage 2 and below of the NGI (i.e. particles with aerodynamic diameter ≤4.64 μm).

7.3. Results

7.3.1. Effect of Blending of Formulation Characteristics

Particle size data of lactose prior to blending results performed in triplicate (dry dispersion): d_5 = 2.97 ± 0.03 μm; d_{10} = 9.51 ± 0.07 μm; d_{50} = 68.87 ± 0.34 μm. Table 7.1 and Table 7.2 show particle size data for cholesterol and vitamin C blends respectively at various SEIs, along with the formulation homogeneity, expressed in coefficient of variation (CV) (see section 3.5) and the average drug composition by mass (both expressed in percentage terms).

As seen in previous chapters (Fig. 4.11, Fig. 4.26, Fig. 4.27 and Table 5.2), and work by Bridson *et al.*, (2007), an increase in SEI is generally associated with an increase in particle size. This is particularly apparent at the fine end of the distribution, where a d_5 increase of around 1.5 μm is observed with a SEI of ~600 kJ kg^{-1} using this bowl size, impeller speed, and mass fill (0.13 m diameter bowl, 500 rpm, 500 g). Likewise, the same orders of change are observed in both the d_{10} and d_{50} particle sizes as previous chapters. This suggests that blending inhalation-grade lactose with the mimic APIs cholesterol and vitamin C does not affect the size distribution of the bulk formulation. This is to be expected since the mimic drugs only make up less than 2% of the formulation by mass, thus would not affect the size distribution substantially enough to be observed in laser diffraction particle sizing.

Based on the previous work described in Fig. 4.26 and Fig. 4.27, chemical homogeneity (defined by CV <6% - Crooks and Ho, 1976) was observed in all the blends produced with SEI greater than ~200 kJ kg^{-1}. Therefore, the formulations were suitably homogeneous for use in the fluidised bed, AJS, and NGI tests to assess the effect of blending on fine particles. There was no observed difference in the ability of the high shear blender to disperse the mimic drugs throughout the bulk lactose, despite there being differences in the cohesivity of cholesterol and vitamin C. As seen in section 3.4.5, cholesterol is more cohesive than vitamin C, and thus may have been more difficult to achieve suitably cohesive formulations. In addition, there was no observed improvement in the cohesivity of the formulations beyond ~200 kJ kg^{-1} SEI, in line with the results found in section 4.3.10.

Table 7.1. Particle size data, content uniformity and fine particle content of model cholesterol formulations, post blending.

Specific Energy Input (kJ kg^{-1})	d_5 (μm)	d_{10} (μm)	d_{50} (μm)	*CV* (%)	*Average drug loading*	*Total Mass Elutriated (g)*	*Drug mass elutriated from 20 g sample (mg)*	*% drug elutriated*	*Drug composition in elutriated fraction*	*Alpine air jet sieve drug removed* from 10 g initial sample			*NGI Fine particle mass*	
										10s	5 min	30 min	Generic	Cyclohaler
188	3.29	9.57	68.54	5.70	1.43%	1.711	130	45.45%	7.60%	52.45%	65.03%	98.60%	16.46%	26.29%
193	3.25	9.60	68.12	5.11	1.40%	1.448	135	48.21%	9.32%	-	-	-	-	-
197	3.21	9.62	68.79	5.33	1.44%	1.319	129	44.79%	9.78%	50.35%	61.54%	99.30%	15.57%	24.20%
200	3.27	9.56	69.73	5.33	1.23%	1.511	130	52.85%	8.61%	-	-	-	-	-
203	3.23	9.49	69.04	5.48	1.45%	1.742	124	42.76%	7.12%	48.25%	65.73%	97.90%	15.99%	27.42%
206	3.27	9.54	68.7	5.03	1.19%	1.216	125	52.65%	10.31%	-	-	-	-	-
268	3.31	9.61	69.15	5.51	1.52%	1.780	132	43.42%	7.42%	-	-	-	-	-
271	3.35	9.43	69.37	5.49	1.32%	1.608	133	50.38%	8.27%	-	-	-	-	-
284	3.36	9.54	69.03	5.29	1.20%	1.154	122	50.83%	10.58%	-	-	-	-	-
349	3.58	9.76	69.89	6.07	1.33%	1.534	121	45.49%	7.89%	-	-	-	-	-
365	3.60	9.83	68.35	5.44	1.24%	1.567	119	47.98%	7.59%	-	-	-	-	-
371	3.64	9.90	69.61	5.95	1.42%	1.760	117	41.20%	6.65%	-	-	-	-	-
387	3.71	9.99	69.44	4.51	1.42%	1.682	131	46.13%	7.79%	49.65%	60.84%	97.20%	14.99%	25.99%
392	3.77	10.11	69.66	4.71	1.48%	1.571	128	43.24%	8.15%	46.85%	63.64%	97.20%	16.85%	24.50%
408	3.78	10.03	68.89	4.80	1.40%	1.353	120	42.86%	8.87%	49.65%	58.74%	96.50%	15.36%	23.66%
434	3.86	10.21	69.4	5.1	1.39%	1.345	141	50.79%	10.50%	-	-	-	-	-
457	3.99	10.46	69.62	6.1	1.27%	1.269	127	49.86%	9.98%	-	-	-	-	-
487	4.23	10.53	68.35	4.85	1.34%	1.566	126	47.01%	8.05%		-	-	-	-
574	4.32	10.78	68.72	5.93	1.24%	1.540	139	56.05%	9.02%	-	-	-	-	-
587	4.35	10.96	69.84	5.92	1.43%	1.392	124	43.36%	8.91%	49.65%	62.94%	97.90%	16.20%	27.14%
598	4.41	11.33	68.35	5.7	1.36%	1.339	111	40.81%	8.29%	-	-	-	-	-
602	4.47	11.48	70.04	5.00	1.42%	1.341	129	45.42%	9.62%	49.65%	63.64%	97.90%	16.72%	25.40%
605	4.42	11.29	69.06	6.03	1.24%	1.469	124	50.04%	8.45%	-	-	-	-	-
611	4.53	11.37	69.89	5.75	1.42%	1.791	127	44.72%	7.09%	49.65%	63.64%	97.20%	15.88%	26.32%

Table 7.2. Particle size data, content uniformity and fine particle content of model vitamin C formulations, post blending.

Specific Energy Input (kJ kg^{-1})	d_5 (μm)	d_{10} (μm)	d_{50} (μm)	*CV* (%)	*Average drug loading*	*Total Mass Elutriated (g)*	*Drug mass elutriated from 20 g sample (mg)*	*% drug elutriated*	*Drug composition in elutriated fraction*	*Alpine air jet sieve drug removed* from 10 g initial sample			*NGI Fine particle mass*	
										10s	5 min	30 min	Generic	Cyclohaler
191	3.24	9.78	69.1	5.52	1.41%	1.699	131	46.20%	7.69%	47.39%	59.33%	96.48%	8.76%	18.34%
198	3.31	9.65	68.75	4.87	1.44%	1.435	121	42.01%	8.45%	49.82%	62.90%	95.49%	8.00%	20.53%
202	3.29	9.69	68.69	5.01	1.46%	1.646	155	53.20%	9.43%	48.44%	63.58%	97.40%	8.79%	15.63%
394	3.65	10.21	69.35	5.59	1.45%	1.402	136	46.90%	9.70%	48.88%	62.05%	94.94%	8.54%	14.65%
401	3.74	9.97	69.54	6.04	1.49%	1.537	134	44.90%	8.72%	46.93%	62.46%	95.99%	7.60%	19.08%
403	3.78	10.2	69.55	4.35	1.46%	1.528	123	42.09%	8.06%	48.07%	64.46%	94.51%	9.84%	15.69%
599	4.49	10.87	69.98	4.98	1.43%	1.604	128	44.67%	7.95%	48.78%	61.17%	96.01%	9.48%	18.06%
604	4.57	11.21	70.17	5.44	1.45%	1.532	147	50.65%	9.60%	50.14%	64.04%	95.25%	9.91%	18.57%
613	4.44	11.04	69.88	5.78	1.46%	1.799	138	47.34%	7.66%	48.42%	61.94%	94.56%	8.54%	16.37%

7.3.2. Effects of Blending on Fine Mimic API Particles

7.3.2.1. Fluidised Bed

The total amount of drug elutriated from a 20 g sample of formulation (corresponding to ~290 mg drug) typically ranged between 120 and 130 mg for both cholesterol and vitamin C at all SEIs – roughly 45-50% by weight of the formulation. Thus at this SGV (6.27 cm s^{-1}), approximately half of the available drug can be removed from these formulations. As seen previously in chapter 5, the total amount of formulation (drug and lactose) elutriated was not affected by SEI either. Thus, the mass elutriated from the bed was similar for both cholesterol and vitamin C containing formulations, and was consistent with data from chapter 5 (mass was between 1600 and 1800 mg for each sample).

AFM methods used in the CAB work reported by Begat *et al*., (2004) and Young and Price, (2004), amongst others, showed differences between the adhesive force holding drug-lactose pairs together, however these experiments were on single pairs of particles, unlike this bulk detachment method. It was shown in their work that the adhesive force between budesonide and lactose was smaller than the force between salbutamol sulphate and lactose, and that the cohesive forces between two budesonide crystals were greater than those between two salbutamol sulphate crystals; indicating that budesonide was far more cohesive than salbutamol sulphate. Based on that data, it would be expected that the less cohesive vitamin C used in this study would have a greater affinity to lactose than cholesterol, and thus elutriate less mass from the fluidised bed.

Fig. 7.3 shows the amount of drug elutriated as a percentage of the initial amount in the bed for both cholesterol and vitamin C (data from Table 7.1 and Table 7.2). Interestingly, no significant differences were observed in the behaviour of cholesterol and vitamin C with regards the amount of drug elutriated from the fluidised bed. It could be the case that the cohesive and adhesive forces experienced between cholesterol and lactose, and vitamin C and lactose were largely similar, and therefore similar amounts of drug would be elutriated. On the other hand, the elutriation process used in this study may not be subtle enough to remove individual particles, which could possibly be used to identify differences in adhesive strength. Since the fluidised bed requires removal of particles of the order of 25 μm, (sufficient airflow to suitably

fluidise the bed), it may be the case that the particles removed reside in entities (including lactose-drug agglomerates) that are readily removed, and separation of carrier and individual drug particle may not occur in this system.

Jones *et al*., (2008) report that the micronisation process has the effect of normalising the physical properties of drugs, thus they may appear to behave in similar ways, despite their differences in properties in their natural state. It could be the case that upon blending with lactose (and only making up less than 2% of the formulation by weight) that elutriation from a fluidised bed is too crude to identify differences between the drugs when in formulation.

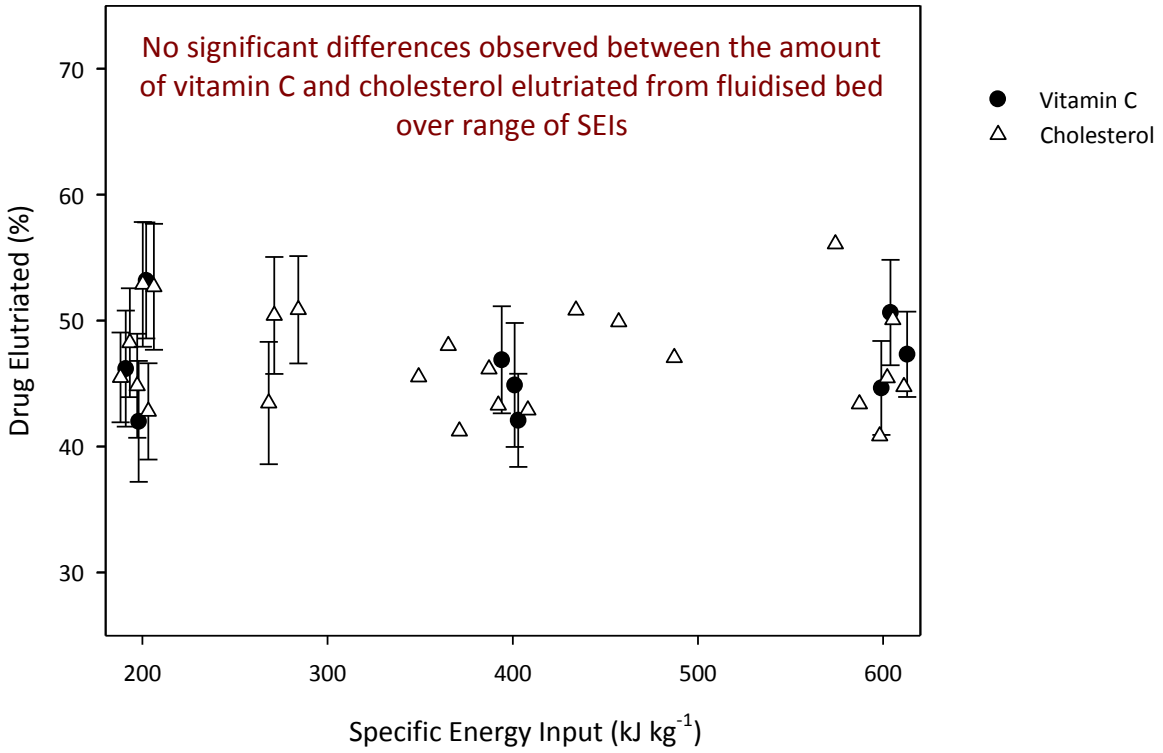

Fig. 7.3. Amount of drug elutriated as a function of SEI, using a fixed formulation mass of 20g. Error bars represent average of three independent experiments on each sample. □ - cholesterol, ▲ - vitamin C.

7.3.2.2. Air Jet Sieve

Results from the AJS experiments showed that at 30 s, approximately 70 mg drug could be removed from 10 g formulation – roughly half of the initial drug mass. After 5 min, this increased to roughly 90 mg (~60% initial mass), and after 30 min, about 140 mg could be removed (~95% initial mass). As with the fluidised bed results, there were no observed differences between the mass removed from formulations containing cholesterol or vitamin C. In addition, SEI did not affect the amount of formulation removed, such that formulations blended with ~200 kJ kg^{-1} displayed similar results to those blended with ~600 kJ kg^{-1} (Kruskal-Wallis test - page 119). The differences

observed in the amount of mass removed between formulations exposed to low SEIs (~70 kJ kg^{-1}) and high SEIs (~600 kJ kg^{-1}) seen in chapter 6 were not observed with chemically homogenous formulations, thus suggesting that the differences seen in lactose-only formulations only apply to lower SEIs corresponding to the de-agglomerated lactose (see chapter 4). This provides further evidence that blending beyond the point of homogeneity may not be beneficial, as no improvement in the delivery of drug has been observed.

The same arguments hold for AJS data, with it being likely that the AJS is not discriminating enough to distinguish between cholesterol and vitamin C in terms of amount of drug removed, at any of the pressures or sieving times tested. As with the FBE method, the AJS method is designed to view bulk changes in formulation adhesion and cohesion, unlike the AFM methods, which measured single-particle pairs.

7.3.2.3. Next Generation Impactor

Differences between cholesterol and vitamin C

Unlike FBE and AJS data, NGI data showed slight differences between formulations containing each compound. Using the Cyclohaler device, between 15 and 20% of the mass of vitamin C in the formulation at present was delivered beyond stage 2 of the NGI, whereas for cholesterol, between 24 and 28% of the formulation was delivered beyond stage 2 (Table 7.1 and Table 7.2).

Although these raw values are much smaller than the percentage drug elutriated or removed by the AJS, it should be remembered that stage 2 represents particles with aerodynamic diameters <4.64 μm. When compared to the cut off aerodynamic diameter and sieve aperture size of 25 μm used in the fluidised bed and AJS techniques, these values are expectedly lower.

Based on particle size alone, it would be expected that vitamin C had a greater delivery past stage 2 than cholesterol, since prior to blending, the particles were finer (see Table 3.2). There are two possible explanations which describe the superior FPF formulation performance of the more cohesive cholesterol over vitamin C. Firstly, a more cohesive system represents a weaker dug-carrier adhesion, thus a smaller force is required to detach a drug particle from the carrier, resulting in aerosolisation of a greater number of drug particles (Jones *et al*., 2008). Secondly, the formation of larger drug-only agglomerates can result in improved performance via an agglomeration

method proposed for other types of DPI formulations (Begat *et al*., 2004). Previous work focussing on CAB ratios suggests that as cohesive materials tend to form larger agglomerates, they experience greater shear and drag forces during aerosolisation (see Equation 7.1 and Equation 7.2). An explanation for this centred around the drag forces and kinetic energies experienced upon entrainment into an airstream. Equation 7.1 and Equation 7.2 describe the drag force, F_{drag} and kinetic energy, E_k of agglomerates in an air stream respectively.

$$F_{drag} = C_d \frac{\pi}{8} \rho_g \phi_{agg} v^2 \qquad \textbf{Equation 7.1}$$

where, C_d is the drag coefficient, ρ_g is the gas density, ϕ_{agg} is the effective diameter of the agglomerates, and v is the velocity of gas (in Equation 7.1, this is the gas velocity relative to the particle velocity, whereas in Equation 7.2 it is the absolute velocity of the particle).

$$E_k = \frac{\pi}{12} \rho_{agg} \phi_{agg} v^2 \qquad \textbf{Equation 7.2}$$

where, E_K is the kinetic energy of the agglomerate moving in the gas stream, and ρ_{agg} is the density of the agglomerate. It was hypothesized that the both the drag force which breaks up agglomerates and the kinetic energy which affects the drag efficiency by increasing the number and energy of collisions, increase in proportion with ϕ^3 and ϕ^2 respectively, thus larger agglomerates are subjected to greater deagglomeration forces (Begat *et al*., 2004). Whilst this suggests that materials that are more cohesive may offer superior formulation performance, a balance needs to be made since excessive cohesivity could result in the formation of agglomerates that resist the separation and de-agglomeration forces, resulting in poorer formulation performance.

Effects of SEI on formulation behaviour

Despite differences being observed between cholesterol and vitamin C behaviour, in the FPF, effects of SEI on formulation aerodynamic behaviour were still not observed by the NGI. For both vitamin C and cholesterol, the delivery of fine drug particles showed no change with respect to increasing SEI (Fig. 7.4), backing up the results in chapter 4, and the elutriation and AJS results earlier in this chapter that suggest additional HSB beyond the point at which chemical homogeneity is achieved does not improve fine particle drug delivery.

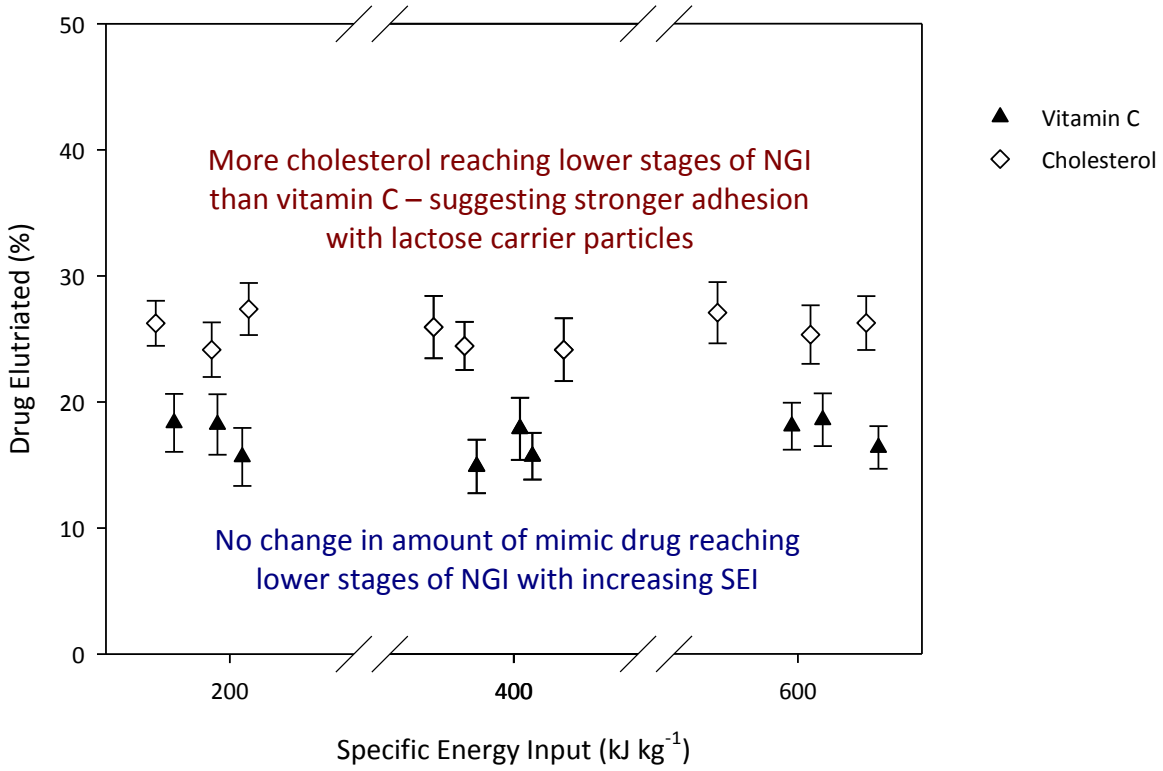

Fig. 7.4. Percentage mass delivered to stage 2 and beyond (FPF) from NGI as a function of SEI for cholesterol and vitamin C formulations.

Despite affecting the PSD of formulations, increased SEI has not been observed to alter the separation of fine drug particles from carrier particles. This suggests that the press-on forces attaching drug particles to carrier particles imparted during HSB do not increase beyond a certain point, and once the drug particles are attached – further application of blend energy will not increase the strength of attraction. Instead, the additional energy is used to create agglomerates of particles observed previously in this study. This has implications for the manufacture of DPI formulations since the primary indicator of performance is the amount of drug delivered to the respiratory zone, and if this amount is not seen to increase with additional SEI, it may be deemed unnecessary to perform extended blending.

Effect of device in NGI trials

In addition, the de-agglomeration and dispersion effects of the Cyclohaler® device were observed in this study, as an increased fine particle mass was observed with formulation delivered through the inhaler, rather than the generic stainless steel device. Typically, around 25% of the drug loaded into the Cyclohaler® capsule was delivered to stage 2 or lower with cholesterol as the mimic drug, compared to around

15% using the generic device (Table 7.1 and Table 7.2). This also applied to vitamin C, with around 18% of the available drug being deposited beyond stage 2 using the Cyclohaler device, whereas around 9% was delivered using the generic device. The remainder of the formulation either stayed in the capsule, device, preseparator or stage 1. This can be explained by the dispersion mechanism found within the Cyclohaler device that is not featured on the generic sample holder. This device creates a tortuous path for the particles suspended in the airstream, and enhances de-agglomeration of particles, thus increasing the number of fine particles that can be deposited in the latter stages of the NGI.

7.3.3. Effect of Storage on Formulation Characteristics

7.3.3.1. Particle Size

Fig. 7.5, Fig. 7.6, and Fig. 7.7 show the d_5, d_{10} and d_{50} particle size of cholesterol formulations stored at 40% and 60% RH for 12 weeks respectively. It can be shown that 40% RH stabilises the particle size of the formulations, with d_5, d_{10} and d_{50} remaining constant throughout the storage period. However, 60% RH storage conditions cause the powder to agglomerate, an effect seen previously, and probably due to the formation of liquid bridges (Finot *et al*., 1996; Bérard *et al*., 2002; Young *et al*., 2003). PSD increases occur through fines adhering to the surfaces of larger particles, and through formation of agglomerates or multiplets of a series of smaller particles. This effect has been previously observed by Bridson *et al*., (2007) and in chapters 4 and 5 of this thesis.

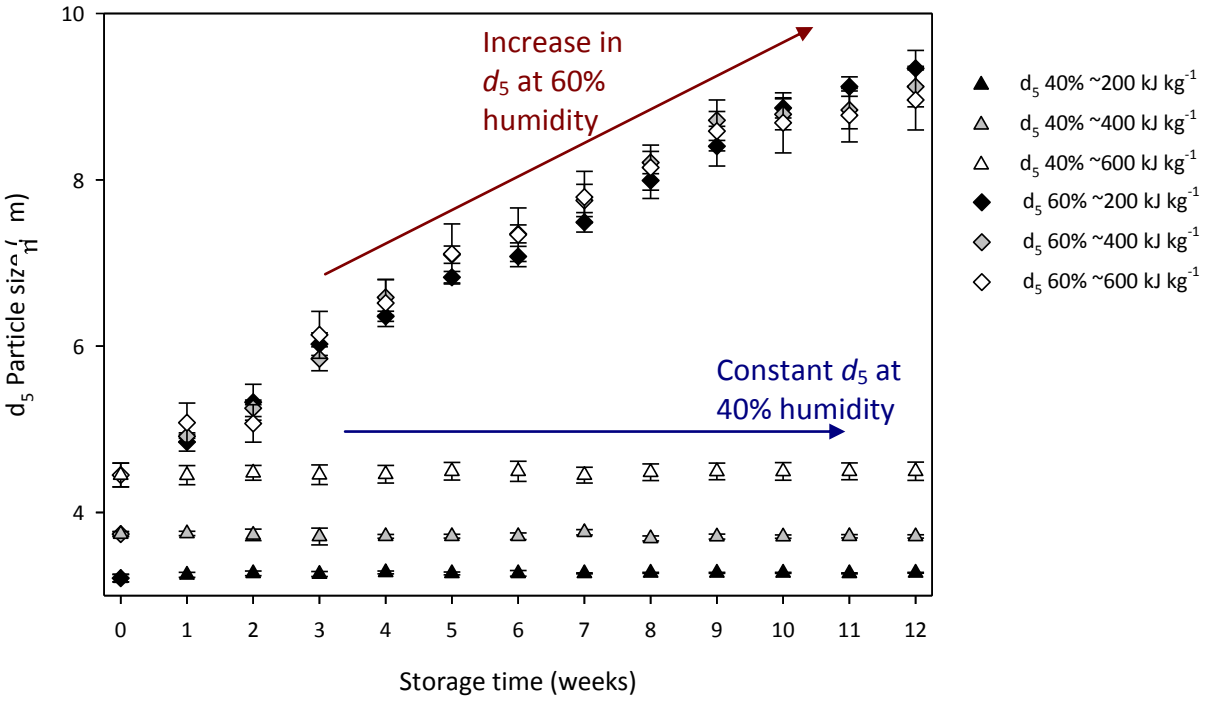

Fig. 7.5. Effect of storage time and humidity on cholesterol formulation d_5 particle size. Results shown are averaged from three independent experiments on three separate formulations at each energy input ± SEM.

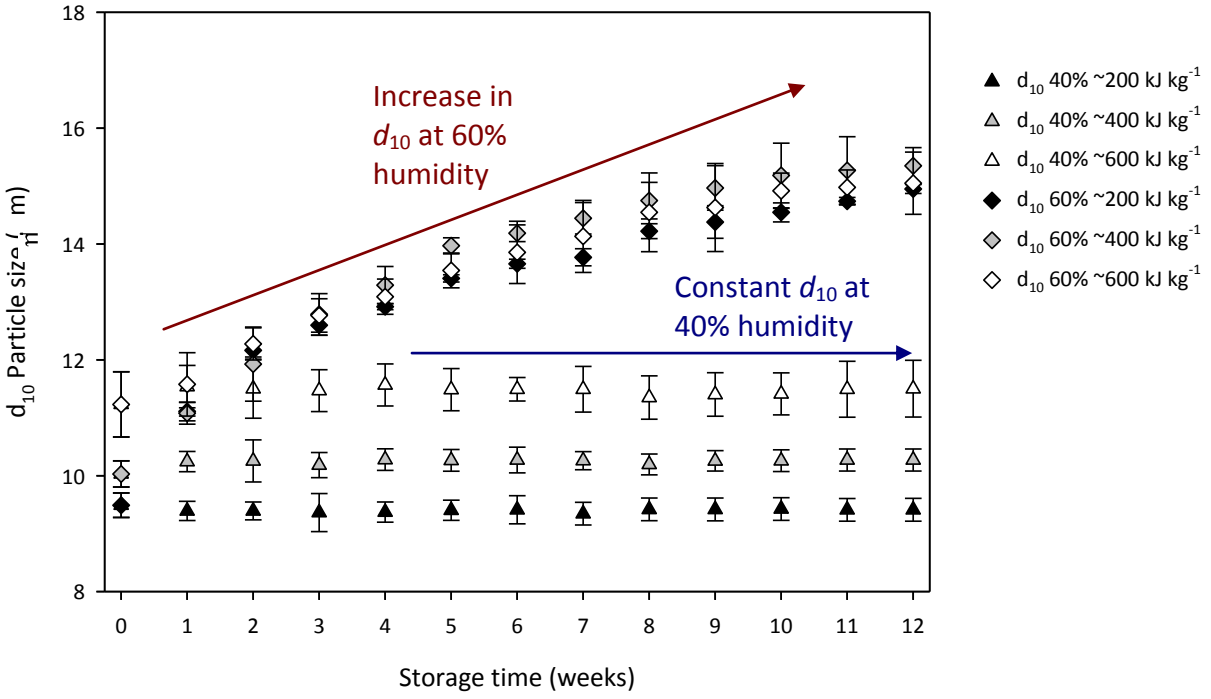

Fig. 7.6. Effect of storage time and humidity on cholesterol formulation d_{10} particle size. Results shown are averaged from three independent experiments on three separate formulations at each energy input ± SEM.

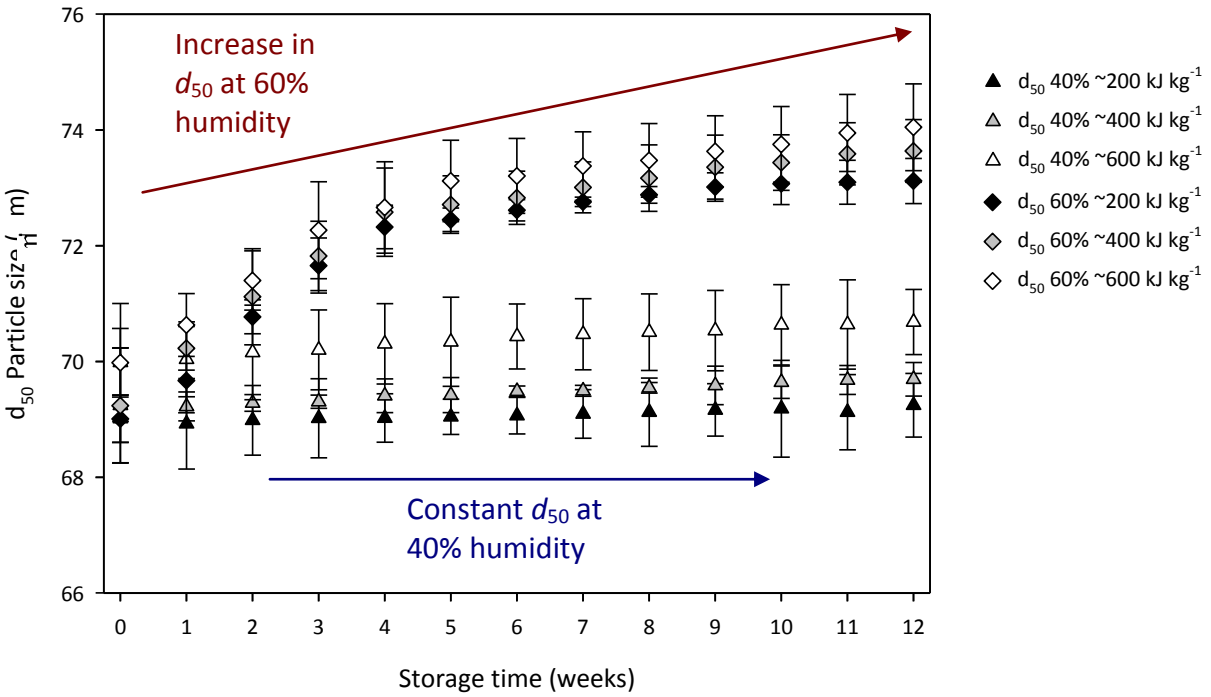

Fig. 7.7. Effect of storage time and humidity on cholesterol formulation d_{50} particle size. Results shown are averaged from three independent experiments on three separate formulations at each energy input ± SEM.

It can also be seen that storage effects dominate over blending effects (Fig. 7.9). Immediate post-blending (time = 0) data shows that there are significant differences in particle size between formulations exposed to different SEI (especially in the d_5 and d_{10} values). However, after just one week of storage at high humidity, these effects become less apparent, and the difference between these formulations is greatly reduced, providing further evidence that the capillary forces described by Finot *et al.*, (1996); Bérard *et al.*, (2002), and Young *et al.*, (2003) are present.

Trends for vitamin C containing formulations match those found in cholesterol containing formulations, which is to be expected since the mimic drug makes up less than 2% of the formulation by weight. Fig. 7.8 shows vitamin C d_5 particle size as a function of storage time, to highlight the similarity with the cholesterol formulation (Fig. 7.5), and emphasising the effects of storage dominating the effects of blending.

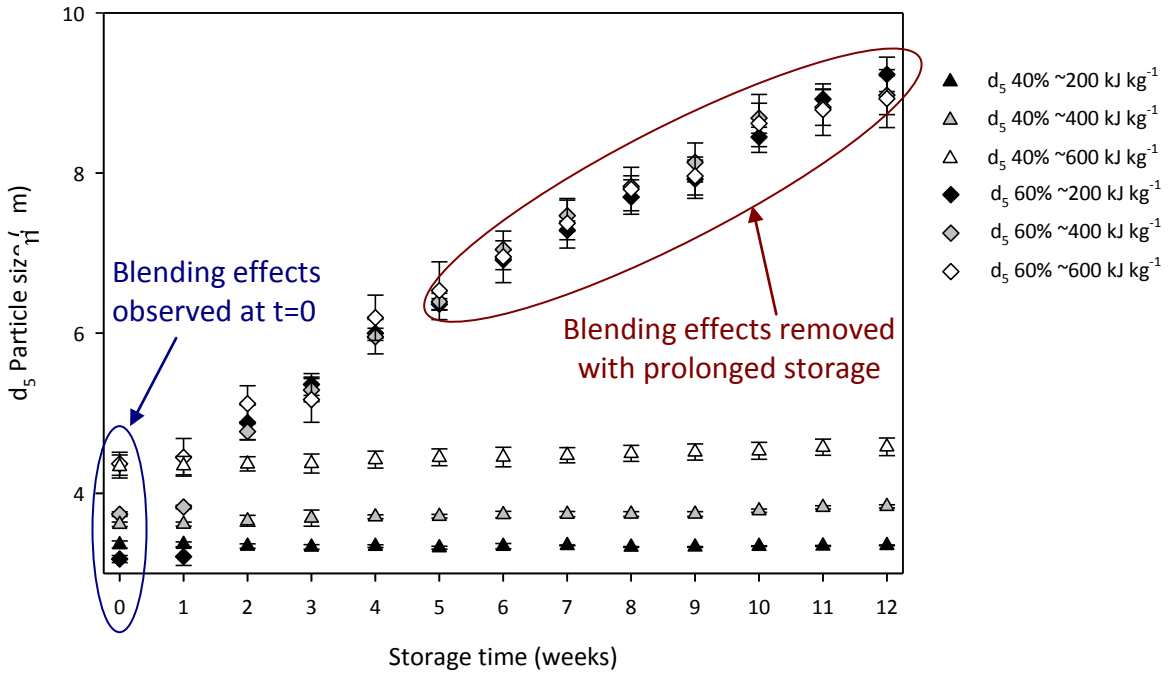

Fig. 7.8. Effect of storage time and humidity on vitamin C formulations d_5 particle size. Results shown are averaged from three independent experiments on three separate formulations at each energy input ± SEM.

7.3.3.2. Homogeneity

The chemical homogeneity of formulations was found to remain below 6% CV as specified in previous literature (Crooks and Ho, 1976; Flament *et al.*, 2004) over the time of the study, thus the formulations were suitable for FBE, AJS and NGI analyses. This was the case for all formulations stored at 40% and 60% RH.

7.3.4. Effects of Storage on Fine Mimic API Particles

Tests were performed using the FBE, AJS, and NGI methods to assess the effects of different storage conditions on the behaviour of formulations.

7.3.4.1. Fluidised Bed Elutriation

Fig. 7.9 shows the effect of storage time and RH on the total amount of cholesterol elutriated from a 20 g ± 0.1 g sample of formulation, using a SGV of 6.27 cm s^{-1}.

The results show that storage at 60% humidity causes less cholesterol to be elutriated from the bed than storage at 40%. This was apparent after just one week of storage and was consistent across the timescale of the experiment. However, unlike the particle size data shown above, the amount of material elutriated did not decrease with prolonged storage; instead, it remained consistent across the 12-week timescale. This suggests that the fluidisation process may alter the behaviour of the blend, since

material stored for 12 weeks at 60% RH behaved in the same way as material stored for just one week at 60% RH. Effectively, the fluidisation process may be "normalising" any storage effects such that they cannot be observed. However, the fluidisation process appears to be insufficient to reverse the effects of storage completely, hence the different amounts of total material that can be elutriated from formulations stored at 40% and 60% RH.

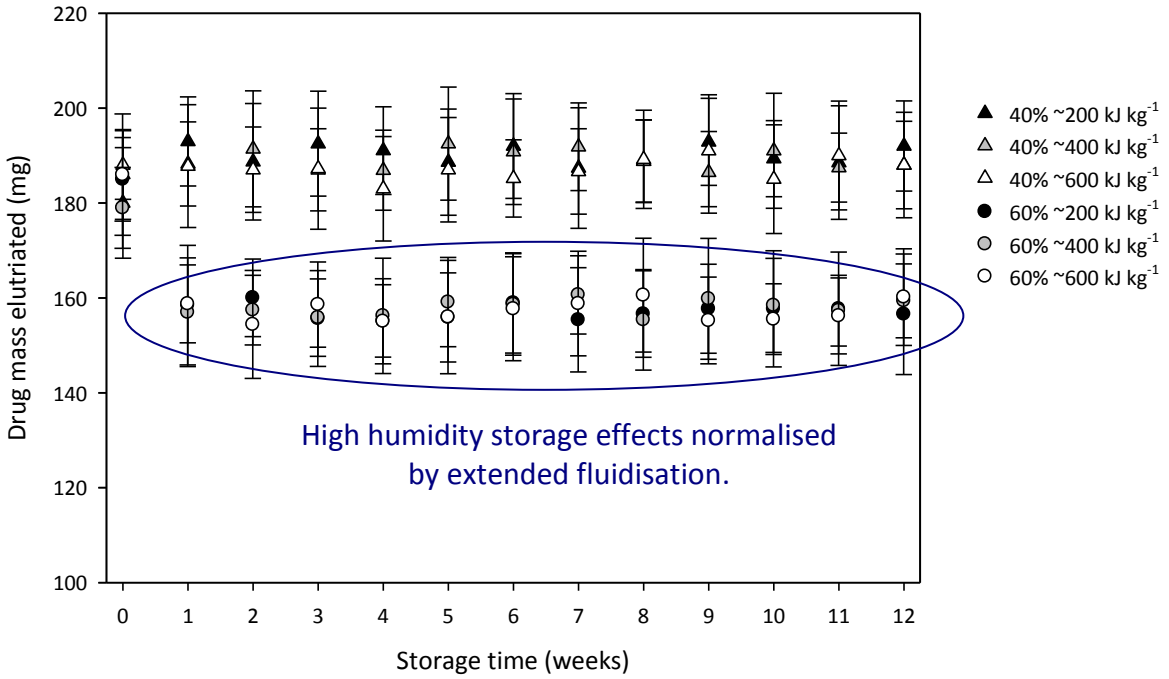

Fig. 7.9. Effect of storage time and RH on total amount of cholesterol elutriated from 20 g ± 0.1 g formulation fluidised with 6.27 cm s^{-1} SGV. Results shown are averaged from three independent experiments on three separate formulations at each energy input ± SEM.

Fig. 7.10 shows the amount of cholesterol elutriated following 10 min of fluidisation as a function of storage time and storage RH. Whilst the amount of cholesterol elutriated remains constant when stored at 40% RH, prolonged storage appears to decrease the amount elutriated. Unlike Fig. 7.9 which appears to show the ~120 min fluidisation process normalising storage effects, just 10 min of fluidisation time does not appear to have this effect, hence the reduced amount of cholesterol elutriated from formulations stored for longer periods of time at 60% RH. Statistically significant differences between cholesterol formulations stored at 40% and 60% RH were first observed (found by application of the Kruskal-Wallis test - page 119) following three weeks of storage, and the difference increased with further storage.

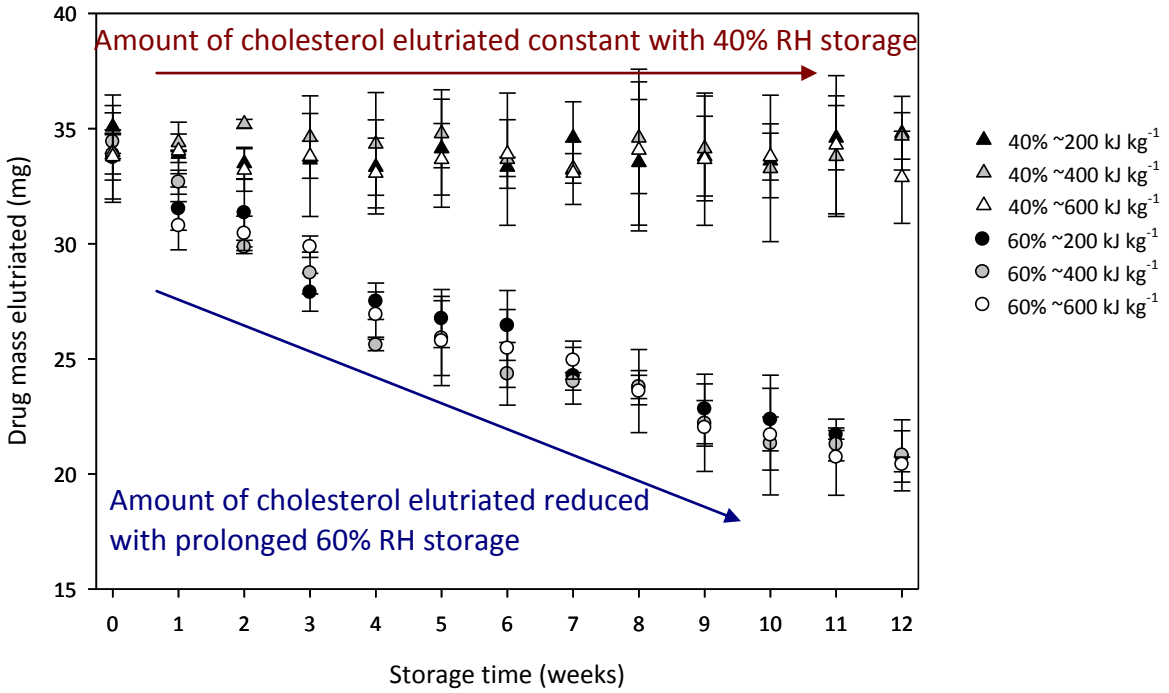

Fig. 7.10. Effect of storage time and RH on amount of cholesterol elutriated from 20 g ± 0.1 g formulation after 10 min fluidisation at 6.27 cm s^{-1} SGV. Results shown are averaged from three independent experiments on three separate formulations at each energy input ± SEM.

This reduction in amount of cholesterol elutriated appears to correlate with the particle size data that showed a coarsening of particle size with prolonged high-humidity storage, suggesting that the same process affects both particle size and elutriation of drug. Previous literature supports this theory with Zeng *et al.*, (2001), Price *et al.*, (2002), Young *et al.*, (2004), and Zhu *et al.*, (2008) reporting a decrease in salbutamol sulphate FPF due to high humidity storage, whilst Das *et al.*, (2009) shows this with salmeterol xinafoate, each due to an increase in interparticulate (capillary) forces associated with high humidity storage. Harjunen *et al.*, (2003) also show this effect occurs at low budesonide doses; however, at high doses, they report the opposite effect, with moisture sorption causing electrostatic forces to decrease, thus allowing easier detachment from the carrier surface. Since the formulations in this study use relatively low doses (1.46% w/w), it is likely that the increase in capillary interaction theory applies, causing the reduction in elutriated fraction with increased storage.

Vitamin C experiments (Fig. 7.11) showed the same trends as cholesterol (Fig. 7.10), however slightly less drug was elutriated than from the cholesterol formulations, suggesting the adhesion between vitamin C and lactose is greater than between cholesterol and lactose.

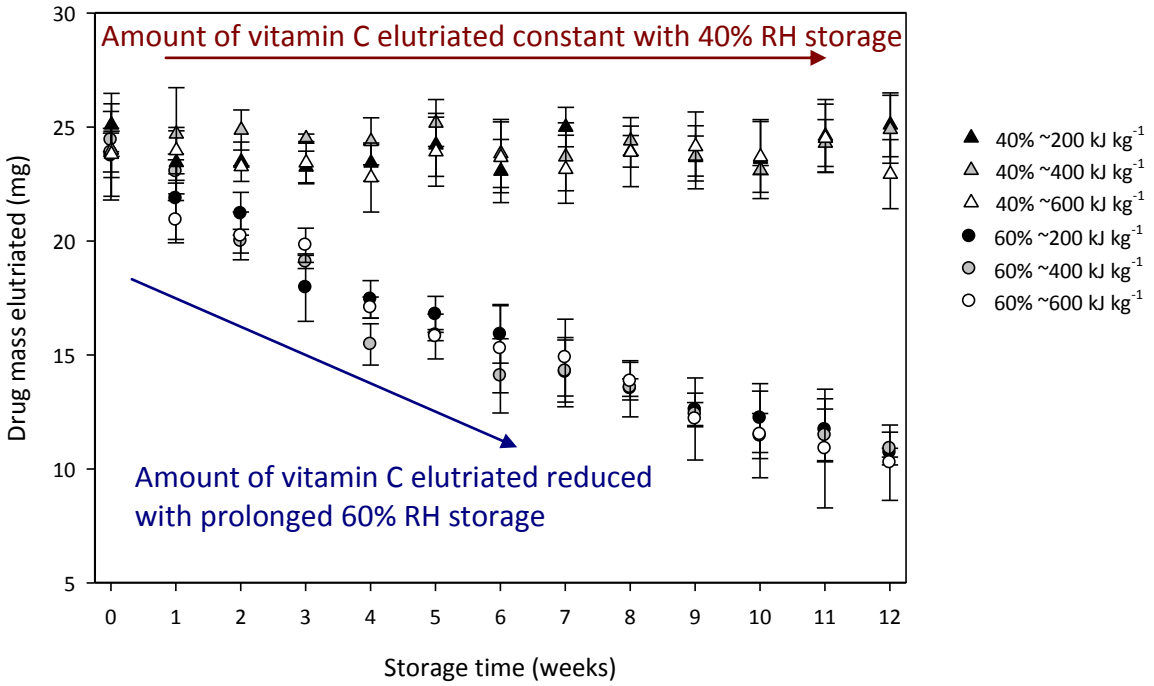

Fig. 7.11. Effect of storage time and RH on amount of vitamin C elutriated from 20 g ± 0.1 g formulation after 10 min fluidisation at 6.27 cm s^{-1} SGV. Results shown are averaged from three independent experiments on three separate formulations at each energy input ± SEM.

7.3.4.2. Air Jet Sieve

Removal of drug by AJS pressure was not seen to alter with storage time at either 40% or 60% RH. Results from cholesterol formulations showed that the amount of drug removed after 10 s from formulations stored at both 40% and 60% RH remained at ~85 mg (Fig. 7.12) over the course of the experiment, whereas the amount removed after 30 min was ~145 mg (Fig. 7.13).

Again, the effects of storage appear to have been cancelled by the AJS, similar to the effects seen in the fluidised bed. This removes the possibility to distinguish between samples stored over different periods of time under high humidity conditions, thus the amount of mimic drug removed were similar for formulations stored at both 40% and 60% and also for formulations stored for just one week and those stored for 12 weeks.

As seen with the FBE method, the amount of vitamin C removed was less than the amount of cholesterol removed (Fig. 7.14, Fig. 7.15), suggesting that the adhesion between vitamin C particles and lactose was greater than between cholesterol and lactose. This agrees with previous literature that suggest more hydrophilic drug substances show a stronger affinity to lactose than hydrophobic substances, hence removal of these particles from carrier surfaces is more difficult, this is explained in

the CAB literature, which assesses the adhesive/cohesive balance in various drug-excipient systems (Begat *et al.*, 2004; Young and Price, 2004).

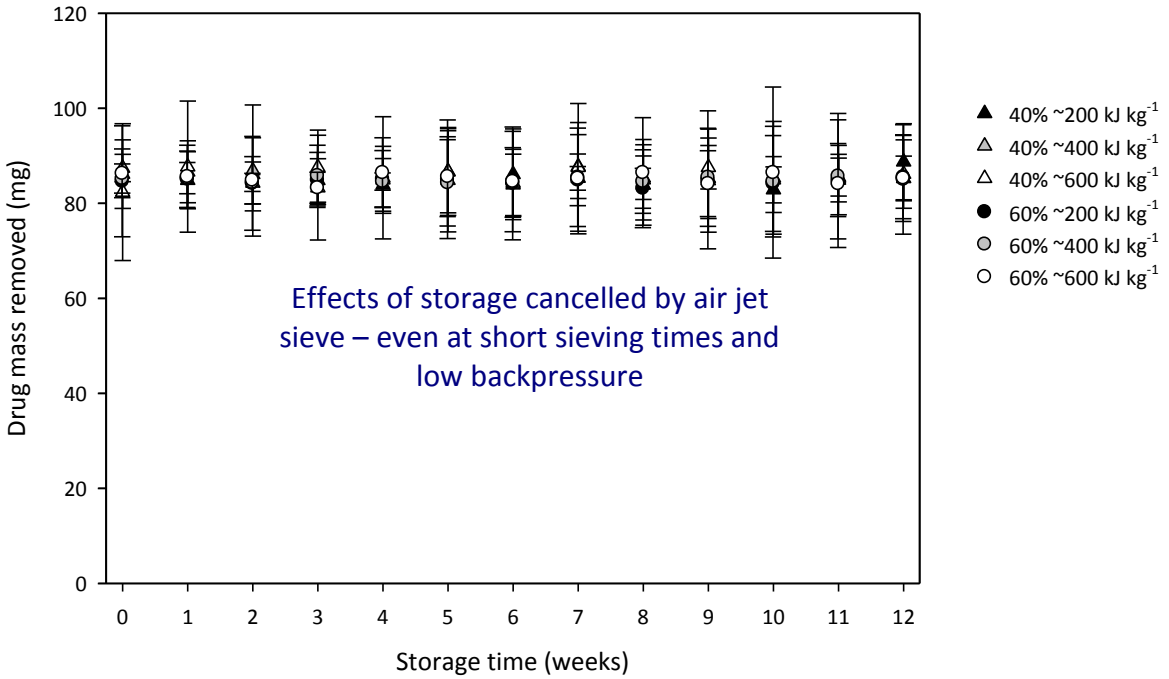

Fig. 7.12. Effect of storage time and RH on the amount of cholesterol removed from 10 g ± 0.1 g initial sample using AJS following 10 s sieving time, with 25 μm sieve and 600 Pa backpressure.

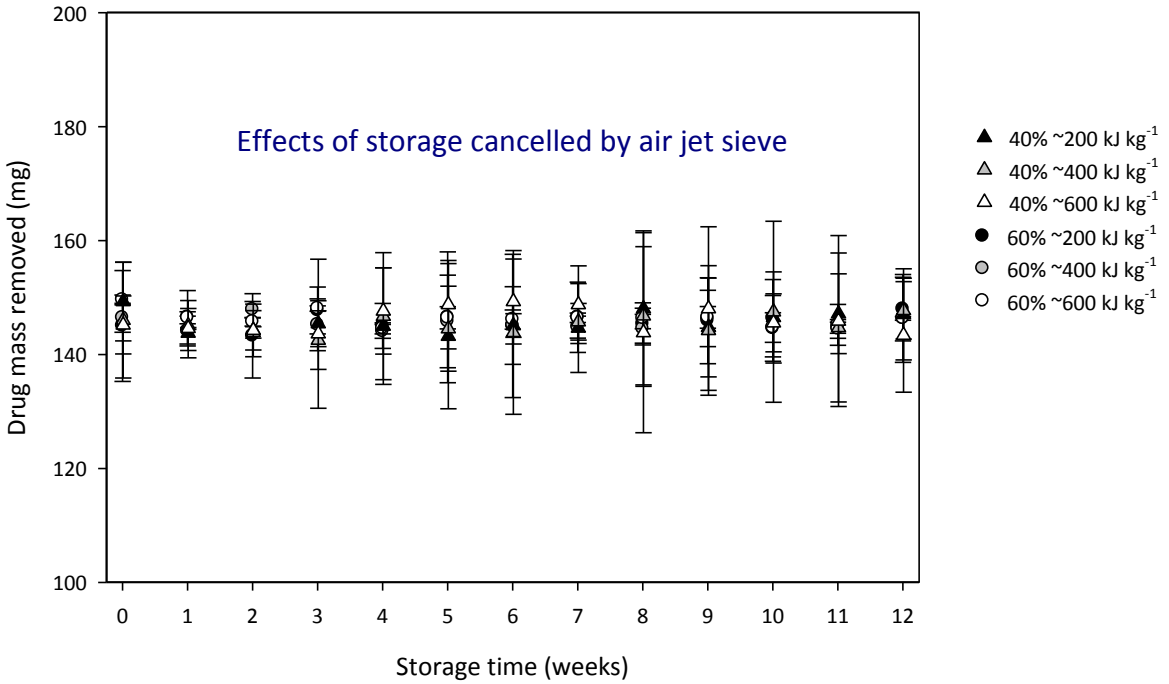

Fig. 7.13. Effect of storage time and RH on the amount of cholesterol removed from 10 g ± 0.1 g initial sample using AJS following 30 min sieving time, with 25 μm sieve and 600 Pa backpressure.

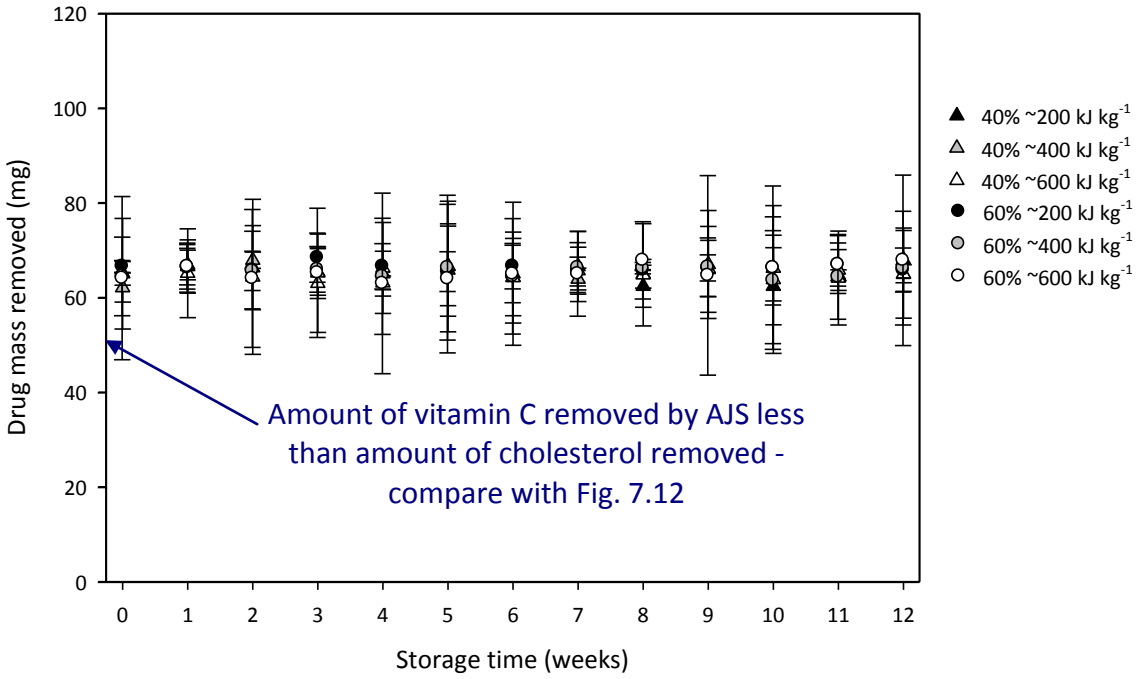

Fig. 7.14. Effect of storage time and storage RH on the amount of vitamin C removed from 10 g ± 0.1 g initial sample using AJS following 10 s sieving time, with 25 μm sieve and 600 Pa backpressure.

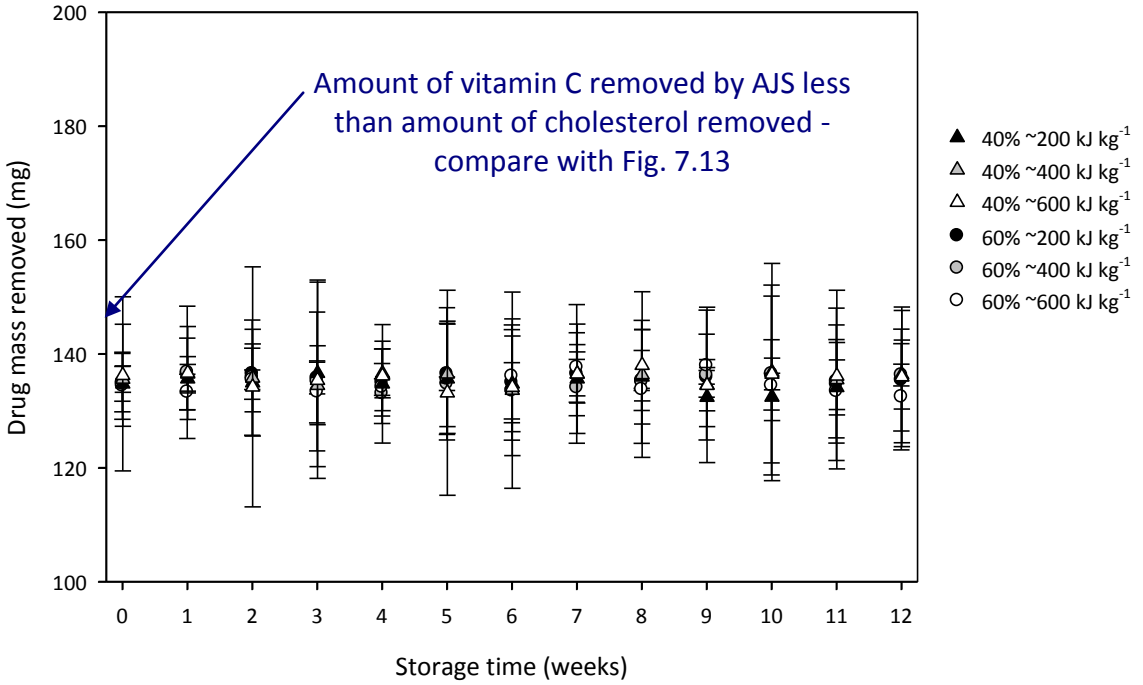

Fig. 7.15. Effect of storage time and storage RH on the amount of vitamin C removed from 10 g ± 0.1 g initial sample using AJS following 30 min sieving time, with 25 μm sieve and 600 Pa backpressure.

7.3.4.3. Next Generation Impactor

Cascade impactor data shows cholesterol-containing formulations unaffected by storage conditions; in both cases, the amount of drug deposited at stage 2 or further in the NGI is around 90 μg, irrespective of the storage conditions or time. Fig. 7.16 shows data from three formulations blended with SEI ~400 kJ kg^{-1} (formulations blended with ~200 kJ kg^{-1} and ~600 kJ kg^{-1} showed similar trends and magnitude of fine particle mass).

The greater delivery of cholesterol compared to vitamin C is does not concur with the particle size data that suggests vitamin C is finer, however previous work suggests that more hydrophobic compounds can produce a greater FPF during aerosolisation testing than more hydrophilic compounds (Price *et al*., 2002; Young *et al*., 2004; Zeng *et al*., 2007). In addition, as described in section 7.3.2.3, formulations that are more cohesive have been shown to have better FPF performance, which concurs with the results found here as the cholesterol used in this study was found to be more cohesive than the vitamin C (Table 3.3).

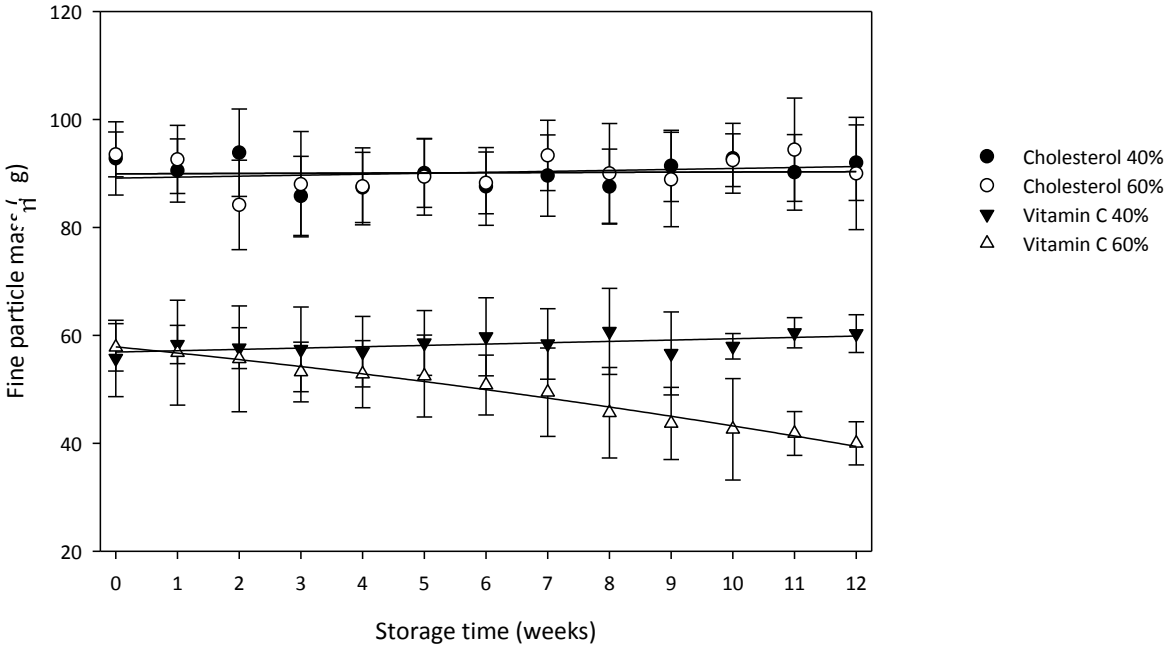

Fig. 7.16. Effect of storage time and storage RH on cholesterol and vitamin C fine particle mass determined by NGI using Cyclohaler® device operating at 60 l min^{-1} flow rate with 250 mg formulation loaded into size three capsules. Results are averaged from three independent samples from three independent formulations with SEI ~400 kJ kg^{-1} stored at each humidity.

Price *et al*., (2002) show that the separation energy for salbutamol sulphate (hydrophilic) particles is much greater than budesonide (hydrophobic) at high

humidity. Young *et al*., (2004) found a decrease in FPF due to high-humidity storage of salbutamol sulphate, caused by increased capillary forces and possible liquid bridge formation, supporting previous work by Zeng *et al*., (2001), Price *et al*., (2002), and Harjunen *et al*., (2003). In addition, Borgstrom *et al*., (2005) and Zeng *et al*., (2007) have reported significant reductions in FPF due to increased RH storage conditions, whilst Traini *et al*., (2006) used AFM to find that the separation energy required to detach salbutamol sulphate, budesonide, and formoterol fumarate dihydrate drug particles from carrier increased in high-humidity environments.

Results from NGI impaction experiments show a decrease in the fine particle delivery of vitamin C with prolonged storage at high humidity. Statistically significant differences were observed from 8 weeks storage; however, the trend appeared to begin at just 3 weeks (Kruskal-Wallis test - page 119). Despite this, corresponding FBE and AJS experiments do not show similar reductions. A likely explanation is such that the fine particle definition of the NGI is $\leq$4.64 μm, whereas with the FBE and AJS tests developed, the fine particles removed are $\leq$25 μm, thus the NGI offered greater discrimination between formulations. It is able to de-agglomerate any groups of drug that may have formed and thus is more representative of an inhalation event than the other two methods. Whereas the fluidised bed and AJS methods will remove every object (single particle or agglomerate) less than 25 μm, the NGI will only assess those less than 4.64 μm, hence seeing differences that occur in this population of particles.

In addition, the increased PSD of the formulations with prolonged storage at high humidity (Fig. 7.5 - Fig. 7.8), explains the reduced elutriation and NGI FPF, as the coarser formulations possess fewer free fines. This is backed up by shear cell analysis that showed that formulations stored at 60% RH for a prolonged period had a smaller FF, and were hence more cohesive (Table 7.3). This can again be explained by the increased liquid bridge formation and enhanced capillary forces that occur in high humidity formulations and has been shown previously in Fig. 5.5 where the amount of mass elutriated from the fluidised bed reduced for lactose only samples stored at high humidity. Although no statistically significant differences could be observed between cholesterol and vitamin C formulations, this was expected as the shear cell analysis is a bulk characterisation technique and the effects of the mimic drug on the mechanical properties of the powders is minimal. Results for the FFs immediately post blending

concur with previous results for blended formulations (Table 4.4), and storage at 40% RH was not seen to affect the cohesivity, as with PSD and fine particle separation data.

Table 7.3. Flow functions (f_c) of cholesterol and vitamin C formulations used in this study. Results show average values from three formulations at each energy input with three independent experiments performed on each batch. Errors represent ± SEM and are rounded to two decimal places.

	40% storage		*60% storage*	
Material	***Week 0***	***Week 12***	***Week 0***	***Week 12***
Vitamin C (~200 kJ kg^{-1})	4.02 ± 0.58	4.32 ± 0.44	4.02 ± 0.67	2.32 ± 0.56
Vitamin C (~400 kJ kg^{-1})	4.18 ± 0.54	4.06 ± 0.83	3.93 ± 0.61	2.56 ± 0.63
Vitamin C (~600 kJ kg^{-1})	4.45 ± 0.64	4.30 ± 0.42	4.28 ± 0.97	2.22 ± 0.76
Cholesterol (~200 kJ kg^{-1})	4.21 ± 0.54	4.46 ± 0.61	4.15 ± 0.86	2.20 ± 0.59
Cholesterol (~400 kJ kg^{-1})	4.47 ± 0.78	4.05 ± 0.58	4.36 ± 0.66	2.47 ± 0.50
Cholesterol (~600 kJ kg^{-1})	4.11 ± 0.54	3.99 ± 0.73	4.03 ± 0.71	2.31 ± 0.72

Humidity conditions have affected vitamin C more strongly than cholesterol due to their relative hydrophobicities and the greater solubility of vitamin C with respect to cholesterol is likely to be a factor in its decreased performance following prolonged high RH storage. It has previously been shown that more hydrophobic compounds (cholesterol) are less strongly affected by high humidity conditions than more hydrophilic compounds (vitamin C). Price *et al*., (2002) found that the separation energy and adhesive force was much greater for salbutamol sulphate (hydrophilic) - lactose interactions than budesonide (hydrophobic) - lactose interactions, whilst Harjunen *et al*., (2003) reported an increase in FPF of budesonide associated with prolonged high humidity storage. Zeng *et al*., (2001), Young *et al*., (2004), and Zhu *et al*., (2008) report a decrease in FPF of salbutamol sulphate due to storage at high RH, whilst Das *et al*., (2009) show a decrease in FPF with the hydrophilic salmeterol xinafoate.

7.4. Conclusion

This chapter has shown that HSB regimes do not appear to affect the ability of micronised cholesterol and vitamin C to separate from inhalation-grade α-lactose monohydrate, based on FBE, AJS, and NGI studies. These tests showed no significant differences in the amount of fine (≤25 μm) particles elutriated, removed by sieving, or comprising the FPF based on NGI experiments (which focussed on fines ≤4.64 μm). Tests were performed on chemically homogeneous formulations and showed that extended SEI past the point of homogeneity did not affect the separation of drug

particles, despite a continual increase in the particle size distribution of the formulations.

On the other hand, storage regimes were shown to affect the performance of DPI formulations. Storage of formulations at 60% RH has been shown to reduce the ability of fine vitamin C particles to separate from lactose carriers compared to formulations stored at 40% using both the FBE and NGI methods. Elutriation of cholesterol from the fluidised bed was also seen to decrease with 60% RH storage, whereas NGI data showed no difference in the FPF of cholesterol from formulations stored at 40% or 60%.

However, the AJS method was seen to cancel storage effects, with no differences observed between the formulations stored at 40% and those stored at 60% with respect to fine particles removed for both vitamin C and cholesterol containing formulations.

The FBE and AJS methods showed no difference in the amount of drug elutriated/removed between cholesterol and vitamin C with respect to SEI. However, this is most likely due to these methods not being quite as sensitive to fine particles as the NGI, and thus removing the mimic drug particles in small agglomerates with lactose particles, and not just single particles being removed. Overall, the FBE has shown that it can be used as a tool to assess mimic DPI formulations, however unlike the NGI method; it does not have the sensitivity to very fine particles in the respirable size range of 1-5 μm. Instead, it measures performance based on the elutriation of particles with aerodynamic diameter ≤25 μm. It is useful to compare the velocities experienced in each analysis technique used. As previously mentioned, the FB method uses a SGV of 6.27 cm s^{-1}, which is by far the lowest velocity used. By application of Bernoulli's equation $P = ½\rho v^2$, where P is the dynamic pressure applied to the system, ρ is the density of air (1.2 kg m^{-3}), and v is the gas velocity, the velocity of air through the AJS can be estimated to be ~ 32 ms^{-1} (at 600 Pa). Finally, velocities in the NGI can be estimated by using the cross sectional areas of the nozzle at the collection plate, and at the capsule, along with the flow rate used to mimic an inhalation event (60 l min^{-1}). At the capsule, with diameter through which the powder flows estimated to be 0.5 mm, the velocity is approximately 2 ms^{-1}, whereas this increases to approximately 200 ms^{-1} at the collection plate nozzle (diameter ~ 5 μm).

8.0. Conclusion

8.1. Importance of Work and Review of Findings

The main aims and conclusions of this work have been discussed below, with reference to the aims outlined in chapter 1.

The effects of the scale of HSB regimes on the properties of mimic DPI formulations, including PSD, SSA, and chemical homogeneity were investigated to compare against previous literature.

HSB was shown to affect the particle size of inhalation-grade lactose such that an increased SEI was shown to coarsen the powder by agglomeration of fine particles with each other to form multiplets of fine particles, and by attachment to larger carrier particles. This agglomeration followed an initial decrease in particle size at low SEIs, an event that was previously unseen during the HSB of inhalation-grade lactose and was attributed to the redistribution of particles, and the break-up of agglomerates found in the unprocessed lactose, before reagglomeration occurred with further energy input. Changes to the particle size of lactose were characterised by laser diffraction and SSA studies, which were used as tools to confirm the mechanism by which particle changes occurred.

The initial decrease and subsequent increase in PSD was observed across a series of laboratory-scale, geometrically similar HSB equipment. However, their magnitude and rate at which they occurred differed over the scales tested in this study, with the larger bowls appearing to increase both the rate and magnitude at which these changes occurred. A novel feature of this work was the use of equipment with distinct *high shear* blending process, previous studies exploring blending effects on DPI formulations have often used blenders which do not utilise a high shear process, instead using tumbling methods or even equipment with a milling action.

Regime maps were produced to highlight preferential blending conditions for each high shear blender bowls and impellers. Such knowledge was required in order to achieve optimal blending conditions for the production of mimic formulations that were produced for work later in the thesis.

Despite the lactose used in this study being the same inhalation-grade powder used by the manufacturer, closer investigation proved that the initial PSD was slightly finer

than that used in a previous study. This highlighted the importance of characterisation of materials used in DPI formulations prior to manufacture of the final product. It showed that even slight changes in the initial properties of materials have profound effects on the behaviour of such powders, and could have implications for the performance of these formulations.

In addition, the chemical homogeneity of mimic DPI formulations was tested using vitamin C and cholesterol as mimic APIs, the rationale of their choice being their notably different cohesivities. It was found that a suitably homogenous formulation was produced with relatively low SEI, roughly corresponding to the point at which the PSD of the formulations began to re-agglomerate. However, unlike the PSD, the homogeneity was not seen to alter with additional SEI, and remained below the prescribed limit of $\leq$6% CV as stated in previous literature. This has implication for the pharmaceutical industry as it indicates that extended blending regimes may not be beneficial to the quality of formulation in terms of chemical homogeneity.

It was found that the point at which homogeneity is achieved varies depending on the cohesivity of the mimic drugs and hence their particles' relative affinity to lactose. It was shown that the more cohesive cholesterol required a greater energy input to achieve chemical homogeneity than vitamin C, which due to its weaker cohesivity, the agglomerates present in its micronised state, were more readily distributed throughout the bulk lactose powder.

A classical FB was designed, built, and used to test DPI formulations, with the principles of elutriation employed to separate fine particles from the bulk powder within the bed.

A classical fluidised bed was designed and built to explore the effects of passing an air stream through formulations to explore the effects of blending and storage on the separation of fine particles from coarse particles using the principles of elutriation. Elutriation of particles is often an undesired effect of fluidisation in chemical engineering processes; however, in this project it has been used to classify particles according to aerodynamic particle size. Separation of drug particles from carrier particles is a key process involved in the delivery of API to the lungs, and although not attempting to mimic an inhalation event, the use of classical fluidised bed equipment

enabled separation mechanisms similar to those in a DPI to be employed, without requiring the use of a real device.

Tests on lactose-only formulations immediately post-blending showed that measurements of pressure drop across the bed vs SGV was not sufficient to distinguish between samples exposed to different SEIs, although the bed could differentiate batches that had been deliberately coarsened by sieving (section 3.4.5.1) to produce samples with significantly different cohesivities. In addition, the amount (mass) of material elutriated was not sufficient to differentiate between samples exposed to different SEIs. However, closer analysis of the elutriated fraction showed a change in the size distribution of particles elutriated, suggesting that the blending process affected the particles in the ~25 μm size range, along with the fine particles that were seen to be affected previously.

Therefore, the FBE method described in this thesis has shown to be a potential tool for assessing formulation behaviour at various stages during the secondary manufacturing process. This is a particularly useful technique as it deals with formulations in their actual state (does not require suspension of particles in fluids etc.) immediately post-blending and eliminates the need to fill devices or other equipment to perform such adhesion tests. In addition, statistically significant numbers of particles were examined; therefore, the bulk properties are being assessed, rather than individual particles or pairs of particles, without wasting an excessive amount of valuable formulation.

The effects of HSB regimes on the in vitro performance of mimic DPI formulations using the novel FBE technique were investigated, and compared to conventional AJS and NGI separation techniques used to assess the properties of DPI formulations.

Tests were performed on mimic DPI formulations using cholesterol and vitamin C as mimic APIs. Tests were performed using the newly developed FBE technique for separating fine particles, and compared to AJS and cascade impactor methods. It was found that the effects of blending could not be determined using any of the separation techniques, with the amount of drug removed by each method being consistent over a range formulation SEIs. This suggested that extended blending regimes might not be

beneficial to the formulation performance. Earlier work in this study showed that additional SEI beyond the point at which suitable chemical homogeneity was achieved increased the PSD of the formulation.

Differences were observed between the amount of cholesterol removed and the amount of vitamin C removed, with the NGI method showing a greater delivery of fine cholesterol particles to the latter stages of the impactor than vitamin C. This concurred with previous literature that found more cohesive APIs offered greater *in vitro* performance due to the reduced affinity to the larger lactose particles. The FBE and AJS methods showed no difference in the amount of drug elutriated/removed between cholesterol and vitamin C; however, this is most likely due to these methods not being quite as sensitive to fine particles as the NGI, and thus removing the mimic drug particles in small agglomerates with lactose particles, and not just single particles being removed.

The effects of storage regimes on the in vitro performance of mimic DPI formulations using the novel FBE technique were investigated, and compared to conventional AJS and NGI, separation techniques used to assess the properties of DPI formulations.

The effects of storage were seen to predominate over the effects of blending, with particle size distributions of all formulations seen to increase with prolonged storage at 60% RH. This was due the formation of liquid bridges and enhanced capillary forces causing particles to agglomerate; this effect was seen in both cholesterol and vitamin C formulations to the same degree.

Fine particle studies using the AJS were inconclusive, with the amount of vitamin C and cholesterol removed being similar over all storage periods. However, both the NGI and FBE methods showed differences in the amount of vitamin C removed with respect to storage conditions. Both methods showed a decrease in fine particle delivery with continued storage at 60% RH, an effect explained by the increased capillary forces between mimic drug and carrier. Cholesterol fine particle delivery was seen to decrease with extended 60% RH storage using the FBE method, although no differences were observed using the NGI method. This again was due to the FBE method being a method analysing agglomerates of particles, rather than the NGI

method that analysed individual particle separation. Cholesterol, due to its hydrophobicity was less sensitive to high-humidity storage conditions than the more hydrophilic vitamin C, hence the lack of change in fine particle delivery over time.

With current pharmaceutical emphasis being placed on Quality by Design and Process Analytical Technologies, monitoring the performance and behaviour of products at each stage of manufacture is vitally important to minimise waste and associated costs. Overall, this thesis has shown that the FBE technique can be used to analyse mimic DPI formulations, and detect blending and storage induced changes in these powders. It can be used in conjunction with existing cascade impactor studies to evaluate the performance of formulations throughout the secondary manufacturing process. The major limitation is the lack of ability to elutriate the very fine particles since the SGV required to elutriate particles solely in the 1-5 μm size range required for pulmonary deposition is insufficient to fluidise the powder bed, thus collection of these powders is difficult.

Each of the FBE, AJS, and NGI tests used in this study has used bulk separation methods. Many previous AFM studies have separated individual drug particles from larger carrier particles, and are able to assign values to the adhesive force required to separate the particles. A quantitative evaluation of the forces involved in separation of drug particles from carriers on a bulk scale would be useful, in order to compare to the values attributed to single pairs of particles found through AFM, and provide a value for the force required to liberate a given amount of drug. However, due to the range of separation mechanisms involved (shear forces, gravitational forces, particle-particle, and particle-wall collisions) and the range of particle properties (size, shape, surface rugosity, density etc.) featured in DPI formulations, measuring values in bulk is extremely difficult.

Despite the wide range of literature regarding interactive forces in DPI formulations, prediction of powder behaviour will continue to be difficult due to the three-dimensional particle shapes with unknown number and strength of contact points between drug and carrier. It should also be considered that minimising the interparticulate forces might not always be desirable if the clinical physiological response or reliability of treatment is not improved in turn.

8.2. Opportunities for Further Work

The importance of this work was to develop and understand ways to reduce batch variability, and increase process understanding in order to eliminate batch failure. In addition, increasing the depth of understanding of formulation processing and the development of new analysis techniques that allows formulations at different energy states to be identified.

There are several options that could be explored to further the work described in this thesis. Firstly, the use of *active* drugs could be used rather than the mimics used in this study, thus enhancing the knowledge of their formulation performance. Secondly, alternative blending methods could be explored. As increased HSB was observed to not significantly improve the chemical homogeneity of formulations beyond given SEIs, it may be useful to determine the effects of other blending regimes on the performance of formulations.

Discrete Element Modelling (DEM) of the interactions present within DPI formulations during both the manufacturing process and delivery to the lungs could be explored further, although this is often difficult to achieve satisfactorily given the wide range of variables that are a feature of these powders. The size, shape surface features, variations of forces, non-linear airflow patterns (amongst other variables) make modelling difficult for an ensemble of particles making up an interactive mixture with multimodal distribution. However, idealised particles can readily be used and each one of the factors listed above can be studied independently to enhance knowledge and understanding of how they affect DPI performance.

Finally, a study into the importance of HSB, and the extent to which it is used in DPI manufacture could also be undertaken. As shown in the results, extended HSB may be preventable if it is seen to not improve performance of the final product. A comparison involving low-shear or tumbling blending regimes may be useful in this study.

References

Adi, H., Larson, I., Stewart, P. (2007). Laser diffraction particle sizing of cohesive lactose powders. Powder Technology 179, 90–94.

Adi, S Adi, H., Chan, H-K., Young, P. M., Traini, D., Yang, R., Yu, A. (2008). Scanning White-Light Interferometry as a Novel Technique to Quantify the Surface Roughness of Micron-Sized Particles for Inhalation. Langmuir, 24, 11307-11312

Agnew, J. E. (1984) in Aerosols and the Lung: Clinical and Experimental Aspects (Clarke, S.W. and Pavia, D., eds), pp. 49–70, Butterworths & Co. London, UK

Ahlneck, C. and Zografi, G. (1990) The molecular basis of moisture effects on the physical and chemical stability of drugs in the solid state. International Journal of Pharmaceutics. 62, 87–95.

Alexander, A. W., Shinbrot, T., Johnson, B., Muzzio, F. J. (2004). V-blender segregation patterns for free-flowing materials: effects of blender capacity and fill level. International Journal of Pharmaceutics. 269,1, 19–28.

Alexander, A. W., Muzzio, F. J. (2005). Batch size increase in dry blending and mixing. In Pharmaceutical Process Scale-Up. 2nd edition, Levin, M., (Editor). Dekker, New York. Vol 118, pp 115-132.

Allen, S. (2008). Are inhaled systemic therapies a viable option for the treatment of the elderly patient? Drugs Aging. 25,2, 85-94.

Ashurst, I., Malton, A., Prime, D., Sumby, B., (2000). Latest advances in the development of dry powder inhalers. Pharmaceutical Science & Technology Today. 3,7, 246-256

Atkins, P. (1998). Physical chemistry, 6th ed. New York: WH Freeman.

Baeyens, J., Geldart, D., Wu, S. Y. (1991). Elutriation of fines from gas fluidized beds of Geldart A-type powders - effect of adding superfines. Powder Technology, 71, 71-80

Barber, T. A. (2000). Control of particulate matter contamination in healthcare manufacturing. Interpharm Press. pp487-492

Barry, P. W., O'Callaghan, C. (2003). The influence of inhaler selection on efficacy of asthma therapies. Advanced Drug Delivery Review. 55,7, 879–923.

Bates, D. V., Fish, B. R., Hatch, T. F., Mercer, T. T., Morrow, P. E. (1966). Deposition and retention models for internal dosimetry of the human respiratory tract. Task group on lung dynamics. Health Physics. 12,2, 173–207.

Begat, P., Young, P. M., Edge, S., Kaerger, J. S., Price, R. (2003). The effect of mechanical processing on surface stability of pharmaceutical powders: visualization by atomic force microscopy. Journal of Pharmaceutical Science, 92,3, 611–620.

Begat, P., Morton, D. A., Staniforth, J. N., Price, R. (2004). The cohesive-adhesive balances in dry powder inhaler formulations I: Direct quantification by atomic force microscopy. Pharmaceutical Research. 21,9, 1591–1597.

Begat, P., Morton, D. A., Shur, J., Kippax, P., Staniforth, J. N., Price, R. (2009). The role of force control agents in high-dose dry powder inhaler formulations. Journal of Pharmaceutical Science. 98, 8, 2770-2783

Bentham, A. C., Kwan, C. C., Boerefijn, R., Ghadiri, M. (2004). Fluidsed bed jet milling of pharmaceutical powders. Powder Technology. 141,3, 233-238.

Bérard, V., Lesniewska, E., Andrès, C., Pertuy, D., Laroche, C., Pourcelot, Y. (2002). Dry powder inhaler: influence of humidity on topology and adhesion studied by AFM. International Journal of Pharmaceutics. 232, 213-224.

Boerefjin, R., Ning, Z., Ghadiri, M. (1998). Disintegration of weak agglomerates for inhalation applications. International Journal of Pharmaceutics. 172, 199-209.

Böhme, G., Egey, Z., Krupp, H. (1964). in Overbeek, J.Th.G. (editor.), Chemistry, Physics and Application of Surface Active Substances, Vol. II, Gordon and Breach, New York, 1964, p. 419.

Borgstrom, L., Derom, E., Stahl, E., Wahlin-Boll, E., Pauwels, R. (1996). The inhalation device influences lung deposition and bronchodilating effect of terbutaline. American Journal of Respiratory Critical Care Medicine. 153,5, 1636–1640.

Borgstrom, L., Asking, L., & Lipniunas, P. (2005). An in vivo and in vitro comparison of two powder inhalers following storage at hot/humid conditions. Journal of Aerosol Medicine—Deposition Clearance and Effects in the Lung, 18, 304–310.

Bosquillon, C., Lombry, C., Préat, V., Vanbever, R. (2001a). Influence of formulation excipients and physical characteristics of inhalation dry powders on their aerosolisation performance. Journal of Controlled Release. 70, 329-339.

Bosquillon, C., Lombry, C., Préat, V., Vanbever, R. (2001b). Comparison of particle sizing techniques in the case of inhalation dry powders. Journal of Pharmaceutical Science. 90, 2032-2041.

Braun, M. A., Oschmann, R., Schmidt, P. C. (1996). Influence of excipients and storage humidity on the deposition of disodium cromoglycate (DSCG) in the Twin Impinger. International Journal of Pharmaceutics. 135, 53–62

Bridson, R. H., Robbins, P. T., Chen, Y., Westerman, W., Gillham, C. R., Roche, T. C., Seville, J. P. K. (2007). The effects of high shear blending on α-lactose monohydrate. International Journal of Pharmaceutics. 339, 84–90.

Broadhead, J., Edmond Rouan, S. K., Rhodes, C. T. (1995). Dry powder inhalers: evaluation of testing methodology and effect of inhaler design. Pharmaceutica Acta Helvetiae. 70, 125-131.

Brodka-Pfeiffer, K., Langguth, P., Grab, P., Haüsler, H. (2003). Influence of mechanical activation on the physical stability of salbutamol sulphate. European Journal of Pharmaceutics and Biopharmaceutics. 56, 393–400.

Brone D., and Muzzio, F. J. (2000). Enhanced mixing in a double-cone blender. Powder Technology, 110,3, 179-189.

Brown, H. G., (1986). Adaptation of an HPLC System to Quantify Cholesterol. Journal of the American Oil Chemists' Society, 64, 1, 106-108.

Brown, D. P., Kauppinen, E. I., Jokiniemi, J. K. (2003). Agglomerate deaggregation potential during dry powder inhaler operation and characterization under steady and unsteady conditions. Journal of Aerosol Science, 34, 1417–1428.

Brunauer, S., Deming, L., Deming, W. and Teller, E. (1940). Journal of the American Chemical Society. 62, 1732.

Brunauer, S., Emmett P. H., and Teller, E. (1938). Adsorption of gases in multimolecular layers Journal of the American Chemical Society. 60, 309.

Buckton, G. (1995). Surface characterisation: understanding sources of variability in the production and use of pharmaceuticals, Journal of Pharmaceutics and Pharmacology. 47, 265–275.

Byron, P. R., Patton, J. S. (1994). Drug Delivery via the Respiratory Tract. Journal of Aerosol Medicine. 7,1, 49-75.

Callahan, J., Cleary, G., Elefant, M., Kaplan, G., Kensler, T., Nash, R. (1982). Equilibrium moisture content of pharmaceutical excipients. Drug Developments and Industrial Pharmacy. 8,355–369.

Callen, A., Moghtaderi, B., Galvin, K.P. (2007). Use of parallel inclined plates to control elutriation from a gas fluidized bed. Chemical Engineering Science. 62, 356 – 370

Castellanos, A., Valverde, J. M., Perez, A. T., Ramos, A., and Watson, P. K. (1999). Flow regimes in fine cohesive powders. Physical Review Letters. 82, 1156–1159

Castellanos, A. (2005). The relationship between attractive interparticle forces and bulk behaviour in dry and uncharged fine powders. Advances in Physics. 54, 263–376.

Carroll, N., Cooke, C., James, A. (1997). The distribution of eosinophils and lymphocytes in the large and small airways of asthmatics. European Respiratory Journal. 10, 292-300.

Cegla, U. H. (2004). Pressure and inspiratory flow characteristics of dry powder inhalers. Respiratory Medicine. 98 Supplement A: S22–S28.

Cember, H. (1996). Introduction to Health Physics. McGraw-Hill Professional. pp. 42–43.

Chander, S., Hogg, R., Fuerstenau, D.W. (2007). Characterization of the wetting and dewetting behavior of powders, KONA 25, 56

Chandratilleke, G. R., Zhou, Y. C., Yu, A. B., Bridgwater, J. (2010). Effect of Blade Speed on Granular Flow and Mixing in a Cylindrical Mixer. Industrial and Engineering Chemical Research. 49, 5467–5478

Chang, Y-M., Chou, C-M., Su, K-T., Hung, C-Y., Wu, C-H. (2005). Elutriation characteristics of fine particles from bubbling fluidized bed incineration for sludge cake treatment. Waste Management. 25, 249–263

Chaplin, G., Pugsley, T., Winters, W. (2005). The S-statistic as an early warning of entrainment in a fluidized bed dryer containing pharmaceutical granule. Powder Technology. 149, 148-156

Chawla, A., Taylor, K. M. G, Newton, J. M., Holbrook, P. (1994) Production of spray dried salbutamol sulfate for use in dry powder aerosol formulation. International Journal of Pharmaceutics. 108, 233–240.

Chen, B-Y., Lee, Y-H., Lin, W-C., Lin, F-H., Lin, K-F. (2006). Understanding the characteristics of L-ascorbic acid-montmorillonite nanocomposite: chemical structure and biotoxicity. Biomedical engineering applications, basis & communications. 18, 1, 30-36.

Chen, W., Su, B., Xing, H., Yang, Y., Ren, Q. (2009). Solubilities of cholesterol and desmosterol in binary solvents of n-hexane + ethanol. Fluid Phase Equilibria. 287, 1-6.

Chen, Y., Ding, Y., Papadopoulos, D.G., Ghadiri, M., (2004). Energy-based analysis of milling alpha-lactose monohydrate. Journal of Pharmaceutical Science. 93, 886–895.

Chew, N. Y.K ., Chan, H. K. (2002). The role of particle properties in pharmaceutical powder inhalation formulations. Journal of Aerosol Medicine. 15,3, 325–330.

Chirone, R., Massimilla, L., Russo, S. (1993). Bubble-free fluidization of a cohesive powder in an acoustic field. Chemical Engineering Science, 48,1, 41–52.

Chirone, R., Massimilla, L. (1994). Sound-assisted aeration of beds of cohesive solids. Chemical Engineering Science, 49,8, 1185–1194.

Choi, J-H., Suh, J-M., Chang, I-Y., Shun, D-W., Yi, C-K., Son, J-E., Kim, S-D. (2001). The effect of fine particles on elutriation of coarse particles in a gas fluidized bed. Powder Technology. 121, 190-194

Choi, W. S., Hyun I. K., Kwak, S. S., Chung, H. Y., Chung, H. Y., Yamamoto, K., Oguchi, T., Tozuka, Y., Yonemochi, E., Terada, K. (2004). Amorphous ultrafine particle preparation or improvement of bioavailability of insoluble drugs: grinding characteristics of fine grinding mills. International Journal of Mineral Processes 74, 165–172.

Choudhari, K.B., Jayanthi, S., Murty, R.B., Matharu R.R. (1996). A high-performance liquid chromatographic method for the analysis of lipids from lyophilized formulations. Journal of Chromatography A, 724, 343-347.

Clark, A. R. and Egan, M. (1994). Modelling the deposition of inhaled powder drug aerosols. Journal of Aerosol Science. 25, 175–186.

Clarke, M. J., Peart, J., Cagnani, S., Byron, P. R. (2002) Adhesion of powders for inhalation: an evaluation of drug detachment from surfaces following deposition from aerosol streams. Pharmaceutical Research. 19,3, 322-329.

Cline, D., Dalby, R. (2002). Predicting the quality of powders for inhalation from surface energy and area. Pharmaceutical Research. 19,9, 1274–1277.

Colakyan, M., and Levenspiel, O. (1984). Elutriation from fluidised beds. Powder Technology, 38, 223-232.

Columbano, A., Buckton, G., Wikeley, P. (2002). A study of the crystallisation of amorphous salbutamol sulphate using waster vapour sorption and near infrafed spectroscopy. International Journal of Pharmaceutics. 237, 171-178.

Colombo, P., Catellani, P. L. Massimo, G., Santi, P., Bettini, R., Cocconi, D., Cagnani, S., Ventura, P. (2000). Surface smoothing of lactose particles for dry powder inhalers. In: Dalby, R. N., Byron, P. R., Farr, S. J., Peart, J. (Eds.) Respiratory Drug Delivery VII. Serentec Press, Inc. Raleigh, England. pp 629-631

Concessio, N. M., van Oort, M., Knowles, M. R., Hickey, A. J. (1999). Pharmaceutical dry aerosols: Correlation of powder properties with dose delivery and implications for pharmacodynamic effect. Pharmaceutical Research. 16, 828–834.

Cosgrove, T. (2005). Colloid Science: Principle Methods and Applications. In Electron Microscopy by Sean Davis Chapter 14. Blackwell Publishing, Oxford.

Crooks, M., Ho, R. (1976). Ordered mixing in direct compression of tablets. Powder Technology. 14, 161-167.

Crooks, P. A., Damani, L.A. (1990). Drug application to the respiratory tract: metabolic and pharmacokinetic considerations. Respiratory Drug Delivery I. 1, 61–90.

Crowder, T. M. (2003). A guide to pharmaceutical particulate science. Boca Raton, Florida: Interpharm Press/CRC.

Crowder, T. M. (2004). Vibration technology for active dry-powder inhalers. Pharmaceutical Technology. 28, 52–61.

Crowder, T. M., Hickey, A. J., (2000). The physics of powder flow applied to pharmaceutical solids. Pharmaceutical Technology. 24, 50–58.

Crowder, T. M., Hickey, A. J. (2006). Powder specific active dispersion for generation of pharmaceutical aerosols. International Journal of Pharmaceutics. 327, 65–72.

Crowder, T. M., Louey, M. D., Sethuraman, V. V., Smyth, H. D., Hickey, A. J. (2001). An odyssey in inhaler formulations and design. Pharmaceutical Technology. 25, 99–113.

Czekai, D. A., and Seaman, L. P. (1999). US Patent Number 5,862,999

Danesh, A., Chen, X., Davies, M. C., Roberts, C. J., Sanders, G. H., Tendler, S. J. (2000). Polymorphic discrimination using atomic force microscopy: distinguishing between two polymorphs of the drug cimetidine. Langmuir, 16,2, 866–870.

Daniher, D.I., Zhu, J. (2008). Dry Powder Platform for Pulmonary Drug Delivery. Particuology, 6, 225-238

Danjo, K., Kinoshita, K., Kitagawa, K., Lida, K., Sunada, H., Otsuka, A. (1989). Effect of particle shape on the compaction and flow properties of powders. Chemical and Pharmaceutical Bulletin 37, 3070–3073.

Das, S., Larson, I., Young, P., Stewart, P. (2009). Agglomerate properties and dispersibility changes of salmeterol xinafoate from powders for inhalation after storage at high relative humidity. European Journal of Pharmaceutical Sciences. 37, 442-450.

Davies, C. N. (1961). A formalized anatomy of the human respiratory tract. In: Inhaled Particles and Vapours. C. N. Davies, ed. Pergamon Press, London

de Boer, A. H., Hagedoorn, P., Gjaltema, D., (1997). Design and development of a novel disintegraton principle for the ASTA Medica multi dose dry powder inhaler. European Respiratory Journal. 10, 236.

de Boer, A. H., Gjaltema, D., Hagedoorn, P., Frijlink, H. W. (2002a). Characterization of inhalation aerosols: a critical evaluation of cascade impactor analysis and laser diffraction technique. International Journal of Pharmaceutics. 249, 219-231.

de Boer, A. H., Gjaltema, D., Hagedoorn, P., Schaller, M., Witt, W., Frijlink, H. W. (2002b). Design and application of a new modular adapter for laser diffraction characterization of inhalation aerosols. International Journal of Pharmaceutics. 249:233–245

de Boer, A. H., Hagedoorn, P., Dickhoff, B. H. J., Frijlink, H. W. (2002c). Investigating the relevant parameters for the performance of adhesive mixtures in an air classifier during inhalation. Drug Delivery to the Lungs XIII, London, The Aerosol Society.

de Boer, A. H., Hagedoorn, P., Gjaltema, D., Goede, J., Frijlink, H. W., (2003a). Air classifier technology (ACT) in dry powder inhalation. Part 1. Introduction of a novel force distribution concept (FDC) explaining the performance of a basic air classifier on adhesive mixtures. International Journal of Pharmaceutics. 260: 187–200

de Boer, A. H., Hagedoorn, P., Gjaltema, D., Goede, J., Kussendrager, K., Frijlink, H. W., (2003b). Air classifier technology (ACT) in dry powder inhalation. Part 2. The effect of lactose carrier surface

properties on the de-agglomeration of adhesive mixtures in a basic classifier. International Journal of Pharmaceutics. 260: 201-216

de Boer, A. H., Hagedoorn, P., Gjaltema, D., Lambregts, D., Irngartinger, M., Frijlink, H. W. (2004). The mode of drug particle detachment from carrier crystals in an air classifier-based inhaler. Pharmaceutical Research, 21, 2167-2174.

De Jongh, F.H.C. (1995). Ventilation modelling of the human lung. Thesis, University of Delft, pp27-43.

de Koning, J. P., van der Mark, Th. W., Coenegracht, P. M. J., Tromp, Th. F. J., Frijlink, H. W. (2002). Effect of an external resistance to airflow on the inspiratory flow curve. International Journal of Pharmaceutics. 234,1-2, 257-266.

Deng, T., Paul, K. A., Bradley, M. S. A., Immins, L., Preston, C., Scott, J. F., Welfare, E. H. (2010). Investigations on air induced segregation of pharmaceutical powders and effect of material flow functions, Powder Technology. 203, 2, 354-358

de Villiers, M. M. (1995). Influence of cohesive properties of micronized drug powders on particle size analysis. Journal of Pharmaceutical and Biomedical Analysis. 13,3, 191-198.

Dickhoff, B. H. J., (2006), Ph.D. Thesis: Adhesive mixtures for powder inhalation: The effect of carrier (surface and bulk) properties, carrier payload and mixing conditions on the performance of adhesive mixtures for inhalation. University of Groningen, The Netherlands.

Dickhoff, B. H. J., de Boer A. H., Lambregts, D., Frijlink, H. W. (2006). The effect of carrier surface treatment on drug particle detachment from crystalline carriers in adhesive mixtures for inhalation. International Journal of Pharmaceutics. 327, 17–25.

Dolovich, M. B., Ahrens, R. C., Hess, D. R., Anderson, P., Dhand, R., Rau, J. L., (2005). Device selection and outcomes of aerosol therapy: evidence based guidelines. American College of Chest Physicians/American College of Asthma, Allergy, and Immunology. 127,1, 335–371.

Donovan, M. J., Smyth, H. D. C. (2010). Influence of size and surface roughness of large lactose carrier particles in dry powder inhaler formulations. International Journal of Pharmaceutics. 402, 1-2, 1-9.

Dubois, E. F., Roder, E., Ifle, R. G. (2003). Bronchodilating effects of cumulative doses of formoterol from a novel multi-dose inhaler (Airmix). Respiratory Medicine. 97,1, 71-4

Duddu, S. P., Sisk, S. A., Walter, Y. H., Tarara, T. E., Trimble, K. R., Clark, A. R., Eldon, M. A., Elton, R. C., Pickford, M., Hirst, P. H., Newman S. P., Weers, J. G. (2002). Improved lung delivery from a passive dry powder inhaler using an Engineered PulmoSphere powder. Pharmaceutical Research 19, 689–695.

Dudognon, E., Willart, J. F., Caron, V., Capet, F., Larsson, T., Descamps, M. (2006). Formation of budesonide/α-lactose monohydrate glass solutions by ball-milling. Solid State Communications. 138, 68–71.

Dunbar, C. A., Morgan, B., Van Oort, M., Hickey, A. J. (2000). A comparison of dry powder inhaler dose delivery characteristics using a power criterion. PDA Journal of Pharmaceutical Science Technology. 54,6, 478–484.

Dunbar, C. A., Hickey, A. J., Holzner, P. (1998). Dispersion and characterization of pharmaceutical dry powder aerosols. Kona. 16, 7–44.

Dutta, A., Dullea, L. V. (1991). Effects of external vibration and the addition of fibers on the fludization of a fine powder. Fluidization and Fluid-Particle Systems, Chicago, IL, USA, 87(281), 38–46.

Edwards, A., Murphy, J., Aldous, B., Cheyne, J., Brody, R., Harding, L. (2009). Investigating Blend Relaxation Effects on Lactose Blends Produced Using a High Shear Process. Pfizer Global Research and Development, Sandwich, Kent.

Edwards, D. A., Hanes, J., Caponetti, G., Hrkach, J., Ben-Jebria, A., Eskew, M-L., Mintzes, J., Deaver, D., Lotan, N., Langer R. (1997). Large Porous Particles for Pulmonary Drug Delivery. Science, 276,5320, 1868–1871.

El-Hagrasy, A. S., Morris, H. R., D'Amico, F., Lodder, R. A., Drennen III, J. K. (2001). Near-infrared spectroscopy and imaging for the monitoring of powder blend homogeneity. Journal of Pharmaceutical Science. 90,9, 1298-1307.

El-Hagrasy, A. S., D'Amico, F., Drennen III, J. K. (2006). A Process Analytical Technology Approach to Near-Infrared Process Control of Pharmaceutical Powder Blending. Part I: D-Optimal Design for Characterization of Powder Mixing and Preliminary Spectral Data Evaluation. Journal of Pharmaceutical Sciences. 95,2, 392-406

Ennis, B.J., Litster, J.D. (1997). Principles of size enlargement. In: D. Green and R. Perry, Editors, Perry's Chemical Engineers. Handbook (seventh ed), McGraw Hill, New York (1997)

Ergun, S. (1952). Fluid Flow through Packed Columns. Chemical Engineering Progress. 48, 89-94.

Eve, J. K., Patel, N., Luk, S. Y., Ebbens, S. J., Roberts, C. J. (2002). A study of single drug particle adhesion interactions using atomic force microscopy. International Journal of Pharmaceutics. 238,1–2, 17–27.

Faqih, A. M. N., Mehrotra, A., Hammond, S. V., Muzzio, F. J. (2007). Effect of moisture and magnesium stearate concentration on flow properties of cohesive granular materials. International Journal of Pharmaceutics. 336, 338-345.

Ferron, G.A., Kreyling,W.G. and Haider, B. (1988). Inhalation of salt aerosol particles--II. growth and deposition in the human respiratory tract. Journal of Aerosol Science. 19, 611–631

Fincher, J. (1968). Particle size of drugs and its relationship to absorption and activity. Journal of Pharmaceutical Science. 57,11, 1825-1835.

Finlay, W. H. (2001). The mechanics of inhaled pharmaceutical aerosols. San Diego: Academic Press.

Finot, E., Lesniewska, E., Mutin, J.C., Hosain, S.I., Goudonnet, J.P. (1996). Contact force dependence on relative humidity: investigations using atomic force microscopy. Scanning Microscopy. 10, 697–708.

Fisher, E. S. (2007). Milling of Active Pharmaceutical Ingredients. In, Encyclopedia of Pharmaceutical Technology, Informa Healthcare, USA. pp 2239-2351.

Flament, M-P., Leterme, P., Gayot, A. (2004). The influence of carrier roughness on adhesion, content uniformity and the in vitro deposition of terbutaline sulphate from dry powder inhalers. International Journal of Pharmaceutics. 275, 201-209.

Flament, M-P., Leterme, P., Gayot, A. (2006). The influence of carrier on the performance of Dry Powder Inhalers. International Journal of Pharmaceutics. 334, 35-91

Fournol, A. B., Bergougnou, M. A. and Baker, G. G. J. (1973). Solids Entrainment in a Large Gas Fluidized Bed. Canadian Journal of Chemical Engineering. 51, 401.

Frijlink, H. W., de Boer, A. H., (2004). Dry powder inhalers for pulmonary drug delivery. Expert Opinion on Drug Delivery. 1(1): 67-86

French, D. L., Edwardsd, D. A., Niven, R. W. (1996). The influence of formulation on emission, deaggregation and deposition of dry powders for inhalation. Journal of Aerosol Science. 27(5): 769-783

Fukumori, Y., Fukuda, T., Hanyu, Y., Takeuchi, Y., Osako, Y. (1987). Coating of pharmaceutical powders by fluidized bed process. I. Aqueous enteric coating with methacrylic acid–ethylacrylate copolymer and the dissolution behaviour of products. Chemical and Pharmaceutical Bulletin. 35, 2494–2957

Fults, K. A., Miller, I. F., Hickey, A.J. (1997). Effect of particle morphology on emitted dose of fatty acid-treated disodium cromoglycate powder aerosols. Pharmaceutical Developments and Technology. 2,1, 67–79.

Ganderton, D. (1997). General factors influencing drug delivery to the lung. Respiratory Medicine. 91, Supplement A: 13–16.

Ganderton, D., Kassem, N. M. (1992). Dry powder inhaler. Ganderton. D. (Ed.), Advances in Pharmaceutical Sciences. London, Academic Press: 165-191

Ganesh, M., Narasimharao, C. V., Saravana Kumar A., Kamalakannan, K. Vinoba, M., Mahajan, H. S. Sivakuamar, T. (2009). UV Spectrophotometric Method for the Estimation of Valacyclovir HCl in Tablet Dosage Form. E-Journal of Chemistry. 6, 3, 814-818.

Ganguly, U. P., (1982). Characteristics of Solids from Liquid-Fluidized Bed Systems. Part I. Onset of Elutriation, Canadian Journal of Chemical Engineering. 60(4): 466

Ganguly, U. P., (1993). Prediction of Polydispersed Fluidized Bed System Properties: A New Approach, American Institute of Chemical Engineering Journal. 39(11): 1777-1782

Garcia, T. P., Wilkinson, S. J, Scott, J. F. (2001). The development of a blend sampling technique to assess the uniformity of a powder mixture. Drug Development and Industrial Pharmacy. 27,4, 297-307

Gebhart, J., Heyder, J. and Stahlhofen,W. (1981). Use of aerosols to estimate pulmonary air-space dimensions. Journal of Applied Physiology. 51, 465–476.

Geldart, D. (1973). Types of gas fluidisation. Powder Technology. 7, 285

Geldart, D. (1986). Particle Entrainment and Carryover in Gas Fluidization Technology edited by Geldart, D. pp. 123-154, John Wiley, New York.

Giraud, V., Roche, N. (2002). Misuse of corticosteroid metered-dose inhaler is associated with decreased asthma stability. European Respiratory Journal. 19,2, 246–251.

Giry, K., Péan, J.M., Giraud, L., Marsas, S., Rolland, H., Wüthrich, P. (2006). Drug/lactose co-micronization by jet milling to improve aerosolization properties of a powder for inhalation. International Journal of Pharmaceutics. 321. pp. 162–166.

Godard, K., Richardson, J. F. (1969). The use of slow speed stirring to initiate particulate fluidization. Chemical Engineering Science, 24, 194–195.

Gonda, I., (1990). Aerosols for delivery of therapeutic and diagnostic agents to the respiratory tract, Critical Review in Therapeutic Drug Carrier Systems. 6: 273

Gonda, I. (2006). Systemic delivery of drugs to humans via inhalation. Journal of Aerosol Medicine. 19,1, 47-53.

Greenspan, L. (1977). Journal of Research of the National Bureau of Standards-A, vol. 81A (1), 89-96.

Grimsey, I. M., Feeley, J. C., York, P. (2002). Analysis of the surface energy of pharmaceutical powders by inverse gas chromatography. Journal of Pharmaceutical Science. 91,2, 571–583.

Grossman, J. (1954). The evolution of inhaler technology. Journal of Asthma. 31,1, 55-64

Guenette, E., Barrett, A., Kraus, D., Brody, R., Harding, L., Magee, G. (2009). Understanding the effect of lactose particle size on the properties of DPI formulations using experimental design. International Journal of Pharmaceutics. 380, 80-88

Gugnoni, R. J., Zenz, F. A. (1980). Particle Entrainment from Bubbling Fluidized Beds in Fluidization III edited by Grace, J. R. and Matsen, J. M. pp. 501-508.

Gupta, M. K., Vanwert, A., Bogner, R. H. (2003). Formation of physically stable amorphous drugs by milling with neuslin. Journal of Pharmaceutical Sciences. 92,3, 536-551

Hahn, I., Scherer, P. W. and Mozell, M. M. (1993). Velocity profiles measured for airflow through a large-scale model of the human nasal cavity. Journal of Applied Physiology. 75, 2273–2287

Hailey, P. A., Doherty, P., Tapsell, P., Oliver, T., Aldridge, P. K. (1996). Automated system for the on-line monitoring of powder blending processes using near-infrared spectroscopy Part I. System development and control. Journal of Pharmaceutical and Biomedical Analysis. 14, 551-559.

Hancock, B. C., Shamblin, S. L., Zografi, G. (1995). Molecular mobility of amorphous pharmaceutical solids below their glass transition temperatures. Pharmaceutical Research. 12, 799–806.

Hancock, B. C., Zografi, G. (1997). Characteristics and significance of the amorphous state in pharmaceutical systems. Journal of Pharmaceutical Science. 86, 1–12.

Harjunen, P., Lehto, V., Martimo, K., Suihko, E., Lankinen, T., Paronen, P., Jarvinen, K. (2002). Lactose modifications enhance its drug performance in the novel multiple dose Taifun ® DPI. International Journal of Pharmaceutics. 263(1-2) 151-163.

Harjunen, P., Lankinen, T., Salonen, H., Lehto, V-P., Jarvinen, K. (2003). Effects of carriers and storage of formulation on the lung deposition of a hydrophobic and hydrophillic drug fro a DPI. International Journal of Pharmaceutics. 263(1-2), 151-163

Harris, D. (2007). Testing Inhalers. Pharmaceutical Technology Europe. 29-35

Hartge, E-U., Werther, J. (2003). Elutriation and Entrainment. In Yang, W-C., Handbook of Fluidization and Fluid-Particle Systems. Taylor and Francis Group Publishing LLC.

Heath, T. D., and Aconsky, L. (1963). Fluidized Bed Classifier. U.S. Patent 3,102,092 (Aug. 27, 1963).

Hegedüs, H., Gergely, A., Veress, T., Horváth, P. (1999). Novel derivatization with Sanger's reagent (2,4-dinitrofluorobenzene [DNFB]) and related methodological developments for improved detection of amphetamine enantiomers by circular dichroism spectroscopy. Analysis, 27, 458-463

Hein, S., Picker-Freyer, K.M., Langridge, J. (2008). Simulation of roller compaction with subsequent tableting and characterisation of lactose and microcrystalline cellulose. Pharmaceutical Developments and Technology. 13, 523-532.

Heng, P. W., Chan, L. W., Lim, L. T. (2000). Quantification of the surface morphologies of lactose carriers and their effect on the in vitro deposition of salbutamol sulphate. Chemical and Pharmaceutical Bulletin. 48,3, 393-8

Heng, D., Tang, P., Cairney, J. M., Chan, H., Cutler, D. J., Salama, R. (2007). Focused-ion-beam milling: A novel approach to probing the interior of particles used for inhalation aerosols. Pharmaceutical Research, 24,9, 1608–1617.

Hennart, S. L. A., Domingues, M. C., Wildeboer, W. J., van Hee, P., Meesters, G. M. H. (2010). Study of the process of stirred ball milling of poorly water soluble organic products using factorial design. Powder Technology. 198, 56-60

Hersey, J. A., (1975). Ordered mixing: A new concept in powder mixing practice. Powder Technology. 11: 41-44

Hickey, A. J., Martonen, T. B. (1993). Behaviour of hygroscopic pharmaceutical aerosols and the influence of hydrophobic additives. Pharmaceutical Research. 10,1, 1-7.

Hickey, A. J., Concessio, N. M., Van Oort, M. M., Platz, R. M., (1994). Factors influencing the dispersion of dry powders as aerosols. Pharmaceutical Technology. 18, 58-64

Hinds, W. C. (1999). Aerosol technology: properties, behaviour, and measurement of airborne particles, 2nd ed. New York: Wiley.

Hindle, M., Byron, P. R. (1995). Dose emissions from marketed dry powder inhalers. International Journal of Pharmaceutics. 116, 169-177.

Hoornaert, F., Wauters, P.A.L., Meesters, G.M.H., Pratsinis, S. E., Scarlett, B. (1998) Agglomeration behaviour of powders in a Lodige mixer granulator. Powder Technology. 96, 2, 116-128

Hooton, J. C., German, C. S., Allen, S., Davies, M.C., Roberts, C. J., Tendler, S. J., Williams P. (2003). Characterization of particle-interactions by atomic force microscopy: effect of contact area. Pharmaceutical Research. 20,3, 508–514.

Hou, H., Sun, C. (2008). Quantifying Effects of Particulate Properties on Powder Flow Properties Using a Ring Shear Tester. Journal of Pharmaceutical Sciences, 97,9, 4030-4039.

Hoving, B. (1995). Chromatographic methods in the analysis of cholesterol and related lipids. Journal of Chromatography B, 671, 341-362.

Hristov, J. (2000). The fluidization in a magnetic field is more than 40 years old: It is time to strike the balance in front of the new century. Lavoisier Technique, Paris, 14(75), 251–260.

Hu, G., Otaki, H., Watanuki, K. (2001). Optimization of grinding performance of tumbling ball mill. International Journal Series C-Mechanical Systems Machine Elements and Manufacturing. 44, 267–274

Hu, J., Johnston, K. P., Williams Iii, R. O. (2004). Nanoparticle engineering process for enhancing the dissolution rates of poorly water soluble drugs. Drug Development and Industrial Pharmacy. 30,3, 233-245.

Iida, K., Okomato, H., Hayakawa, Y., Danjo, K., Leuenberger, H., (2001). Evaluation of flow properties of dry powder inhalation of salbutamol sulphate with lactose carrier. Chemical and Pharmaceutical Bulletin. 49,10, 1326-1330.

Iida, K., Hayakawa, Y., Danjo, K., Leuenberger, H., (2003). Preparation of dry powder inhalation by surface treatment of lactose carrier particles. Chemical and Pharmaceutical Bulletin. 51, 1, 1–5.

Ikegami, K., Kawashima, Y., Takeuchi, H., Yamamoto, H., Momose, D-I., Saito, N., Isshki, N. (2000). In vitro inhalation behaviour of spherically agglomerated steroid particles with carrier lactose. Advanced Powder Technology. 11,3, 323-332.

Ikegami, K., Kawashima, Y., Takeuchi, H., Yamamoto, H., Isshki, N., Momose, D-I., Ouchi, K. (2003). Simultaneous particulate design of primary and agglomerated crystals of steroid by spherical agglomeration in liquid for dry powder inhalation. Powder Technology. 130, 290-297.

Islam, N., Stewart, P., Larson, I., Hartley, P. (2004). Lactose surface modification decantation: are drug-fine lactose ratios the key to better dispersion of salmeterol xinafoate from lactose-interactive mixture? Pharmaceutical Research 21, 492-499.

Israelachvili, J. N. (1991). Intermolecular and surface forces, 2nd ed. London: Academic Press.

Jackson, C. and Lipworth, B. (1995). Optimizing inhaled drug delivery in patients with asthma. British Journal of General Practice 45, 683–687

Jaraiz, E., Kimura, S., Levenspiel, O. 1992. Vibrating beds of fine particles: estimation of interparticle forces from expansion and pressure drop experiments. Powder Technology. 72, 23-30.

Jashnani, R. N., Byron, P. R. (1996). Dry powder aerosol generation in different environments: performance comparisons of albuterol, albuterol sulfate, albuterol adipate and albuterol stearate. International Journal of Pharmaceutics. 130, 13-24.

Jenike, A.W. (1964). "Storage and Flow of Solids" in Utah Engineering Experiment Station Bulletin 123, 16th ed., (University of Utah, Salt Lake City).

Jones, T. M., Pilpel, N. (1965). Some physical properties of lactose and magnesia. Journal of Pharmaceutics and Pharmacology. 17: 440-448

Jones, M.D., Hooton, J. C., Dawson, M. L., Ferrie, A. R., Price, R. (2008). An investigation into the dispersion mechanisms of ternary dry powder inhaler formulations by the quantification of interparticle forces. Pharmaceutical Research. 25, 2, 337-348

Jones, M. D., Santo, J. G. F., Yakub, B., Dennison, M., Master, H., Buckton, G. (2010). The relationship between drug concentration, mixing time, blending order, and ternary dry powder inhalation performance. International Journal of Pharmaceutics. 391, 1-2, 137-147.

Kanig, J. L., Lachman, L., Lieberman, H., A. (1986). The Theory and Practice of Industrial Pharmacy (3 ed.). Philadelphia: Lea & Febiger

Karhu, M., Kuikka, J., Kauppinen, T., Bergstrom, K., Vidgren, M. (2000). Pulmonary deposition of lactose carriers used in inhalation powders. International Journal of Pharmaceutics. 196(1): 95-103

Kassem, N. M., and Ganderton, D. (1990). The influence of carrier surface on the characteristics of inspiratory powder aerosols. Journal of Pharmaceutics and Pharmacology. 42, 11.

Kawashima Y., Serigano, T., Hino, T., Yamamoto, H., Takeuchi, H. (1998a). Effect of surface morphology of carrier lactose on dry powder inhalation property of pranlukast hydrate. International Journal of Pharmaceutics. 172, 179-188.

Kawashima, Y., Serigano, T., Hino, T. (1998b) Design of inhalation dry powder of pranlukast hydrate to improve dispersibility by the surface modification with light anhydrous silicic acid (AEROSIL 200). International Journal of Pharmaceutics. 173, 243–251.

Kim, C. S., Fisher, D. M., Lutz, D. J., Gerrity, T. R. (1994). Particle deposition in bifurcating airway models with varying airway geometry. Journal of Aerosol Science. 25, 567–581

Kim, S. W., Namkung, W., Kim, S. D. (1999). Solids flow characteristics in loop-seal of a circulating fluidized bed. Korean Journal of Chemical Engineering. 16,1 82-88

Kinnarinen, T., Jarhoa, P., Järvinen, K., Järvinen, J. (2003). P ulmonary deposition of a budesonide/γ -cyclodextrin complex in vitro. Journal of Controlled Release. 90, 197-205

Kleiner O, Ramesh J, Huleihel M, Cohen B, Kantarovich K, Levi C, Polyak B, Marks R. S, Mordehai J, Cohen Z, Mordechai S. (2002). A comparative study of gallstones from children and adults using FTIR spectroscopy and fluorescence microscopy. BMC Gastroenterology.2, 3

Knight, P. C. (1993). An investigation into the kinetics of granulation using a high shear mixer. Powder Technology. 77, 159-169

Kraemer, J., Svensson, J. R., Melgaard, H. (1995). Sampling bias in blending validation and a different approach to homogeneity assessment. Drug Development and Industrial Pharmacy. 25,2, 217-222.

Krishna, M. T., Springall, D. R., Meng, Q-H., Withers, N. J., Macleod, D. P., Frew, A.J. , Polak, J. M., Holgate, S. T. (1997). Effects of ozone on epithelium and sensory nerves in the bronchial mucosa of healthy humans. American Journal of Respiratory Critical Care Medicine. 156, 943-950.

Kumon, M., Suzuki, M., Kusai, A., Yonemochi, E., Terada, K. (2006). Novel approach to DPI carrier lactose with mechanofusion process with additives and evaluation by IGC. Chemical and Pharmaceutical Bulletin. 54, 1508–1514.

Kunii, D., and Levenspiel, O. (1991). Fluidization Engineering, 2ed, Butterworth, Boston.

Kwakye, J. K. (1997). Development of a UV spectrophotometric method of assay of ascorbic acid (vitamin C) in pharmaceutical formulations. West African Journal of Pharmacology 11, 2, 65–75.

Kwakye, J. K. (2000). The use of stabilizers in the UV assay of ascorbic acid. Talanta 51, 197-200.

Kwok, P. C. L., Chan, H. K. (2007). Effect of relative humidity on the electrostatic charge properties of dry powder inhaler aerosols. Pharmaceutical Research. 25,2, 277-288

Labiris, N. R., Dolovich, M. B. (2003) Pulmonary drug delivery. Part I: physiological factors affecting therapeutic effectiveness of aerosolized medications. British Journal of Clinical Pharmacology. 56,6, 588–599.

Lachman, L., Lieberman, H.A., Kanig, J.L. (1976). The Theory and Practice of Industrial Pharmacy, Second edition, Henry Kimpton, London.

Lai, F., Hersey, J., Staniforth, J. (1981). Segregation and mixing of fine particles in an ordered mixture, Powder Technology. 28, 17–23.

Larhrib, H., Zeng, X. M., Martin, G. P., Marriott, C., Pritchard, J., (1999). The use of different grades of lactose as a carrier for aerosolised salbutamol sulphate. International Journal of Pharmaceutics. 191,1, 1-14.

Larhrib, H, Martin, G. P., Marriott, C., Prime, D. (2003a). The influence of carrier and drug morphology on drug delivery from dry powder formulations. International Journal of Pharmaceutics. 257, 283-296

Larhrib, H., Martin, G. P., Prime, D., Marriott, C. (2003b). Characterisation and deposition studies of engineered lactose crystals with potential for use as a carrier for aerosolised salbutamol sulphate from dry powder inhalers. European Journal of Pharmaceutical Science. 19: 211-221

Lazghab, M., Saleh, K., Pezron, I., Guigon, P., Komunjer, L. (2005). Wettability assessment of finely divided solids, Powder Technology. 157, 79

Leach, C. (1998). Improved delivery of inhaled steroids to the large and small airways. Respiratory Medicine. 92, 3

Leva, M. (1951). Elutriation of Fines from Fluidized Systems. Chemical Engineering Progress. 47,1, 39

Levy, E. K., and Celeste, B. (2006). Combined effects of mechanical and acoustic vibrations on fluidization of cohesive powders. Powder Technology. 163, 41-50.

Li, J., and Kato, K. (2001). Effect of electrostatic and capillary forces on the elutriation of fine particles from a fluidized bed. Advanced Powder Technology. 12,2, 287-205.

Li, J., Nakazato, T., Kato, K. (2004). Effect of cohesive powders on the elutriation of particles from a fluid bed. Chemical Engineering Science. 59: 2777 – 2782

Liew, C. V., Karande, A. D., Heng, P. W. S. (2010). In-line quantification of drug and excipients in cohesive powder blends by near-infrared spectroscopy. International Journal of Pharmaceutics. 386, 138-148.

Litster, J. D., Hapgood, K. P., Michaels, A. N., Sims, A., Roberts, M., Kameneni, S. K. (2002). Scale-up of mixer granulators for effective liquid distribution. Powder Technology. 124, 3, 272-280.

Liu, Y. A., Hamby, R. K., Colberg, R. D. (1991). Fundamental and practical developments of magnetofluidized beds - A review. Powder Technology, 64,1–2, 3–41.

Louey, M. D., Mulvaney, P., Stewart, P. J., (2001). Characterisation of adhesional properties of lactose carriers using atomic force microscopy. Journal of Pharmaceutics and Biomedical Analysis. 25(3-4): 559-67

Louey, M. D., Stewart, P. J. (2002). Particle interactions involved in aerosol dispersion of ternary interactive mixtures. Pharmaceutical Research. 19,10, 1524–1531.

Louey, M. D., Razia, S., Stewart, P. J., (2003). Influence of physico-chemical carrier properties on the in vitro aerosol deposition from interactive mixtures. International Journal of Pharmaceutics. 252(1-2): 87-98

Lucas, P., Anderson, K., Staniforth, J.N., (1998). Protein deposition from dry powder inhalers: fine particle multiplets as performance modifiers. Pharmaceutical Research. 15, 562–569.

Ma, X., and Kato, K., (1997). Effect of interparticle adhesion forces on elutriation of fine powders from a fluidized bed of a binary particle mixture. Powder Technology. 95: 93-101

Ma, X., Honda, Y., Nakagawa, N., Kato, K. (1996). Elutriation of fine powders from a fluidized bed of a binary particle-mixture. Journal of Chemical Engineering of Japan, 29,2, 330–335.

Mackin, L., Sartnurak, S., Thomas, I., Moore, S., (2002). The impact of low levels of amorphous material (<5%) on the blending characteristics of a direct compression formulation. International Journal of Pharmaceutics. 231, 213–226.

Maggi, L., Bruni, R., Conte, U. (1999). Influence of the moisture on the performance of a new dry powder inhaler. International Journal of Pharmaceutics. 177,1, 83–91.

Mahmoud, E. H., Nakazato, T., Nakajima, S., Nakagawa, N., Kato, K. (2004). Separation rate of fine powders from a circulating powder-particle fluidized bed (CPPFB). Powder Technology. 146, 46-55.

Malcolmson, R. J., and Embleton, J. K. (1998). Dry powder formulations for pulmonary delivery. Pharmaceutical Science & Technology Today. 1, 9, 394-398

Makkawi, Y. T., Wright, P. C., The voidage function and effective drag force for fluidized beds. Chemical Engineering Science 58, 2035 – 2051

Marple, V. A., Rubow, K. L., Olson, B. A. (2001). Inertial, gravitational, centrifugal, and thermal collection techniques. In: Baron, P. A., Willeke, K. editors. Aerosol measurement: principles, techniques and applications. New York: Wiley Interscience; pp 229–260.

Marple, V. A., Olson, B. A., Santhanakrishnan, K., Roberts, D. L., Mitchell, J. P., Hudson-Curtis, B. L. (2004). Next generation pharmaceutical impactor: a new impactor for pharmaceutical inhaler testing. Part III: Extension of archival calibration to 15 L/min. Journal of Aerosol Medicine. 17,4, 335–343.

Marriott, C., MacRitchie, H. B., Zeng, X-M., Martin, G. P., (2006). Development of a laser diffraction method for the determination of the particle size of aerosolised powder formulations. International Journal of Pharmaceutics. 326: 39-4

Martonen, T. B. and Katz, I. (1993). Deposition patterns of aerosolized drugs within human lungs: effects of ventilatory parameters. Pharmaceutical Research. 10, 871–878.

Mawatari, Y., Koide, T., Tatemoto, Y., Takeshita, T., Noda K. (2000). Comparison of Three Vibrational Modes (Twist, Vertical And Horizontal) For Fluidization Of Fine Particles. Advanced Powder Technology. 12,2, 157–168

Mawatari, Y., Tatemoto, Y., Noda, K. (2003). Prediction of minimum fluidization velocity for vibrated fluidized bed. Powder Technology. 131, 66–70.

Mazalli, M. R., Sawaya A. C. H. F., Eberlin M. N., and Bragagnolo N. (2006). HPLC Method for Quantification and Characterization of Cholesterol and Its Oxidation Products in Eggs. Lipids, 41, 6, 615-622.

Melveger, A. J., Huynh-Ba, K. (2008). Critical Regualtory Requirements for a Stability Program. In: Handbook of Stability Testing in Pharmaceutical Development: Regulations, Methodologies and Best Practices. Hyunh-Ba, K (Editor). Springer, pp 9-16.

Merisko-Liversidge, E., Liversidge, G. G., Cooper, E. R. (2003). Nanosizing: a formulation approach for poorly-water-soluble compounds. European Journal of Pharmaceutical Sciences. 18, 113-120.

Merkus, H. G. (2009). Particle Size Measurements. Springer, The Netherlands. 259-285

Mitchell, J. P., Nagel, M. W. (2003). Cascade impactors for the size characterization of aerosols from medical inhalers: their uses and limitations. Journal of Aerosol Medicine. 16,4, 341–377.

Montz, K. W., Beddow, J. K., Butler, P. B. (1988). Adhesion and removal of particulate contaminants in a high-decibel acoustic field. Powder Technology, 55,2, 133–140.

Mori, S., Yamamoto, A., Iwata, S., Haruta, T., Yamada, I., Mizutani, E. (1990). Vibro-fluidization of group-C particles and its industrial applications. Advances in Fluidization Engineering, San Francisco, CA, USA, 86,276, 88–94.

Morse, R. D. (1955). Sonic energy in granular solid fluidization. Industrial and Engineering Chemistry, 47(6), 1170–1175.

Moulton, B., Zaworotko, M. J. (2001). From molecules to crystal engineering: supramolecular isomerism and polymorphism in network solids. Chemical Review. 101,6, 1629–1658.

Mullarney, M. P., Leyva, N. (2009). Modelling Pharmaceutical Powder-Flow Performance Using Particle-Size Distribution Data. Pharmaceutical Technology. 33,3, 126-134

Müller, R. H., Krause, K., Mäder, K. (2000). Method for controlled production of ultrafine microparticles and nanoparticles. PCT Patent Application 2001/03670 A1 July 10, 2000

Müller, R. H., Jacobs, C., Kayser, O. (2001). Nanosuspensions as particulate drug formulation in therapy rational for development and what we can expect for the future. Advanced Drug Delivery Reviews. 47, 3-19.

Murnane, D., Marriott, C., Martin, G.P. (2008). Comparison of salmeterol xinafoate microparticle production by conventional and novel antisolvent crystallization. European Journal of Pharmaceutics and Biopharmaceutics. 69, 94–105.

Muzzio, F. J., Alexander, A. W. (2005). Scale up of powder blending operations. Pharmaceutical Technology Supplement. 34-42.

Naini, V., Byron, P. R., Phillips, E. M. (1998). Physicochemical stability of crystalline sugars and their spray-dried forms: Dependence on relative humidity and suitability for use in powder inhalers. Drug Development and Industrial Pharmacy. 24, 895-909.

Nakach, M., Authelin, J-R., Chamayou, A., Dodds, J. (2004). Comparison of various milling technologies for grinding pharmaceutical powders. International Journal of Mineral Processing. 74,1, S173-S181.

Newman, S.P., Clarke, S.W. (1983). Therapeutic aerosols. I. Physical and practical considerations. Thorax 38, 881–886.

Newman, S. P., Clarke, S. W. (1993). Bronchodilator delivery from Gentlehaler, a new low-velocity pressurized aerosol inhaler. Chest. 103,5, 1442–1446.

Newman, S., Hollingworth, A., Clark, A. (1994). Effect of different modes of inhalation on drug delivery from a dry powder inhaler. International Journal of Pharmaceutics. 102,1, 127-132.

Nezzal, A., Large, J. F., Guigon, P. (1998). Fluidisation behaviour of very cohesive powders under mechanical agitation. In Fluidization VIII, Proceedings of the Eighth Engineering Foundation Conference on Fluidization (pp. 77–82), May 14–19. American Institute of Chemical Engineering

Ng, W. H., Kwek, J. W., Tan, R. B. H. (2007). Anomalous particle size shift during post-milling storage. Pharmaceutical Research. 25,5, 1175-1185

Ng, B. H., Kwan, C. C., Ding, Y. L., Ghadiri, M., Fan, X. F., Parker, D. J. (2008). Granular Flow Fields in Vertical High Shear Mixer Granulators. AIChE Journal. 54, 2, 415-426

Nguyen, T. T., Rambanapasi, C., de Boer, A. H., Frijlink, H. W., v.D. Ven, P. M., de Vries, J., Busscher, H. J., v.D. Voort Maarschalk, K. (2010). A centrifuge method to measure particle cohesion forces to substrate surfaces: The use of a force distribution concept for data interpretation. International Journal of Pharmaceutics, 393,1-2, 89-96

Niven, R.W., Lott, F. D., Ip, A. Y., Cribbs, J. M. (1994).Pulmonary delivery of powders and solutions containing recombinant human granulocyte colony-stimulating factor (rhG-CSF) to the rabbit. Pharmaceutical Research. 11(8):1101–1109.

Norwood, D. L., Prime, D., Downey, B. P., Creasey, J., Sethi, S. K., Haywood, P. (1995). Analysis of polycyclic aromatic hydrocarbons in metered dose inhaler drug formulations by isotope dilution gas chromatography / mass spectrometry. Journal of Pharmaceutics and Biomedical Analysis. 13,3, 293–304.

Nowak,W., Hasatani, M., Derczynski, M. (1993). Fluidization and heat transfer of fine particles in an acoustic field. AIChE Symposium Series, 89,296, 137–149.

O'Connor B.J. (2004). The ideal inhaler: design and characteristics to improve outcomes. Respiratory Medicine. 98, Supplement A:S10–S16.

Ohta, M., Buckton, G. (2004). Determination of the changes in surface energetics of cefditoren pivoxil as a consequence of processing induced disorder and equilibration to different relative humidities. International Journal of Pharmaceutics. 269,1, 81–88.

Ógáin, O. N., Li, J., Tajber, L., Corrigan, O. I., Healy, A. M. (2011). International Journal of Pharmaceutics. 405, 1-2, 23-35.

Paradkar, M.M. and Irudayaraj, J., (2002). Determination of cholesterol in dairy products using infrared techniques: 1. FTIR spectroscopy. International Journal of Dairy Technology. 55, 3. 127-132

Park, A-H., Bi, H., Grace, J., (2002). Reduction of electrostatic charges in gas–solid fluidized beds. Chemical Engineering Science. 57: 153-162

Patton, J. S. (2000). Pulmonary delivery of drugs for bone disorders. Advanced Drug Delivery Review. 42,3, 239–248.

Patton, J. S., Bukar, J., Nagarajan, S. (1999). Inhaled Insulin. Advanced Drug Delivery Review. 35,2-3, 235-247.

Pell, M. (1990). Gas Fluidization in Handbook of Powder Technology. Elsevier Science Publishers, Amsterdam. pp 15, 21-31, 65-73.

Pell, M., Dunson, J. B. (1999). Gas-solid operations and equipment. In: Green, D. W., editor. Perry's chemical engineers' handbook. New York: McGraw-Hill.

Pemberton, S. T., and Davidson, J. F. (1986). Elutriation from Fluidized Beds–II. Disengagement of Particles from Gas in the Freeboard. Chemical Engineering Science. 41, 253

Perry, R. H., and Green, D. (1997). Perry's Chemical Engineers' Handbook (7th Edition). McGraw Hill, USA.

Pilcer, G., Amighi, K. (2010). Formulation strategy and use of excipients in pulmonary drug delivery. International Journal of Pharmaceutics. 392, 1-19.

Pikal, M. J., Lukes, A. L., Lang, J. E. (1977). Thermal Decomposition of amorphous β-lactam antibacterials. Journal of Pharmaceutical Science. 66,9, 1312–1316

Pitchayajittipong, C., Price, R., Shur, J. Kaerger, J. S., Edge, S. (2010). Characterisation and functionality of inhalation anhydrous lactose. International Journal of Pharmaceutics. 390, 134-141

Plank, R., Diehl, B., Grinstead, H., Zega, J. (2002). Quantifying liquid coverage and powder flux in high-shear granulators. Powder Technology. 134, 3, 223-234.

Podczeck, F., (1996a). Optimization of the operation conditions of an Andersen-Cascade impactor and the relationship to centrifugal adhesion measurements to aid the development of dry powder inhalations. International Journal of Pharmaceutics. 149: 51-61

Podczeck, F., (1996b). Assessment of the mode of adherence on the deformation characteristics of micronized particles adhering to various surfaces. International Journal of Pharmaceutics. 145: 65-76

Podczeck, F. (1997). The relationship between physical properties of lactose monohydrate and the aerodynamic behaviour of adhered drug particles. International Journal of Pharmaceutics. 160, 119–130

Podczeck, F. (1998a). The relationship between physical properties of lactose monohydrate and the aerodynamics behaviour of adhered drug particles. International Journal of Pharmaceutics. 160, 119-130.

Podczeck, F., (1998b). Adhesion forces in interactive powder mixtures of micronized drug and carrier particles of various particle size distributions. Journal of Adhesion Science and Technology. 12(12): 1323-1339

Podczeck, F. (1999). The influence of particle size distribution and surface rougness of carrier particles on the in vitro properties of dry powder inhalations. Aerosol Science Technology. 31, 301-321.

Podczeck, F., and Newton, J.M. (1995). The development of an ultracentrifuge technique to determine the adhesion and friction properties between particles and surfaces. Journal of Pharmaceutical Sciences. 84, 1067–1071.

Podczeck, F., Newton, J. M., James, M. B., (1995). Adhesion and friction between powders and polymer or aluminium surfaces determined by a centrifuge technique. Powder Technology. 83, 201-209.

Podczeck, F., Newton, J. M., James, M. B., (1996). The influence of constant and changing relative humidity of the air on the autoadhesion force between pharmaceutical powder particles. International Journal of Pharmaceutics. 145: 221-229

Podczeck, F., Newton, J. M., James, M. B., (1997). Variations in the adhesion force between a drug and carrier particles as a result of changes in the relative humidity of the air. International Journal of Pharmaceutics. 149: 151-160

Popo, M., Romero-Torres, S., Conde, C., Romañach, R. J. (2002). Blend Uniformity Analysis Using Stream Sampling and Near Infrared Spectroscopy. AAPS PharmSciTech. 3(3) article 24.

Popov, K. I., Pavlovic, M. G., Pavlovic, L. J., Ivanovic, E. R., Krstic, S. B., Obradovic, M. C. (2003). The effect of the particle shape and structure on the flowability of electrolytic copper powder II. The experimental verification of the model of the representative powder particle. Journal of the Serbian Chemical Society. 68 779–783.

Price, R., Young, P. M., Edge, S., Staniforth, J. N. (2002). The influence of relative humidity on particluate interactions in carrier-based dry powder inhaler formulations. International Journal of Pharmaceutics. 246: 47-59

Price, R., Young, P. M. (2004). Visualization of the crystallization of lactose from the amorphous state. Journal of Pharmaceutical Science. 93,1, 155–164.

Rao, A., Curtis, J. S., Hancock, B. C., Wassgren, C. (2010). The effect of column diameter and bed height on minimum fluidisation velocity. American Institute of Chemical Engineers' Journal. 56, 2304-2311.

Räsänen, E., Antikainen, O., Yliruusi, J. (2003). A new method to predict flowability using a microscale fluid bed. AAPS Pharmaceutical Science and Technology. 4,4, 418-424.

Reed, T. M., Fenske, M. R. (1955). Effect of agitation on gas fluidization of solids. Industrial and Engineering Chemistry, 47,2, 275–282.

Richardson, J. F. (1971). Incipient Fluidization and Particulate Systems. In: Davidson, J. F. and Harrison, D., Eds., Academic Press London

Rodriguez-Hornedo, N., Sinclair, B. D. (2002). Crystallization: significance in product development, processing, and performance. In: Swarbrick, J., Boylan, J. C., editors. Encyclopedia of pharmaceutical technology. New York: Dekker.

Rogers, T. L., Johnston, K. P., Williams III, R. O. (2001). Solution-based particle formation of pharmaceutical powders by supercritical or compressed fluid CO2 and cryogenic spray-freezing technologies. Drug Development and Industrial Pharmacy. 27,10, 1003-1015.

Roth, Y., Chapnik, J. S., Cole, P. (2003). Feasibility of aerosol vaccination in humans. Annals of Otology, Rhinology and Laryngology. 112,3, 264–270.

Russo, P., Chirone, R., Massimilla, L., Russo, S. (1995). The influence of the frequency of acoustic waves on sound-assisted fluidization of beds of fine particles. Powder Technology, 82,3, 219–230.

Saint-Lorant, G., Leterme, P., Gayot, A., Flament, M. P. (2007). Influence of carrier on the performance of dry powder inhalers. International Journal of Pharmaceutics. 334, 85-91.

Saleh, K., Cami, X. B., Thomas, A., Guigon, P. (2006). An Experimental Study on the Fluidisation Behaviour of Geldart C Class Powders. KONA, 24, 134-145

Saleki-Gerhard, A., Ahlneck, C., and Zografi, G. (1994). Assessment of disorder in crystalline solids. International Journal of Pharmaceutics. 101, 237.

Santana, D., Rodriguez, J.M., Macıas-Machın, A., (1999). Modelling fluidised bed elutriation of fine particles. Powder Technology. 106, 110-118

Sarkari, M., Brown, J. N., Chen, X., Swinnea, S., Williams III, R. O., Johnston, K. P. (2002). Enhanced drug dissolution using evaporative precipitation into aqueous solution. International Journal of Pharmaceutics. 243, 17-31.

Saxena, S.C. and Jadav, S. (1983). A two-dimensional gas fluidized bed for hydrodynamic and elutriation studies, Powder Technology. 36, 61–70.

Schiavone, H., Palakodaty, S., Clark, A., York, P., Tzannis, S. T. (2004). Evaluation of SCF-engineered particle-based lactose blends in passive dry powder inhalers. International Journal of Pharmaceutics. 281,102, 55–66.

Schiewe, J., Zierenberg, B. (2004). How easy is powder de-agglomeration? A critical assessment of particle interaction techniques. In: Respiratory Drug Delivery IX. Dalby, R.N., Byron, P.R., Peart, J., Surman, J.D., Farr, S. J. (Eds.), Davis Healthcare International Publishing, Tiver Grove, Il, USA. p 303-311

Schlimmer, P. (2002). Single dose comparison of formoterol (Oxis) Turbuhaler 6 μg and formoterol Aerolizer 12 μg in moderate to severe asthma: a randomised, crossover study. Pulmonary Pharmacology & Therapeutics. 15,4, 369-74

Schulze, D. (2005). Flow properties testing with ring shear testers RST-01.01, RST-01.pc and RST-XS. Schwedes + Schulze Schüttguttechnik GmbH, Braunschweig.

Sebti, T., Vanderbist, F., Amighi, K. (2007). Evaluation of the content homogeneity and dispersion properties of fluticasone DPI compositions. Journal of Drug Delivery Science and Technology. 17, 223–229.

Seville, J. P. K., (1987) in Tribology in Particle Technology, Briscoe, B. J. and Adams, M. J. (eds.), Adam Hilger, Bristol.

Seville, J. P. K., Tùzùn, U., Clift, R. (1997). Processing of Particulate Solids. Blackie Academic and Professional (Kluwer).

Schafmayer, C., Hartleb, J., Tepel, J., Albers, S., Freitag, S., Völzke, H., Buch, S., Seeger, M., Timm, B., Kremer, B., Fölsch, U. R., Fändrich, F., Krawczak, M., Schreiber, S., Hampe, J. (2006). Predictors of gallstone composition in 1025 symptomatic gallstones from Northern Germany. BMC Gastroenterology. 6: 36

Shahi, S. R., Agrawal, G.R., Rathi, P.B., Shinde, N.V., Somani, V.G., Mahamuni, S.B., Padalkar, A.N. (2008). Development and validation of UV spectrophotmetric determination of Etoricoxib in bulk and tablet formulation. Rasayan Journal of Chemistry 1, 2, 390-394.

Shariare, M.H., de Matas, M., York, P., Shao, Q. (2011). The impact of material attributes and process parameters on the micronisation of lactose monohydrate. International Journal of Pharmaceutics. doi:10.1016/j.ijpharm.2011.01.047

Shekunov, B. Y., Feeley, J. C., Chow, A. H. L., Tong, H. H. Y, York, P. (2003). Aerosolisation behaviour of micronised and supercritically-processed powders. Journal of Aerosol Science. 34,5, 553-568.

Shur, J., Harris, H., Jones, M. D., Kaerger, J. S., Price, R. (2008). The Role of Fines in the Modification of the Fluidization and Dispersion Mechanism Within Dry Powder Inhaler Formulations. Pharmaceutical Research, 25,7, 1931-1940

Siekmeier, R., Scheuch, G. (2008) Systemic Treatment by Inhalation of Macromolecules – Principles, Problems and Examples. Journal of Physiology and Pharmacology. 59, 6, 53-79.

Smolders, K., and Baeyens, J. (1997). Elutriation of fines from gas fluidized beds: mechanisms of elutriation and effect of freeboard geometry, Powder Technology. 92, 35–46.

Smyth, H. D., Hickey, A. J. (2005). Carriers in drug powder delivery: implications for inhalation system design. American Journal of Drug Delivery. 3,2, 117–132.

Snow, R. H., Allen, T., Ennis, B. J., Litster, J. D. (1999). Size reduction and size enlargement. In: Perry RH, Green, D. W., editors. Perry's chemical engineers' handbook. New York: McGraw-Hill.

Srichana, T., Martin, G. P., Marriott, C. (1998). On the relationship between drug and carrier deposition from dry powder inhalers in vitro. International Journal of Pharmaceutical Technology and Product Manufacture. 2,1, 7-12.

Staniforth, J. N., Rees, J. E., Lai, F. K., Hersey, J. A., (1981). Interparticle forces in binary and ternary ordered powder mixes. Journal of Pharmaceutics and Pharmacology. 34(3): 141-145

Staniforth, J. N., (1996). Preformulation aspects of dry powder aerosols. In: Byron, P.R., Dalby, R.N., Farr, S.J. (Eds.), Respiratory Drug Delivery V. Interpharm Press, Buffalo Grove, IL, pp. 65-73

Steckel, H. and Bolzen, N. (2004). Alternative sugars as potential carriers for dry powder inhalations. International Journal of Pharmaceutics. 270, 297-306

Steckel, H. and Müller, B. W. (1997a). In vitro evaluation of dry powder inhalers I: Drug deposition of commonly used devices. International Journal of Pharmaceutics. 154, 19-29

Steckel, H. and Müller, B. W. (1997b). In vitro evaluation of dry powder inhalers II: influence of carrier particle size and concentration on in vitro deposition. International Journal of Pharmaceutics. 154, 31-37.

Steckel, H., Borowski, M., Eskander, F., Villax, P., (2004). Selecting lactose for a capsule- based dry powder inhaler. Pharmaceutical Technology Europe (April): 23-35

Strauss, W., (1975). Industrial Gas Cleaning. Pergamon, London.

Sudah, O. S., Coffin-Beach, D., Muzzio, F. J. (2002a). Effects of blender rotational speed and discharge on the homogeneity of cohesive and free-flowing mixtures. International Journal of Pharmaceutics. 247,1–2, 57–68.

Sudah, O. S., Coffin-Beach, D., Muzzio, F. J. (2002b). Quantitative characterization of mixing of free-flowing granular material in tote (bin) blenders. Powder Technology. 126, 191-200.

Swift, D.L. and Proctor, D.F. (1988). A Dosimetric Model for Particles in the Respiratory Tract above the Trachea. Annala of Occupational Hygiene. 32, 1035–1044

Takano, K., Nishii, K., Horio, M., (2003). Binderless granulation of pharmaceutical fine powders with coarse lactose for dry powder inhalation. Powder Technology. 131: 129-138

Taki, M., Marriott, C., Zeng, X-M., Martin, G. P. (2010). Aerodynamic deposition of combination dry powder inhaler formulations in vitro: A comparison of three impactors. International Journal of Pharmaceutics. 388, 1-2, 40-51

Taylor, L. J., Papadopoulos, D. G., Dunn, P. J., Bentham, A. C., Mitchell, J.C., Snowden, M. J. (2004). Mechanical characterisation of powders using nanoindentation. Powder Technology, 143–144, 179–185.

Tee, S. K., Marriott, C., Zeng, X. M., Martin, G.P. (2000). The use of different sugars as fine and coarse carriers for aerosolised salbutamol sulphate. International Journal of Pharmaceutics. 208,1–2, 111–123.

Telko, M. and Hickey, A. J. (2005). Dry powder inhaler formulations. Respiratory Care 50, 1209–1227.

Telko, M. J., Kujanpaa, J., Hickey, A. J. (2007). Investigation of triboelectric charging in dry powder inhalers using electrical low pressure impactor (ELPI). International Journal of Pharmaceutics, 336,2, 352– 360.

Thi, T. H. H., Dane, F., Descamps, M., Flament, M-P. (2008). Comparison of physical and inhalation properties of spray-dried and micronized terbutaline sulphate. European Journal of Pharmaceutics and Biopharmaceutics. 70, 380-388.

Ticehurst, M. D., Basford, P. A., Dallman, C. I., Lukas, T. M., Marshall, P. V., Nichols, G. et al. (2000). Characterisation of the influence of micronisation on the crystallinity and physical stability of revatropate hydrobromide. International Journal of Pharmaceutics, 193, 247–259.

Timsina, M. P., Martin, G. P., Marriott, C., Ganderton, D., Yianneskis, M., (1994). Drug delivery to the respiratory tract using dry powder inhalers. International Journal of Pharmaceutics. 101, 1–13.

Tinke, A. P., Govoreanu, R., Weuts, I., vanhoutte, K., De Smaele, D. (2009). A review of underlying fundamentals in wet dispersion size analysis of powders. Powder Technology. 196,2, 102-114.

Tobyn, M., Staniforth, J. N., Morton, D., Harmer, Q., Newton, M. E. (2004). Active and intelligent inhaler device development. International Journal of Pharmaceutics. 277,1–2, 31–37.

Traini, D., Young, P. M., Jones, M., Edge, S., & Price, R. (2006). Comparative study of erythritol and lactose monohydrate as carriers for inhalation: Atomic force microscopy and in vitro correlation. European Journal of Pharmaceutical Sciences, 27, 243–251.

Trojak, A., Kocevar, K., Musevic, I., Srcic, S. (2001). Investigation of the felodipine glassy state by atomic force microscopy. International Journal of Pharmaceutics. 218,1–2, 145–151.

Tsukada, M., irie, R., Yonemochi, Y,. Noda, R., Kamiya, H., Watanabe, W., (2004). Adhesion force measurement of a DPI size pharmaceutical particle by colloid proc=be atomic force microscopy. Powder Technology. 141: 262-269

Tu, W-D., Ingram, A., Seville, J., Hsiau, S-S. (2009). Exploring the regime map for high-shear mixer granulation. Chemical Engineering Journal. 145, 505-513

Tuley, R., Shrimpton, J., Jones, M. D., Price, R., Palmer, M., Prime, D. (2008). Experimental observations of dry powder inhaler dose fluidisation. International Journal of Pharmaceutics 358. 238–247

Turki, D., Fatah, N. (2008). Behavior and fluidization of the Cohesive powders: agglomerates Sizes approach. Brazilian Journal of Chemical Engineering. 25,4, 697 - 711

Valverde, J. M., Rasenack, N., Castellanos, A., Watson, P. K. (1998). The tensile strength of cohesive powders and its relationship to consolidation, free volume and cohesivity. Powder Technology. 97, 237–245

Vanderbist, F., Maes, P. (1998). Dry powder inhaler excipient, process for its preparation and pharmaceutical compositions containing it. European Patent No. 0876814 A1.

Vanbever, F., Mintzes, J. D., Wang, J., Nice, J., Chen, D. ,Batycky, R., Langer, R., Edwards, D. A. (1999). Formulation and physical characterisation of large porous particles for inhalation. Pharmaceutical Research. 16, 1735-1742.

van Drooge, D. J., Hinrichs, W. L. J., Dickhoff, B. H. J., Elli, W. N. A., Visser, M. R., Zijsltra, G. S., Frijlink, H. W. (2005). Spray freeze drying to produce a stable (delta) 9-tetrahydrocannabinol containing insulin based solid dispersion powder suitable for inahlation. European Journal of Pharmaceutical Science. 26(2): 231-240

Versteeg, H., Hargreave, G., Hind, R. (2005). An optical study of aerosol generation in dry powder inhalers. In: Drug Delivery to the Lungs, vol. 16. The Aerosol society, pp. 3–6.

Vidgren, M. T., Vidgren, P. A., Paronen, T. P. (1987). Comparison of physical and inhalation properties of spray-dried and mechanically micronized disodium-cromoglycate. International Journal of Pharmaceutics. 35, 139–144.

Visser, J., (1989). Van der Waals and other cohesive forces affecting powder fluidization. Powder Technology. 58: 1-10

Wagner, D. H., Ramanthan, S., Taylor, M. L., Brown, A. B., Staben-Wobker, M. E., Prior, M. (2009). The thermodynamics of high shear blending. Powder Technology. 193, 195-199

Waites, M. J., Morgan, N. L. (2001). Industrial Microbiology: An Introduction. Blackwell Science Ltd. Oxford, UK. pp113-114.

Walker, G. M., Bell, S. E. J., Andrews, G., Jones, D. (2007). Co-melt fluidised bed granulation of pharmaceutical powders: Improvements in drug bioavailability. Chemical Engineering Science 62, 451 – 462

Waltersson, J., Lundgren, P. (1985). The effect of mechanical communition on drug stability. Acta Pharmaceutica Suecica. 22, 291–300.

Wang, R.H., Fan, L.T. (1974). Methods for scaling-up tumbling mixers. Chemical Engineering. 81, pp. 88–94.

Wang, T-J., Jin, Y., Tsutsumi, A., Wang, Z., Cui, Z., (2000). Energy transfer mechanism in a vibrating fluidised bed. Chemical Engineering Journal. 78: 115-123

Watling, C. P., Elliott, J. A., Cameron, R. E. (2010). Entrainment of lactose inhalation powders: A study using laser diffraction. European Journal of Pharmaceutical Sciences. 40, 352-358.

Watson, P. K., Valverde, J. M., Castellanos, A. (2001). The tensile strength and free volume of cohesive powders compressed by gas flow. Powder Technology. 115, 45–50.

Weibel, E.R. (1963). Morphometry of the Human Lung. Heidelberg: Springer Verlag.

Wellm, A. B. (1997). Investigation of a high shear mixer=agglomerator. Ph.D. Thesis, The University of Birmingham, Birmingham, UK.

Wen, C.Y., Chen, L.H., (1982). Fluidized bed freeboard phenomena: entrainment and elutriation. American Institute of Chemical Engineers' Journal. 28: 117–128.

Williams III, R.O., Brown, J. Liu, J. (1999). Influence of micronization method on the performance of a suspension triamcinolone acetonide pressurized metered-dose inhaler formulation, Pharmaceutical Development Technology. 4, 167–179.

Wood, W. M. L. (2001). A bad (crystal) habit: and how it was overcome. Powder Technology. 121, 53–59.

Wu, S. Y., Baeyens, J. (1991) Effect of operating temperature on minimum fluidization velocity. Powder Technology, 67, 217-220

Wu, S.Y., Baeyens, J. (1998). Segregation by size difference in gas fluidized beds. Powder Technology 98, 139-150

Xu, C., and Zhu, J-X. (2006). Effects of gas type and temperature on fine particle fluidization. China Particuology. 4,3-4, 114-121.

Xu, R. (2000). Particle Characterization: Light Scattering Methods, Kluwer Academic Publishing, Dordrecht.

Xu, R., Guida, O.A.D. (2003). Comparison of sizing small particles using different technologies. Powder Technology. 132, 145–153.

Yip C. W., Hersey, J. A. (1977). Ordered or random mixing: Choice of system and mixer. Drug Development and Industrial Pharmacy. 3, 429 - 438.

Young, P. M., Cocconi, D., Colombo, P., Bettini, R., Price, R., Steele, D. F., Tobyn, M. J. (2002). Characterization of a surface modified dry powder inhalation carrier prepared by "particle smoothing". Journal of Pharmaceutics and Pharmacology. 54, 1339-1344.

Young, P. M., Price, R., Tobyn, M. J., Buttrum, M., & Dey, F. (2003). Effect of humidity on aerosolization of micronized drugs. Drug Development and Industrial Pharmacy, 29, 959–966.

Young, P. M., Price, R., Tobyn, M. J., Buttrum, M., Dey, F. (2004). The influence of relative humidity on the cohesion properties of micronized drugs used in inhalation therapy. Journal of Pharmaceutical Science. 93,3, 753–761.

Young, P. M., Edge, S., Traini, D., Jones, M. D., Price, R., El-Sabawi, D., Urry, C., Smith, C., (2005). The influence of dose on the performance of dry powder inhalation systems. International Journal of Pharmaceutics. 296: 26-33

Young, P. M., Chan, H. K., Chiou, H., Edge, S., Tee, T. H., Traini, D. (2007a). The influence of mechanical processing of dry powder inhaler carriers on drug aerosolization performance. Journal of Pharmaceutical Sciences. 96, 1331-1341.

Young, P. M., Sung, A., Traini, D., Kwok, P., Chiou, H., & Chan, H. K. (2007b). Influence of humidity on the electrostatic charge and aerosol performance of dry powder inhaler carrier based systems. Pharmaceutical Research, 24, 963–970.

Zanen, P., Go, L. T., Lammers, J. W. (1994). The optimal particle-size for betaadrenergic aerosols in mild asthmatics. International Journal of Pharmaceutics. 107, 211– 217.

Zeng, X. M., Martin, G. P., Tee, S. K., Marriott, C. (1998). The role of fine particle lactose on the dispersion and de-agglomeration of salbutamol sulphate in an air stream in vitro. International Journal of Pharmaceutics. 176, 99-110.

Zeng, X. M., Martin, G. P., Marriott, C., Pritchard, J., (2000a). The influence of carrier morphology on drug delivery by dry powder inhalers. International Journal of Pharmaceutics. 200, 93–106.

Zeng, X. M., Pandhal, K. H., Martin, G. P., (2000b). The influence of lactose carrier on the content homogeneity and dispersibility of beclomethasone dipropionate from dry powder aerosols. International Journal of Pharmaceutics. 197: 41-52

Zeng, X. M., Martin, G. P., Marriott, C., Pritchard, J., (2001). Lactose as a carrier in dry powder formulations: The influence of surface characteristics on drug delivery. Journal of Pharmaceutical Sciences. 90,9, 1424-1434.

Zeng, X. M., MacRitchie, H. B., Marriott, C., & Martin, G. P. (2007). Humidity-induced changes of the aerodynamic properties of dry powder aerosol formulations containing different carriers. International Journal of Pharmaceutics, 333, 45–55.

Zenz, F. A., Weil, N. A. (1958). A Theoretical-Emperical Approach to the Mechanism of Particle Entrainment from Fluidized Beds," American Institute of Chemical Engineers' Journal. 4, 4, 472

Zhou, T., Li, H. (1999). Effects of adding different size particles on fluidization of cohesive particles. Powder Technology, 102,3, 215–220.

Zhou, Q., Armstrong, B., Larson, I., Stewart, P.J., Morton, D.A.V. (2009). Effect of host particle size on the modification of powder flow behaviours for lactose monohydrate following dry coating. Dairy Science Technology. doi:10.1051/dst/2009046.

Zhou, Q. T., Qu, L., Larson, I., Stewart, P. J., Morton, D. A. V. (2010).Improving aerosolization of drug powders by reducing powder intrinsic cohesion via a mechanical dry coating approach. International Journal of Pharmaceutics. 394, 50-59

Zhu, K., Tan, R. B. H., Ng, W. K., Shen, S., Zhou, Heng, P. W. S. (2008). Analysis of the influence of relative humidity on the moisture sorption of particles and the aerosolization process in a dry powder inhaler. Journal of Aerosol Science. 39, 6, 510-524

Zijlstra, G. S., Hinrichs, W. L. J., de Boer, A. H. and Frijlink, H. W. (2004). The role of particle engineering in relation to formulation and de-agglomeration principle in the development of a dry powder formulation for inhalation of cetrorelix. European Journal of Pharmaceutical Science. 23(2): 139-149

Zimon, A. D. (1982). Adhesion of dust and powder. R. K. Johnston. New York, Consultants Bureau: 154, pp 310-319.

Appendix

Example density and cumulative distribution curves from dry laser diffraction measurements:

Example Raw PSD data of unblended lactose

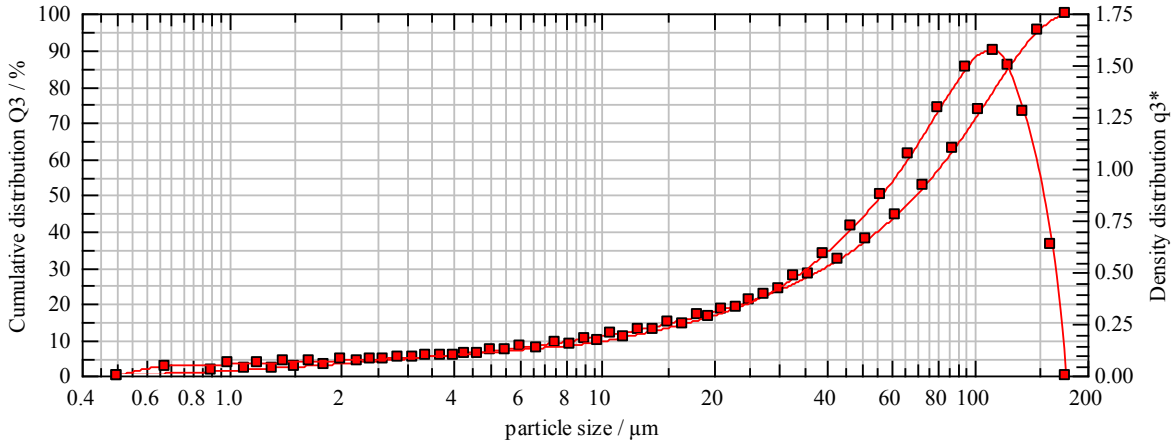

Example Raw PSD data of blended lactose (197 kJ kg^{-1})

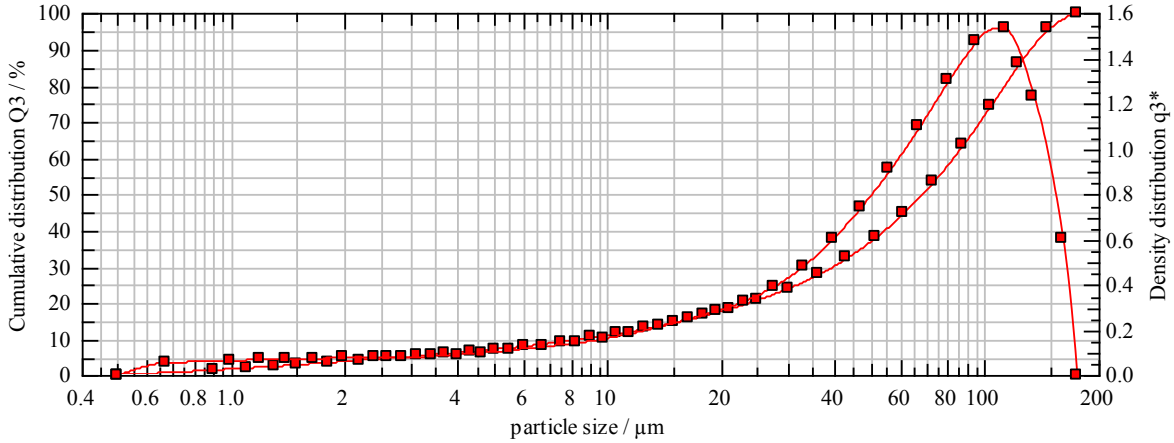

Example Raw PSD data of blended lactose (399 kJ kg^{-1})

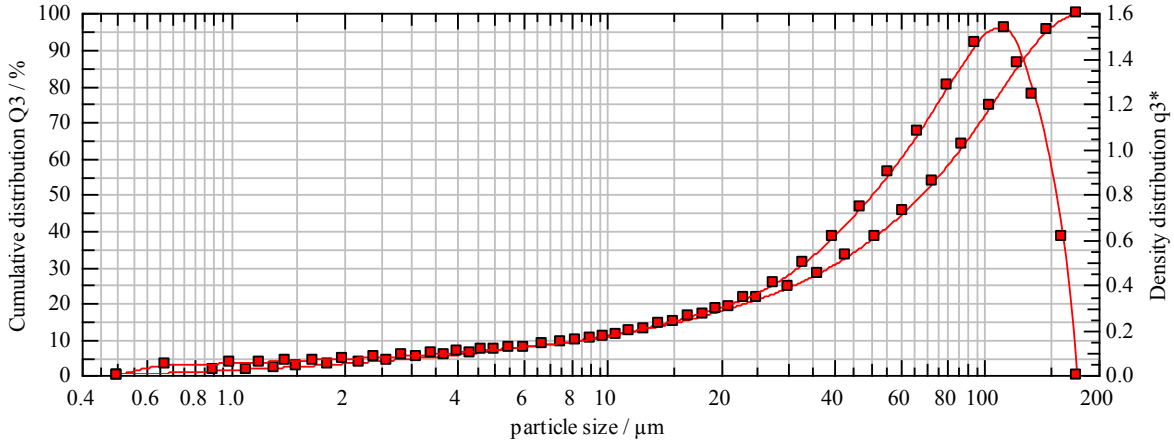

Example Raw PSD data of blended lactose (618 kJ kg^{-1})

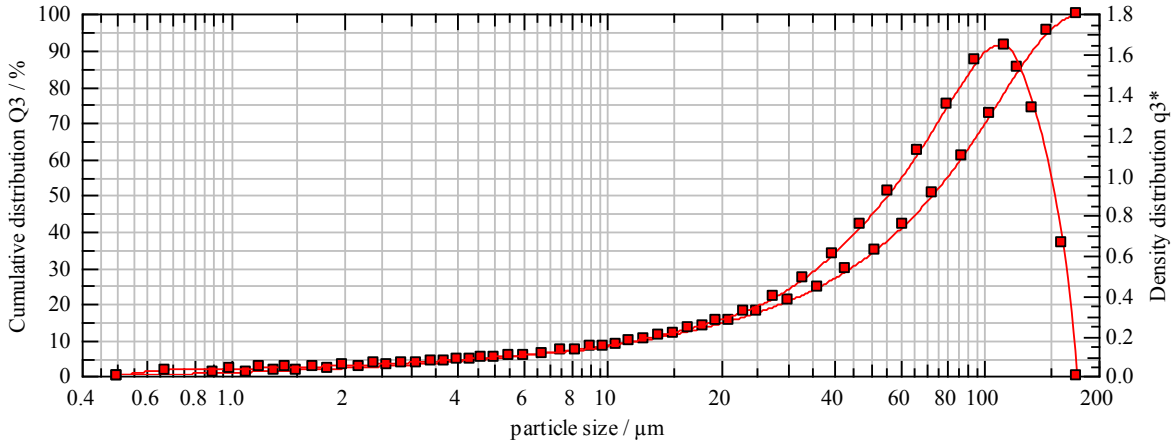

Example Raw PSD data of 71 µm lactose

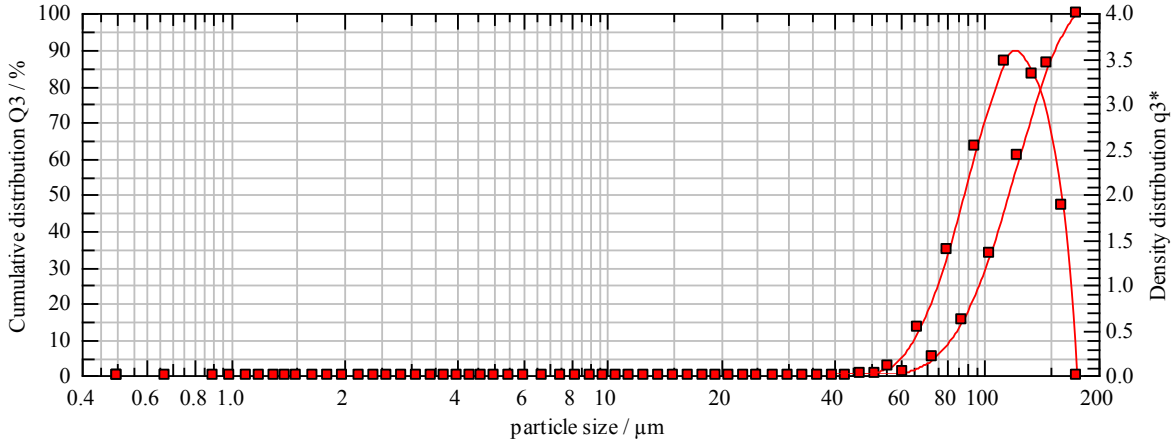

Example shear cell measurements of unconfined yield stress (σ), against consolidation stress (τ)

Example Mohr's Circles for Unblended Lactose

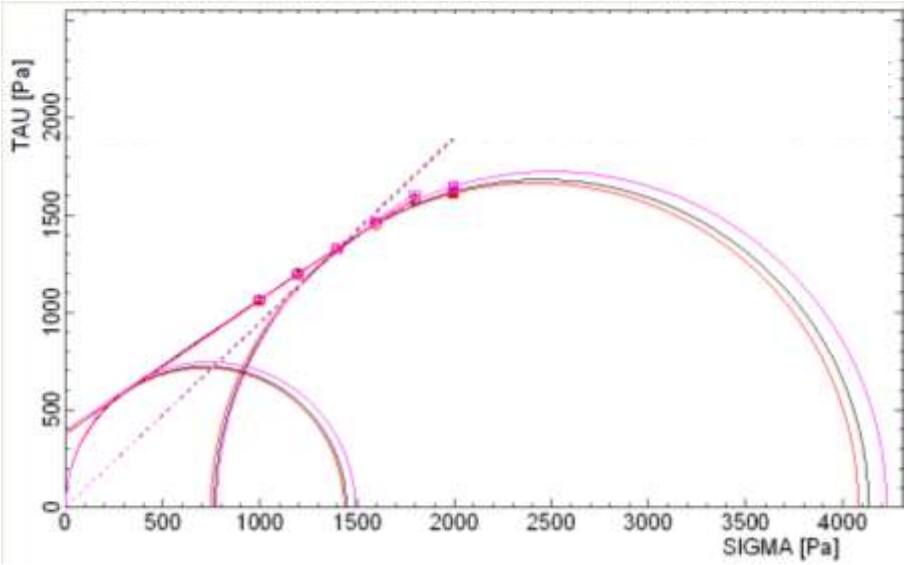

Example Mohr's Circles for "Deagglomerated" Lactose (Blended for 88 kJ kg^{-1})

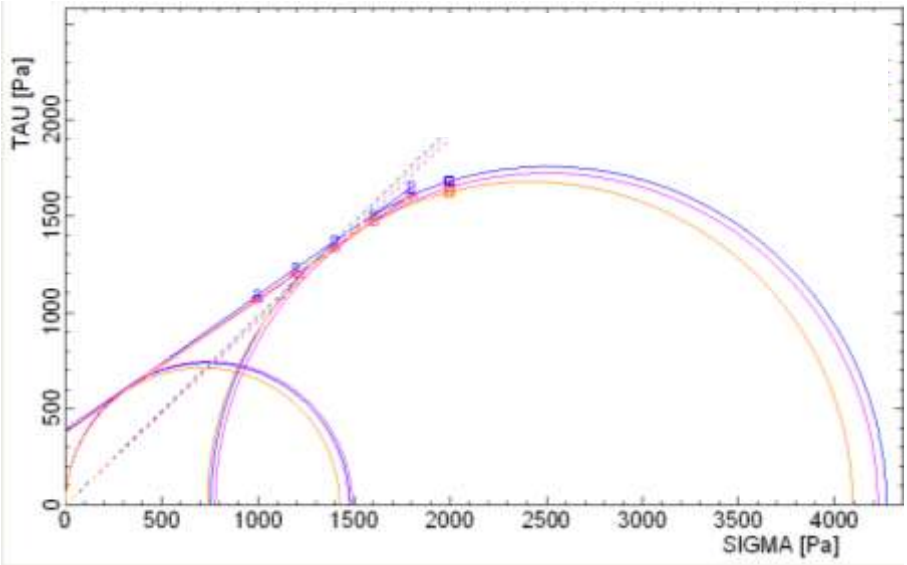

Example Mohr's Circles for "Agglomerated" Lactose (Blended for 602 kJ kg^{-1})

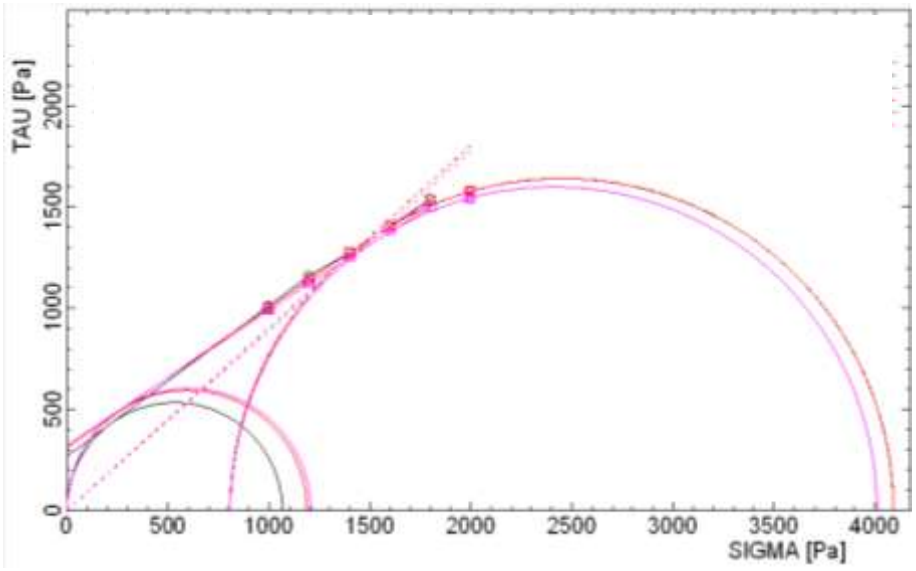

Example Mohr's Circles for "25 μm" Lactose

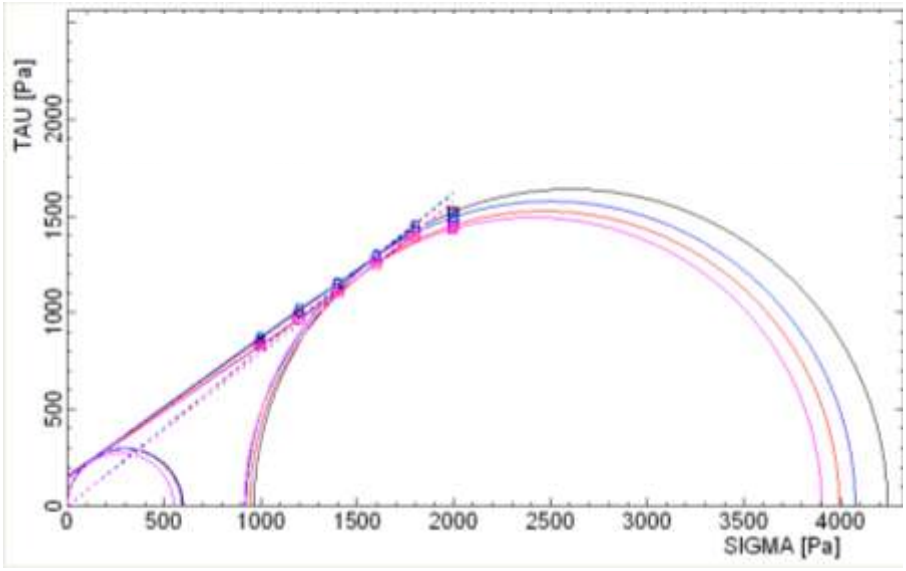

Example Mohr's Circles for "71 μm" Lactose

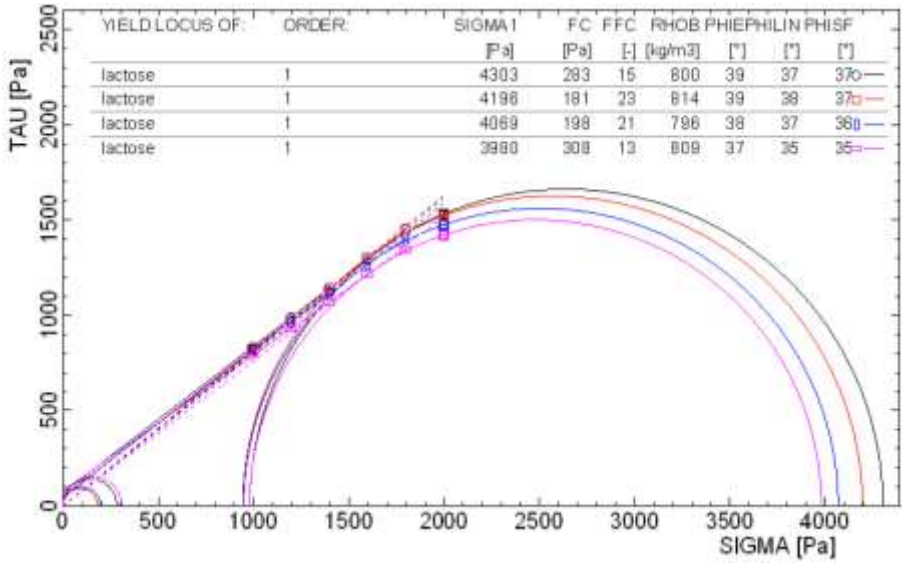

Publications

Willetts, J., Robbins, P.T., Bowley, M.A., Roche, T., Bridson, R. (2009). Investigation into the effects of blend energy input at different scales on α-lactose monohydrate. Journal of Pharmacy and Pharmacology, Volume 61, p94-95

Willetts, J., Robbins, P.T., Bridson, R., Bowley, M.A., Roche, T. (2010). Development of a fluidised bed method for assessing fine/coarse particle interactions in inhalation-grade lactose. Journal of Pharmacy and Pharmacology, Volume 62, p1416

Development of a fluidised bed method for assessing fine/coarse particle interactions in inhalation-grade lactose

John Willetts[1*], Phil Robbins[1], Rachel Bridson[1], Michael Bowley[2], Trevor Roche[3],
[1]Centre for Formulation Engineering, School of Chemical Engineering, University of Birmingham, U.K., B15 2TT
[2]GlaxoSmithKline, Global Manufacturing and Supply, Priory Street, Ware, Hertfordshire, U.K. SG12 0DJ
[3]GlaxoSmithKline, Research and Development, Inhaled Product Development, Park Road, Ware, Hertfordshire, U.K. SG12 0DP
* Email: jpw281@bham.ac.uk

INTRODUCTION

While fluidised beds are commonly used in the pharmaceutical industry for applications such as coating, granulation and drying, it is uncommon for them to be used for the deliberate separation of fine particles from coarse particles; indeed particle elutriation from fluidised beds is often considered a problem. In this work, the elutriation of lactose particles from a classic fluidised bed system has been exploited to explore the behaviour of lactose particles that have been exposed to different high shear blending conditions. While the fluidisation conditions employed do not attempt to mimic those of an inhalatory event, the behaviour of particles under varying fluidisation regimes will provide fundamental insight into particle-particle interactions and the effects that blending has on these. This abstract describes the fluidised bed system and comparisons between the fluidisation and elutriation behaviour of blended and unblended materials.

MATERIALS AND METHODS

A small-scale vibrational fluidised bed was designed to enable analysis of both unprocessed and high shear blended inhalation grade lactose (approx 20 g). Key design features included apparatus for the humidification of the air stream and for the effective collection of elutriated fines. Control of humidification allowed balance of electrostatic and capillary forces encountered within the fluidised bed [1]. In addition, the apparatus was designed to enable collection of various size fractions of elutriated material, based on the superficial gas velocity of fluidising air.

Particle characterisation was performed using: dry laser diffraction (Sympatec HELOS/RODOS), wet laser diffraction (Malvern Mastersizer 2000) with propan-2-ol as dispersant [2], water sorption characteristics and BET surface area analysis with octane as the probe molecule [3] (DVS Advantage II, Surface Measurement Systems, UK). In addition, scanning electron microscope (SEM) images of the surface morphology and uniformity of material were obtained. Blending was performed using a high shear blender, as described in previous work. [4],[5].

RESULTS AND DISCUSSION

Both blended and unblended lactose were difficult to fluidise; no measurable differences were seen between the fluidisation curves (*pressure drop vs. flow rate*) of blended and unblended lactose. In addition, there were no statistically significant differences in the mass of material elutriated over a fixed periods of time and flow rates. However, there were measurable and consistent differences between particle size distributions of the elutriated fractions when comparing unblended and blended lactose. This provided information on how blending affected the distribution of different-sized lactose particles.

CONCLUSIONS

A vibrational fluidised bed has been used to assess the bulk behaviour of dry powder inhaler grade lactose, and in assessing DPI performance, the elutriated fraction is likely to be important. Experimentation here has shown that measurement of this elutriated fraction can be related to the effects of high shear blending. This method could prove important in assessing the behaviour of DPI formulations.

ACKNOWLEDGMENTS

Funding for this project was provided by the Engineering and Physical Sciences Research Council (EPSRC) and GlaxoSmithKline.

Both the Sympatec HELOS detector and RODOS dispersion unit, and the DVS Advantage II used in this research were obtained through Birmingham Science City: Innovative Uses for Advanced Materials in the Modern World (Advanced Materials 2) with support from Advantage West Midlands (AWM) and part funded by the European Regional Development Fund (ERDF).

REFERENCES

[1] Li, J., and Kato, K. (2001). Effect of electrostatic and capillary forces on the elutriation of fine particles from a fluidized bed. Advanced Powder Technology. 12,2, 287-205.
[2] Adi, H., Larson, I., Stewart, P. (2007). Laser diffraction particle sizing of cohesive lactose powders. Powder Technology 179, 90–94.
[3] Brunauer, S., Emmett P. H., and Teller, E. (1938). Adsorption of gases in multimolecular layers. Journal of the American Chemical Society. 60, 309.
[4] Bridson, R. H., Robbins, P. T., Chen, Y., Westerman, W., Gillham, C. R., Roche, T. C., Seville, J. P. K. (2007). The effects of high shear blending on α-lactose monohydrate. International Journal of Pharmaceutics. 339, 84–90.
[5] Knight, P. C., Seville, J. P. K., Wellm, A. B., Instone, T. (2001). Prediction of impeller torque in high shear powder mixers. Chemical Engineering Science. 56, 4457–4471.

Development of a fluidised bed elutriation method for assessing fine/coarse particle interactions in inhalation-grade lactose

John Willetts[1], Phil Robbins[1], Michael Bowley[2], Trevor Roche[3], Rachel Bridson[1]*

1. Centre for Formulation Engineering, School of Chemical Engineering, University of Birmingham, U.K., B15 2TT
2. GlaxoSmithKline, Global Manufacturing and Supply, Priory Street, Ware, Hertfordshire, U.K. SG12 0DJ
3. GlaxoSmithKline, Research and Development, Inhaled Product Development, Park Road, Ware, Hertfordshire, U.K. SG12 0DP
** Email: jpw281@bham.ac.uk*

investing in your future · Advantage West Midlands · UNIVERSITY OF BIRMINGHAM · gsk GlaxoSmithKline · EPSRC Engineering and Physical Sciences Research Council

Introduction

Fluidised beds are commonly used in the pharmaceutical industry for applications such as coating, granulation and drying. However, it is uncommon for them to be used for the deliberate separation of fine particles from coarse particles; indeed particle elutriation from fluidised beds is often considered a problem. In this work, the elutriation of lactose particles from a classic fluidised bed system has been exploited to explore the behaviour of lactose particles that have been exposed to different high shear blending conditions. While the fluidisation conditions employed do not attempt to mimic those of an inhalatory event, the hypothesis is that blending-induced changes in model DPI formulations can be explored by assessing changes in their fluidisation and elutriation performance and behaviour.

Materials & Methods

A vibrating fluidised bed was designed (Fig.1) to enable analysis of both unprocessed and high shear blended inhalation grade lactose (approx 20 g from a 500 g blend). Key design features included apparatus for the humidification of the air stream (Fig.2) and a filter for the collection of elutriated fines. Control of humidification allowed balance of electrostatic and capillary forces encountered within the fluidised bed[1]. The apparatus was designed to enable collection of various size fractions of elutriated material, based on the superficial gas velocity of fluidising air.

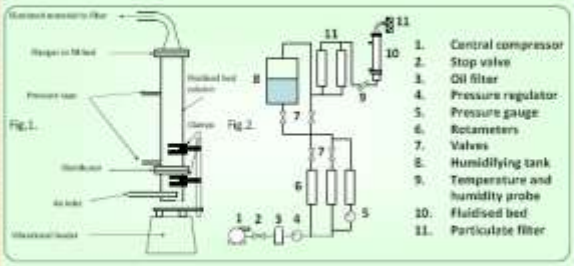

Formulations were prepared using a high shear blender designed to allow real-time torque monitoring on the bowl during blending; this allowed the specific energy input (kJ kg^{-1}) to be calculated from equations 1 & 2. Inhalation grade lactose (Friesland Foods Domo, Netherlands) was used as supplied. Cholesterol was micronised using a Pulverisette 7 (Fritsch, Germany) with 1mm zirconium oxide grinding media, suspended in 1:3 w/w cholesterol:water suspension (Fig.3).

$$P = \frac{2\pi RFN}{60} \quad \text{(Eq. 1)} \qquad E = \int_{t_1}^{t_2} P dt \quad \text{(Eq. 2)}$$

P = Power (W), F = Force (N), E = Energy (J)
N = Rotational speed (rpm)
R = Radius from centre of bowl to force transducer (m)

Blending conditions – 500 g initial mass; 500 rpm

- 140 mm internal diameter stainless steel bowl
- Three-blade impeller with constant width in the horizontal plane (50 mm); depth of blade 10 mm with 11° bevelled edge on forward face; front 1 mm of bevelled edge was left vertical to ensure the blades were not sharp[2]
- Lactose stored at 20°C and 40% RH in a humidity and temperature controlled cabinet (Binder, Germany)
- Satisfactory mixing conditions achieved through visual observations and torque readings

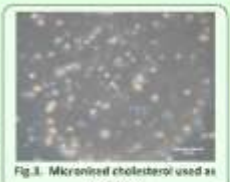
Fig.3. Micronized cholesterol used as model drug

Measurements

- Samples of lactose were taken at regular intervals during blending and analysed using laser diffraction (HELOS sensor with RODOS dispersion unit, Sympatec, Germany)
- Elutriated material weighed gravimetrically and particle size distributions determined using laser diffraction (Wet dispersion in Propan-2-ol – Malvern Mastersizer 2000)[3]
- Blend homogeneity determined using UV Spectroscopy (Jasco V-670, Jasco, UK) Methanol used to dissolve cholesterol; centrifugation to separate non-dissolved lactose; supernatant removed by pipette and analysed using λ = 205 nm

References

[1] Li, J., and Kato, K. (2001). Effect of electrostatic and capillary forces on the elutriation of fine particles from a fluidized bed. *Adv. Powder. Tech.* **12**,2, 287-205.
[2] Knight, P.C., Seville, J.P.K., Wellm, A.B., Instone, T., (2001). *Chem. Eng. Sci.* **56**, 4457–4471.
[3] Adi, H., Larson, I., Stewart, P. (2007). *Powder Tech.* **179**, 90–94.
[4] Bridson, R.H., Robbins, P.T., Chen, Y., Westerman, D., Gillhams, C.B., Roche, T.C., Seville, J.P.K. (2007). *Int. J. Pharm.* **339**, 84-90

Results

Extended high-shear blending regimes have previously been shown to affect the fines content of lactose[4]. In this work, samples were taken at regular intervals (energy inputs) and fluidised at superficial gas velocity of 6.25 cms^{-1}. Elutriated material was weighed (Fig.4) and particle size distributions were determined at regular fluidisation intervals.

Fig. 4. Cumulative mass elutriated as a function of time for lactose subjected to various specific blend energy inputs, and deliberately agglomerated (by humidity) lactose. Results are the overall mean of three independent experiments ± SEM.

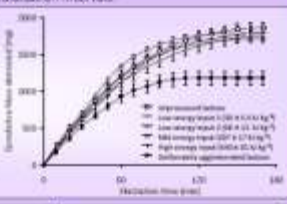

No significant differences are apparent in the fluidisation performance of lactose-based formulations. However, significantly less mass is elutriated from deliberately agglomerated samples - showing the ability of the fluidised bed system to discriminate between formulations.

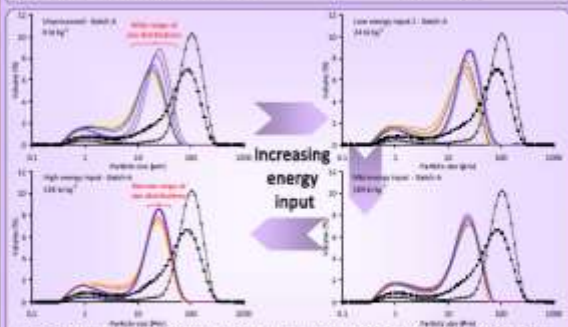

Fig.5. Particle size distributions of elutriated material as a function of fluidisation time for various specific energy inputs: ■ - 10 min; ■ - 20 min; ■ - 30 min; ■ - 50 min; ■ - 110 min; ■ - 120 min; ■ - 130 min; ■ - unprocessed lactose; ▲ - non elutriated lactose.

These differences in elutriation performance due to blending show this method to be of potential importance for assessing the performance of both lactose and other DPI excipients upon fluidisation; understanding the behaviour of lactose-drug systems (including adhesion), and relating formulation behaviour to different manufacturing processes.

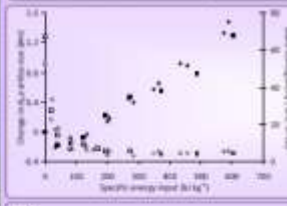

Fig.6. Change in d_v particle size (△,□,◇) and blend homogeneity (◆,■,▲) as a function of specific energy input for three independent 1:67.5 w/w cholesterol:lactose blends.
Here it is shown that whilst extended high shear blending affects the PSD of this model active formulation, the chemical homogeneity (quality of blend) does not increase beyond specific energy inputs ~200 kJ kg^{-1}. This could have implications for use in end-point determination of processes to eliminate unnecessary powder changes.

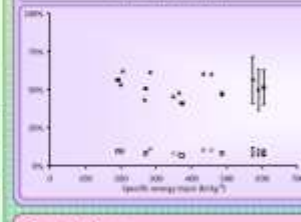

Fig.7. % drug in elutriated material (△,□,◇) and emitted drug % (◆,■,▲) as a function of specific energy input for three independent 1:67.5 w/w cholesterol:lactose blends. Error bar available for final data set due to sample availability.
This shows that extended high shear blending does not affect the elutriation behaviour of this model actives from the fluidised bed. Based on this study, excessive blending beyond the point at which homogeneity is achieved is unnecessary.

Conclusion

A vibrational fluidised bed has been used to assess the bulk behaviour of DPI grade lactose, both with and without model API. In assessing DPI performance, the elutriated fraction has been shown to be important and the changes in this behaviour due to blending show that this may be a useful tool in understanding a variety of processes including: end-point determination to reduce over processing and eliminate unnecessary powder changes; understanding of different excipient behaviour and drug interactions (including adhesion), and relating changes in manufacturing processes to formulation behaviour. Further studies examining behaviour of formulations using a Next Generation Impactor and Alpine air jet sieve are ongoing.

Investigation into the effects of blend energy input at different scales on α-lactose monohydrate

John Willetts[1], Phil Robbins[1], Michael Bowley[2], Trevor Roche[3], Rachel Bridson[1]*

1. Centre for Formulation Engineering, School of Chemical Engineering, University of Birmingham, U.K., B15 2TT
2. GlaxoSmithKline, Global Manufacturing and Supply, Priory Street, Ware, Hertfordshire, U.K. SG12 0DJ
3. GlaxoSmithKline, Research and Development, Inhaled Product Development, Park Road, Ware, Hertfordshire, U.K. SG12 0DP
** Email: jpw281@bham.ac.uk*

investing in your future | Advantage West Midlands | UNIVERSITY OF BIRMINGHAM | gsk GlaxoSmithKline | EPSRC Engineering and Physical Sciences Research Council

Introduction

The properties and behaviour of lactose play an important role in the delivery of drug to the lower airways in several dry powder inhaler (DPI) formulations. It is known that high shear blending can affect lactose properties and that there is a relationship between blend energy input and the distribution of lactose fines[1]. However, this previous work was carried out at a single scale with one bowl size. The current study therefore focuses on establishing whether a similar relationship is seen at other, larger scales.

Materials & Methods

Experiments were carried out with a high shear blender designed to allow real-time torque monitoring on the bowl during blending; this allowed the specific energy input (kJ kg^{-1}) to be calculated from equations 1 & 2. Inhalation grade lactose (Friesland Foods Domo, Netherlands) was blended at three different scales using bowls of 140, 168 and 220 mm diameter (Fig.1).

Fig. 1. Three bowls with internal diameters 140, 168 and 220 mm, and corresponding high shear blades

$$P = \frac{2\pi RFN}{60} \quad \text{(Eq. 1)} \qquad E = \int_{t_1}^{t_2} P\,dt \quad \text{(Eq. 2)}$$

P = Power (W), F = Force (N), E = Energy (J)
N = Rotational speed (rpm)
R = Radius from centre of bowl to force transducer (m)

Experimental conditions

- Three-blade impellers were used, with constant width in the horizontal plane (50 mm)
- Depth of blade 10 mm with 11° bevelled edge on forward face
- Front 1 mm of bevelled edge was left vertical to ensure the blades were not sharp[2]
- Lactose stored at 20°C and 40% RH in a humidity and temperature controlled cabinet (Binder, Germany)
- Satisfactory mixing conditions achieved through visual observations and torque readings

Variables

- Impeller speed (200 – 700 rpm)
- Bowl fill (typically between V_1 and V_2 fill)

Measurements

- Samples of lactose were taken at regular intervals during blending and analysed using:
  - Laser diffraction (HELOS sensor with RODOS dispersion unit, Sympatec, Germany)
  - BET analysis (octane)[3] (QVS Advantage II, Surface Measurement Systems, UK)
- Scanning electron microscope (SEM) images of the lactose surface morphology and uniformity of material were taken using a JEOL 6060 SEM (JEOL, Japan) at 10 keV. Each sample was mounted on a carbon sticky tab and gold coated (10 nm thickness), prior to analysis. Images were obtained at magnification of 1500x

Results

Blending regime maps (example in Fig. 2) were constructed for each of the three bowls. These show the experimental space that can be employed for each bowl in order to work in "good" blending conditions.

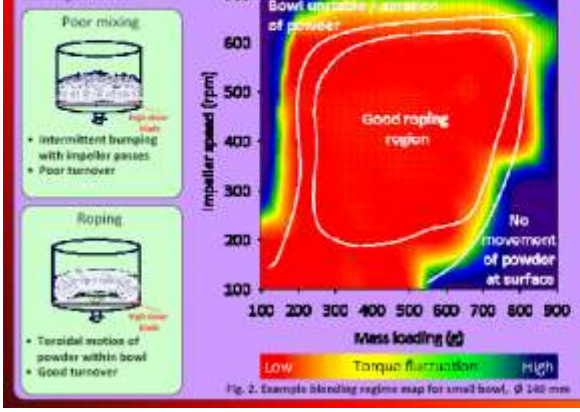

Fig. 2. Example blending regime map for small bowl, Ø 140 mm

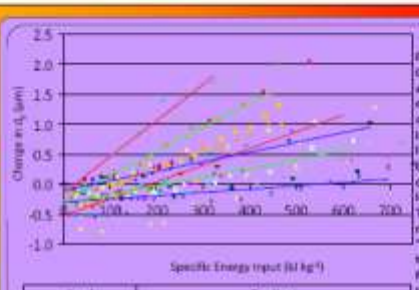

Fig. 3. Change in d_5 particle size as a function of specific energy input. Results shown are from independent samples of lactose blended in three bowl sizes across a range of mass loadings and impeller speeds. Trend lines allow the minimum and maximum "agglomeration gradients" to be seen for each bowl. Note the reduction in d_5 particle size at low energy inputs – indicating that de-agglomeration or milling was occurring before agglomeration.

Bowl	Gradient	
	Range	Average
Small	0.001-0.0033	0.00203 ± 0.00095
Medium	[illegible]	[illegible]
Large	0.0014-0.0064	0.00358 ± 0.00214

For lactose blended in regimes where there was good bed turnover, cumulative energy input during blending was found to be the most important factor affecting lactose particle size distribution. The observed trends were similar at all of the investigated scales. However, the overall effect for a given energy input appeared to increase with bowl size (Fig. 3). Blade speed and bowl fill were not found to be important for individual bowls.

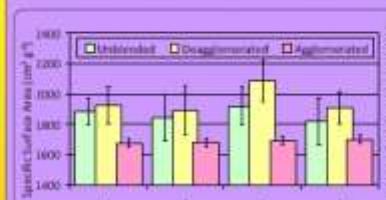

Fig. 4. Specific surface area (SSA) measurements of independent blends, showing unblended, de-agglomerated and agglomerated material. Results obtained by application of the Brunauer, Emmett, Teller (BET)[3] equation using octane as the probe molecule and are shown as the average of at least three separate (120 ± 5 mg) measurements of each sample.

Surface area measurements were performed using a QVS Advantage II, through application of the BET equation using octane as the probe molecule. Results indicate a deagglomeration of material at low energies – shown by an increase in surface area, and the expected agglomeration at higher energies – shown by a reduction in surface area (Fig. 4).

Fig. 5. SEM images of: a) unblended material, b) deagglomerated material, and c) agglomerated material

In order to determine if the reduction in specific surface area was due to deagglomeration or particle breakage (milling), scanning electron microscope (SEM) images were taken (Fig. 5). The images show that particle breakage is an unlikely mechanism for the reduction in particle size / increase in specific surface area. No new surfaces are apparent in the deagglomerated material, thus suggesting that finer material may be knocked from the surface of larger particles at low energy inputs, which then re-agglomerate with additional energy input.

Conclusion

Energy input has a significant and reproducible effect on the particle size distribution of lactose during blending. Scaling effects have been observed on lactose blends, such that larger bowls increase the rate of change of particle size with respect to specific energy input, when compared to smaller bowls. Hence careful control and understanding of this process parameter during DPI development and manufacture is important as it may impact product performance.

References

[1] Brisson, R.M., Robbins, P.T., Chen, Y., Westerman, D., Gillham, C.R., Roche, T.C., Seville, J.P.K. (2007) *Int. J. Pharm.* **335**: 84-90.
[2] Knight, P.C., Seville, J.P.K., Wellm, A.B., Instone, T., (2001). *Chem. Eng. Sci.* **56**: 4457–4471.
[3] Brunauer, S., Emmett P.H., and Teller, E. (1938) *J. Am. Chem. Soc.*, **60**: 309.